Glycoproteomics characterization of immunoglobulins in health and disease

Plomp, H.R.

Glycoproteomics Characterization of Immunoglobulins in Health and Disease

Henriëtte Rosina Plomp

ISBN: 978-94-6295-651-3

The work presented in this thesis was done at the Center for Proteomics and Metabolomics at the Leiden University Medical Center (LUMC), Leiden, The Netherlands.

This work was supported financially by the European Union Seventh Framework Programme HighGlycan project (grant nr. 278535).

Cover design and layout by Henriëtte Rosina Plomp

Printing by Proefschriftmaken.nl, Uitgeverij BOXPress

Glycoproteomics Characterization of Immunoglobulins in Health and Disease

Proefschrift

Ter verkrijging van de graad van Doctor aan de Universiteit Leiden,

op gezag van Rector Magnificus Prof. Mr. C.J.J.M. Stolker,

volgens besluit van het College voor Promoties

te verdedigen op woensdag 31 mei 2017

klokke 15:00 uur

door

Henriëtte Rosina Plomp

geboren te Leiderdorp

op 13 november 1987

Promotoren:

Prof. Dr. M. Wuhrer
Prof. Dr. A.M. Deelder

Co-promotor:

Dr. P. Hensbergen

Leden promotiecommissie:

Prof. Dr. M. de Haas
Dr. G. Vidarsson (Department of Experimental Immunohematology, Sanquin Research, and Landsteiner Laboratory, Academic Medical Center, University of Amsterdam)
Prof. Dr. C. van Kooten
Dr. R. Dolhain (Department of Rheumatology, Erasmus University Medical Center)

Table of Contents

Chapter 1: Introduction

Modified from: *Mol Cell Proteomics* 2016, 15(7), 2217-28

Authors: Rosina Plomp[1], Albert Bondt[1,2], Noortje de Haan[1], Yoann Rombouts[1,3], Manfred Wuhrer[1]

[1]*Center for Proteomics and Metabolomics, Leiden University Medical Center, Leiden, The Netherlands;*
[2]*Department of Rheumatology, Leiden University Medical Center, Leiden, The Netherlands;*
[3]*present address: Institut de Pharmacologie et de Biologie Structurale, Université de Toulouse, CNRS, UPS, France;*

Table of Contents

1.1: General introduction

Carbohydrates, also known as sugars or saccharides, are commonly thought of solely as energy repositories, but they are also a vital part of many other cellular biomolecules. In plants and fungi, respectively cellulose and chitin give the cell wall its strength, and in nucleic acids the sugars deoxyribose and ribose form the backbone involved in storage of the genetic code. A lesser known function of carbohydrates is the alteration of proteins by attachment of an oligosaccharide, called a glycan. It is estimated that half of all mammalian proteins is glycosylated (1), and the purpose of these glycans is manifold: some alter the stability or half-life of proteins, others influence the interaction with ligands, and for many others the function is still unknown.

1.1.1: Glycan structure

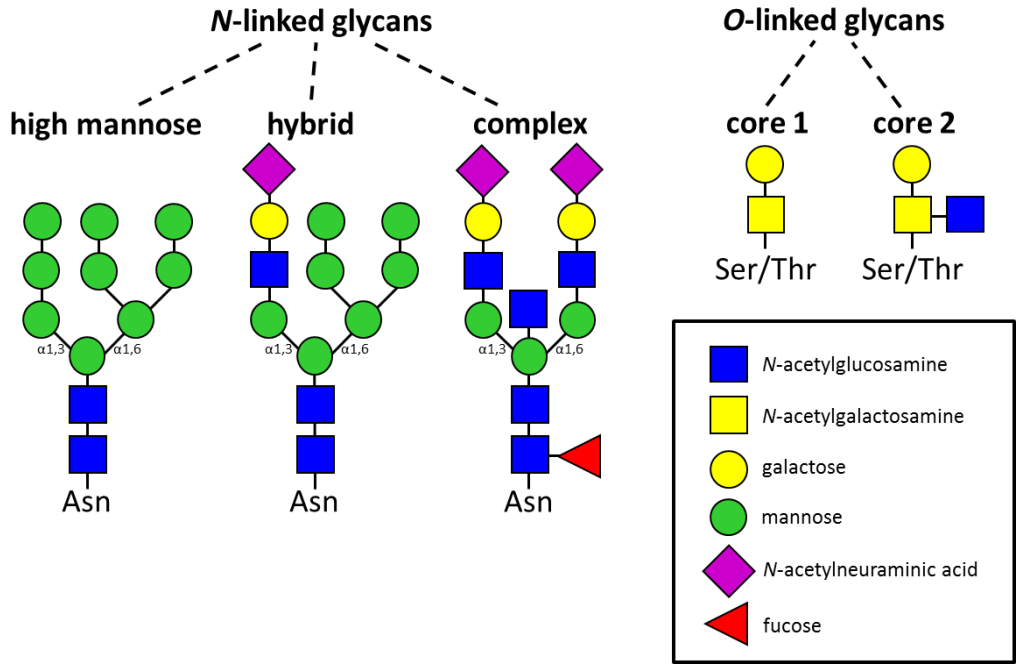

Figure 1.1: *N*-linked and *O*-linked glycosylation, and the most common types thereof. Monosaccharides are represented schematically.

Glycans consist of monosaccharides which are linked together by enzymes through glycosidic linkages. The number of monosaccharide building blocks in humans is limited: glycans can consist of hexoses (mannose, galactose, glucose and fucose), *N*-acetylhexosamines (*N*-acetylglucosamine and *N*-acetylgalactosamine), and sialic acid (*N*-acetylneuraminic acid). Additional types of monosaccharides can be found in other organisms, such as *N*-glycolylneuraminic acid in other mammals and xylose in plants.

Each glycosylation site is usually occupied by a range of glycan structures, called glycoforms. Glycans are an exceedingly heterogeneous class of polysaccharides. Most are oligosaccharides consisting of less than 20 monosaccharides, but some are large sprawling structures with the total mass of glycans exceeding that of their carrier protein (2). Glycans can be linear, but more often are branched. The reason for this vast diversity of glycan structures lies in their synthesis: this is not a template-driven process as with DNA or proteins, but rather the types of monosaccharides and glycosidic linkages are governed by the activity of glycosyltransferases and glycosidases which assemble and trim the glycan as the glycoprotein travels through various compartments within the cell. Even after secretion, glycans can still be altered by glycosyltransferases and glycosidases which are present in the extracellular matrix (3). Furthermore, the surrounding protein structure influences the structure of the glycan, by stereochemically restricting enzyme access to a site. Moreover, sorting sequences guide the path of proteins through cell compartments, thereby controlling their access to the glycosylation machinery. Hence, two glycosylation sites on the same protein can be occupied by very different glycan structures, exhibiting different functions. There are two main types of protein glycosylation: *N*- and *O*-glycosylation.

1.1.2: *N*-glycosylation

The presence of an *N*-glycosylation site in mammalian proteins is relatively easy to predict when the protein sequence is known: *N*-glycans are covalently attached to the nitrogen (N) of the amino acid asparagine (Asn) in the consensus sequence Asn-X-Ser/Thr, with X being any amino acid except for proline. However, even though the consensus sequence is necessary, this alone is not sufficient for *N*-glycosylation, and many potential *N*-glycosylation sites remain unoccupied. All *N*-glycans share a common core which consists of 5 monosaccharides: two *N*-acetylglucosamines (GlcNAcs) and three mannoses (Figure 1.1).

Synthesis is initiated with the assembly of an *N*-glycan precursor onto a lipid dolichol embedded in the membrane of the endoplasmic reticulum (ER). This precursor consists of an *N*-glycan core with 2 additional mannoses, facing the cytoplasm. The orientation of the phospholipid is then reversed by the enzyme flippase, so that the *N*-glycan precursor faces the lumen of the ER, followed by the addition of mannoses to a total of 9, as well as 3 glucose residues. The glycan is then covalently attached to the substrate asparagine, several monosaccharides are trimmed and the glycoprotein is transported to the Golgi system. Here, the *N*-glycan is subjected sequentially to various glycosidases and glycosyltransferases as it

moves through compartments of the Golgi. These glycosidases and glycosyltransferases are generally very specific and can remove or add only one type of monosaccharide with a specific linkage.

In the Golgi, first the glucose residues and outer mannoses are removed. Then, the sequential addition of GlcNAc, galactose and sialic acid leads to the formation of branches, called antennae; most *N*-glycans are diantennary, but tri- and tetra-antennary *N*-glycans are also frequently observed. In addition, a fucose can be added either to the protein-bound GlcNAc (core fucosylation) or in some cases to an antennary GlcNAc (antennary fucosylation). Furthermore, a GlcNAc can be added to the innermost mannose with a β1-4 linkage (bisecting GlcNAc). This concise summary of *N*-glycan diversity applies to humans as well as some other mammals, whilst other vertebrates have a slightly different set of glycosylation-related enzymes.

N-glycans can be subdivided into three types: high mannose (also known as mannosidic), hybrid and complex. High mannose *N*-glycans consist of only the core structure with up to six additional mannoses; these glycans underwent only the first part of the *N*-glycan synthesis pathway. In contrast, complex *N*-glycans have been fully processed in the Golgi and contain at least two antennary GlcNAc residues. Hybrid *N*-glycans fall in between: they have one complex arm bearing a GlcNAc, often elongated with galactose and sialic acid, and one mannosidic arm.

1.1.3: *O*-glycosylation

Compared to *N*-glycans, *O*-glycans are less predictable both in structure as well as in their site of attachment. *O*-glycans are usually attached to the oxygen in either a serine (Ser) or a threonine (Thr), but tyrosine (Tyr) or modified hydroxyl-amino acids may also serve as attachment site. A range of different types of *O*-glycan classes exist which are distinguished on the basis of the nature of the first sugar which is attached to the protein (4). In the following, mucin-type *O*-glycosylation will be considered, which is the most common form of protein *O*-glycosylation in humans.

For mucin-type *O*-glycosylation, a GalNAc is first added to the protein in the Golgi, then various types of monosaccharides are added sequentially. The two most common core structures can be seen in Figure 1.1, but a variety of different structures have been found. *O*-glycans usually have a more linear structure than *N*-glycans, and they can vary greatly in size: many consist of only a few monosaccharides while others can consist of as many as a

hundred, often organised into tandem repeats. There is no clear consensus sequence for *O*-glycosylation, which is in part due to the fact that humans express 20 different GalNAc transferases initiating the first step of protein *O*-glycosylation. However, mucin-type *O*-glycosylation often occurs in protein regions rich in proline (preferentially at +3 or -1 relative to the *O*-glycosylation site) and alanine residues.

1.1.4: Functions of glycosylation

Much like their structures, the functions of glycans are highly diverse as well (5). Firstly, addition of a glycan can alter the folding or basic thermodynamic properties of a protein. In some cases, a protein cannot be produced in its non-glycosylated form, because incorrect folding leads to degradation or otherwise prevents secretion. Glycosylation can also influence the interaction with other proteins, such as receptors. In some cases, interaction with another protein occurs exclusively through the glycan, as is the case for lectins, which recognize specific glycan motifs.

In addition, glycosylation plays a role in the management of protein quality. The chaperone proteins calnexin and calreticulin exist to ensure correct folding of proteins, and incorrectly labelled proteins are tagged by the addition of glucose on their *N*-glycan structures, preventing them from leaving the ER and sending them back to be re-folded (4, 6). Furthermore, asialo receptors capture extracellular non-sialylated glycoproteins and target them for degradation. It is speculated that this pathway clears proteins which have been in the circulation for some time and are thus prone to loss of sialic acids, thereby introducing a kind of expiration date on proteins (4).

Finally, some glycans appear to fulfil a purely structural role. Mucins contain extensively *O*-glycosylated regions which retain water and form a mucous layer, while a separate kind of *O*-glycans, proteoglycans, provide a firm padding in structures like cartilage (7). It should be noted that glycosylation, while it is essential for the functioning of higher organisms, is not necessary for the survival of many single-cell organisms. This is reflected by the fact that bacteria do not produce *N*-glycoproteins and that archaea, which lack a Golgi system, produce only simple precursor-like *N*-glycans. The glycosylation machinery fulfills an important task by managing inter-cell interaction and signalling, and it has evolved to become more complex in multicellular organisms. Lower eukaryotes such as yeast produce solely high mannose *N*-glycans with extensive branching of mannoses. Furthermore, pathogen

evasion is thought to have provided additional evolutionary pressure in favour of heterogeneity of glycan structures.

1.1.5: Glycosylation of immunoglobulins

The importance of immunoglobulins (Igs) in the immune system is well-known: they can function independently to impede pathogens, as well as mount an organized defence reaction by activating the adaptive immune system. They are produced by B-cells and are either secreted or presented on the plasma membrane. Igs are constructed of two heavy chains and two light chains, held together by disulphide bridges. Igs are usually referred to by the name of the heavy chain, of which there are five isotypes: IgG, IgA, IgM, IgD and IgE. The light chains occur in two varieties: lambda and kappa. Each heavy chain is composed of a variable domain (V_H) and 3 or 4 constant domains (C_H), while a light chain consists of two domains (V_L and C_L). Igs can also be structurally subdivided by function: the antigen-binding Fab portion, which encompasses the variable and the C_H1 domain and binds to the antigen, and the fragment crystallizable (Fc) portion, which encompasses C_H2-3/4 and binds to Fc receptors and complement to activate the immune system. Within the five antibody isotypes there are still variations in the protein sequences, and based on this IgG and IgA are further categorized into respectively 4 and 2 subclasses. Based on genetic differences between individuals, these can be further subdivided into allotypes. IgG, IgE and IgD exist only as monomers, while IgA and IgM can also be present as secretory protein complexes in dimeric and pentameric form, respectively, bonded together by a J-chain and secretory component (8).

All human antibodies carry one or multiple glycosylation structures, many of which have been shown to influence their properties and function. A single well-characterized complex *N*-glycan is located in the Fc region of IgG, and this glycan has been shown to influence receptor binding (9). In their constant domain, IgA1 and IgA2 carry 2 and 5 *N*-glycans, respectively. IgM carries 5 *N*-glycans, while IgD carries three (9). IgE is the most heavily glycosylated with six *N*-glycans in the conserved protein sequence (10). In addition, IgA1 and IgD exhibit multiple *O*-glycosylation sites in their hinge region (9). The J-chain and secretory component found in multimeric antibody complexes are also glycosylated. Furthermore, the variable domain of both the heavy and light chain, which varies for each antigen-specific type of Ig due to somatic hypermutation, can sometimes contain glycosylation sites (11).

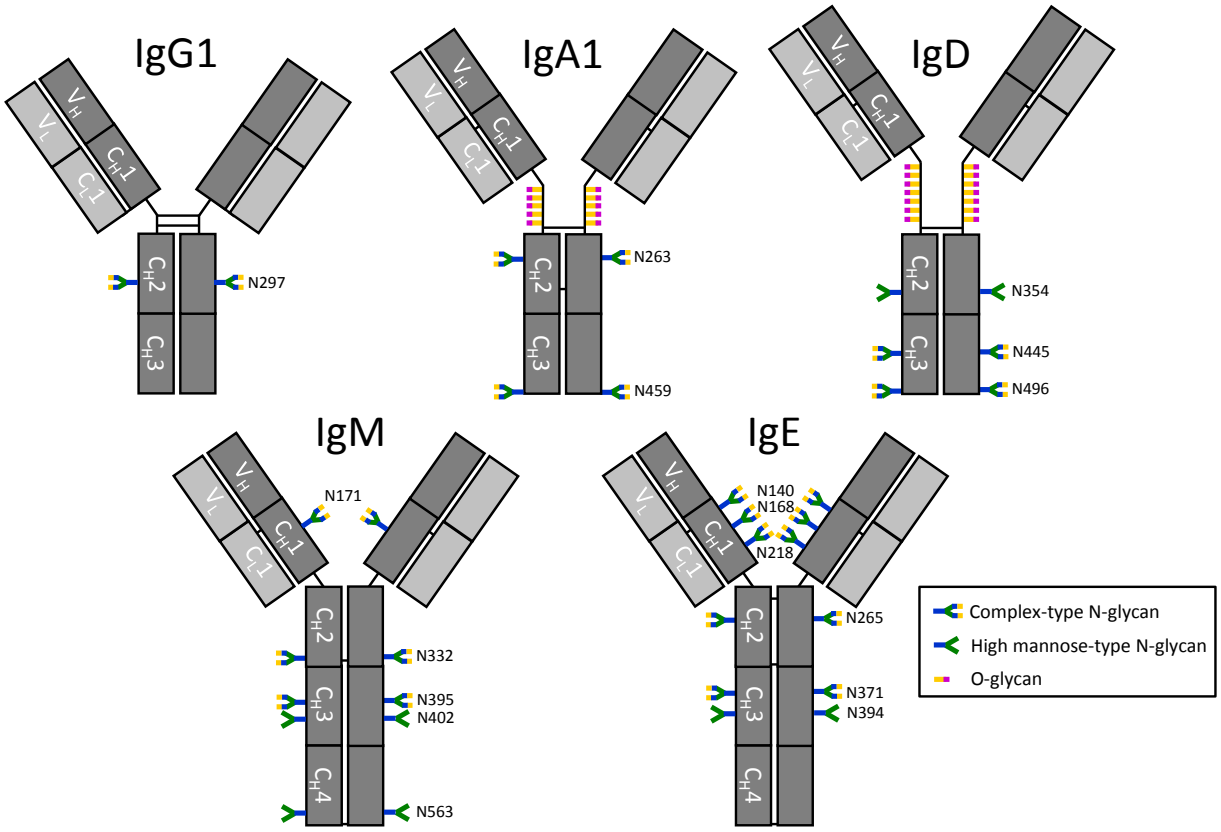

Figure 1.2: The main immunoglobulin isotypes with their reported *N*- and *O*-glycosylation sites. Heavy chain domains, conserved (C) and variable (V), are shown in dark grey, while the light chains are shown in light grey.

1.2: Recent advances in clinical glycoproteomics of immunoglobulins (Igs)

1.2.1: Introduction

Glycosylation of immunoglobulins (Igs) plays a key role in the regulation of immune reactions: glycans located at various sites modulate a diversity of immunoglobulin properties including protein conformation and stability, serum half-life, as well as binding affinities to antigens, receptors and glycan-binding proteins (GBP) (12-14).

The five classes of human antibodies – IgG, IgA, IgM, IgE and IgD – each contain one to six sites for *N*-linked glycosylation within the conserved sequence of each heavy chain (9). IgA1, IgD and IgG3 also carry *O*-linked glycans on their hinge-region (9, 15). In addition, immunoglobulins can be glycosylated in the variable domain of the Fab (antigen-binding fragment) (16-18). Importantly, glycosylation adds a formidable degree of complexity to protein species, since a range of glycan structures is usually present at each glycosylation site.

Studies on the functional consequences of immunoglobulin glycosylation, especially for IgG, have shown that glycans linked to the Fc (fragment crystallizable) part of the antibody influence the interaction with Fc receptors and GBPs, thereby regulating the pro- or anti-inflammatory immune response (12, 19-22). For example, lack of a fucose on the IgG Fc glycan can enact a 100-fold increase in antibody-dependent cellular cytotoxicity (ADCC) (23, 24). Fc-linked glycans may also influence the endocytosis, transcytosis and half-life of some classes of immunoglobulin, such as IgA (25, 26). Next to Fc-linked glycosylation, glycans attached to the Fab region also influence Ig properties and inflammation, especially by modulating antigen recognition and antibody aggregation, as well as through the binding to GBP (11, 17). Importantly, antibody glycosylation has been shown to reflect the physiological and pathological condition of an organism (27-29).

Because of the impact on the immunological response and thus the efficacy of therapeutic antibody treatment, it is crucial to monitor and in some cases alter the glycosylation profile in order to optimize antibody effector functions (19, 23). Glycosylation of antibodies can vary widely depending on the expression system and cell culture conditions during production (23). Because non-human glycan structures can trigger immunogenic responses, therapeutic antibodies are currently produced exclusively in mammalian cell cultures. Due to improvements in glyco-engineering, it is expected that non-mammalian expression systems will soon be applicable as well (23, 30). Robust and high-throughput methods are needed to

monitor the glycosylation of therapeutic antibodies. Additionally, glycosylation analysis should be site-specific since the function of a glycan can depend on its location, as illustrated by the different influence of glycans located at the Fc and at the Fab part of IgG (11, 22).

Glycosylation profiling of antibodies is usually done using one of the following approaches: 1) by releasing glycans from the protein, which is easily done for *N*-glycans by digestion with PNGase F, while *O*-glycans can be released chemically through hydrazinolysis or beta-elimination; 2) by using a proteolytic enzyme to digest the glycoprotein, resulting in glycopeptides; or 3) by analyzing the intact glycoprotein or portions thereof (e.g. Ig heavy and light chains) (31-33). Recent years have seen major methodological advances in all three approaches as detailed in this review. In addition, selected examples are given of antibody glycosylation studies in both biotechnological and biomedical research.

In the field of immunoglobulin (glyco)proteomics, several nomenclatures for the glycosylation sites are used (Table 1.1). The one most commonly used refers to the Asn positions as determined in the old days based on Edman sequencing of both variable and heavy chains (e.g. (9)). Alternatively, the homology-based nomenclature by the international ImMunoGeneTics information system (IMGT) is available for immunoglobulins, which has the advantage of a more intuitive comparison between the different immunoglobulins (e.g. site homology between CH2 84.4 on IgG and IgD, as well as similarity with CH3 84.4 on IgE and IgM). (34). In this review we will use the UniProt based site annotation, since this is more easily integrated with proteomic databases (35).

Analysis of the antibodies themselves is complicated by the variable domain which dictates the specificity of the antigen-binding site. Protein sequencing of monoclonal antibodies or affinity-purified antibodies is done using high resolution liquid chromatography tandem mass spectrometry methods, coupled to DNA sequence information generated by next-generation sequencing of the B-cell antibody repertoire (36, 37). Post-translational modifications, such as glycosylation, further complicate antibody analysis and require specific analysis strategies, as will be detailed in this review.

Table 1.1: Several different immunoglobulin protein sequence nomenclatures are used in literature. The nomenclature most frequently used in literature is based on archaic sequencing data of both immunoglobulin variable and constant domains, whereas the UniProt numbering is based on the conserved sequences, and the IMGT nomenclature is based on homology between the immunoglobulins.

Ig	conventional literature[1]	UniProt[2]	IMGT[3]
IgG1	297	180	CH2-84.4
IgG2	297	176	CH2-84.4
IgG3	297	227	CH2-84.4
IgG3	392	322	CH3-79
IgG4	297	177	CH2-84.4
IgA1	263	144	CH2-20
IgA1	459	340	CHS-7
IgA2	166	47	CH1-45.2
IgA2	211	92	CH1-114
IgA2	263	131	CH2-20
IgA2	337	205	CH2-120
IgA2	459	327	CHS-7
IgM	171	46	CH1-45
IgM	332	209	CH2-120
IgM	395	272	CH3-81
IgM	402	279	CH3-84.4
IgM	563	439	CHS-7
IgE	140/145[4]	21	CH1-15.2
IgE	168/173[4]	49	CH1-45.2
IgE	218/219[4]	99	CH1-118
IgE	265	146	CH2-38
IgE	371	252	CH3-38
IgE	394	275	CH3-84.4
IgD	354	225	CH2-84.4
IgD	445	316	CH3-45.4
IgD	496	367	CH3-116

[1] As used in e.g. (9)

[2] (35)

[3] (34)

[4] alternative nomenclature used in (38)

1.2.2: IgG

1.2.2.1: Fc glycosylation at Asn180/176/227/177 ('Asn297')

The majority of IgG glycosylation analysis has been focused on the Fc glycan because of both the known influence of this glycan on IgG effector functions and the established high-throughput methods which are available to selectively monitor this glycosylation site (22, 32, 33). In human IgG, the conserved *N*-glycosylation site is located at Asn180 (IgG1; UniProt P01857), Asn176 (IgG2; P01859), Asn227 (IgG3; P01860) or Asn177 (IgG4; P01861), alternatively referred to as position CH2-84.4 (34) or Asn297 (e.g. in (9); Table 1.1). In all IgG subclasses, the Fc-glycosylation site has been shown to harbor complex type diantennary *N*-glycans which carry between zero and two galactoses, with the majority carrying a core fucose, and a minority having a bisecting *N*-acetylglucosamine (GlcNAc) and one or two sialic acids (39). The glycan at this site has been shown to influence the inflammatory capacity of IgG through modulation of the binding to Fc-gamma receptors (FcγRs) and C-type lectins: in general, the absence of a core fucose and/or absence of galactoses and sialic acids appear to convey pro-inflammatory properties, while the presence of terminal sialic acids triggers an anti-inflammatory response (12, 22, 40).

Changes in Fc glycosylation, i.e. a decrease in galactosylation and sialylation which contributes to a more inflammatory antibody profile, have been observed in various autoimmune disorders, most recently inflammatory bowel disease (IBD), systemic lupus erythematosus (SLE), multiple sclerosis (MS) and chronic inflammatory demyelinating polyneuropathy (CIDP) (41-44). In addition to autoimmune disorders, IgG glycosylation changes can also occur in infectious diseases, as was shown by recent studies on HIV infection, chronic hepatitis B and the parasitic disease visceral leishmaniasis (45-47). Furthermore, new reports reaffirm the potential role for IgG glycosylation as a biomarker for cancer progression (48, 49). Finally, congenital defects in glycosylation or carbohydrate metabolism also alter IgG glycosylation, as shown recently for Man1B1 deficiency and galactosemia (50, 51).

1.2.2.1.1: Analysis of released glycans

The gold standard for studying IgG glycosylation relies on enzymatic *N*-glycan release, subsequent fluorescent labeling by reductive amination and analysis of the labeled glycans by high-performance liquid chromatography (HPLC) using hydrophilic interaction liquid chromatography (HILIC) with fluorescence detection (52). First, this approach has been

further developed by implementing HILIC stationary phases for ultra-performance liquid chromatography (UPLC) instrumentation, thereby improving both throughput and resolution (53). Second, sample preparation has been simplified through the use of 96-well filter plates to increase the throughput of glycan purification (54), as well as by introducing fluorescent tags to label the glycosylamine species released by PNGase F, instead of targeting the aldehyde species that arise from acid-catalyzed hydrolysis of the glycosylamine (55). Of note, the increased throughput capacity allowed for analyses of large sample sets, which could for example show the potential of the IgG *N*-glycans as a marker of chronological and biological age (56). Third, sample preparation has been robotized, resulting in a highly automated, higher-throughput workflow and leading to more robust results (55). However, this method has a disadvantage: because the glycans are released from the IgG, it is impossible to distinguish between Fab and Fc glycans as well as between glycans originating from different IgG subclasses.

Next to HILIC UPLC of fluorescently labeled glycans, various methods for repetitive IgG glycosylation analysis ("profiling") have reached maturity as evidenced by the high consistency of the results obtained in extensive method comparison studies (31-33). Remarkably, various mass spectrometric methods showed very good performance with respect to resolution, sensitivity and robustness, which opened the way to their broad application in both biotechnological (32, 33) and biomedical applications (31).

1.2.2.1.2: Analysis of glycopeptides

A bottom-up proteomics approach, with trypsin digestion followed by liquid chromatography (LC) coupled to mass spectrometric analysis, is most commonly applied for site-specific analysis of IgG Fc glycosylation (32). Tryptic digestion results in distinct glycopeptides that allow discrimination of the different IgG subclasses – with the peptide moieties EEQYNSTYR for IgG1, EEQFNSTFR for IgG2 and EEQFNSTYR for IgG4. The peptide sequence of the IgG3 glycopeptide shows allotype variation in the amino acid at the position *N*-terminal of the Asn227, causing a mass that is identical to either the IgG2 peptide (EEQFNSTFR; predominant allotype in Caucasian populations) or the IgG4 sequence (EEQYNSTFR; predominant allotype in Asian and African populations) (57). While trypsin digestion forms the gold standard for Fc IgG glycopeptide analysis, we have recently found that incomplete denaturation and digestion of IgG might lead to biases in glycoprofiling (58).

To prevent ion suppression of the glycopeptides by unglycosylated peptides during mass spectrometric analysis, a glycopeptide separation or enrichment step is often applied. This separation is usually performed using either reverse phase LC with C18 or graphitized carbon as a stationary phase, or by HILIC (13). While a variety of stationary phases exist for HILIC, amide is most frequently used, although polysaccharide-based stationary phases may show similar performance. Notably, the affinity of current HILIC materials is often dependent on glycan structure, which can lead to a bias in enrichment (13). The lack of a gold standard method has led to the development of various new HILIC materials for glycopeptide enrichment of tryptic IgG (glyco)peptides, with stationary phases consisting of various polysaccharides (chitosan, dextran, cyclodextrin, maltose) coupled to magnetic particles, silica particles or metallo-organic frameworks (59-62), or functionalized amide polymers embedded in a monolith capillary (63). Furthermore, electrostatic repulsion HILIC (also known as ERLIC) has been successfully employed to enrich IgG glycopeptides, although a thorough analysis of the potential skewing of IgG glycoforms in ERLIC enrichment is still lacking (64). Zwitterionic (ZIC) HILIC has also gained popularity: this technique makes use of highly hydrophilic materials carrying both positive and negative charges and shows a very good performance in glycopeptide enrichment (65). Novel ZIC HILIC materials, consisting of zwitterionic polymers coupled to silica particles or magnetic nanoparticles, have been developed and feature high sensitivity in post-enrichment MALDI-MS measurements (66-68).

Multiple reaction monitoring (MRM) is well-suited for high-throughput quantitative analysis of complex samples and has only recently been applied to glycopeptide Ig analysis (69-71). Hong *et al.* developed a method which simultaneously performs glycoprofiling of IgG and absolute quantitation of IgG and its separate subclasses, which can help determine if a relative change in glycosylation is due to changes in post-translational modification or changes in the level of protein production (71). For the quantification of glycopeptides, MRM was set to specifically detect oxonium ions, fragment ions that originate during the fragmentation of glycopeptides. Similar methods are being developed for IgA and IgM (69). A comparable protocol describing MRM detection of IgG glycoforms was separately developed by Yuan *et al.*, with the added feature of a prior separation of IgG3 so that glycosylation could be observed separately for each of the four IgG subclasses (72).

Capillary electrophoresis (CE) coupled to MS has likewise been applied for tryptic IgG analysis and shows a vastly increased sensitivity compared to the LC-MS approach (73). The sensitivity gain may be largely ascribed to the very low flow rates achieved in CE-MS.

Compared to LC-ESI-MS or CE-MS, MALDI-MS offers higher sample throughput as well as lower data complexity. However, detection of glycopeptides is complicated by the loss of sialic acids through in-source decay. Of note, this can be prevented by neutralizing the charge on the sialic acid by (dimethyl-)amidation (39, 74) or ethyl esterification (75). The derivatization methods target carboxyl groups on the peptide moiety as well as on the glycan, which can provide useful structural information from a combination of positive- and negative-ion MS/MS analyses (74). An additional advantage of these methods is the introduced mass difference between α2,3- and α2,6-linked sialic acids, caused by the sialic acid linkage-specificity of the reactions. While the ethyl esterification method is highly specific for sialic acid linkages on the level of released glycans (76), the modification of the peptide moiety of glycopeptides was found to be not completely specific, resulting in unwanted byproducts. This issue has been addressed and overcome by a recently published method using dimethylamidation, which provides sialic acid linkage information on a stably modified glycopeptide (Figure 1.3) (39). Currently, the dimethylamidation of sialylated glycopeptides is optimized for IgG Fc-glycopeptides and would need further optimization when used for different glycoproteins, such as other immunoglobulins. MALDI-TOF-MS/MS of sialylated glycopeptides, using laser induced fragmentation, highly benefits from the derivatization, as the loss of the sialic acid is no longer the dominant fragment. In addition to analysis with MALDI-TOF-MS(/MS), the derivatization method has been shown to be applicable for the analysis of IgG Fc-glycopeptides, using LC-MS(/MS), enabling differentiation between differently linked sialic acids, without having a major influence on the fragmentation of the analytes (data not published). Pyrene derivatization is an alternative method for glycopeptide analysis by MALDI-MS and also allows discrimination between α2,3- and α2,6-linked sialic acids, although its application on immunoglobulins has not been established (77, 78).

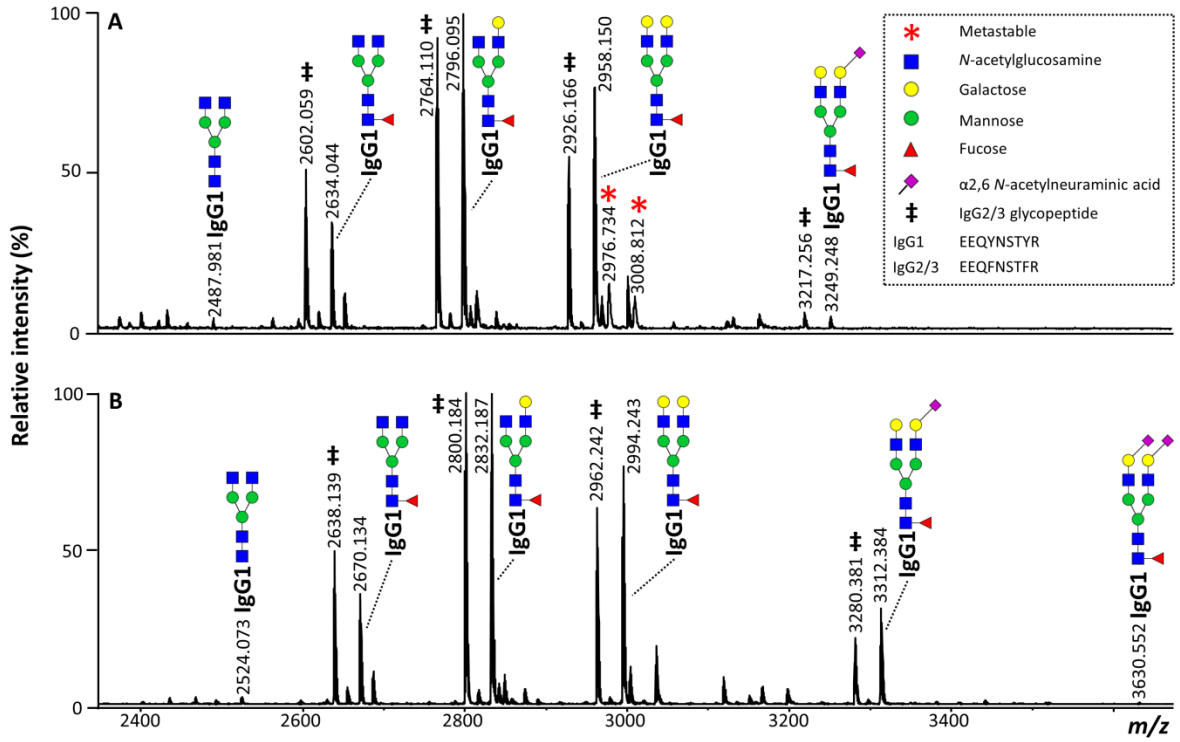

Figure 1.3: MALDI-TOF-MS spectra of human plasma IgG Fc-glycopeptides (A) without derivatization, and (B) after dimethylamidation. Derivatization results in the stabilization of the sialylated glycopeptides, improving their detection and preventing the formation of metastable signals. With the use of dimethylamidation, no unspecific side reactivity on the peptides was observed and the linkage of the sialic acids could be determined (39).

Furthermore, stable isotope labeling of glycopeptides has recently been achieved: succinic anhydride was used to introduce a mass increment of 8 Da to tryptic IgG1 glycopeptides (79). This method can be used to perform absolute quantification of IgG glycopeptides, or can be used to reduce bias during sample analysis by parallel analysis of two samples. Isobaric labeling using tandem mass tags (TMTs), which lead to different masses upon fragmentation, has also been used for the analysis of pepsin-generated IgG glycopeptides (80).

1.2.2.1.3: Analysis of intact glycoprotein or glycoprotein fragments

Alternatively, a middle-down or middle-up proteomics approach can be applied for assessing IgG Fc glycosylation. The Fc portion can be cleaved from the Fab portion in whole IgG, or from fused proteins in Fc-fusion proteins, by limited proteolytic digestion with the protease IdeS (FabRICATOR®), followed by either mass spectrometric analysis of the protein fragment or purification of the Fc portion and release of the glycans using PNGase F (16, 81-83). The latter method has recently been applied to a clinical sample set, as is discussed later in this review (16).

Finally, technical advances in the recent years have allowed for top-down mass spectrometric analysis of monoclonal antibodies, allowing the integrated analysis of post-translational modifications (32, 83-86). An extensive review has been recently published by Zhang *et al.*, describing several applications of these techniques, and a comparison between 'normal' and native MS, furthermore including ion mobility (87). More recently, ultra-high resolution machinery (e.g. Fourier transform ion cyclotron resonance (FTICR)) allowed for the detection of intact monoclonal antibodies with isotopic resolution, showing several glycoforms (85). Additional top-down MS/MS information was obtained in conjunction with online electrochemical reduction of the antibody (85). Furthermore, isobaric labeling has been applied to intact antibody-drug conjugates (80). Native MS is often applied to analyze intact mAbs (86). The advantage of this approach is the limitation of charge states because of the native 3D protein configuration, causing increased signal-to-noise for the few charge states that do occur. The downside of native MS is a lack of information regarding the glycosylation site(s) or the precise structure of the glycan(s) (86, 87).

1.2.2.2: Fab glycosylation

The structural features of IgG Fab glycosylation and its emerging importance in immunity have been recently reviewed (11). It has been estimated that approximately 15-25% of serum IgG of healthy individuals contain *N*-glycosylation sites and carry *N*-glycans (Fab-glycosylation) in their variable domains, in addition to the almost fully occupied IgG Fc *N*-glycosylation site (88, 89). Of note, the percentage of Fab-glycosylation and glycan structures varies during certain pathological and physiological conditions, as shown in RA, lymphoma and pregnancy (16, 17, 90, 91). Since only a few germline-encoded sequences contain an *N*-glycosylation site, the sites present in the variable domains of immunoglobulins are mainly introduced by somatic hypermutation during the process of affinity maturation (18, 92). Within an affinity-purified population of antigen-specific IgG, identification of Fab glycosylation sites has been achieved by labeling the sites with ^{18}O during deglycosylation with PNGase F. This was followed by mass spectrometry-assisted proteomics analysis which revealed the mass shift denoting the site of glycosylation and the peptide sequence surrounding the site (17). The human immune system comprises of an enormous antibody repertoire, recognizing an estimated billion or more different antigens. Antibody specificity is determined by a unique amino acid sequence in the Fab portion, thus making the analysis of Fab *N*-glycopeptides derived from polyclonal antibodies very difficult, if feasible at all.

Therefore, in order to analyze polyclonal IgG Fab glycosylation, the currently used analytical methods consist of the release of *N*-glycans from purified Fab fragments followed by their analysis using capillary electrophoresis with laser-induced fluorescence detection (CE-LIF), (ultra)high performance liquid chromatography and/or mass spectrometry (16, 17, 93). In order to improve the throughput of IgG Fab glycosylation analysis, we recently set up a new sample preparation method. The method relies on IgG affinity capturing in a 96-well filter plate, on-bead proteolytic release of the Fab portions, and collection of Fab (flow-through) and Fc portions (eluate) followed by enzymatic glycan release. Detailed glycan information was obtained by MALDI-TOF-MS after sialic acid stabilization. The method was applied to study the differences between Fab and Fc glycosylation in young women, and the pregnancy associated changes thereof (16). The levels of galactosylation, sialylation and bisection were significantly higher on the Fab portion compared to the Fc. During pregnancy Fab and Fc glycans showed similar patterns in their changes. Interestingly, the Fab portion was also shown to carry minor amounts of α2,3-linked sialic acids. In general, the *N*-glycans on the Fab are more extended, and some species seem to be Fab-specific. Diantennary fucosylated glycans with two sialic acids are hardly present on the Fc, while they are the major species on Fab. Similarly, the presence of a bisecting GlcNAc on glycans with two galactoses appears to be more prominent in Fab versus Fc (16). Of note, these data result from the analysis of solely young women, while characterization of Fab glycosylation in males as well as different age groups is still lacking.

High-sensitivity analysis of released Fab glycans can also be performed by CGE-LIF (93). However, the glycosylation data obtained via these techniques, especially regarding both the levels of *N*-glycan bisection in IgG Fab portions and various glycosylation features of murine IgG, has shown some discrepancies as compared to results obtained with other analytical methods (16, 94, 95). Additional studies are needed to further unravel Fab glycosylation changes with age, sex and diseases.

1.2.2.3: Additional *N*- and *O*-glycosylation of IgG3

In addition to the well-known Fc *N*-glycosylation site, several allotypes of IgG3 possess a second *N*-linked site in the CH3 domain at Asn322 (UniProt P01860; alternatively referred to as CH3-79 (34) or Asn392; Table 1.1) (96). Only 10% of Asn322 was found to be occupied; the *N*-glycans found at this site were mainly complex type diantennary structures, which differ from those at Asn227 in that the majority is afucosylated and contains a bisecting

GlcNAc, and a minority of high mannose type *N*-glycans is also present (96). Since trypsin digestion produces a very large glycopeptide containing this site, the glycan structures may alternatively be examined after digestion with aspecific proteases. Aspecific proteases such as pronase are particularly useful for the study of glycoproteins since they tend to produce small glycopeptides which are well suited for mass spectrometric analysis (97, 98). Sequential chromatography of resulting digests on a C18 reversed phase (RP) column and a porous graphitized carbon column provides the broad retention range necessary to observe all glycopeptides regardless of the heterogeneous retention properties of both the glycan and the peptide moiety. Using collision-induced dissociation with a combination of lower- and enhanced-energy, which produced both glycan and peptide fragmentation, respectively, identification of both the glycan and the peptide moiety in one run could be achieved (96).

Next to *N*-glycosylation, IgG3 may carry up to 3 *O*-glycosylation sites per heavy chain within a triple repeat in the hinge region (15). Proteolytic digestion with trypsin, proteinase K or pronase followed by LC-MS/MS analysis revealed that approximately 10% of each of these sites is occupied, mainly by sialylated core 1 type *O*-glycan structures (15, 96). As both the Fc *N*-glycosylation at Asn322 and the *O*-glycans of IgG3 have been described only recently, their function and clinical relevance remain to be investigated.

1.2.2.4: Antigen-specific IgG

The glycoprofiling of antigen-specific antibodies in clinical samples after vaccination or during disease started less than a decade ago. This was made possible by the numerous improvements in sensitivity and throughput of methods for both antibody purification and glycosylation analysis. Antigen-specific antibodies are generally purified by affinity chromatography using antigens coated on 96-well plates or on chromatography beads/columns. Antigens are usually synthetic peptides or recombinant (glyco)proteins. For instance, the high-throughput purification of anti-citrullinated peptide/protein antibodies (ACPA), i.e. autoantibodies specific for rheumatoid arthritis (RA), has been achieved by repeated capturing on 96-well plates coated with a synthetic circular peptide containing citrulline, called CCP2 (cyclic citrullinated peptide 2) (28, 99, 100). Likewise, antibodies directed against multiple HIV and influenza antigens (e.g. HIV gp41 and gp120 or influenza hemagglutinin) have been enriched using amino-link antigen resin or antigen-functionalized streptavidin resins packed into cartridges (46, 101, 102). Alternatively, antigen-specific antibodies can be captured by using viral particles, microorganisms or cells. Thus, Vidarsson

and coworkers have isolated anti-platelet antibodies (causing neonatal alloimmune thrombocytopenia) and anti-red blood cell antibodies (responsible for haemolytic disease of the fetus and newborn) by incubating serum of pregnant women directly on platelets and red blood cells (103-105). Fc- and/or Fab-linked glycosylation of antigen-specific IgG has been analyzed either at the glycopeptide level mainly using LC-MS, or by releasing glycans using a middle-down/middle-up proteomics approach as described above. Of note, unlike glycopeptide detection, analysis of released glycans from antigen-specific IgG requires another purification step prior to or after antigen-specific capturing in order to separate IgG from other serum glycoproteins or other immunoglobulins (101).

Antigen-specific IgG displays different sialylation, galactosylation, fucosylation and/or bisection patterns compared to total IgG isolated from the same individuals. Importantly, these structural differences are clearly associated with clinical and functional consequences including disease outcome, disease severity and/or antiviral control responses. For instance, as compared to total IgG, anti-platelet IgGs found in the serum of pregnant women exhibit an exceptionally low level of fucosylation in their Fc-glycans, which enhances the binding affinity for the FcγRIIIa/b and the phagocytosis of platelets, and correlates with increased severity of neonatal alloimmune thrombocytopenia (105). Likewise, HIV-specific IgG antibodies isolated from HIV-positive subjects present a higher frequency of afucosylated, agalactosylated, and asialylated *N*-glycans compared to total IgG. Importantly, this glycan difference, especially the greater percentage of agalactosylated glycoforms, is far more pronounced in HIV elite controllers than in (un)treated chronic progressors and is associated with an enhanced capacity to bind to FcγRIIIa, probably explaining the more potent antibody-dependent cellular viral inhibition activity that characterizes antibody from elite controllers (46). A disruption in the balance between type I (part of the Ig receptor superfamily which includes FcγRI, II and III) and type II (C-type lectin receptors) Fc receptor signaling also very likely occurs in several autoimmune diseases such as rheumatoid arthritis and granulomatosis with polyangiitis (GPA), in which changes in autoantibody-specific glycosylation have been observed. Thus, the Fc-galactosylation, sialylation, and bisection of anti-proteinase 3 (PR3) antibodies IgG1 are reduced compared to total IgG1 in GPA patients (106). Despite an early study reporting a negative correlation between the level of anti-PR3 specific IgG sialylation and disease activity as measured by the Birmingham Vasculitis Activity Score (BVAS), recent evidence demonstrated that the BVAS is strongly associated with the presence of bisecting GlcNAc on anti-PR3 IgG but not with

galactosylation/sialylation percentages (106, 107). Interestingly, the level of anti-PR3 IgG galactosylation was associated with pro-inflammatory cytokine concentrations and time to remission (106). Similarly, in RA patients, ACPA-IgG autoantibodies exhibit a decrease in Fc galactosylation and sialylation levels that occurs a few months before disease presentation, correlates with disease severity, and potentially determines osteoclast differentiation and bone loss during RA (28, 99, 108). Variations in antigen-specific IgG glycosylation have also been observed following vaccination and, more importantly, can predict the efficacy of vaccination (102, 109). Ravetch and coworkers recently showed that the sialylated Fc glycan abundance on anti-hemagglutinin IgG produced by day 7 following influenza virus vaccination predicts the quality of the vaccine response (102). It was proposed that immune complexes formed with Fc-sialylated IgG signal through the type II FcR CD23 on activated B cells and triggers the expression of FcγRIIb, thereby driving the selection of higher affinity B cells and the generation of higher affinity and more protective anti-HA IgG (102).

1.2.3: IgA

There are two subclasses of immunoglobulin A (i.e. IgA1 and IgA2), and two known allotypes for the IgA2 subclass (i.e. A2m(1) and A2m(2)). IgA1 contains a slightly elongated hinge region compared to IgA2. This elongated hinge contains 9 potential *O*-glycosylation sites, of which up to six have been reported to be occupied (110). In addition, IgA1 harbors two *N*-glycosylation sites at Asn144 and Asn340 (UniProt P01876; alternatively referred to as CH2-20 and CHS-7, respectively (34), or Asn263 and Asn459 (e.g. in (9)); Table 1.1), whereas IgA2 harbors four sites at Asn47, Asn131, Asn205, and Asn327 (UniProt P01877; also referred to as CH1-45.2, CH2-20, CH2-120, CHS-7 (34), or Asn166, Asn263, Asn337, and Asn459 (e.g. in (9)); Table 1.1). In the A2m(2) allotype of IgA2 an additional consensus sequence is present due to the replacement of a proline by a serine, thus forming a glycosylation site at Asn92 (CH1-114 / Asn211; Table 1.1). The analysis of (s)IgA glycosylation is generally performed at the level of released glycans (111) or by lectin ELISA, although a few glycopeptide-based LC-MS/MS methods have been described (110, 112-115).

For the analysis of tryptic *O*-glycopeptides, the use of FTICR-MS/MS coupled online to an RP-LC system has been described (110). Electron transfer dissociation, which preferentially fragments the peptide backbone and not the glycan, was used to determine the location of

each glycosylation site. By applying a few additional separation steps using less advanced laboratory techniques, others have achieved similar results by MALDI-TOF/TOF-MS (116).

The IgA *N*-glycosylation is less frequently studied, although it may have important functional consequences as demonstrated by the influence of *N*-glycan sialylation on the transportation of secretory IgA across an *in vitro* model of follicle-associated epithelium via binding to Dectin-1 and Siglec-5 (26).

Nowadays, the use of IgA instead of IgG monoclonal antibodies for biopharmaceutical purposes is being explored, with a focus on anti-HIV drugs (117-119). Therefore, several site-specific glycosylation analysis methods have recently been developed. An LC-ESI-MS/MS method primarily developed for the analysis of HIV gp140 has been adapted and applied to secretory IgA1 produced in plants as well as to human IgA (119, 120). In brief, IgA was digested by sequential application of trypsin and GluC after reduction and alkylation. Next, glycopeptide analysis was performed by first identifying the elution position of deglycosylated peptide moieties. Glycopeptides are known to elute a short time ahead of the deglycosylated variant, with some spread due to the various glycans attached. The addition of a buffered formic acid solution to the flow ascertained very close or even identical elution times for glycosylated peptides bearing sialylated structures. A targeted search for the peptide plus potential glycan *m/z* using selected ion chromatograms completed the analysis. Several high mannose type structures were identified using the applied technique. The analysis did not reveal any hinge region *O*-glycosylation, which could be attributed to the production in plants.

The *N*-glycans of IgA are nevertheless still mainly studied at the level of released glycans. For example, the comparison of released glycans from different IgA constructs obtained from various cell lines showed profound differences, especially regarding the level of sialylation, which correlated with the half-life of these antibodies (121).

Of note, the secreted form of IgA consists of a dimer, which forms a complex with the (also glycosylated) joining (J)-chain and the secretory component. The J-chain harbors a single glycosylation site at Asn71 (UniProt P01591; also referred to as Asn48), which appears to be important for IgA dimerization (122). This site bears mainly highly sialylated diantennary *N*-glycans (111, 114). The secretory component is also highly glycosylated, with seven *N*-glycosylation sites at Asn83, Asn90, Asn135, Asn186, Asn421, Asn469 and Asn499 (UniProt P01833; also referred to as Asn65, Asn72, Asn117, Asn168, Asn403, Asn451, and

Asn481, e.g. in (123); Table 1.1). The protein contains a wide variety of glycan species: di-, tri- and tetraantennary glycans, bearing all Lewis epitopes (111, 114). It was suggested that these glycans are meant to bind to lectins of bacteria (111).

1.2.4: IgM

Human serum IgM mainly circulates as a pentamer of 950 kDa consisting of ten light chains, ten heavy chains and one joining chain (J-chain). Each IgM monomer contains five conserved *N*-glycosylation sites at Asn46, Asn209, Asn272, Asn279 and Asn439 (UniProt P01871; also known as CH1-45, CH2-120, CH3-81, CH3-84.4, CHS-7 (34), or Asn171, Asn332, Asn395, Asn402, and Asn563; Table 1.1) located within the constant region of the heavy chain. In addition, the previously mentioned J-chain contains one *N*-glycosylation site at Asn71 (UniProt P01591). In two recent studies, a site-specific *N*-glycosylation mapping of human serum IgM was achieved by analyzing IgM glycopeptides, generated by trypsin or trypsin/GluC digestion, using either the classical LC-ESI-MS method or a nano-LC-microarray-MALDI-MS platform (124, 125). The latter consists of a nano-LC reverse phase separation of IgM (glyco)peptides, including the J-chain glycopeptide, followed by high frequency droplet-based fractionation of the nano-LC outflow on microarray chips. Each spot on the microarray is then analyzed by MALDI-MS, with or without pre-digestion with PNGase F to remove *N*-glycans. Both studies demonstrated that glycans linked to Asn279 and Asn439 are predominantly oligomannose structures, whereas glycans attached to Asn46, Asn209 and Asn272 mainly consist of complex-type structures (124, 125). The glycosylation site Asn71 of the J-chain also exhibits complex-type *N*-glycans. The main complex-type *N*-glycans found in IgM heavy chains are diantennary species carrying one or two sialic acids, bisecting GlcNAc and/or a core fucose. Minor proportions of oligomannosidic and hybrid-type glycans were also detected on Asn46 (124). Likewise, Asn279 carries 10% of hybrid-type structures, which are also present in very low amount on Asn209. Based on computer modeling of the IgM structure, the clear distinction between glycosylation sites carrying oligomannose structures (on Asn279 and Asn439) or complex-type *N*-glycans (on Asn46, Asn209, Asn272) has been proposed to be the consequence of the low accessibility of glycans on Asn279 and Asn439 for the glycosyltransferase/glycosidases within the Golgi (125). Finally, although the functional aspect of IgM glycosylation on immunity has not been examined yet, the recent possibility of producing human-like glycoengineered heteromultimeric IgM in plants may help to provide new insights in this field (125).

1.2.5: IgE

With six oligosaccharides on each heavy chain at Asn21, Asn49, Asn99, Asn146, Asn252 and Asn275 (10) (UniProt P01854; also referred to as CH1-15.2, CH1-45.2, CH1-118, CH2-38, CH3-38 and CH3-84.4 (34), or Asn140, Asn168, Asn218, Asn265, Asn371 and Asn394 e.g. in (9); Table 1.1), IgE is the most heavily glycosylated of the immunoglobulins. Characterization of the glycan structures on polyclonal IgE was achieved with a combination of proteolytic enzymes and LC-MS/MS analysis (10). Glycosylation sites Asn21, Asn49, Asn99, Asn146 and Asn252 are occupied by complex type *N*-glycans, which are primarily fully galactosylated diantennary structures, containing a core fucose and one or two sialic acids (10, 126). A high mannose type glycan is present at Asn275, the sixth site, which is homologous to the Fc glycosylation site in IgG. Glycosylation at this site has recently been shown to be essential for the binding of IgE to the high affinity receptor FcεRI and initiation of anaphylaxis (127). Individuals with PGM3-related hyper IgE syndrome or with a hyperimmune condition displayed similar IgE glycosylation compared to healthy individuals (10, 126). Glycosylation analysis of IgE is challenging due to the low concentration in biological fluids: at approximately 130-300 ng/mL, the concentration in human serum is roughly 50 000 times lower than that of IgG (128, 129). Due to this limitation, no large-scale glycosylation analysis of IgE in clinical cohorts has been performed as of yet. However, recent advances in LC- and CE-MS sensitivity and robustness may allow for some attempts in the near future.

1.2.6: Conclusions and perspectives

Thanks to the improvement of sample preparation methods and analytical technologies, recent years have seen an increase in sensitivity, accuracy and robustness of IgG glycosylation analysis. These methodological and technological advances are beneficial for biopharmaceutical companies, allowing a better characterization of antibody-based biopharmaceuticals, biosimilars and bio-betters, but are also crucial tools in both basic and clinical research. Thus, this enables, among others, the characterization of glycosylation of antigen-specific IgG, including autoantibodies, alloantibodies and some anti-pathogen antibodies, which directly impact the immune response and the outcome, progression and/or severity of diseases (28, 46, 99, 101-105, 109). Therefore, methodologies and technologies dedicated to IgG glycosylation analysis have great prospects regarding the early detection and diagnostic of some diseases. Of note, most studies on IgG glycosylation have focused on serum/plasma antibodies, while IgG in other biofluids and tissue remain largely unstudied.

In addition to IgG, the substantial recent advances in purifying and analyzing small amounts of samples have helped to analyze the glycosylation of other immunoglobulin subclasses (i.e. IgA, IgM and IgE) in a more precise and comprehensive manner. Today's technological level allows for the simultaneous analysis of multiple immunoglobulin classes in one run (70).

We expect that in the near future, several hiatuses in immunoglobulin-related glycomics will be covered. Not only by thorough analysis of the glycosylation of all immunoglobulin classes, but additionally by complementary glycoproteomics analysis of many interacting proteins, such as cell surface derived Fc receptors. This may reveal a regulatory role of both antibody and receptor glycomic variation and the interaction thereof in the regulation of antibody effector functions (24).

1.3: Scope of thesis

The aim of the studies presented in this thesis is to contribute to the knowledge within the field of immunoglobulin glycosylation. The glycosylation of IgG, specifically the *N*-glycan located in the Fc portion, has been extensively studied, but its function as well as its regulation still in part eludes us. Glycosylation of the other antibody isotypes has attracted much less attention from researchers. This can be attributed both to the lower abundance of the other Ig isotypes, which can make analysis challenging, and to the fact that the pharmaceutical industry focusses on IgG for monoclonal antibody therapeutics.

IgE is the antibody which is responsible for allergic reactions: it can trigger the strongest reaction of all of the immunoglobulins, and conversely is found at the lowest concentration in blood. IgE is also the most abundantly glycosylated, with roughly 12% of its mass consisting of saccharides (38). In **chapter 2**, we provide a detailed profile of the *N*-glycan structures present at each of the six *N*-glycosylation sites, in a polyclonal sample from pooled plasma of healthy donors. A seventh site was found to be unoccupied. Since the publication of this paper, compelling evidence has arisen that the *N*-glycan at Asn394 (Asn275 using the Uniprot nomenclature) can influence receptor binding, analogous to the IgG Fc glycan (127).

While research in the past few decades has largely mapped the glycosylation sites on antibodies and is now moving on to functional and clinical studies, structural analysis can still turn up new findings. **Chapter 3** describes a hitherto unreported *O*-glycan found in the hinge region of IgG3. Because only 10% of each of the two to three *O*-glycosylation sites on IgG3 are occupied, this glycan has evaded discovery until recently.

Chapter 4 describes the application of the same analysis method to a cohort of patients with ANCA-associated vasculitis, an autoimmune disease with an established pathogenic role of autoantibodies (130). Various glycosylation features were found to be associated with a relapse of disease symptoms. This study reinforces the potential of IgG glycosylation as a biomarker to reflect disease severity.

In **chapter 5**, the glycosylation of Fc IgG is examined in a large population cohort of healthy individuals using liquid chromatography mass spectrometry (LC-MS). A clear association was observed between specific glycosylation features and the inflammation-associated proteins C-reactive protein and interleukin-6.

Finally, concluding notes and points of further discussion are presented in **chapter 6**.

References

1. Apweiler, R., Hermjakob, H., and Sharon, N. (1999) On the frequency of protein glycosylation, as deduced from analysis of the SWISS-PROT database. *Biochim Biophys Acta* 1473, 4-8
2. Chandran, P. L., and Horkay, F. (2012) Aggrecan, an unusual polyelectrolyte: review of solution behavior and physiological implications. *Acta Biomater* 8, 3-12
3. Jones, M. B., Oswald, D. M., Joshi, S., Whiteheart, S. W., Orlando, R., and Cobb, B. A. (2016) B-cell-independent sialylation of IgG. *Proc Natl Acad Sci U S A* 113, 7207-7212
4. Varki, A., Cummings, R. D., Esko, J. D., Stanley, P., Hart, G., Aebi, M., Darvill, A., Kinoshita, T., Packer, N. H., Prestegard, J. J., Schnaar, R. L., and Seeberger, P. H. (2015) *Essentials of Glycobiology*, 3rd Edition Ed., Cold Spring Harbor Laboratory Press, Cold Spring Harbor (NY)
5. Varki, A. (1993) Biological roles of oligosaccharides: all of the theories are correct. *Glycobiology* 3, 97-130
6. Roth, J., and Zuber, C. (2016) Quality control of glycoprotein folding and ERAD: the role of N-glycan handling, EDEM1 and OS-9. *Histochem Cell Biol*, R110.003251
7. Vertel, B. M. (1995) The ins and outs of aggrecan. *Trends Cell Biol* 5, 458-464
8. Schroeder, H. W., Jr., and Cavacini, L. (2010) Structure and function of immunoglobulins. *J Allergy Clin Immunol* 125, S41-52
9. Arnold, J. N., Wormald, M. R., Sim, R. B., Rudd, P. M., and Dwek, R. A. (2007) The impact of glycosylation on the biological function and structure of human immunoglobulins. *Annu Rev Immunol* 25, 21-50
10. Plomp, R., Hensbergen, P. J., Rombouts, Y., Zauner, G., Dragan, I., Koeleman, C. A., Deelder, A. M., and Wuhrer, M. (2014) Site-specific N-glycosylation analysis of human immunoglobulin e. *J Proteome Res* 13, 536-546
11. van de Bovenkamp, F. S., Hafkenscheid, L., Rispens, T., and Rombouts, Y. (2016) The Emerging Importance of IgG Fab Glycosylation in Immunity. *J Immunol* 196, 1435-1441
12. Karsten, C. M., Pandey, M. K., Figge, J., Kilchenstein, R., Taylor, P. R., Rosas, M., McDonald, J. U., Orr, S. J., Berger, M., Petzold, D., Blanchard, V., Winkler, A., Hess, C., Reid, D. M., Majoul, I. V., Strait, R. T., Harris, N. L., Kohl, G., Wex, E., Ludwig, R., Zillikens, D., Nimmerjahn, F., Finkelman, F. D., Brown, G. D., Ehlers, M., and Kohl, J. (2012) Anti-inflammatory activity of IgG1 mediated by Fc galactosylation and association of FcgammaRIIB and dectin-1. *Nat Med* 18, 1401-1406
13. Zauner, G., Selman, M. H., Bondt, A., Rombouts, Y., Blank, D., Deelder, A. M., and Wuhrer, M. (2013) Glycoproteomic analysis of antibodies. *Mol Cell Proteomics* 12, 856-865
14. Schwab, I., Lux, A., and Nimmerjahn, F. (2015) Pathways Responsible for Human Autoantibody and Therapeutic Intravenous IgG Activity in Humanized Mice. *Cell Rep* 13, 610-620
15. Plomp, R., Dekkers, G., Rombouts, Y., Visser, R., Koeleman, C. A., Kammeijer, G. S., Jansen, B. C., Rispens, T., Hensbergen, P. J., Vidarsson, G., and Wuhrer, M. (2015) Hinge-Region O-Glycosylation of Human Immunoglobulin G3 (IgG3). *Mol Cell Proteomics* 14, 1373-1384
16. Bondt, A., Rombouts, Y., Selman, M. H., Hensbergen, P. J., Reiding, K. R., Hazes, J. M., Dolhain, R. J., and Wuhrer, M. (2014) Immunoglobulin G (IgG) Fab glycosylation analysis using a new mass spectrometric high-throughput profiling method reveals pregnancy-associated changes. *Mol Cell Proteomics* 13, 3029-3039
17. Rombouts, Y., Willemze, A., van Beers, J. J., Shi, J., Kerkman, P. F., van Toorn, L., Janssen, G. M., Zaldumbide, A., Hoeben, R. C., Pruijn, G. J., Deelder, A. M., Wolbink, G., Rispens, T., van Veelen, P. A., Huizinga, T. W., Wuhrer, M., Trouw, L. A., Scherer, H. U., and Toes, R. E. (2015) Extensive glycosylation of ACPA-IgG variable domains modulates binding to citrullinated antigens in rheumatoid arthritis. *Ann Rheum Dis* 75, 578-585
18. Dunn-Walters, D., Boursier, L., and Spencer, J. (2000) Effect of somatic hypermutation on potential N-glycosylation sites in human immunoglobulin heavy chain variable regions. *Mol Immunol* 37, 107-113

19. Thomann, M., Schlothauer, T., Dashivets, T., Malik, S., Avenal, C., Bulau, P., Ruger, P., and Reusch, D. (2015) In vitro glycoengineering of IgG1 and its effect on Fc receptor binding and ADCC activity. *PLoS One* 10, e0134949
20. Anthony, R. M., Nimmerjahn, F., Ashline, D. J., Reinhold, V. N., Paulson, J. C., and Ravetch, J. V. (2008) Recapitulation of IVIG anti-inflammatory activity with a recombinant IgG Fc. *Science* 320, 373-376
21. DiLillo, D. J., and Ravetch, J. V. (2015) Fc-Receptor Interactions Regulate Both Cytotoxic and Immunomodulatory Therapeutic Antibody Effector Functions. *Cancer Immunol Res* 3, 704-713
22. Anthony, R. M., and Nimmerjahn, F. (2011) The role of differential IgG glycosylation in the interaction of antibodies with FcgammaRs in vivo. *Curr Opin Organ Transplant* 16, 7-14
23. Costa, A. R., Rodrigues, M. E., Henriques, M., Oliveira, R., and Azeredo, J. (2014) Glycosylation: impact, control and improvement during therapeutic protein production. *Crit Rev Biotechnol* 34, 281-299
24. Ferrara, C., Grau, S., Jager, C., Sondermann, P., Brunker, P., Waldhauer, I., Hennig, M., Ruf, A., Rufer, A. C., Stihle, M., Umana, P., and Benz, J. (2011) Unique carbohydrate-carbohydrate interactions are required for high affinity binding between FcgammaRIII and antibodies lacking core fucose. *Proc Natl Acad Sci U S A* 108, 12669-12674
25. Basset, C., Durand, V., Jamin, C., Clement, J., Pennec, Y., Youinou, P., Dueymes, M., and Roitt, I. M. (2000) Increased N-linked glycosylation leading to oversialylation of monomeric immunoglobulin A1 from patients with Sjogren's syndrome. *Scand J Immunol* 51, 300-306
26. Rochereau, N., Drocourt, D., Perouzel, E., Pavot, V., Redelinghuys, P., Brown, G. D., Tiraby, G., Roblin, X., Verrier, B., Genin, C., Corthesy, B., and Paul, S. (2013) Dectin-1 is essential for reverse transcytosis of glycosylated SIgA-antigen complexes by intestinal M cells. *PLoS Biol* 11, e1001658
27. Maverakis, E., Kim, K., Shimoda, M., Gershwin, M. E., Patel, F., Wilken, R., Raychaudhuri, S., Ruhaak, L. R., and Lebrilla, C. B. (2015) Glycans in the immune system and The Altered Glycan Theory of Autoimmunity: a critical review. *J Autoimmun* 57, 1-13
28. Rombouts, Y., Ewing, E., van de Stadt, L. A., Selman, M. H., Trouw, L. A., Deelder, A. M., Huizinga, T. W., Wuhrer, M., van Schaardenburg, D., Toes, R. E., and Scherer, H. U. (2015) Anti-citrullinated protein antibodies acquire a pro-inflammatory Fc glycosylation phenotype prior to the onset of rheumatoid arthritis. *Ann Rheum Dis* 74, 234-241
29. Bondt, A., Selman, M. H., Deelder, A. M., Hazes, J. M., Willemsen, S. P., Wuhrer, M., and Dolhain, R. J. (2013) Association between galactosylation of immunoglobulin G and improvement of rheumatoid arthritis during pregnancy is independent of sialylation. *J Proteome Res* 12, 4522-4531
30. Frenzel, A., Hust, M., and Schirrmann, T. (2013) Expression of recombinant antibodies. *Front Immunol* 4, 217
31. Huffman, J. E., Pucic-Bakovic, M., Klaric, L., Hennig, R., Selman, M. H., Vuckovic, F., Novokmet, M., Kristic, J., Borowiak, M., Muth, T., Polasek, O., Razdorov, G., Gornik, O., Plomp, R., Theodoratou, E., Wright, A. F., Rudan, I., Hayward, C., Campbell, H., Deelder, A. M., Reichl, U., Aulchenko, Y. S., Rapp, E., Wuhrer, M., and Lauc, G. (2014) Comparative performance of four methods for high-throughput glycosylation analysis of immunoglobulin G in genetic and epidemiological research. *Mol Cell Proteomics* 13, 1598-1610
32. Reusch, D., Haberger, M., Falck, D., Peter, B., Maier, B., Gassner, J., Hook, M., Wagner, K., Bonnington, L., Bulau, P., and Wuhrer, M. (2015) Comparison of methods for the analysis of therapeutic immunoglobulin G Fc-glycosylation profiles-Part 2: Mass spectrometric methods. *MAbs* 7, 732-742
33. Reusch, D., Haberger, M., Maier, B., Maier, M., Kloseck, R., Zimmermann, B., Hook, M., Szabo, Z., Tep, S., Wegstein, J., Alt, N., Bulau, P., and Wuhrer, M. (2015) Comparison of methods for the analysis of therapeutic immunoglobulin G Fc-glycosylation profiles--part 1: separation-based methods. *MAbs* 7, 167-179

34. IMGT® (2001) Protein display: Human IGH C-REGIONs. [last updated 20/12/2012; accessed 01/2016] http://www.imgt.org/IMGTrepertoire/Proteins/protein/human/IGH/IGHC/Hu_IGHCallgenes.html
35. (2015) UniProt: a hub for protein information. *Nucleic Acids Res* 43, D204-212
36. Lavinder, J. J., Horton, A. P., Georgiou, G., and Ippolito, G. C. (2015) Next-generation sequencing and protein mass spectrometry for the comprehensive analysis of human cellular and serum antibody repertoires. *Curr Opin Chem Biol* 24, 112-120
37. Cheung, W. C., Beausoleil, S. A., Zhang, X., Sato, S., Schieferl, S. M., Wieler, J. S., Beaudet, J. G., Ramenani, R. K., Popova, L., Comb, M. J., Rush, J., and Polakiewicz, R. D. (2012) A proteomics approach for the identification and cloning of monoclonal antibodies from serum. *Nat Biotechnol* 30, 447-452
38. Dorrington, K. J., and Bennich, H. H. (1978) Structure-function relationships in human immunoglobulin E. *Immunol Rev* 41, 3-25
39. de Haan, N., Reiding, K. R., Haberger, M., Reusch, D., Falck, D., and Wuhrer, M. (2015) Linkage-specific sialic acid derivatization for MALDI-TOF-MS profiling of IgG glycopeptides. *Anal Chem* 87, 8284-8291
40. Lin, C. W., Tsai, M. H., Li, S. T., Tsai, T. I., Chu, K. C., Liu, Y. C., Lai, M. Y., Wu, C. Y., Tseng, Y. C., Shivatare, S. S., Wang, C. H., Chao, P., Wang, S. Y., Shih, H. W., Zeng, Y. F., You, T. H., Liao, J. Y., Tu, Y. C., Lin, Y. S., Chuang, H. Y., Chen, C. L., Tsai, C. S., Huang, C. C., Lin, N. H., Ma, C., Wu, C. Y., and Wong, C. H. (2015) A common glycan structure on immunoglobulin G for enhancement of effector functions. *Proc Natl Acad Sci U S A* 112, 10611-10616
41. Akmacic, I. T., Ventham, N. T., Theodoratou, E., Vuckovic, F., Kennedy, N. A., Kristic, J., Nimmo, E. R., Kalla, R., Drummond, H., Stambuk, J., Dunlop, M. G., Novokmet, M., Aulchenko, Y., Gornik, O., Campbell, H., Pucic Bakovic, M., Satsangi, J., and Lauc, G. (2015) Inflammatory bowel disease associates with proinflammatory potential of the immunoglobulin G glycome. *Inflamm Bowel Dis* 21, 1237-1247
42. Wuhrer, M., Selman, M. H., McDonnell, L. A., Kumpfel, T., Derfuss, T., Khademi, M., Olsson, T., Hohlfeld, R., Meinl, E., and Krumbholz, M. (2015) Pro-inflammatory pattern of IgG1 Fc glycosylation in multiple sclerosis cerebrospinal fluid. *J Neuroinflammation* 12, 235
43. Vuckovic, F., Kristic, J., Gudelj, I., Teruel, M., Keser, T., Pezer, M., Pucic-Bakovic, M., Stambuk, J., Trbojevic-Akmacic, I., Barrios, C., Pavic, T., Menni, C., Wang, Y., Zhou, Y., Cui, L., Song, H., Zeng, Q., Guo, X., Pons-Estel, B. A., McKeigue, P., Leslie Patrick, A., Gornik, O., Spector, T. D., Harjacek, M., Alarcon-Riquelme, M., Molokhia, M., Wang, W., and Lauc, G. (2015) Association of systemic lupus erythematosus with decreased immunosuppressive potential of the IgG glycome. *Arthritis Rheumatol* 67, 2978-2989
44. Wong, A. H., Fukami, Y., Sudo, M., Kokubun, N., Hamada, S., and Yuki, N. (2015) Sialylated IgG-Fc: a novel biomarker of chronic inflammatory demyelinating polyneuropathy. *J Neurol Neurosurg Psychiatry* 87, 275-279
45. Gardinassi, L. G., Dotz, V., Hipgrave Ederveen, A., de Almeida, R. P., Nery Costa, C. H., Costa, D. L., de Jesus, A. R., Mayboroda, O. A., Garcia, G. R., Wuhrer, M., and de Miranda Santos, I. K. (2014) Clinical severity of visceral leishmaniasis is associated with changes in immunoglobulin g fc N-glycosylation. *MBio* 5, e01844
46. Ackerman, M. E., Crispin, M., Yu, X., Baruah, K., Boesch, A. W., Harvey, D. J., Dugast, A. S., Heizen, E. L., Ercan, A., Choi, I., Streeck, H., Nigrovic, P. A., Bailey-Kellogg, C., Scanlan, C., and Alter, G. (2013) Natural variation in Fc glycosylation of HIV-specific antibodies impacts antiviral activity. *J Clin Invest* 123, 2183-2192
47. Ho, C. H., Chien, R. N., Cheng, P. N., Liu, J. H., Liu, C. K., Su, C. S., Wu, I. C., Li, I. C., Tsai, H. W., Wu, S. L., Liu, W. C., Chen, S. H., and Chang, T. T. (2015) Aberrant serum immunoglobulin G glycosylation in chronic hepatitis B is associated with histological liver damage and reversible by antiviral therapy. *J Infect Dis* 211, 115-124

48. Chen, G., Wang, Y., Qin, X., Li, H., Guo, Y., Wang, Y., Liu, H., Wang, X., Song, G., Li, F., Li, F., Guo, S., Qiu, L., and Li, Z. (2013) Change in IgG1 Fc N-linked glycosylation in human lung cancer: age- and sex-related diagnostic potential. *Electrophoresis* 34, 2407-2416
49. Kawaguchi-Sakita, N., Kaneshiro-Nakagawa, K., Kawashima, M., Sugimoto, M., Tokiwa, M., Suzuki, E., Kajihara, S., Fujita, Y., Iwamoto, S., Tanaka, K., and Toi, M. (2015) Serum immunoglobulin G Fc region N-glycosylation profiling by matrix-assisted laser desorption/ionization mass spectrometry can distinguish breast cancer patients from cancer-free controls. *Biochem Biophys Res Commun* 469, 1140-1145
50. Saldova, R., Stockmann, H., O'Flaherty, R., Lefeber, D. J., Jaeken, J., and Rudd, P. M. (2015) N-Glycosylation of Serum IgG and Total Glycoproteins in MAN1B1 Deficiency. *J Proteome Res* 14, 4402-4412
51. Maratha, A., Stockmann, H., Coss, K. P., Estela Rubio-Gozalbo, M., Knerr, I., Fitzgibbon, M., McVeigh, T. P., Foley, P., Moss, C., Colhoun, H. O., van Erven, B., Stephens, K., Doran, P., Rudd, P., and Treacy, E. (2016) Classical galactosaemia: novel insights in IgG N-glycosylation and N-glycan biosynthesis. *Eur J Hum Genet*
52. Rudd, P. M., Guile, G. R., Kuster, B., Harvey, D. J., Opdenakker, G., and Dwek, R. A. (1997) Oligosaccharide sequencing technology. *Nature* 388, 205-207
53. Ahn, J., Bones, J., Yu, Y. Q., Rudd, P. M., and Gilar, M. (2010) Separation of 2-aminobenzamide labeled glycans using hydrophilic interaction chromatography columns packed with 1.7 microm sorbent. *J Chromatogr B Analyt Technol Biomed Life Sci* 878, 403-408
54. Akmacic, I. T., Ugrina, I., Stambuk, J., Gudelj, I., Vuckovic, F., Lauc, G., and Pucic-Bakovic, M. (2015) High-Throughput Glycomics: Optimization of Sample Preparation. *Biochemistry (Mosc)* 80, 934-942
55. Stockmann, H., Duke, R. M., Millan Martin, S., and Rudd, P. M. (2015) Ultrahigh throughput, ultrafiltration-based n-glycomics platform for ultraperformance liquid chromatography (ULTRA(3)). *Anal Chem* 87, 8316-8322
56. Kristic, J., Vuckovic, F., Menni, C., Klaric, L., Keser, T., Beceheli, I., Pucic-Bakovic, M., Novokmet, M., Mangino, M., Thaqi, K., Rudan, P., Novokmet, N., Sarac, J., Missoni, S., Kolcic, I., Polasek, O., Rudan, I., Campbell, H., Hayward, C., Aulchenko, Y., Valdes, A., Wilson, J. F., Gornik, O., Primorac, D., Zoldos, V., Spector, T., and Lauc, G. (2014) Glycans are a novel biomarker of chronological and biological ages. *J Gerontol A Biol Sci Med Sci* 69, 779-789
57. Dard, P., Lefranc, M. P., Osipova, L., and Sanchez-Mazas, A. (2001) DNA sequence variability of IGHG3 alleles associated to the main G3m haplotypes in human populations. *Eur J Hum Genet* 9, 765-772
58. Falck, D., Jansen, B. C., Plomp, R., Reusch, D., Haberger, M., and Wuhrer, M. (2015) Glycoforms of Immunoglobulin G Based Biopharmaceuticals Are Differentially Cleaved by Trypsin Due to the Glycoform Influence on Higher-Order Structure. *J Proteome Res* 14, 4019-4028
59. Fang, C., Xiong, Z., Qin, H., Huang, G., Liu, J., Ye, M., Feng, S., and Zou, H. (2014) One-pot synthesis of magnetic colloidal nanocrystal clusters coated with chitosan for selective enrichment of glycopeptides. *Anal Chim Acta* 841, 99-105
60. Sheng, Q., Su, X., Li, X., Ke, Y., and Liang, X. (2014) A dextran-bonded stationary phase for saccharide separation. *J Chromatogr A* 1345, 57-67
61. Ji, Y., Xiong, Z., Huang, G., Liu, J., Zhang, Z., Liu, Z., Ou, J., Ye, M., and Zou, H. (2014) Efficient enrichment of glycopeptides using metal-organic frameworks by hydrophilic interaction chromatography. *Analyst* 139, 4987-4993
62. Li, S., Wang, L., Zhao, S., Lin, J., Zheng, J., and Lin, Z. (2015) Preparation of phenyl-functionalized magnetic mesoporous silica microspheres for the fast separation and selective enrichment of phenyl-containing peptides. *J Sep Sci* 38, 3954-3960
63. Jiang, H., Yuan, H., Qu, Y., Liang, Y., Jiang, B., Wu, Q., Deng, N., Liang, Z., Zhang, L., and Zhang, Y. (2016) Preparation of hydrophilic monolithic capillary column by in situ photo-

polymerization of N-vinyl-2-pyrrolidinone and acrylamide for highly selective and sensitive enrichment of N-linked glycopeptides. *Talanta* 146, 225-230
64. Cao, L., Yu, L., Guo, Z., Li, X., Xue, X., and Liang, X. (2013) Application of a strong anion exchange material in electrostatic repulsion-hydrophilic interaction chromatography for selective enrichment of glycopeptides. *J Chromatogr A* 1299, 18-24
65. Wohlgemuth, J., Karas, M., Eichhorn, T., Hendriks, R., and Andrecht, S. (2009) Quantitative site-specific analysis of protein glycosylation by LC-MS using different glycopeptide-enrichment strategies. *Anal Biochem* 395, 178-188
66. Shen, A., Guo, Z., Yu, L., Cao, L., and Liang, X. (2011) A novel zwitterionic HILIC stationary phase based on "thiol-ene" click chemistry between cysteine and vinyl silica. *Chem Commun (Camb)* 47, 4550-4552
67. Huang, G., Xiong, Z., Qin, H., Zhu, J., Sun, Z., Zhang, Y., Peng, X., ou, J., and Zou, H. (2014) Synthesis of zwitterionic polymer brushes hybrid silica nanoparticles via controlled polymerization for highly efficient enrichment of glycopeptides. *Anal Chim Acta* 809, 61-68
68. Chen, Y., Xiong, Z., Zhang, L., Zhao, J., Zhang, Q., Peng, L., Zhang, W., Ye, M., and Zou, H. (2015) Facile synthesis of zwitterionic polymer-coated core-shell magnetic nanoparticles for highly specific capture of N-linked glycopeptides. *Nanoscale* 7, 3100-3108
69. Ruhaak, L. R., and Lebrilla, C. B. (2015) Applications of Multiple Reaction Monitoring to Clinical Glycomics. *Chromatographia* 78, 335-342
70. Hong, Q., Ruhaak, L. R., Stroble, C., Parker, E., Huang, J., Maverakis, E., and Lebrilla, C. B. (2015) A Method for Comprehensive Glycosite-Mapping and Direct Quantitation of Serum Glycoproteins. *J Proteome Res* 14, 5179-5192
71. Hong, Q., Lebrilla, C. B., Miyamoto, S., and Ruhaak, L. R. (2013) Absolute quantitation of immunoglobulin G and its glycoforms using multiple reaction monitoring. *Anal Chem* 85, 8585-8593
72. Yuan, W., Sanda, M., Wu, J., Koomen, J., and Goldman, R. (2015) Quantitative analysis of immunoglobulin subclasses and subclass specific glycosylation by LC-MS-MRM in liver disease. *J Proteomics* 116, 24-33
73. Heemskerk, A. A., Wuhrer, M., Busnel, J. M., Koeleman, C. A., Selman, M. H., Vidarsson, G., Kapur, R., Schoenmaker, B., Derks, R. J., Deelder, A. M., and Mayboroda, O. A. (2013) Coupling porous sheathless interface MS with transient-ITP in neutral capillaries for improved sensitivity in glycopeptide analysis. *Electrophoresis* 34, 383-387
74. Nishikaze, T., Kawabata, S., and Tanaka, K. (2014) In-depth structural characterization of N-linked glycopeptides using complete derivatization for carboxyl groups followed by positive- and negative-ion tandem mass spectrometry. *Anal Chem* 86, 5360-5369
75. Gomes de Oliveira, A. G., Roy, R., Raymond, C., Bodnar, E. D., Tayi, V. S., Butler, M., Durocher, Y., and Perreault, H. (2015) A systematic study of glycopeptide esterification for the semi-quantitative determination of sialylation in antibodies. *Rapid Commun Mass Spectrom* 29, 1817-1826
76. Reiding, K. R., Blank, D., Kuijper, D. M., Deelder, A. M., and Wuhrer, M. (2014) High-throughput profiling of protein N-glycosylation by MALDI-TOF-MS employing linkage-specific sialic acid esterification. *Anal Chem* 86, 5784-5793
77. Amano, J., Nishikaze, T., Tougasaki, F., Jinmei, H., Sugimoto, I., Sugawara, S., Fujita, M., Osumi, K., and Mizuno, M. (2010) Derivatization with 1-pyrenyldiazomethane enhances ionization of glycopeptides but not peptides in matrix-assisted laser desorption/ionization mass spectrometry. *Anal Chem* 82, 8738-8743
78. Nishikaze, T., Nakamura, T., Jinmei, H., and Amano, J. (2011) Negative-ion MALDI-MS2 for discrimination of alpha2,3- and alpha2,6-sialylation on glycopeptides labeled with a pyrene derivative. *J Chromatogr B Analyt Technol Biomed Life Sci* 879, 1419-1428
79. Pabst, M., Benesova, I., Fagerer, S. R., Jacobsen, M., Eyer, K., Schmidt, G., Steinhoff, R., Krismer, J., Wahl, F., Preisler, J., and Zenobi, R. (2016) Differential Isotope Labeling of Glycopeptides for Accurate Determination of Differences in Site-Specific Glycosylation. *J Proteome Res* 15, 326-331

80. Gautier, V., Boumeester, A. J., Lossl, P., and Heck, A. J. (2015) Lysine conjugation properties in human IgGs studied by integrating high-resolution native mass spectrometry and bottom-up proteomics. *Proteomics* 15, 2756-2765
81. An, Y., Zhang, Y., Mueller, H. M., Shameem, M., and Chen, X. (2014) A new tool for monoclonal antibody analysis: application of IdeS proteolysis in IgG domain-specific characterization. *MAbs* 6, 879-893
82. Lynaugh, H., Li, H., and Gong, B. (2013) Rapid Fc glycosylation analysis of Fc fusions with IdeS and liquid chromatography mass spectrometry. *MAbs* 5, 641-645
83. Tran, B. Q., Barton, C., Feng, J., Sandjong, A., Yoon, S. H., Awasthi, S., Liang, T., Khan, M. M., Kilgour, D. P., Goodlett, D. R., and Goo, Y. A. (2015) Comprehensive glycosylation profiling of IgG and IgG-fusion proteins by top-down MS with multiple fragmentation techniques. *J Proteomics* 134, 93-101
84. Stoll, D. R., Harmes, D. C., Danforth, J., Wagner, E., Guillarme, D., Fekete, S., and Beck, A. (2015) Direct identification of rituximab main isoforms and subunit analysis by online selective comprehensive two-dimensional liquid chromatography-mass spectrometry. *Anal Chem* 87, 8307-8315
85. Nicolardi, S., Deelder, A. M., Palmblad, M., and van der Burgt, Y. E. (2014) Structural analysis of an intact monoclonal antibody by online electrochemical reduction of disulfide bonds and Fourier transform ion cyclotron resonance mass spectrometry. *Anal Chem* 86, 5376-5382
86. Rosati, S., Yang, Y., Barendregt, A., and Heck, A. J. (2014) Detailed mass analysis of structural heterogeneity in monoclonal antibodies using native mass spectrometry. *Nat Protoc* 9, 967-976
87. Zhang, H., Cui, W., and Gross, M. L. (2014) Mass spectrometry for the biophysical characterization of therapeutic monoclonal antibodies. *FEBS Lett* 588, 308-317
88. Holland, M., Yagi, H., Takahashi, N., Kato, K., Savage, C. O., Goodall, D. M., and Jefferis, R. (2006) Differential glycosylation of polyclonal IgG, IgG-Fc and IgG-Fab isolated from the sera of patients with ANCA-associated systemic vasculitis. *Biochim Biophys Acta* 1760, 669-677
89. Stadlmann, J., Pabst, M., and Altmann, F. (2010) Analytical and Functional Aspects of Antibody Sialylation. *J Clin Immunol* 30 Suppl 1, S15-19
90. Radcliffe, C. M., Arnold, J. N., Suter, D. M., Wormald, M. R., Harvey, D. J., Royle, L., Mimura, Y., Kimura, Y., Sim, R. B., Inoges, S., Rodriguez-Calvillo, M., Zabalegui, N., de Cerio, A. L., Potter, K. N., Mockridge, C. I., Dwek, R. A., Bendandi, M., Rudd, P. M., and Stevenson, F. K. (2007) Human follicular lymphoma cells contain oligomannose glycans in the antigen-binding site of the B-cell receptor. *J Biol Chem* 282, 7405-7415
91. Coelho, V., Krysov, S., Ghaemmaghami, A. M., Emara, M., Potter, K. N., Johnson, P., Packham, G., Martinez-Pomares, L., and Stevenson, F. K. (2010) Glycosylation of surface Ig creates a functional bridge between human follicular lymphoma and microenvironmental lectins. *Proc Natl Acad Sci U S A* 107, 18587-18592
92. Sabouri, Z., Schofield, P., Horikawa, K., Spierings, E., Kipling, D., Randall, K. L., Langley, D., Roome, B., Vazquez-Lombardi, R., Rouet, R., Hermes, J., Chan, T. D., Brink, R., Dunn-Walters, D. K., Christ, D., and Goodnow, C. C. (2014) Redemption of autoantibodies on anergic B cells by variable-region glycosylation and mutation away from self-reactivity. *Proc Natl Acad Sci U S A* 111, E2567-2575
93. Mahan, A. E., Tedesco, J., Dionne, K., Baruah, K., Cheng, H. D., De Jager, P. L., Barouch, D. H., Suscovich, T., Ackerman, M., Crispin, M., and Alter, G. (2015) A method for high-throughput, sensitive analysis of IgG Fc and Fab glycosylation by capillary electrophoresis. *J Immunol Methods* 417, 34-44
94. Blomme, B., Van Steenkiste, C., Grassi, P., Haslam, S. M., Dell, A., Callewaert, N., and Van Vlierberghe, H. (2011) Alterations of serum protein N-glycosylation in two mouse models of chronic liver disease are hepatocyte and not B cell driven. *Am J Physiol Gastrointest Liver Physiol* 300, G833-842

95. Raju, T. S., Briggs, J. B., Borge, S. M., and Jones, A. J. (2000) Species-specific variation in glycosylation of IgG: evidence for the species-specific sialylation and branch-specific galactosylation and importance for engineering recombinant glycoprotein therapeutics. *Glycobiology* 10, 477-486
96. Stavenhagen, K., Plomp, R., and Wuhrer, M. (2015) Site-Specific Protein N- and O-Glycosylation Analysis by a C18-Porous Graphitized Carbon-Liquid Chromatography-Electrospray Ionization Mass Spectrometry Approach Using Pronase Treated Glycopeptides. *Anal Chem* 87, 11691-11699
97. Nwosu, C. C., Huang, J., Aldredge, D. L., Strum, J. S., Hua, S., Seipert, R. R., and Lebrilla, C. B. (2013) In-gel nonspecific proteolysis for elucidating glycoproteins: a method for targeted protein-specific glycosylation analysis in complex protein mixtures. *Anal Chem* 85, 956-963
98. Dodds, E. D., Seipert, R. R., Clowers, B. H., German, J. B., and Lebrilla, C. B. (2009) Analytical performance of immobilized pronase for glycopeptide footprinting and implications for surpassing reductionist glycoproteomics. *J Proteome Res* 8, 502-512
99. Scherer, H. U., van der Woude, D., Ioan-Facsinay, A., el Bannoudi, H., Trouw, L. A., Wang, J., Haupl, T., Burmester, G. R., Deelder, A. M., Huizinga, T. W., Wuhrer, M., and Toes, R. E. (2010) Glycan profiling of anti-citrullinated protein antibodies isolated from human serum and synovial fluid. *Arthritis Rheum* 62, 1620-1629
100. Scherer, H. U., Wang, J., Toes, R. E., van der Woude, D., Koeleman, C. A., de Boer, A. R., Huizinga, T. W., Deelder, A. M., and Wuhrer, M. (2009) Immunoglobulin 1 (IgG1) Fc-glycosylation profiling of anti-citrullinated peptide antibodies from human serum. *Proteomics Clin Appl* 3, 106-115
101. Brown, E. P., Normandin, E., Osei-Owusu, N. Y., Mahan, A. E., Chan, Y. N., Lai, J. I., Vaccari, M., Rao, M., Franchini, G., Alter, G., and Ackerman, M. E. (2015) Microscale purification of antigen-specific antibodies. *J Immunol Methods* 425, 27-36
102. Wang, T. T., Maamary, J., Tan, G. S., Bournazos, S., Davis, C. W., Krammer, F., Schlesinger, S. J., Palese, P., Ahmed, R., and Ravetch, J. V. (2015) Anti-HA Glycoforms Drive B Cell Affinity Selection and Determine Influenza Vaccine Efficacy. *Cell* 162, 160-169
103. Kapur, R., Della Valle, L., Verhagen, O. J., Hipgrave Ederveen, A., Ligthart, P., de Haas, M., Kumpel, B., Wuhrer, M., van der Schoot, C. E., and Vidarsson, G. (2015) Prophylactic anti-D preparations display variable decreases in Fc-fucosylation of anti-D. *Transfusion* 55, 553-562
104. Kapur, R., Della Valle, L., Sonneveld, M., Hipgrave Ederveen, A., Visser, R., Ligthart, P., de Haas, M., Wuhrer, M., van der Schoot, C. E., and Vidarsson, G. (2014) Low anti-RhD IgG-Fc-fucosylation in pregnancy: a new variable predicting severity in haemolytic disease of the fetus and newborn. *Br J Haematol* 166, 936-945
105. Kapur, R., Kustiawan, I., Vestrheim, A., Koeleman, C. A., Visser, R., Einarsdottir, H. K., Porcelijn, L., Jackson, D., Kumpel, B., Deelder, A. M., Blank, D., Skogen, B., Killie, M. K., Michaelsen, T. E., de Haas, M., Rispens, T., van der Schoot, C. E., Wuhrer, M., and Vidarsson, G. (2014) A prominent lack of IgG1-Fc fucosylation of platelet alloantibodies in pregnancy. *Blood* 123, 471-480
106. Wuhrer, M., Stavenhagen, K., Koeleman, C. A., Selman, M. H., Harper, L., Jacobs, B. C., Savage, C. O., Jefferis, R., Deelder, A. M., and Morgan, M. (2015) Skewed Fc glycosylation profiles of anti-proteinase 3 immunoglobulin G1 autoantibodies from granulomatosis with polyangiitis patients show low levels of bisection, galactosylation, and sialylation. *J Proteome Res* 14, 1657-1665
107. Espy, C., Morelle, W., Kavian, N., Grange, P., Goulvestre, C., Viallon, V., Chereau, C., Pagnoux, C., Michalski, J. C., Guillevin, L., Weill, B., Batteux, F., and Guilpain, P. (2011) Sialylation levels of anti-proteinase 3 antibodies are associated with the activity of granulomatosis with polyangiitis (Wegener's). *Arthritis Rheum* 63, 2105-2115
108. Harre, U., Lang, S. C., Pfeifle, R., Rombouts, Y., Fruhbeisser, S., Amara, K., Bang, H., Lux, A., Koeleman, C. A., Baum, W., Dietel, K., Grohn, F., Malmstrom, V., Klareskog, L., Kronke, G., Kocijan, R., Nimmerjahn, F., Toes, R. E., Herrmann, M., Scherer, H. U., and Schett, G. (2015) Glycosylation of immunoglobulin G determines osteoclast differentiation and bone loss. *Nat Commun* 6, 6651

109. Selman, M. H., de Jong, S. E., Soonawala, D., Kroon, F. P., Adegnika, A. A., Deelder, A. M., Hokke, C. H., Yazdanbakhsh, M., and Wuhrer, M. (2012) Changes in antigen-specific IgG1 Fc N-glycosylation upon influenza and tetanus vaccination. *Mol Cell Proteomics* 11, M111.014563
110. Takahashi, K., Smith, A. D., Poulsen, K., Kilian, M., Julian, B. A., Mestecky, J., Novak, J., and Renfrow, M. B. (2012) Naturally occurring structural isomers in serum IgA1 o-glycosylation. *J Proteome Res* 11, 692-702
111. Royle, L., Roos, A., Harvey, D. J., Wormald, M. R., van Gijlswijk-Janssen, D., Redwan el, R. M., Wilson, I. A., Daha, M. R., Dwek, R. A., and Rudd, P. M. (2003) Secretory IgA N- and O-glycans provide a link between the innate and adaptive immune systems. *J Biol Chem* 278, 20140-20153
112. Kolka, R., Valdimarsson, H., Bodvarsson, M., Hardarson, S., and Jonsson, T. (2013) Defective immunoglobulin A (IgA) glycosylation and IgA deposits in patients with IgA nephropathy. *Apmis* 121, 890-897
113. Iwatani, H., Inoue, T., Wada, Y., Nagasawa, Y., Yamamoto, R., Iijima, H., Takehara, T., Imai, E., Rakugi, H., and Isaka, Y. (2012) Quantitative change of IgA hinge O-glycan composition is a novel marker of therapeutic responses of IgA nephropathy. *Biochem Biophys Res Commun* 428, 339-342
114. Huang, J., Guerrero, A., Parker, E., Strum, J. S., Smilowitz, J. T., German, J. B., and Lebrilla, C. B. (2015) Site-specific glycosylation of secretory immunoglobulin A from human colostrum. *J Proteome Res* 14, 1335-1349
115. Deshpande, N., Jensen, P. H., Packer, N. H., and Kolarich, D. (2010) GlycoSpectrumScan: fishing glycopeptides from MS spectra of protease digests of human colostrum sIgA. *J Proteome Res* 9, 1063-1075
116. Franc, V., Rehulka, P., Raus, M., Stulik, J., Novak, J., Renfrow, M. B., and Sebela, M. (2013) Elucidating heterogeneity of IgA1 hinge-region O-glycosylation by use of MALDI-TOF/TOF mass spectrometry: role of cysteine alkylation during sample processing. *J Proteomics* 92, 299-312
117. Hur, E. M., Patel, S. N., Shimizu, S., Rao, D. S., Gnanapragasam, P. N., An, D. S., Yang, L., and Baltimore, D. (2012) Inhibitory effect of HIV-specific neutralizing IgA on mucosal transmission of HIV in humanized mice. *Blood* 120, 4571-4582
118. Yu, X., Duval, M., Lewis, C., Gawron, M. A., Wang, R., Posner, M. R., and Cavacini, L. A. (2013) Impact of IgA constant domain on HIV-1 neutralizing function of monoclonal antibody F425A1g8. *J Immunol* 190, 205-210
119. Paul, M., Reljic, R., Klein, K., Drake, P. M., van Dolleweerd, C., Pabst, M., Windwarder, M., Arcalis, E., Stoger, E., Altmann, F., Cosgrove, C., Bartolf, A., Baden, S., and Ma, J. K. (2014) Characterization of a plant-produced recombinant human secretory IgA with broad neutralizing activity against HIV. *MAbs* 6, 1585-1597
120. Pabst, M., Chang, M., Stadlmann, J., and Altmann, F. (2012) Glycan profiles of the 27 N-glycosylation sites of the HIV envelope protein CN54gp140. *Biol Chem* 393, 719-730
121. Rouwendal, G. J., van der Lee, M. M., Meyer, S., Reiding, K. R., Schouten, J., de Roo, G., Egging, D. F., Leusen, J. H., Boross, P., Wuhrer, M., Verheijden, G. F., Dokter, W. H., Timmers, M., and Ubink, R. (2016) A comparison of anti-HER2 IgA and IgG1 in vivo efficacy is facilitated by high N-glycan sialylation of the IgA. *MAbs* 8, 74-86
122. Krugmann, S., Pleass, R. J., Atkin, J. D., and Woof, J. M. (1997) Structural requirements for assembly of dimeric IgA probed by site-directed mutagenesis of J chain and a cysteine residue of the alpha-chain CH2 domain. *J Immunol* 159, 244-249
123. Hughes, G. J., Reason, A. J., Savoy, L., Jaton, J., and Frutiger-Hughes, S. (1999) Carbohydrate moieties in human secretory component. *Biochim Biophys Acta* 1434, 86-93
124. Pabst, M., Kuster, S. K., Wahl, F., Krismer, J., Dittrich, P. S., and Zenobi, R. (2015) A Microarray-Matrix-assisted Laser Desorption/Ionization-Mass Spectrometry Approach for Site-specific Protein N-glycosylation Analysis, as Demonstrated for Human Serum Immunoglobulin M (IgM). *Mol Cell Proteomics* 14, 1645-1656

125. Loos, A., Gruber, C., Altmann, F., Mehofer, U., Hensel, F., Grandits, M., Oostenbrink, C., Stadlmayr, G., Furtmuller, P. G., and Steinkellner, H. (2014) Expression and glycoengineering of functionally active heteromultimeric IgM in plants. *Proc Natl Acad Sci U S A* 111, 6263-6268
126. Wu, G., Hitchen, P. G., Panico, M., North, S. J., Barbouche, M. R., Binet, D., Morris, H. R., Dell, A., and Haslam, S. M. (2015) Glycoproteomic studies of IgE from a novel hyper IgE syndrome linked to PGM3 mutation. *Glycoconj J*
127. Shade, K. T., Platzer, B., Washburn, N., Mani, V., Bartsch, Y. C., Conroy, M., Pagan, J. D., Bosques, C., Mempel, T. R., Fiebiger, E., and Anthony, R. M. (2015) A single glycan on IgE is indispensable for initiation of anaphylaxis. *J Exp Med* 212, 457-467
128. Johansson, S. G. (1967) Raised levels of a new immunoglobulin class (IgND) in asthma. *Lancet* 2, 951-953
129. King, C. L., Poindexter, R. W., Ragunathan, J., Fleisher, T. A., Ottesen, E. A., and Nutman, T. B. (1991) Frequency analysis of IgE-secreting B lymphocytes in persons with normal or elevated serum IgE levels. *J Immunol* 146, 1478-1483
130. Little, M. A., Al-Ani, B., Ren, S., Al-Nuaimi, H., Leite, M., Jr., Alpers, C. E., Savage, C. O., and Duffield, J. S. (2012) Anti-proteinase 3 anti-neutrophil cytoplasm autoantibodies recapitulate systemic vasculitis in mice with a humanized immune system. *PLoS One* 7, e28626

Chapter 2:

Site-specific *N*-Glycosylation analysis of human immunoglobulin E

Adapted from: *J Proteome Res* 2014, 13(2), 536-46

Authors: Rosina Plomp[1], Paul J. Hensbergen[1], Yoann Rombouts[1,2,3], Gerhild Zauner[1,4], Irina Dragan[1], Carolien A. M. Koeleman[1], André M. Deelder[1], Manfred Wuhrer[1]

[1]*Center for Proteomics and Metabolomics, Leiden University Medical Center, Leiden, The Netherlands;*
[2]*Department of Rheumatology, Leiden University Medical Center, Leiden, The Netherlands;*
[3]*present address: Institut de Pharmacologie et de Biologie Structurale, Université de Toulouse, CNRS, UPS, France;*
[4]*present address: Imperial Innovations, London, the United Kingdom*

Table of Contents

2.1: Summary

Immunoglobulin E (IgE) is a heterodimeric glycoprotein involved in anti-parasitic and allergic immune reactions. IgE glycosylation is known to exhibit significant inter-individual variation, and several reports have indicated its relevance in determining IgE activity. Here, we present site-specific glycosylation analysis of IgE from three different sources: IgE from the serum of a hyperimmune donor, from the pooled serum of multiple non-diseased donors, and from the pooled serum of 2 patients with IgE myeloma. The heavy chains were isolated and digested with either trypsin, proteinase K or chymotrypsin, which permitted coverage of all seven potential *N*-glycosylation sites. The resulting (glyco-)peptides were analyzed by nano-reverse phase-LC-MS/MS and MALDI-TOF/TOF-MS/MS. Site Asn264 was shown to be unoccupied. In all three samples, site Asn275 contained exclusively oligomannosidic structures with between 2 and 9 mannoses, while sites Asn21, Asn49, Asn99, Asn146 and Asn252 contained exclusively complex-type glycans. For the non-myeloma IgE, the majority of these glycans were biantennary, core-fucosylated and contained one or two terminal *N*-acetylneuraminic acids. In contrast, myeloma IgE showed a higher abundance of triantennary and tetraantennary glycan structures, and a low abundance of species with a bisecting *N*-acetylglucosamine. Our approach allows comparison of the glycosylation of IgE samples in a site-specific manner.

2.2: Introduction

Immunoglobulin E (IgE) is the least abundant of the immunoglobulins in human blood, present at an average concentration of approx. 150-300 ng/ml in serum (1-3). It exists in both a soluble form and as a membrane-bound receptor. Like several other immunoglobulins, IgE consists of two heavy and two light chains, with the variable regions of both chains together forming the antigen binding site. In contrast to other members of the immunoglobulin family, which contain a hinge region, IgE adopts a more rigid, asymmetrically bent conformation (4). IgE is involved in anti-parasitic immune reactions (5), but is mostly known for its role in allergic responses (6). Allergic responses originate when allergen-bound IgE triggers mast cell and basophil degranulation, thereby releasing pro-inflammatory mediators. Furthermore, IgE serum levels have been found to be elevated in individuals with allergies (3).

Roughly 12% of the molecular mass of IgE can be attributed to oligosaccharides, making it the most heavily glycosylated immunoglobulin (7). The biological function of IgE glycosylation is still largely unclear. While glycosylation is essential for the secretion of IgE, further processing of the precursor glycans ($Glc_3Man_9GlcNAc_2$) is not required for secretion, allergen binding or mast cell activation (8). Several IgE Fc receptors have been described. The high affinity IgE receptor FcεRI is expressed on the surface of basophils and mast cells, and is preloaded with IgE under physiological conditions (9). When antigen binds to IgE and crosslinks the receptors, this triggers the release of histamine and other pro-inflammatory mediators from the cells. While a severe loss in binding between IgE and FcεRI after glycan release has been described (10), others observed that glycosylation appears to account for only a minor or no contribution to receptor binding (11-13). CD23, also known as the low affinity IgE receptor FcεRII, is present on the surface of various immune cells, as well as in a soluble form in serum (6). Glycosylation of IgE does not appear to be required for IgE-CD23 binding, but it has been shown to shield IgE from interacting with CD23, as evidenced by an increase in binding affinity observed after enzymatic deglycosylation of myeloma-derived IgE (13). In addition to the Fc-receptors, several galectins have been shown to interact with IgE in a glycosylation-dependent manner. Galectin-3, formerly known as IgE-binding protein, is a secretory protein which can bind to both IgE and FcεRI (14). It is thought to trigger mast cell degranulation by crosslinking IgE and/or FcεRI (14). Galectin-9, a lectin known to suppress mast cell degranulation, also binds to IgE (15).

Human IgE possesses 7 potential *N*-glycosylation sites within the conserved region of the heavy chain. In studies performed on myeloma-derived IgE and on recombinant IgE, six of these sites were found to be occupied (7, 16-18). No *N*-glycans were attributed to site Asn264. Asn275 was found to contain solely oligomannosidic glycans, while the remaining 5 sites were reported to be occupied by complex-type glycan structures (7, 17-19). The presence of a majority (85%) of complex and a minority (14%) of oligomannosidic glycans was confirmed for non-myeloma IgE by Arnold *et al*. using IgE from a single hyperimmune donor (20). Over 20 different kinds of released oligosaccharides were identified in this study. Oligomannosidic glycans were found to carry between 4 and 8 mannose residues, while complex-type glycans appeared to be largely biantennary (97%), core-fucosylated (68%), containing 1 or 2 terminal *N*-acetylneuraminic acids (88%), with a minority (15%) containing a bisecting GlcNAc residue (an *N*-acetylglucosamine β1-4-linked to the innermost mannose) (20). Most studies on IgE have been performed using monoclonal myeloma-derived IgE, which probably does not resemble overall serum IgE glycosylation. In addition, it is known that inter-individual differences are present in the glycosylation of IgE, although this has not been explored using site-specific glycosylation analysis (21). Hence, studies on IgE glycosylation from different sources, resembling different (patho)physiological conditions, preferably in a site-specific manner, are needed.

To this end, an in-depth glycoproteomics analysis of polyclonal IgE is required and the aim of the current study was to develop such a method. IgE heavy chains from different sources (control, hyperimmune and myeloma) were digested using either trypsin, proteinase K or chymotrypsin. Resulting (glyco-)peptides, covering all 7 potential *N*-glycosylation sites, were analyzed by nano-reverse phase (RP)-LC-ESI-ion trap (IT)-MS/MS and MALDI-TOF/TOF-MS/MS. These techniques have been shown to be well suited for glycopeptide detection and characterization (22-24). From these spectra, the *N*-glycans present at each site were inferred, and a site-specific glycosylation profile was established for each of the three types of IgE.

2.3: Methods

2.3.1: IgE sources

Polyclonal IgE was acquired from 3 commercial sources. IgE from Athens Laboratories (Athens, GA) was derived from the serum of a single donor with a hyperimmune condition. IgE from US Biological (Swampscott, MA) was isolated from the pooled serum of non-diseased donors. IgE from Scripps Laboratories (San Diego, CA) was purified from the pooled serum of two IgE myeloma (kappa and lambda) patients.

2.3.2: SDS-PAGE and in-gel enzymatic digestion

Five µg of IgE was reduced with 2-mercaptoethanol (Sigma-Aldrich, St. Louis, MO) at 95°C for 10 min and analyzed by SDS-PAGE on a NuPage 4-12% gradient Bis-Tris gel (Life Technologies, Carlsbad, CA) using NuPage MES SDS running buffer (Life Technologies). The gel was stained with Coomassie G-250 (SimplyBlue SafeStain, Life Technologies). The bands containing the heavy chain (at approx. 75 kDa) and the light chain (at approx. 27 kDa) were excised and cut into pieces. The gel pieces were washed with 25 mM ammonium bicarbonate (Sigma-Aldrich) and dehydrated with acetonitrile (ACN) (Biosolve, Valkenswaard, the Netherlands). The proteins were then reduced in-gel for 30 min at 56°C with 50 µl of a 10 mM DL-dithiothreitol (DTT) (Sigma-Aldrich) 25 mM ammonium bicarbonate solution, followed by dehydration of the gel pieces in ACN and cysteine alkylation for 20 min with 50 µl of a 55 mM iodoacetamide (Sigma-Aldrich) 25 mM ammonium bicarbonate solution in the dark. The gel pieces were subsequently incubated in 25 mM ammonium bicarbonate, followed by removal of the solution and incubation in ACN. This was repeated once, and the gel pieces were subsequently dried in a centrifugal vacuum concentrator (Eppendorf, Hamburg, Germany) at 30°C for 5 min.

Proteolytic digestion was performed by adding 30 µl of 25 mM ammonium bicarbonate containing either 0.15 µg trypsin (sequencing grade modified trypsin, Promega, Madison, WI), 1 µg proteinase K (from *Tritirachium album*, Sigma-Aldrich) or 0.25 µg chymotrypsin (sequencing grade from bovine pancreas, Roche Applied Sciences, Penzberg, Germany) to the dried gel particles. The samples were kept on ice for 1 h to observe whether the gel pieces were fully submerged (10 µl 25 mM ammonium bicarbonate was added if this was not the case) and were subsequently incubated overnight at 37°C. The solution surrounding the gel pieces was collected and stored at -20°C. We then added 20 µl of 25 mM ammonium

bicarbonate to the gel pieces, and incubation was continued at 37°C degrees for another hour. The solution was again collected and added to the first fraction prior to freezing.

In order to identify the amino acid sequence of the peptide moiety of glycopeptides, several samples were deglycosylated with *N*-glycosidase F (*N*-glycosidase F of *Flavobacterium meningosepticum*, Roche Applied Sciences), either in-gel (before the addition of a proteolytic enzyme) or in-solution (after in-gel proteolytic digestion had already taken place). For in-gel deglycosylation, the same digestion protocol as described above was implemented, but instead of a proteolytic enzyme, 0.04 µg (1 unit) of *N*-glycosidase F in 30 µl 25 mM ammonium bicarbonate was added to the dried gel particles. After overnight incubation at 37°C, the solution surrounding the gel pieces was discarded, followed by incubation in 25 mM ammonium bicarbonate, dehydration in ACN, drying with a centrifugal vacuum concentrator, and the addition of a proteolytic enzyme. For in-solution deglycosylation, around 1.5 µg of digested IgE and 0.02 µg *N*-glycosidase F (0.5 units) were brought to a total volume of 20 µl with Milli-Q-purified water and incubated overnight at 37°C.

2.3.3: LC-ESI-MS(/MS) and MALDI-TOF-MS(/MS) analysis

(Glyco-)peptides were analyzed by nano-RP-LC-ESI-ion trap-MS(/MS) on an Ultimate 3000 RSLCnano system (Dionex/Thermo Scientific, Sunnyvale, CA) coupled to an HCTultra-ESI-IT-MS (Bruker Daltonics, Bremen, Germany). Five µl of sample was injected and concentrated on a trap column (Acclaim PepMap100 C18 column, 100 µm x 2 cm, C18 particle size 5 µm, pore size 100 Å, Dionex/Thermo Scientific) before separation on an Acclaim PepMap RSLC nano-column (75 µm x 15 cm, C18 particle size 2 µm, pore size 100 Å, Dionex/Thermo Scientific).

A flow rate of 300 nl/min was applied. Solvent A consisted of 0.1% formic acid in water; solvent B of 0.1% formic acid in 95% ACN and 5% water. A linear gradient was applied with the following conditions: t=0 min, 3% solvent B; t=6 min, 3% solvent B; t=54 min, 40% solvent B; t=64 min, 65% solvent B; t=71 min, 65% solvent B; t=71.5 min, 90% solvent B; t=75 min, 90% solvent B.

Samples were ionized in positive ion mode with an online nanospray source (1000-1300 V) using fused-silica capillaries and a Distal Coated SilicaTip Emitter (New Objective, Woburn,

MA) with an internal diameter of 20 µm (10 µm at the tip) and a length of 5 cm. Solvent evaporation was performed at 170°C with a nitrogen flow of 10 l/min.

For the detection of glycopeptides, the MS ion detection window was set at *m/z* 600-1800 and the MS/MS detection window at *m/z* 140-2200, with automated selection of the 5 highest peaks in the spectrum for MS/MS analysis. Singly charged ions were excluded from fragmentation. For the analysis of *N*-glycosidase F-treated peptide samples, the ion detection window was set at *m/z* 300-1800 for MS and *m/z* 140-2200 for MS/MS.

The amino acid sequence of several glycopeptides could not be identified through LC-MS/MS analysis of N glycosidase F-treated samples. Therefore, MS3 was performed on the original glycopeptide sample. For this, the precursors for both MS2 and MS3 were defined manually in the MS software. In the MS2 fragmentation spectrum of the glycopeptide, the peak corresponding to the peptide with only a single *N*-acetylglucosamine (GlcNAc) or with a GlcNAc and a fucose residue was fragmented, leading to an MS3 spectrum containing b and y ion fragments which allow identification of the amino acid sequence.

In addition, MALDI-TOF-MS and MALDI-TOF/TOF-MS/MS with laser-induced dissociation were performed for peptide analysis on an UltrafleXtreme (Bruker Daltonics) using FlexControl 3.3 software (Bruker Daltonics) in positive ion mode. Proteolytic digests were spotted on an MTP 384 polished steel target plate (Bruker Daltonics) together with 1 µl of 2,5-dihydroxybenzoic acid (DHB) matrix (20 mg/ml in 50% ACN, 50% water). A peptide calibration standard (Bruker Daltonics) was used for external calibration. MALDI-TOF(/TOF)-MS/(MS) data was analyzed with FlexAnalysis (Bruker Daltonics).

2.3.4: Data processing

The LC-MS/MS results were analyzed using DataAnalysis 4.0 software (Bruker Daltonics) and screened manually for the masses of common oxonium fragment ions (*m/z* 366.1: [1 hexose + 1 GlcNAc + H]$^+$; *m/z* 657.2: [1 hexose + 1 GlcNAc + 1 *N*-acetylneuraminic acid + H]$^+$; *m/z* 528.2: [2 hexoses + 1 GlcNAc + H]$^+$), which are characteristic for fragmentation spectra of glycopeptides. Glycopeptide MS/MS spectra were further analyzed manually to derive the oligosaccharide structure and the mass of the peptide moiety, which was then searched against a list of theoretical peptide sequences generated by IgE heavy chain digestion, using the ExPASY FindPept software tool

(http://www.expasy.org/tools/findpept.html). This was done with a mass tolerance of 0.5 Da, the enzyme settings on 'no enzyme', and while selecting the option of iodoacetamide-treated cysteines. The resulting candidate peptide sequences were then confirmed with LC-MS/MS analysis of *N*-glycosidase F-treated samples, using Protein Prospector MS-Product (http://prospector.ucsf.edu/prospector/cgi-bin/msform.cgi?form=msproduct) to calculate expected b and y ion fragmentation peaks.

Mascot generic files (.mgf) were generated with DataAnalysis and analyzed automatically with Mascot Daemon version 2.2.2 (Matrix Science, London, UK). The following conditions were used when operating Mascot Daemon: database: SwissProt; taxonomy: Homo sapiens; enzyme: trypsin/ chymotrypsin/ proteinase K; fixed modifications: carbamidomethyl (C); variable modifications: oxidation (M) (and deamidated (NQ) for *N*-glycosidase F-treated samples); maximal amount of missed cleavages: 1; peptide charge: 2+ and 3+; peptide tolerance MS: 0.6 Da; peptide tolerance MS/MS: 0.4 Da; #13C: 1.

Relative quantification of the glycoforms present at each site was achieved by summing the *m/z* over a fixed time window surrounding the elution time of each glycopeptide, and determining the average background-corrected intensity of the two highest isotope distribution peaks of the glycopeptide in the LC-MS data (if the glycopeptide was present in more than one charge state, the background-corrected intensities of multiple peaks were summed). This value was then normalized against the sum of the intensities of all glycopeptides which contained the same peptide moiety. For some glycopeptide species, modifications of approx. +17.0 Da and -18.0 Da were present, which are expected to be the result of ammonia addition and water loss, respectively. If the intensity of the modified peptide peak exceeded 20% of the intensity of the unmodified peptide peak, the total summed intensity of both peaks was used for relative quantification.

To determine the degree of occupancy of potential *N*-glycosylation sites, LC-MS or MALDI-TOF-MS analysis was performed on an *N*-glycosidase F-treated sample. For peaks belonging to peptides containing a potential *N*-glycosylation site, the isotope distribution was investigated to derive the ratio of the deamidated peptide (with the asparagine amino acid modified to an aspartic acid, increasing the mass by 1 Da and indicating that a glycan structure had been attached prior to deglycosylation) versus the unmodified peptide. This was done by using the theoretical isotope distribution of both peptides as determined by the

Isotope Distribution Calculator (IDCalc) 3.0 (University of Washington, Seattle, Washington). If the deamidated peptide was also found in a non-*N*-glycosidase F-treated sample which was incubated under the same conditions as the treated sample, spontaneous deamidation was determined to be present and a correction was performed to account for this phenomenon.

Additionally, a second method was used to calculate the degree of partial occupation. This involved relative quantification of glycopeptides and the corresponding unoccupied peptide from LC-MS data of a non-deglycosylated sample, by normalizing the background-corrected average intensity of the two highest isotope peaks to the total intensity of both glycopeptides and unoccupied peptide. A correction was applied to account for the difference in isotope distribution between glycopeptides and peptides.

Protein sequence alignment was performed using two different algorithms: Protein BLAST (NCBI) and Clustal Omega (EMBL-EBI), using the default parameters.

2.4: Results

Polyclonal IgE was obtained from three different sources: from the serum of a hyperimmune donor (which will be referred to as hyperimmune-IgE), from the pooled serum of multiple healthy donors (healthy-IgE), and from the pooled serum of two patients with IgE myeloma (myeloma-IgE). All three IgE samples were analyzed by SDS-PAGE, the bands were excised and the extracted *N*-glycopeptides subjected to nano-RP-LC-ESI-IT-MS/MS after tryptic digestion, revealing IgE heavy chains and kappa and lambda light chains (Figure 2.1). While the myeloma-IgE was reportedly derived from the pooled serum of both a donor with kappa-type myeloma as well as a donor with lambda-type myeloma, only the kappa chain was found.

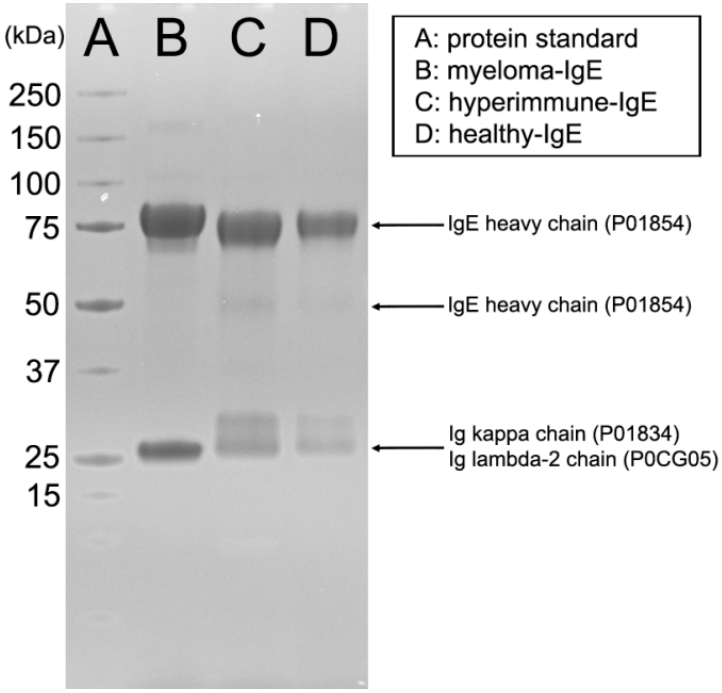

Figure 2.1: SDS-PAGE analysis of IgE derived from the pooled serum of two donors with IgE myeloma (myeloma-IgE), from the serum of a single donor with a hyperimmune condition (hyperimmune-IgE) and from the serum of multiple healthy donors (healthy-IgE). Proteomics analysis of LC-ESI-IT-MS/MS data resulted in the identification of several proteins, of which the most significant are listed with their corresponding primary UniProt accession number. A more comprehensive list of identified proteins can be found in Supplemental Table S2.5.

Hyperimmune-IgE and healthy-IgE displayed a double band containing Ig light chains, while myeloma-IgE showed a single band. Enzymatic deglycosylation of hyperimmune-IgE prior to SDS-PAGE analysis resulted in the appearance of only a single light chain band, indicating that the light chain is present in both a glycosylated and non-glycosylated form in healthy-IgE and hyperimmune-IgE. This was confirmed by LC-ESI-IT-MS/MS analysis of tryptic peptides, which showed that the upper light chain band contained several glycopeptides, whereas none were found in the lower light chain band. Since no consensus *N*-glycosylation site is present in the conserved region of the light chain, we assume that the glycosylation in these samples is present on the variable part of the light chain.

Seven potential *N*-glycosylation sites are present in the constant region of the human IgE heavy chain (Uniprot P01854); Asn21, Asn49 and Asn99 on domain C_H1, Asn146 on C_H2 and Asn252, Asn264 and Asn275 on C_H3. To study site-specific IgE heavy chain glycosylation, in-gel digestions were performed using trypsin, chymotrypsin and proteinase K, and these samples were analyzed by LC-ESI-IT-MS/MS. The LC-MS/MS data was screened for the masses of oxonium fragment ions (*m/z* 366.1: [1 hexose + 1 GlcNAc + H]$^+$; *m/z* 657.2: [1 hexose + 1 GlcNAc + 1 *N*-acetylneuraminic acid + H]$^+$; *m/z* 528.2: [2 hexoses + 1 GlcNAc + H]$^+$), which allowed detection of fragmentation spectra belonging to glycopeptides. Peptide moieties were assigned by matching the peptide mass derived from the fragmentation spectrum (often deduced from the peptide fragment ion with a GlcNAc or a GlcNAc and fucose attached) to theoretical peptide masses from IgE covering the potential *N*-glycosylation sites. In most cases, these peptide moieties were confirmed either by LC-ESI-IT-MS/MS analysis of samples after treatment with *N*-glycosidase F (Supplemental Figure S2.1) or by MS3 experiments. A list of the peptide sequences identified using this methodology is outlined in Supplemental Table S2.1. To exemplify our approach and the different types of glycosylation observed, several MS/MS spectra will be described below.

The fragmentation spectrum in Figure 2.2A shows a proteinase K-generated glycopeptide (*m/z* of 971.36 [M+3H]$^{3+}$) displaying glycan fragments at *m/z* 366.1 and 657.2. Other fragments could be attributed to the glycopeptide after the loss of several sugar residues. Overall this revealed a disialylated, biantennary *N*-glycan structure. While a fragment resembling the peptide moiety is not present, the peptide mass can be deduced from the fragment at *m/z* 764.40 ([M+H]$^+$) corresponding to the peptide with one *N*-acetylglucosamine attached. This peptide mass (561.32 Da, [M+H]$^+$) matches with the peptide TINIT (aa 144-148), containing the *N*-glycosylation site Asn146. This peptide sequence was confirmed by analysis of the deglycosylated sample (Supplemental Table S2.1).

Figure 2.2B shows the fragmentation spectrum of a tryptic glycopeptide covering Asn99 which contains a monosialylated, triantennary glycan moiety. The amino acid sequence was confirmed after analysis of the deglycosylated sample (Supplemental Figure S2.1 and Supplemental Table S2.1).

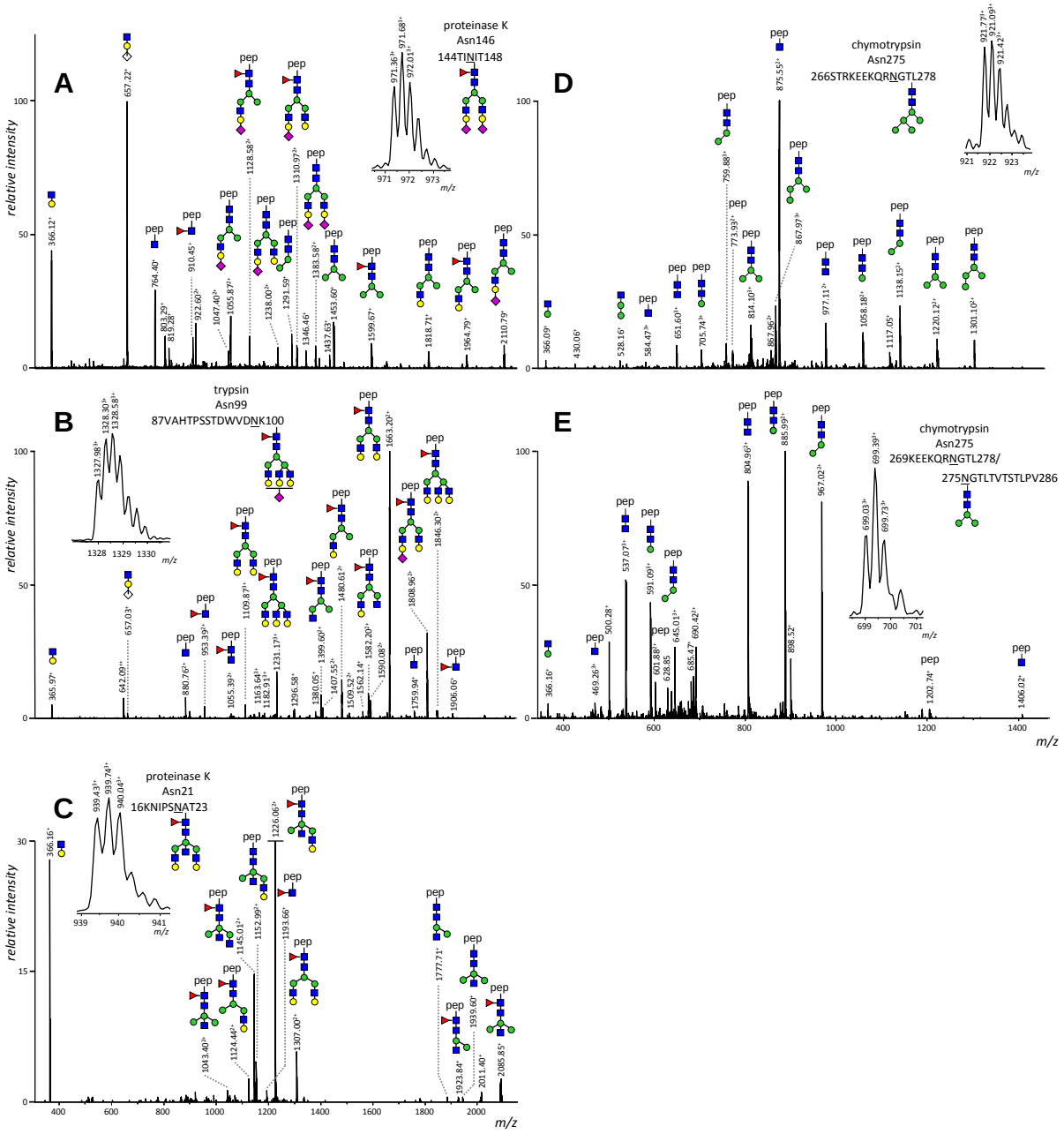

Figure 2.2: Fragmentation spectra obtained by nano-RP-LC-ESI-IT-MS/MS analysis of A) a proteinase K-generated glycopeptide from hyperimmune-IgE consisting of oligosaccharide structure H5N4S2F1 attached to peptide 144TINIT148; B) a trypsin-generated glycopeptide from myeloma-IgE consisting of H6N5S1F1 attached to 87VAHTPSSTDWVDNK100; C) a proteinase K-generated glycopeptide from hyperimmune-IgE consisting of H5N5F1 attached to 16KNIPSNAT23; D) a chymotrypsin-generated glycopeptide from hyperimmune-IgE consisting of H5N2 attached to 266STRKEEKQRNGTL278; and E) a chymotrypsin-generated glycopeptide from myeloma-IgE consisting of H3N2 attached to 269KEEKQRNGTL278/275NGTLTVTSTLPV286. H = hexose; N = *N*-acetylglucosamine; S = *N*-acetylneuraminic acid; F = fucose; pep = peptide; green circle = mannose; yellow circle = galactose; blue square = *N*-acetylglucosamine; red triangle = fucose; purple diamond = *N*-acetylneuraminic acid.

Figure 2.2C displays a proteinase K-generated glycopeptide covering Asn21 which contains a putative bisecting GlcNAc (an *N*-acetylglucosamine which is β1–4 linked to the innermost mannose). In order to confirm that this was indeed a bisected structure, glycans released from hyperimmune-IgE were labeled with 2-aminobenzoic acid (AA) and then characterized using both LC-MS/MS and UHPLC with fluorescence detection. LC-ESI-IT-MS/MS analysis showed an AA-labeled, protonated fragment consisting of 3 GlcNAc residues, 1 fucose and 1 hexose (*m/z* 1057.53) in the fragmentation spectrum of H5N5F1, indicating the presence of a bisecting GlcNAc (Supplemental Figure S2.2). Furthermore, UHPLC analysis of AA-labeled IgE glycans and AA-labeled IVIg glycans shows that the putative bisected structures in IgE elute at the same time as the corresponding structures of human intravenous immunoglobulin (IVIg; polyclonal human IgG), which have previously been shown to be bisected (Supplemental Figure S2.3) (25, 26). Moreover, if these structures were not bisected but instead contained a non-galactosylated third antenna, we would have expected to see non-galactosylated biantennary structures as well, which was not the case.

Oligomannosidic glycans were found on Asn275. The structure with 5 mannoses, exemplified by the MS/MS spectrum of a chymotrypsin-generated glycopeptide (Figure 2.2D), was the most prevalent. Furthermore, paucimannosidic glycans with 4 mannoses were present in all three types of IgE, and structures with 3 or 2 mannoses were found in myeloma-IgE and hyperimmune-IgE (Figure 2.2E). The MS/MS spectra of the oligomannosidic glycopeptides showed intense signals for $[\text{peptide} + \text{GlcNAc} + \text{H}]^+$, and MS3 analysis of this ion was used in some instances to confirm the peptide sequence (Supplemental Figure S2.4).

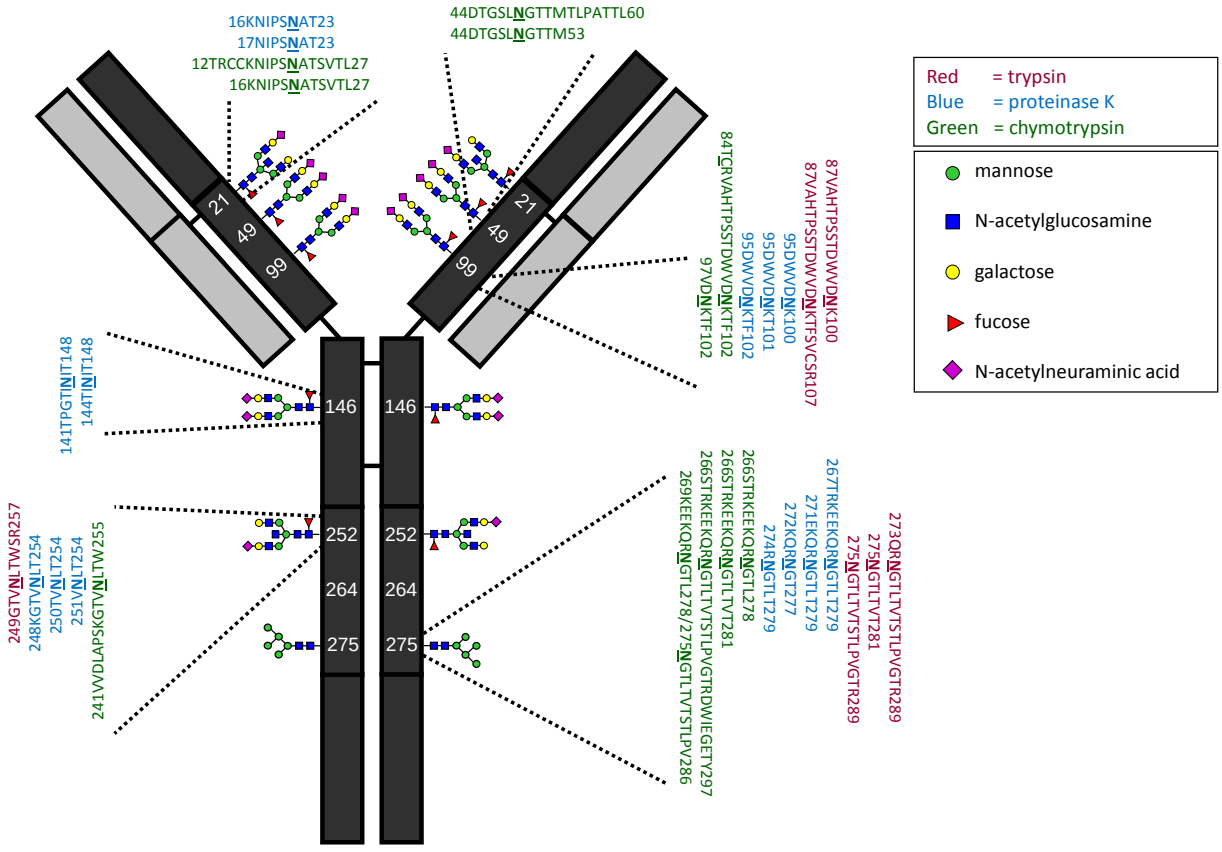

Figure 2.3: A model of IgE, which consists of 2 heavy chains (dark grey) and 2 light chains (light grey). Black lines connecting the chains represent disulfide bonds. Seven potential *N*-glycosylation sites are indicated by their amino acid residue number, and the most common oligosaccharide structure present at each site in IgE from healthy donors (as found by this study) is shown. For each occupied *N*-glycosylation site, several peptide sequences are shown which were observed during digestion with trypsin (shown in red), proteinase K (blue) or chymotrypsin (green).

Overall (Supplemental Figure S2.5), trypsin digestion allowed detection of glycopeptides covering Asn99, Asn252 and Asn275. Using proteinase K, glycopeptides covering Asn21, Asn99, Asn146, Asn252 and Asn275 were observed, while chymotrypsin allowed the analysis of glycans at Asn21, Asn49, Asn99, Asn252 and Asn275. The peptide sequences covered by each of these enzymes are listed in Figure 2.3, along with a scheme of the structure of IgE and its seven potential *N*-glycosylation sites. *N*-glycosylation sites Asn21, Asn49, Asn99, Asn146 and Asn252 were found to be occupied solely by complex-type carbohydrate structures in each of the three types of IgE. The vast majority of complex-type IgE glycan structures were found to contain a core fucose residue. Galactose residues were present on all antennae of complex-type glycans, and most structures also contained one or two terminal *N*-acetylneuraminic acid residues. Structures with a varying number of *N*-acetylneuraminic acids eluted at different time points, as can be seen in the extracted ion

chromatograms (EICs) of the glycopeptides containing Asn99 shown in Figure 2.4. The number of mannose residues present in the oligomannosidic glycan on Asn275 ranged from 2 to 9 mannoses, and all of these structures eluted at roughly the same time (Figure 2.5). To demonstrate the accuracy of our measurements, a comprehensive overview of all glycan species found in hyperimmune-IgE can be seen in Supplemental Table S2.2, along with the corresponding mass measurements and elution times.

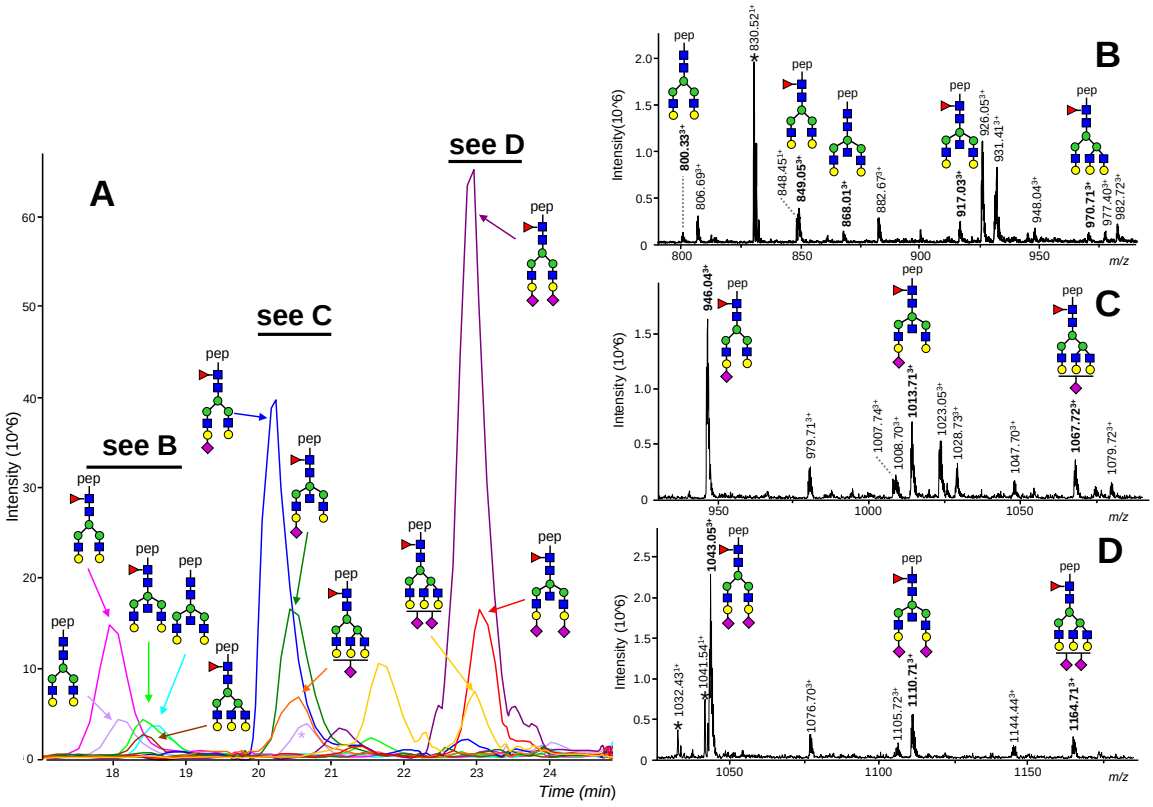

Figure 2.4: NanoLC-ESI-MS of a proteinase K digest of IgE derived from the serum of a single hyperimmune donor. A) Extracted ion chromatogram of the sum of the intensities of MS1 peaks of $[M+2H]^{2+}$ and $[M+3H]^{3+}$ species of glycopeptides corresponding to peptide 95DWVDNK100. Spectra are shown with annotated peaks for neutral glycan species (B), monosialylated glycans (C) and disialylated glycans (D). Peaks which belong to glycopeptides containing the peptide 95DWVDNK100 are shown in bold print; peaks that have been shown not to correspond to glycopeptides are marked with an asterisk. Green circle = mannose; yellow circle = galactose; blue square = *N*-acetylglucosamine; red triangle = fucose; purple diamond = *N*-acetylneuraminic acid; pep = peptide.

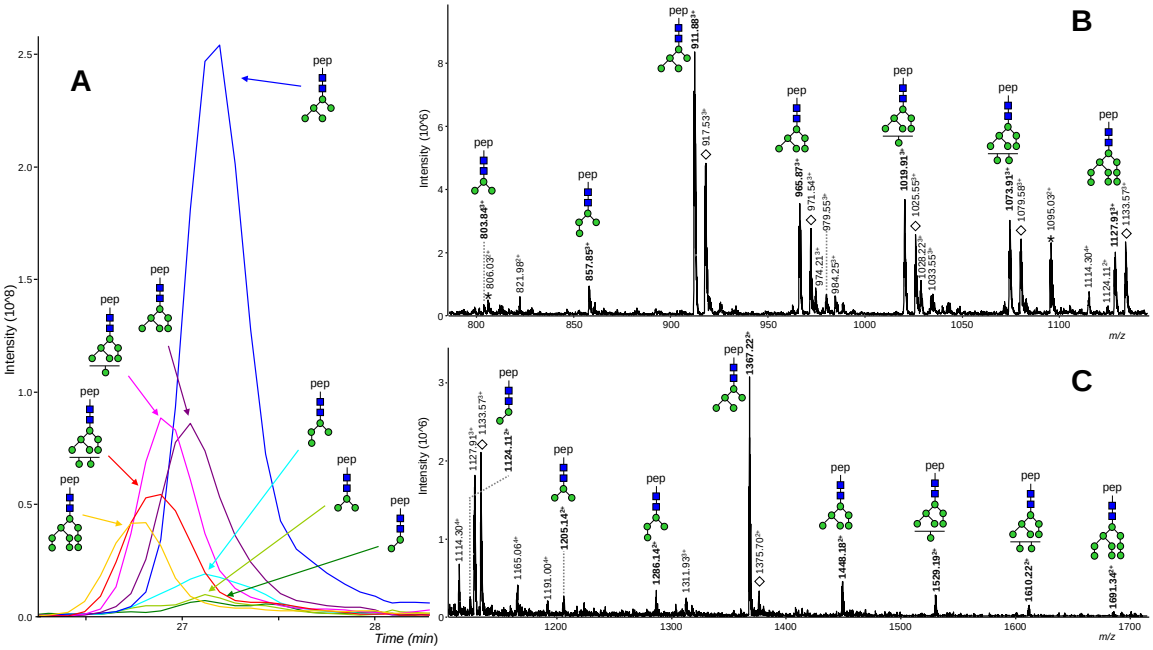

Figure 2.5: NanoLC-ESI-MS of a trypsin digest of IgE derived from the serum of a single hyperimmune donor. A) Extracted ion chromatogram of the sum of the intensities of peaks of [M+2H]2+ and [M+3H]3+ species of glycopeptides corresponding to peptide 275NGTLTVTSTLPVGTR289. Spectra with annotated [M+3H]3+ peaks (B) and [M+2H]2+ peaks (C) are shown. Modified glycopeptides containing an ammonia adduct are present, and are signified by a transparent diamond. Peaks which belong to unmodified glycopeptides containing the peptide 95DWVDNK100 are shown in bold print; peaks that have been shown not to correspond to glycopeptides are marked with an asterisk. Green circle = mannose; yellow circle = galactose; blue square = *N*-acetylglucosamine; red triangle = fucose; purple diamond = *N*-acetylneuraminic acid; pep = peptide.

Relative quantification of the glycan structures at each site was performed by summing the intensity of *m/z* values over a fixed time window around the elution time of each glycopeptide, and determining the background-corrected average intensity of the two highest isotopic peaks. This value was determined for each glycoform (if present in multiple charge states, the intensities of all charge states were summed) and normalized against the total of all glycoforms containing the same peptide moiety. The relative quantification profiles gathered from multiple digest samples were averaged for each glycosylation site, thus combining information from glycopeptides with different peptide moieties. Fortunately, the influence of the variation of the peptide moiety on the quantification profile appeared to be limited. This is illustrated by Supplemental Figure S2.6, which shows 17 relative quantification profiles acquired for site Asn99 in hyperimmune-IgE, based on glycopeptides with 7 different peptide moieties generated by either trypsin, proteinase K or chymotrypsin. The average relative quantification profile and the corresponding standard deviation of each of the six occupied *N*-

glycosylation sites was calculated separately for all three types of IgE, and is shown in the form of bar graphs (Figure 2.6). The number of separate profiles on which each average was based ranged from 2 to 17 (indicated in the inserts). The overall abundance of several *N*-glycosylation features (e.g. core fucose, bisecting GlcNAc, number of antennae, and the number of *N*-acetylneuraminic acids per galactose residue) is presented for each of the sites containing complex-type glycan structures (Figure 2.6, right part and Supplemental Table S2.3).

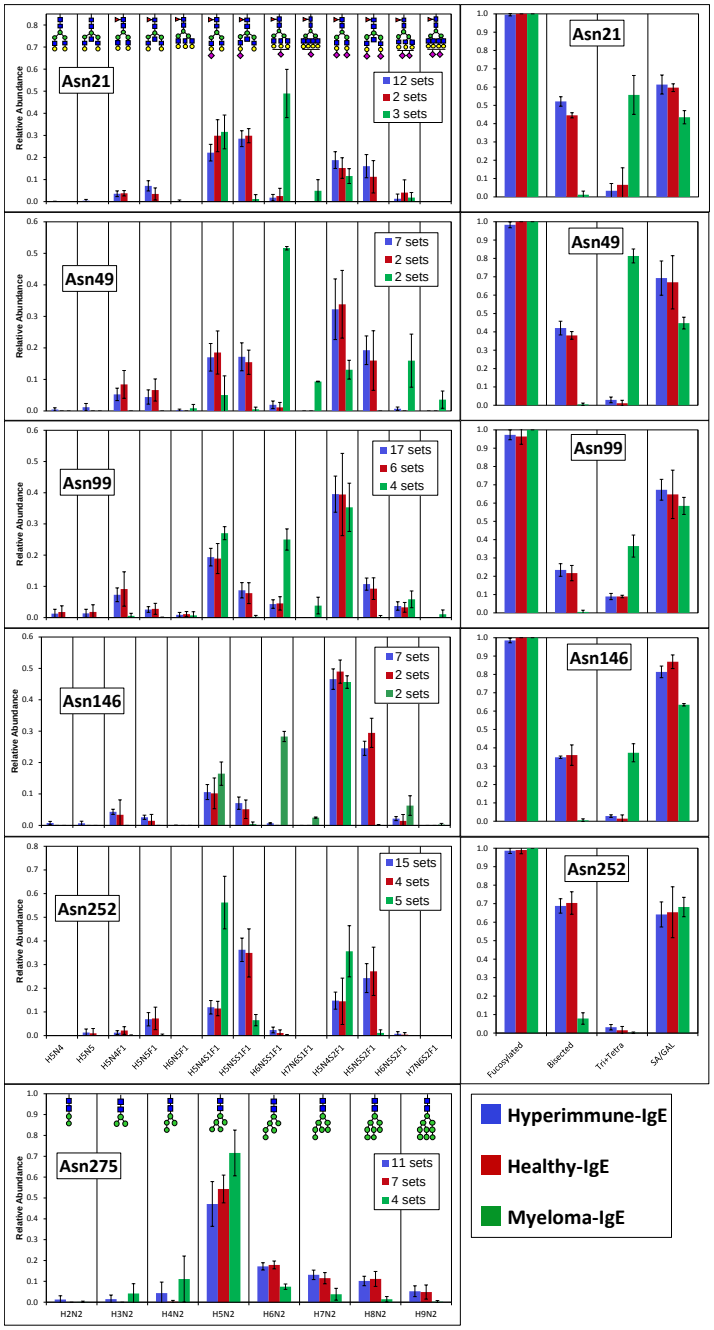

Figure 2.6: Glycosylation profiles of the 6 IgE *N*-glycosylation sites. Peak intensities were normalized to total intensity per glycosylation site, and averages and standard deviations are given based on multiple analyses with different enzymes as detailed in Supplemental Table S2.6. The number written behind the IgE type refers to the number of glycopeptide sets (with one glycopeptide set consisting of various glycoforms on one peptide from a separate enzymatic digest) which were used to calculate the average relative abundance. The complex-type glycosylation sites have an adjacent graph which outlines the following glycosylation features: fucosylation, incidence of bisecting *N*-acetylglucosamine, the number of *N*-acetylneuraminic acids per galactoses and the total percentage of triantennary and tetraantennary glycans. H = hexose; N = *N*-acetylglucosamine; S = *N*-acetylneuraminic acid; F = fucose; green circle = mannose; yellow circle = galactose; blue square = *N*-acetylglucosamine; red triangle = fucose; purple diamond = *N*-acetylneuraminic acid.

Low levels of non-fucosylated structures were observed in hyperimmune-IgE and healthy-IgE, whereas in myeloma-IgE all complex-type glycans were found to contain a core fucose. In all three types of IgE, the majority of complex-type glycans contained one or two terminal *N*-acetylneuraminic acid residues. Structures without *N*-acetylneuraminic acid were present at all five glycosylation sites which contain complex-type glycans in healthy-IgE and hyperimmune-IgE, while they were found only at sites Asn99 and Asn275, at very low levels, in the myeloma-IgE sample. In healthy- and hyperimmune-IgE, roughly 96% of complex-type glycan structures were found to be biantennary, while the remainder was triantennary. The myeloma-IgE sample was characterized by elevated levels of triantennary glycans (37%) and the presence of tetra-antennary structures (5%), at sites Asn21, Asn49, Asn99 and Asn146. Interestingly, at Asn252 myeloma-IgE does not contain tetra-antennary glycan structures, and the level of triantennary glycan structures at this site is actually lower for myeloma-IgE than for healthy- and hyperimmune-IgE. At most *N*-glycosylation sites, bisected glycans form a minority. The exception is formed by site Asn252, where bisected glycan structures are more abundant than non-bisected glycans in healthy-IgE and hyperimmune-IgE. In myeloma-IgE, the level of bisected glycan structures is substantially lower: less than 1.5% of all glycans at Asn21, Asn49, Asn99 and Asn146 and approx. 8% at Asn252.

The potential *N*-glycosylation site Asn264 was not covered by any peptide in the LC-MS/MS results of the proteolytic digests. It was suspected that this was due to the hydrophilicity of the amino acid sequence surrounding this site. This was confirmed by LC-MS/MS analysis of the synthetically produced peptide 258ASGKPVNHSTR268, corresponding to the *in silico* tryptic peptide covering this potential glycosylation site. When this sample was analyzed by LC-MS/MS in the same way as the enzymatic digests, which includes trapping and washing of a pre-column, the peptide was not found. However, by disabling the pre-column and bringing the sample directly onto the nano-column, this peptide was observed in the flow-through (data not shown). Therefore, MALDI-TOF-MS analysis seemed more appropriate to study potential glycosylation at this site. For this purpose, we analyzed tryptic digests of myeloma-IgE and hyperimmune-IgE before and after treatment with *N*-glycosidase F. Both samples displayed a near-identical isotope distribution (shown in Supplemental Figure S2.7 for myeloma-IgE), demonstrating that the apparent partial deamidation was spontaneous and that Asn264 is not occupied by carbohydrate structures.

The sites Asn99, Asn252 and Asn275 were found to be partially unoccupied, as peptides covering these sites were observed in proteolytic digests without *N*-glycosidase F treatment (Supplemental Figure S2.5). This was confirmed by the fact that the unoccupied tryptic peptides 87VAHTPSSTDWVD**N**K100, 249GTV**N**LTWSR257 and 275**D**GTLTVTSTLPVGTR289 (the last one being present only in deamidated form, as has been shown to be characteristic for Asn-Gly sequences (27)) were found in ESI-LC-IT-MS(/MS) and MALDI-TOF(/TOF)-MS/MS analysis of both *N*-glycosidase F-treated and non-*N*-glycosidase F-treated IgE. To calculate the degree of site occupancy, two methods were used.

The first method involved determination of the ratio of deamidated vs. unmodified peptide from the isotope distribution in an *N*-glycosidase F-treated sample. This was corrected for spontaneous deamidation if this was observed in a non-N glycosidase-treated sample which was incubated likewise.

The second method relied on performing relative quantification of both glycopeptides and the corresponding unoccupied peptide from LC-MS data of a non-*N*-glycosidase F-treated sample. Notably, these methods produced comparable results. The degree of occupation (% of peptides occupied by glycans±standard deviation) of Asn99, Asn252 and Asn275 was found to be 80±7% (range: 65-86%), 96±2% (range: 92-98%) and 98±3% (range: 92-100%), respectively, in both hyperimmune- and myeloma-IgE (Supplemental Table S2.4).

2.5: Discussion

In this paper we used a combination of various enzymatic digestions and nano-RP-LC-ESI-IT- and MALDI-TOF/TOF-MS/MS to study site-specific glycosylation in polyclonal immunoglobulin E derived from various sources. Previously, site-specific analysis of the glycosylation of IgE has only been performed on monoclonal myeloma-derived protein using gas-liquid chromatography or on recombinant IgE (7, 16-18). None of these studies have investigated all seven potential IgE *N*-glycosylation sites. We found that by combining the data from proteinase K and chymotrypsin digestion, all 6 occupied *N*-glycosylation sites in the conserved region of the heavy chain can be explored. We confirmed the presence of complex-type *N*-glycosylation structures at Asn21, Asn49, Asn99, Asn146 and Asn252 and oligomannosidic structures at Asn275, in all three types of polyclonal IgE. In accordance with literature, potential *N*-glycosylation site Asn264 was found not to be occupied by *N*-glycans; Asn99, Asn252 and Asn275 were shown to be only partially occupied.

To evaluate the performance of our method in studying site-specific IgE glycosylation profiles and the differences in IgE glycosylation under different physiological conditions, we chose to include a myeloma-derived IgE sample. As expected, the glycosylation profile of the myeloma-IgE sample was found to be markedly different, while the glycosylation of the healthy-IgE and hyperimmune-IgE samples was found to be quite similar. Overall, the level of triantennary and tetraantennary complex-type glycan structures was greatly elevated in myeloma-IgE. Although the linkage types of the antennae within the glycan structures found in this study are not known, it is likely that the increase in tri- and tetraantennary complex-type structures in myeloma-IgE is due to an increase in β1-6-linked branching, which has been observed in previous studies for various types of cancer tissue (28, 29). Accordingly, we found the abundance of glycans with a bisecting *N*-acetylglucosamine to be severely decreased in myeloma-IgE, which is likewise a known glycosylation feature of malignancies (30). Furthermore, no non-fucosylated complex-type glycans were encountered in myeloma-IgE, and the level of complex-type structures which did not contain *N*-acetylneuraminic acids was found to be lower than in healthy-IgE and hyperimmune-IgE. It should be stressed that these results are based on 3 (pooled) samples. Therefore these findings should be considered as examples of how such profiles can be studied using our method, and not as conclusive in describing overall IgE glycosylation under these (patho)physiological conditions.

The validity of nanoLC-ESI-IT-MS for the determination of site occupancy is not undisputed. Recently, Stavenhagen *et al.* studied the influence of (glyco)peptide characteristics in glycoproteomic workflows on signal intensities and consequently on relative site occupancy with MS-based techniques (31). Using a limited set of structurally related (glyco)peptides, they observed lower signal strength of both di- and non-sialylated biantennary *N*-glycopeptides as compared to the non-glycosylated counterparts. Moreover, they observed a slight reduction in intensity upon Asn-Asp exchange (analogous to PNGase F treatment), especially when the aspartic acid was close to the C-terminus of the (tryptic-like) peptide. These ion suppression effects were to a large extent dependent on the ionization source, with nano-ESI allowing to avoid the ionization suppression to a large extent. With regard to our determination of site occupancies, these results imply that comparing signal strengths of glycopeptides and peptides without any correction factor will most likely result in underestimation of the glycopeptide relative abundance and consequently the site-occupancy. Likewise, direct comparison of peptides with a potential *N*-glycosylation site containing the Asn or Asp (generated by PNGase treatment and/or spontaeous deamidation) may result in slightly biased site occupancies. In view of these considerations, it is remarkable that the site occupancies determined in our study by different approaches show a rather good agreement. In addition, the fact that disialylated glycopeptides were reported to generate a lower signal than corresponding non-sialylated species indicates that the level of sialylation found in our study might be somewhat lower than the real values (31).

The type of glycans (complex or oligomannosidic) present at each IgE *N*-glycosylation site as determined by our study matches the findings of previous studies (7, 17, 18). However, this comparison is complicated by the fact that the two previous site-specific IgE characterization studies were performed solely on monoclonal, myeloma-derived IgE, and by the fact that these studies determined only the relative abundance of monosaccharide residues, and not the actual glycan structures (7, 17, 18). These findings do not always correspond with our data. For example, Dorrington *et al.* reported only trace amounts of fucose at Asn99 and Asn146, while our findings show the majority of glycans at these sites to be fucosylated in all three IgE samples (7). A study by Arnold *et al.* on released glycan structures of the IgE heavy chain derived from the serum of a hyperimmune donor also shows several markedly different results (20). Contrary to our findings, they reported no tri- and tetraantennary structures, but they did encounter four different monoantennary glycans and one hybrid-type glycan.

Furthermore, they report that approx. 68% of complex-type IgE glycans contained a core fucose, while the degree of fucosylation in the three samples we analyzed was found to lie between 98.5% and 100%.

Heavy chain glycosylation of several other members of the immunoglobulin family has been shown to influence protein solubility, transport and lectin- and receptor-binding (32, 33). Sequence alignment revealed the IgE *N*-glycosylation site Asn275 to be homologous to Asn297 in IgG, Asn364 in IgD and Asn402 in IgM, indicating functional significance. While Asn275 is occupied by complex-type *N*-glycans in IgG, the homologous sites in IgE, IgD and IgM contain oligomannosidic glycan structures (33). Removal of Asn297 in IgG has been shown to affect thermodynamic stability and receptor binding (34). Further evidence for functional significance of Asn275 emerges from the discovery that, while mutation of potential *N*-glycosylation sites Asn252 or Asn264 (N➔Q) did not influence IgE-FcεRI interaction, mutation of Asn275 or Thr277 resulted in loss of binding (16). However, this loss of binding was also observed when the oligosaccharide occupation of Asn275 was not affected (T277➔S mutation). In general, glycosylation is thought to make only a minor or no contribution to FcεRI binding (11-13), although one account of a severe loss in binding after deglycosylation of IgE has been described (10). Moreover, glycosylation of IgE has been shown to affect binding affinity for CD23 (13). It has been theorized that the presence of glycans at Asn252 could directly affect the interaction between IgE and CD23 (35). The immune regulators galectin-3 and galectin-9 also bind to IgE in a glycosylation-dependent manner, and it is speculated that galectin-IgE binding has a negative effect on IgE-antigen and IgE-receptor binding (14, 36). These are only a few of the ways by which glycosylation of IgE can influence its activity, and more functional research is needed to further elucidate the biological role of IgE glycosylation.

Due to their association with adverse or protective IgE responses, allergy and parasitic diseases are favorable candidates for further studies (5, 6). While this study has uncovered no significant differences between the IgE glycosylation profile of a single hyperimmune donor and that of healthy individuals, it will be interesting to examine if this similarity holds true when comparing large numbers of individuals with various allergic conditions.

In conclusion, this study describes a comprehensive overview of the glycosylation of polyclonal IgE and provides a workflow of how this can be studied in a site-specific manner.

Our aim is to further develop our method in order to determine disease-associated glycosylation changes of IgE. This is motivated by the fact that IgE glycosylation has been known to show inter-individual variation (21) and has been implicated in modulating biological activity. To this end, we are currently working on setting up a robust method for IgE purification from serum, which shall be combined with ultrahigh-sensitivity analysis of glycopeptides (37) in order to comply with the often limited amounts of IgE that can be obtained from serum or plasma samples (1-3).

References

1. King, C. L., Poindexter, R. W., Ragunathan, J., Fleisher, T. A., Ottesen, E. A., and Nutman, T. B. (1991) Frequency analysis of IgE-secreting B lymphocytes in persons with normal or elevated serum IgE levels. *J Immunol* 146, 1478-1483
2. Ghory, A. C., Patterson, R., Roberts, M., and Suszko, I. (1980) In vitro IgE formation by peripheral blood lymphocytes from normal individuals and patients with allergic bronchopulmonary aspergillosis. *Clin Exp Immunol* 40, 581-585
3. Johansson, S. G. (1967) Raised levels of a new immunoglobulin class (IgND) in asthma. *Lancet* 2, 951-953
4. Wan, T., Beavil, R. L., Fabiane, S. M., Beavil, A. J., Sohi, M. K., Keown, M., Young, R. J., Henry, A. J., Owens, R. J., Gould, H. J., and Sutton, B. J. (2002) The crystal structure of IgE Fc reveals an asymmetrically bent conformation. *Nat Immunol* 3, 681-686
5. Gounni, A. S., Lamkhioued, B., Ochiai, K., Tanaka, Y., Delaporte, E., Capron, A., Kinet, J. P., and Capron, M. (1994) High-affinity IgE receptor on eosinophils is involved in defence against parasites. *Nature* 367, 183-186
6. Gould, H. J., and Sutton, B. J. (2008) IgE in allergy and asthma today. *Nat Rev Immunol* 8, 205-217
7. Dorrington, K. J., and Bennich, H. H. (1978) Structure-function relationships in human immunoglobulin E. *Immunol Rev* 41, 3-25
8. Granato, D. A., and Neeser, J. R. (1987) Effect of trimming inhibitors on the secretion and biological activity of a murine IgE monoclonal antibody. *Mol Immunol* 24, 849-855
9. Platzer, B., Ruiter, F., van der Mee, J., and Fiebiger, E. (2011) Soluble IgE receptors--elements of the IgE network. *Immunol Lett* 141, 36-44
10. Bjorklund, J. E., Karlsson, T., and Magnusson, C. G. (1999) N-glycosylation influences epitope expression and receptor binding structures in human IgE. *Mol Immunol* 36, 213-221
11. Woof, J. M., and Burton, D. R. (2004) Human antibody-Fc receptor interactions illuminated by crystal structures. *Nat Rev Immunol* 4, 89-99
12. Basu, M., Hakimi, J., Dharm, E., Kondas, J. A., Tsien, W. H., Pilson, R. S., Lin, P., Gilfillan, A., Haring, P., Braswell, E. H., and et al. (1993) Purification and characterization of human recombinant IgE-Fc fragments that bind to the human high affinity IgE receptor. *J Biol Chem* 268, 13118-13127
13. Vercelli, D., Helm, B., Marsh, P., Padlan, E., Geha, R., and Gould, H. (1989) The B-cell binding site on human immunoglobulin E. *Nature* 338, 649-651
14. Frigeri, L. G., Zuberi, R. I., and Liu, F. T. (1993) Epsilon BP, a beta-galactoside-binding animal lectin, recognizes IgE receptor (Fc epsilon RI) and activates mast cells. *Biochemistry* 32, 7644-7649
15. Niki, T., Tsutsui, S., Hirose, S., Aradono, S., Sugimoto, Y., Takeshita, K., Nishi, N., and Hirashima, M. (2009) Galectin-9 Is a High Affinity IgE-binding Lectin with Anti-allergic Effect by Blocking IgE-Antigen Complex Formation. *Journal of Biological Chemistry* 284, 32344-32352
16. Nettleton, M. Y., and Kochan, J. P. (1995) Role of glycosylation sites in the IgE Fc molecule. *Int Arch Allergy Immunol* 107, 328-329
17. Baenziger, J., Kornfeld, S., and Kochwa, S. (1974) Structure of the Carbohydrate Units of IgE Immunoglobulin: II. Sequence of the Sialic Acid-containing Glycopeptides. *Journal of Biological Chemistry* 249, 1897-1903
18. Baenziger, J., Kornfeld, S., and Kochwa, S. (1974) Structure of the Carbohydrate Units of IgE Immunoglobulin: I. Over-all Composition, Glycopeptide Isolation, and Structure of the High Mannose Oligosaccharide Unit. *Journal of Biological Chemistry* 249, 1889-1896
19. Fridriksson, E. K., Beavil, A., Holowka, D., Gould, H. J., Baird, B., and McLafferty, F. W. (2000) Heterogeneous Glycosylation of Immunoglobulin E Constructs Characterized by Top-Down High-Resolution 2-D Mass Spectrometry†. *Biochemistry* 39, 3369-3376
20. Arnold, J. N., Radcliffe, C. M., Wormald, M. R., Royle, L., Harvey, D. J., Crispin, M., Dwek, R. A., Sim, R. B., and Rudd, P. M. (2004) The Glycosylation of Human Serum IgD and IgE and the

Accessibility of Identified Oligomannose Structures for Interaction with Mannan-Binding Lectin. *The Journal of Immunology* 173, 6831-6840
21. Robertson, M. W., and Liu, F. T. (1991) Heterogeneous IgE glycoforms characterized by differential recognition of an endogenous lectin (IgE-binding protein). *J Immunol* 147, 3024-3030
22. Huddleston, M. J., Bean, M. F., and Carr, S. A. (1993) Collisional fragmentation of glycopeptides by electrospray ionization LC/MS and LC/MS/MS: methods for selective detection of glycopeptides in protein digests. *Anal Chem* 65, 877-884
23. Sullivan, B., Addona, T. A., and Carr, S. A. (2004) Selective detection of glycopeptides on ion trap mass spectrometers. *Anal Chem* 76, 3112-3118
24. Wuhrer, M., Catalina, M. I., Deelder, A. M., and Hokke, C. H. (2007) Glycoproteomics based on tandem mass spectrometry of glycopeptides. *J Chromatogr B Analyt Technol Biomed Life Sci* 849, 115-128
25. Mizuochi, T., Taniguchi, T., Shimizu, A., and Kobata, A. (1982) Structural and numerical variations of the carbohydrate moiety of immunoglobulin G. *J Immunol* 129, 2016-2020
26. Lauc, G., Huffman, J. E., Pucic, M., Zgaga, L., Adamczyk, B., Muzinic, A., Novokmet, M., Polasek, O., Gornik, O., Kristic, J., Keser, T., Vitart, V., Scheijen, B., Uh, H. W., Molokhia, M., Patrick, A. L., McKeigue, P., Kolcic, I., Lukic, I. K., Swann, O., van Leeuwen, F. N., Ruhaak, L. R., Houwing-Duistermaat, J. J., Slagboom, P. E., Beekman, M., de Craen, A. J., Deelder, A. M., Zeng, Q., Wang, W., Hastie, N. D., Gyllensten, U., Wilson, J. F., Wuhrer, M., Wright, A. F., Rudd, P. M., Hayward, C., Aulchenko, Y., Campbell, H., and Rudan, I. (2013) Loci associated with N-glycosylation of human immunoglobulin G show pleiotropy with autoimmune diseases and haematological cancers. *PLoS Genet* 9, e1003225
27. Krokhin, O. V., Antonovici, M., Ens, W., Wilkins, J. A., and Standing, K. G. (2006) Deamidation of -Asn-Gly- sequences during sample preparation for proteomics: Consequences for MALDI and HPLC-MALDI analysis. *Anal Chem* 78, 6645-6650
28. Dennis, J. W., Granovsky, M., and Warren, C. E. (1999) Glycoprotein glycosylation and cancer progression. *Biochim Biophys Acta* 1473, 21-34
29. Kim, Y. J., and Varki, A. (1997) Perspectives on the significance of altered glycosylation of glycoproteins in cancer. *Glycoconj J* 14, 569-576
30. Balog, C. I., Stavenhagen, K., Fung, W. L., Koeleman, C. A., McDonnell, L. A., Verhoeven, A., Mesker, W. E., Tollenaar, R. A., Deelder, A. M., and Wuhrer, M. (2012) N-glycosylation of colorectal cancer tissues: a liquid chromatography and mass spectrometry-based investigation. *Mol Cell Proteomics* 11, 571-585
31. Stavenhagen, K., Hinneburg, H., Thaysen-Andersen, M., Hartmann, L., Varon Silva, D., Fuchser, J., Kaspar, S., Rapp, E., Seeberger, P. H., and Kolarich, D. (2013) Quantitative mapping of glycoprotein micro-heterogeneity and macro-heterogeneity: an evaluation of mass spectrometry signal strengths using synthetic peptides and glycopeptides. *J Mass Spectrom* 48, 627-639
32. Ferrara, C., Grau, S., Jager, C., Sondermann, P., Brunker, P., Waldhauer, I., Hennig, M., Ruf, A., Rufer, A. C., Stihle, M., Umana, P., and Benz, J. (2011) Unique carbohydrate-carbohydrate interactions are required for high affinity binding between FcgammaRIII and antibodies lacking core fucose. *Proc Natl Acad Sci U S A* 108, 12669-12674
33. Arnold, J. N., Wormald, M. R., Sim, R. B., Rudd, P. M., and Dwek, R. A. (2007) The impact of glycosylation on the biological function and structure of human immunoglobulins. *Annu Rev Immunol* 25, 21-50
34. Jefferis, R., Lund, J., and Pound, J. D. (1998) IgG-Fc-mediated effector functions: molecular definition of interaction sites for effector ligands and the role of glycosylation. *Immunol Rev* 163, 59-76
35. Sondermann, P., Pincetic, A., Maamary, J., Lammens, K., and Ravetch, J. V. (2013) General mechanism for modulating immunoglobulin effector function. *Proc Natl Acad Sci U S A* 110, 9868-9872

36. Niki, T., Tsutsui, S., Hirose, S., Aradono, S., Sugimoto, Y., Takeshita, K., Nishi, N., and Hirashima, M. (2009) Galectin-9 is a high affinity IgE-binding lectin with anti-allergic effect by blocking IgE-antigen complex formation. *J Biol Chem* 284, 32344-32352
37. Heemskerk, A. A., Wuhrer, M., Busnel, J. M., Koeleman, C. A., Selman, M. H., Vidarsson, G., Kapur, R., Schoenmaker, B., Derks, R. J., Deelder, A. M., and Mayboroda, O. A. (2013) Coupling porous sheathless interface MS with transient-ITP in neutral capillaries for improved sensitivity in glycopeptide analysis. *Electrophoresis* 34, 383-387
38. Wuhrer, M., Koeleman, C. A., Hokke, C. H., and Deelder, A. M. (2006) Mass spectrometry of proton adducts of fucosylated N-glycans: fucose transfer between antennae gives rise to misleading fragments. *Rapid Commun Mass Spectrom* 20, 1747-1754
39. Selman, M. H., Hemayatkar, M., Deelder, A. M., and Wuhrer, M. (2011) Cotton HILIC SPE microtips for microscale purification and enrichment of glycans and glycopeptides. *Anal Chem* 83, 2492-2499

Supplemental Information

A complete overview of the supplemental information is available online at http://pubs.acs.org/doi/suppl/10.1021/pr400714w.

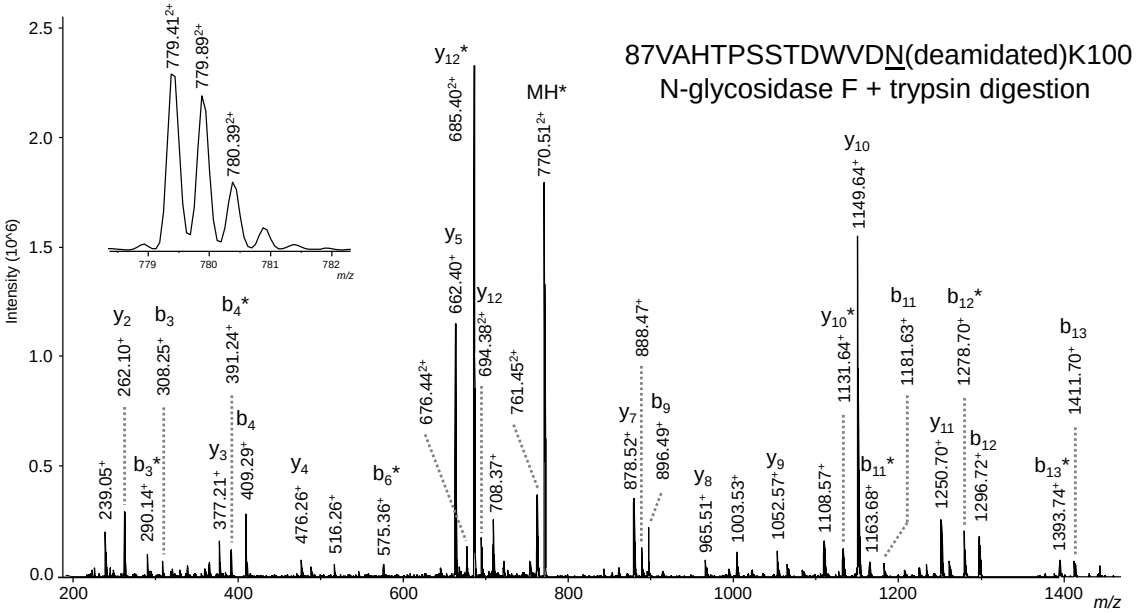

Supplemental Figure S2.1: MS/MS spectrum from LC-ESI-IT-MS analysis corresponding to the deamidated trypsin-generated peptide 87VAHTPSSTDWVDN(deamidated)K100 from myeloma-IgE. Glycan release with *N*-glycosidase F has been performed on the sample, followed by trypsin digestion. The *m/z* values of singly and doubly charged b and y fragment ions are given. Loss of water (-18 Da) is denoted by an asterisk.

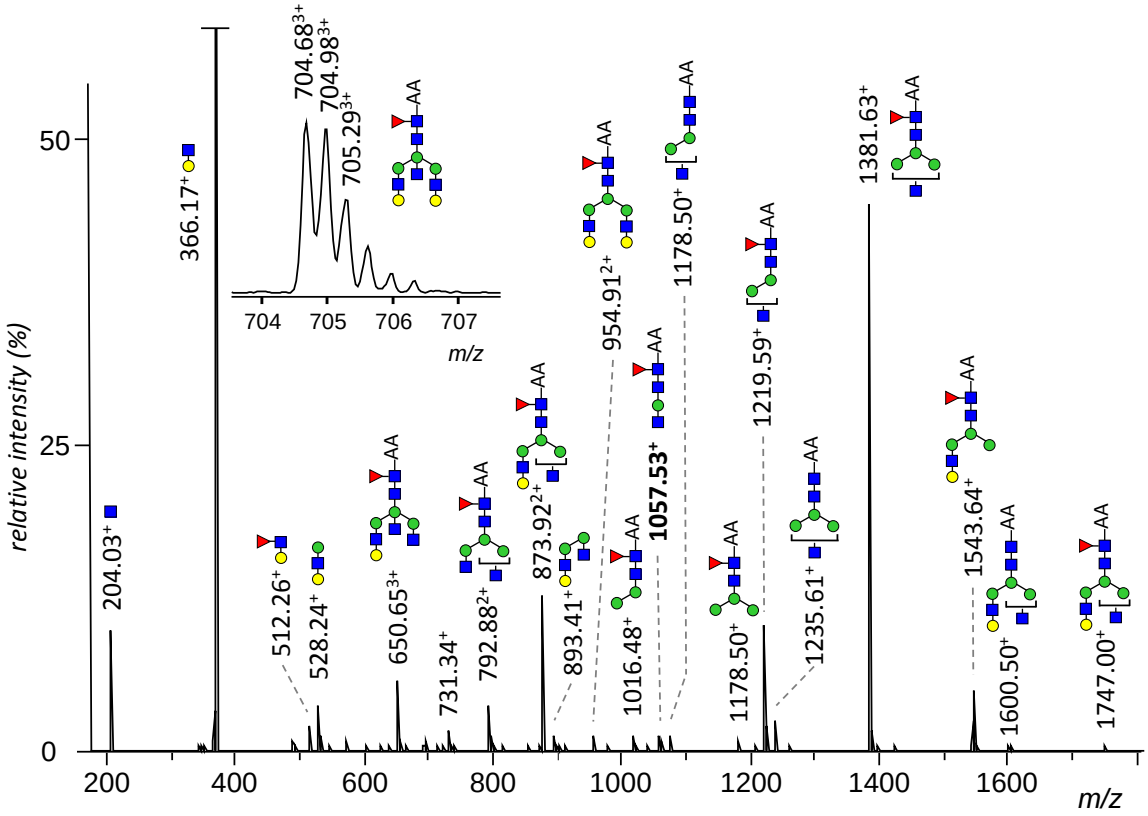

Supplemental Figure S2.2: MS/MS spectrum of the H5N5F1 structure from LC-ESI-IT-MS analysis of 2-aminobenzoic acid-labeled IgE glycans. The peak at *m/z* 1057.53 indicates that the glycan contains a bisecting *N*-acetylglucosamine. The peak at *m/z* 512.26 corresponds to [HexNAc + hexose + fucose + H]$^+$, but this structure is most likely due to fucose migration, as described previously (38). Green circle = mannose; yellow circle = galactose; blue square = *N*-acetylglucosamine; red triangle = fucose; AA = 2-aminobenzoic acid.

For in-solution glycan release, 10 µg of hyperimmune-IgE in 20 µl 1.3%SDS Milli-Q-purified water was first incubated at 60°C for 10 min. Next, 10µl of 2% Tergitol type NP-40, 10 µl of 5xPBS and 1 µl of *N*-glycosidase F (1 unit) were added, and glycan release was performed overnight at 37°C. An AA-label was introduced by adding 15 µl labeling solution (48mg/ml AA in 85%DMSO 15% acetic acid) and 15µl reducing solution (107mg/ml 2-picoline borane in DMSO). The sample was vortexed thoroughly, and incubated at 65°C for 2 h. The glycans were then purified using cotton HILIC SPE, as described by Selman *et al.* (39) The cotton tip was first equilibriated 3x with water and 3x with 85% acetonitrile (ACN). The sample with labeled glycans was brought to 85% ACN and run through the cotton tip around 40x. The cotton tip was then washed 3x with 85% ACN 1% trifluoroacetic acid and 3x with 85% ACN, before the glycans were eluted in 10 µl Milli-Q-purified water.

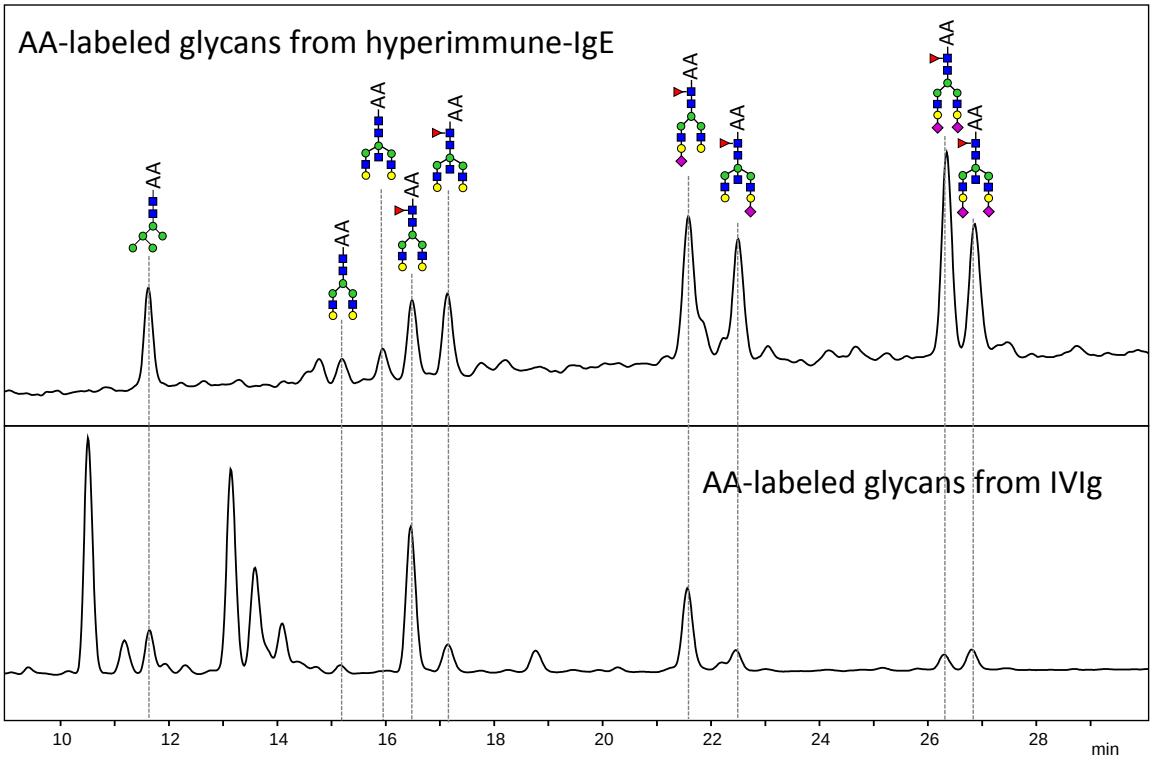

Supplemental Figure S2.3: UHPLC analysis of 2-aminobenzoic acid (AA)-labeled glycans from hyperimmune-IgE and from human IVIg (Nanogam).
Glycan release, labeling and purification were performed as described under Supplemental Figure S2.2. The samples were analyzed on a Dionex Ultimate 3000 UHPLC system, coupled to an FLD-3400RS fluorescence detector (Dionex/Thermo Scientific). Separation was achieved on an AQUITY UPLC BEH Glycan column (2.1 x 100mm, particle size 1.7 µm, Waters), with a flow of 0.6 ml/min and an oven temperature of 60°C. Solvent A consisted of 100 mM ammonium formate in water; solvent B of acetonitrile. A linear gradient was applied with the following conditions: t=0 min, 15% solvent A; t=0.5 min, 15% solvent A; t=0.5 min, 25% solvent A; t=45.5 min; 43% solvent A; t=45.5 min, 60% solvent A; t=49.5 min, 60% solvent A; t=49.5 min, 15% solvent A.
The 2-AA labeled glycans of IgE were identified based on the comparison of their HPLC elution patterns with those of fluorescently labeled IgG *N*-glycans previously described by Lauc *et al.* (26) The H5N5F1, H5N5S1F1 and H5N5S2F1 structures were confirmed by LC-ESI-IT-MS/MS analysis of UHPLC fractions. Green circle = mannose; yellow circle = galactose; blue square = *N*-acetylglucosamine; red triangle = fucose; purple diamond = *N*-acetylneuraminic acid; AA = 2-aminobenzoic acid.

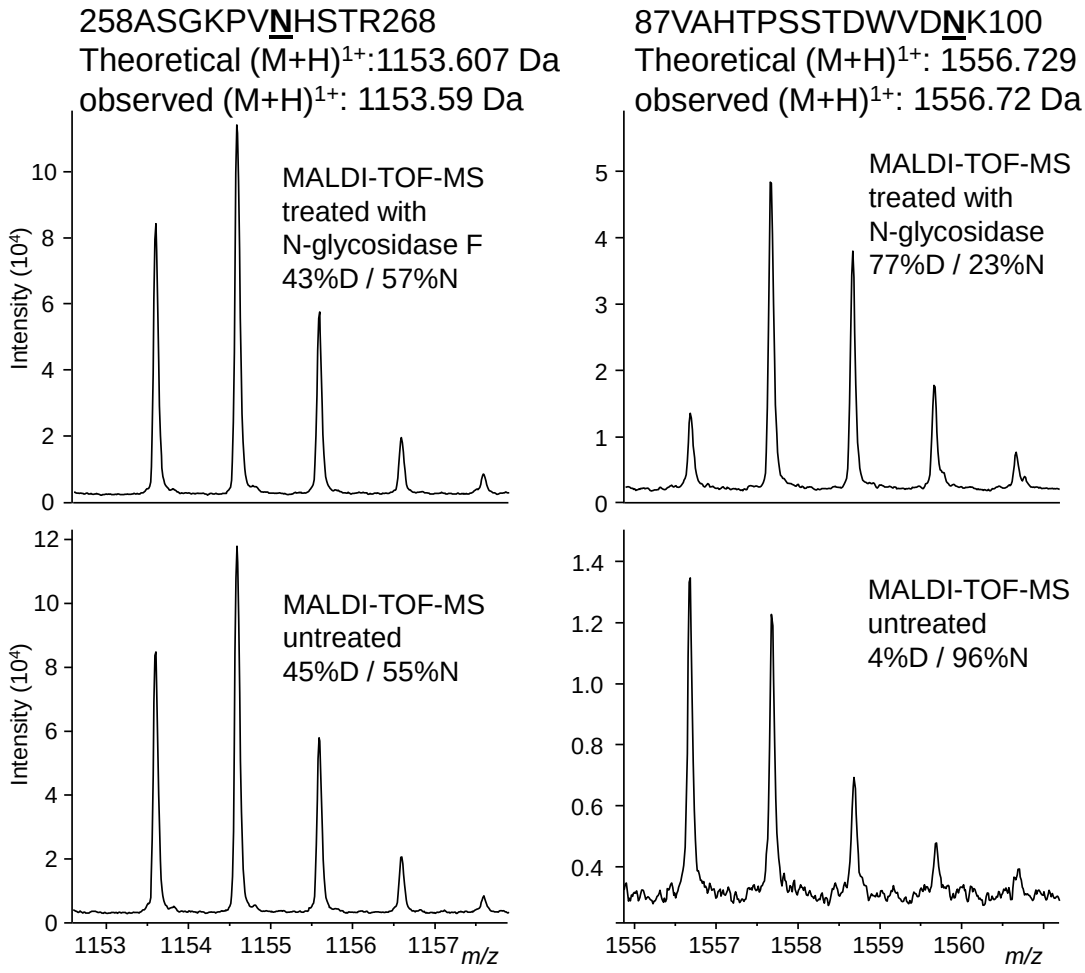

Supplemental Figure S2.7: MALDI-TOF-MS spectra of both a deglycosylated and an untreated trypsin digest of myeloma-IgE. Before trypsin digestion was performed, one of the digests was treated with *N*-glycosidase F, while the other was incubated in buffer. This was done to observe the degree of spontaneous deamidation. The two spectra on the left show the isotope distribution corresponding to a peptide containing the potential *N*-glycosylation site Asn264; the spectra on the right correspond to a peptide containing glycosylation site Asn99. The ratio of deaminated ('D') peptide versus non-deaminated ('N') peptide was determined from the theoretical isotope distribution. Peptide sequences were confirmed with MALDI-TOF/TOF-MS.

Chapter 3:

Hinge-region *O*-glycosylation of human immunoglobulin G3 (IgG3*)*

Adapted from: *Mol Cell Proteomics* 2015, 14(5), 1373-84

Authors: R. Plomp[1], G. Dekkers[2], Y. Rombouts[1,3,4], R. Visser[2], C. A. M. Koeleman[1], G. S. M. Kammeijer[1], B. C. Jansen[1,5], T. Rispens[6], P. J. Hensbergen[1], G. Vidarsson[2], M.Wuhrer[1,7]

[1]*Center for Proteomics and Metabolomics, Leiden University Medical Center, Leiden, The Netherlands;*
[2]*Department of Experimental Immunohematology, Sanquin Research, and Landsteiner Laboratory, Academic Medical Center, University of Amsterdam, Amsterdam, The Netherlands;*
[3]*Department of Rheumatology, Leiden University Medical Center, Leiden, The Netherlands;*
[4]*present address: Institut de Pharmacologie et de Biologie Structurale, Université de Toulouse, CNRS, UPS, France*
[5]*present address: Ludger, Oxford, The United Kingdom*
[6]*Department of Immunopathology, Sanquin Research, and Landsteiner Laboratory, Academic Medical Center, University of Amsterdam, Amsterdam, The Netherlands;*
[7]*Division of BioAnalytical Chemistry, VU University Amsterdam, Amsterdam, The Netherlands*

Table of Contents

3.1: Summary

Immunoglobulin G (IgG) is one of the most abundant proteins present in human serum and a fundamental component of the immune system. IgG3 represents approximately 8% of the total amount of IgG in human serum and stands out from the other IgG subclasses because of its elongated hinge region and enhanced effector functions. This study reports partial *O*-glycosylation of the IgG3 hinge region, observed with nanoLC-ESI-IT-MS(/MS) analysis after proteolytic digestion. The repeat regions within the IgG3 hinge were found to be in part *O*-glycosylated at the threonine in the triple repeat motif. Non-, mono- and disialylated core 1-type *O*-glycans were detected in various IgG3 samples, both poly- and monoclonal. NanoLC-ESI-IT-MS/MS with ETD fragmentation and CE-MS/MS with CID fragmentation were used to determine the site of IgG3 *O*-glycosylation. The *O*-glycosylation site was further confirmed by the recombinant production of mutant IgG3 in which potential *O*-glycosylation sites had been knocked out.

For IgG3 samples from six donors we found similar *O*-glycan structures and site occupancies, whereas for the same samples the conserved *N*-glycosylation of the Fc CH2 domain showed considerable inter-individual variation. The occupancy of each of the 3 *O*-glycosylation sites was found to be approximately 10% in six serum-derived IgG3 samples and approximately 13% in two monoclonal IgG3 allotypes.

3.2: Introduction

Immunoglobulin G (IgG) is one of the most abundant proteins present in human serum and represents approximately three-quarters of the total serum immunoglobulin content (1). As the main mediator of humoral immunity and an important link between the adaptive and innate immune system, IgG is a fundamental component of the immune system. IgG consists of two heavy and light chains, linked by disulfide bonds. The protein can be subdivided into the antigen-binding (Fab) and the receptor-binding (Fc) region. There are four subclasses of IgG, all of which share an overall structure homology but differ slightly in their amino acid sequence; the quantity of the subclasses in human serum is as follows: IgG1 > 2 > 3 > 4 (2).

IgG3 represents approximately 8% of the total amount of IgG in human serum (2), and stands out from the other IgG subclasses for a number of reasons. First of all, IgG3 contains an elongated hinge region with up to a triple repeat sequence (the actual number ranging from one to three depending on the allotype (3)), which is responsible for the increased flexibility between the Fab and the Fc part, as well as the wider and more flexible angle between the two Fab arms (4, 5). This flexibility is likely the cause of the increased affinity of IgG3, compared to the other subclasses, for divalent binding to certain types of antigens (4, 6, 7). Secondly, IgG3 has a higher affinity for C1q, which initiates the classical complement pathway (5, 8). The interaction between IgG3 and C1q is not due to the elongated hinge region, as demonstrated by studies showing that recombinant IgG3 with an IgG1- or IgG4-like hinge sequence exhibited even greater binding affinity for C1q than wild type IgG3 (8-10). Thirdly, IgG3 has a higher overall affinity for the Fcγ receptors (FcγRs), through which it can influence effector cells of the innate immune system (11). The CH2 domain and hinge region of IgG3 were shown to be instrumental in binding to the high affinity FcγRI receptor (12). Finally, IgG3 generally has a shorter half-life compared to the other IgG subclasses (1 versus 3 weeks) (2). This difference was traced back to an H435R mutation that confers a positive charge at physiological pH, resulting in a decreased binding to the neonatal Fc receptor (FcRn), which is involved in recycling IgG targeted for lysosomal degradation (13). The low-efficiency FcRn-mediated transport also gives rise to decreased levels of IgG3 in mucosal tissue and impaired transport of IgG3 across the placenta (14). These properties do not hold true for all types of IgG3, since a large number of IgG3 allotypes have been described, some of which lack the H435R substitution and have a half-life and placental transport rates similar to IgG1 (13-16). IgG3 is more polymorphic than the other IgG

subclasses, as evidenced by the high number of known allotypes (16). Most of the polymorphisms reside in the CH2 or CH3 domain, but the length of the hinge region can also display a high degree of variation. Depending on the number of sequence repeats, the hinge region can vary from 27 to 83 amino acid residues between different IgG3 allotypes (3, 16, 17).

An *N*-linked complex type glycan is highly conserved and found in the CH2 domain of all IgG subclasses and allotypes. The type of glycan present at this site has been shown to influence the effector functions of IgG (18). *N*-glycans which lack a core fucose cause IgG to have an enhanced pro-inflammatory capacity through stronger binding to FcγRIIIa and FcγRIIIb (18-20). In contrast, IgG carrying sialylated *N*-glycans exhibits anti-inflammatory properties, likely due to increased binding affinity to C-type lectins and/or reduced binding to FcγR (18, 21, 22).

O-linked glycosylation has been reported for various immunoglobulins. *O*-glycans are present on the hinge region of human IgA1 and IgD and mouse IgG2b (23-25). IgA1 contains nine potential sites for *O*-glycosylation (serine and threonine) in the hinge region, of which 3-5 are occupied, while IgD has been reported to carry between 4 and 7 *O*-glycans (24-26). The *O*-glycosylation in the hinge of murine IgG2b was observed to protect against proteolytic digestion (23). Likewise, IgA1 was found to be more susceptible to degradation by *Streptococci* proteases after neuraminidase treatment (27).

In this study we report partial *O*-glycosylation of the human IgG3 hinge. We obtained both poly- and monoclonal IgG3 from various sources and performed proteolytic digestion with trypsin or proteinase K. NanoLC-reverse phase (RP)-ESI-ion trap (IT)-MS/MS was used to examine the resulting (glyco)peptides, revealing core 1-type *O*-glycans on multiple sites within the IgG3 hinge region.

3.3: Methods

3.3.1: Immunoglobulin sources

Polyclonal IgG3 from donor sera. IgG3 was purified from 6 serum samples (average donor age: 44.5 ± 9 years; 3 male and 3 female; details are listed in Supplemental Table S3.1). The serum samples were collected from healthy donors with informed consent in compliance with the institutional ethical board. Venous blood was collected in a 9-ml Vacuette serum clot activator tube (Greiner BioOne, Kremsmünster, Austria) and incubated at room temperature for 30 min, followed by centrifugation for 15 min at 1800 g. The serum fraction was then collected and stored at -20°C. IgG was isolated by running the serum over a HiTrap Protein G HP column (GE Healthcare, Buckinghamshire, UK) and eluted with 0.1 M glycine-HCl, pH 2.7. The eluate containing IgG was then applied to a HiTrap MabSelect SuRE column packed with recombinant Protein A (GE Healthcare), and the IgG3-containing flow-through was concentrated using an Amicon Ultra-15 centrifugal filter device 10 kDa (Merck Millipore, Darmstadt, Germany) and dialyzed against PBS using a Slide-A-Lizer Dialysis Cassette, 10K MWCO (Dionex/Thermo Scientific, Sunnyvale, CA).

Polyclonal IgG3 from pooled plasma. IgG3 purified from pooled plasma was obtained commercially from Athens Research and Technology (Athens, GA). Upon inquiry, we learned that this IgG3 had been treated with dextran sulfate, followed by centrifugation to pellet the lipids. The delipidated plasma was then subjected to an ammonium sulfate precipitation, followed by boric acid precipitation. The IgG was isolated with ion exchange chromatography, and further purification of IgG3 was achieved with affinity chromatography (rProtein A), gel filtration chromatography and a jacalin column to remove a minor IgA contaminant. This purification method did not expose the IgG3 to extreme pH conditions or temperatures above 55°C.

Monoclonal IgG3. Two monoclonal recombinant anti-GDob1 IgG3 allotypes, G3m(g) and G3m(s), were produced in a HEK-293F FreeStyle cell line expression system (Life Technologies, Paisley, UK). IgG3m(s) was then purified with a HiTrap MabSelect SuRE column packed with recombinant Protein A (GE Healthcare), while IgG3m(g) was purified with a Protein G HiTrap HP column (GE Healthcare).

Monoclonal IgG3 mutants. Three IgG3 G3m(g) hinge mutants were produced recombinantly, together with wild type IgG3 G3m(g) as a control. The variable regions of

the heavy and light chains (VH, VL) of the mouse IgG1 anti-2,4,6-trinitrophenol (TNP) hapten antibodies were cloned onto human IgG3 and kappa backbones, respectively, as described previously (20, 28). Synthetic DNA encoding for IgG3 mutants, replacing the three threonines (T) and/or serines (S) with alanines (A), was generated as 5'-NheI and 3'Bsu36I fragments by GeneArt (Life Technologies). The NheI-Bsu36I fragments were ligated in anti-TNP IgG3 heavy chain replacing the corresponding fragment in the wild type heavy chain. Antibodies were produced in the HEK-293F FreeStyle cell line expression system (Life Technologies) with co-transfection of vectors encoding p21, p27 and pSVLT genes as described (29) to increase protein production. The antibodies were purified on a protein G HiTrap HP column (GE Healthcare) using the ÄKTAprime plus system (GE Healthcare) and dialyzed against PBS overnight.

Monoclonal IgG3/4 Fc constructs. Four recombinant IgG3 and IgG4 Fc constructs were produced in a HEK-293F FreeStyle cell line (Life Technologies) and purified with a Protein G column (Protein G Sepharose 4 fast flow; GE Healthcare), as described by Rispens *et al* (30). All constructs contained an IgG4 hinge region, together with either the CH2 and CH3 regions of two IgG3 allotypes (G3m(b)-Fc-h4 and G3m(c3c5)-Fc-h4) or the CH2 and CH3 regions of two IgG4 variants (IgG4-Fc-V397M and IgG4-Fc-V397M,K392N).

Polyclonal & monoclonal IgG4. Several IgG4 samples were collected. A polyclonal IgG4 sample was affinity-purified from the plasma of a rheumatoid arthritis patient using anti-IgG4 coupled to Sepharose (clone MH164.4, Sanquin, Amsterdam, The Netherlands). A second IgG4 sample was enriched from the serum of an LUMC patient with an extremely high IgG4 serum titre (14.4 mg/ml). The serum was heat-inactivated and subjected to a 33% cut ammonium sulfate precipitation, followed by dialysis to decrease the salt content. The IgG4 was then enriched on a HiTrap DEAE Sepharose and a Superdex 200 column (GE Healthcare) using an ÄKTAprime plus chromatography system (GE Healthcare); IgG4-containing fractions were identified using ELISA and pooled. A monoclonal anti-TNP IgG4 sample produced in HEK cells was purified with a protein G column and dialyzed against PBS, in the same way as described for the IgG3 mutants. In addition, we obtained a recombinant humanized IgG4 sample in the form of the therapeutic antibody natalizumab (Tysabri; Biogen Idec, Badehoevedorp, The Netherlands), which is produced in murine myeloma cells.

The protein sequences of the recombinant samples can be found in Supplemental Table S3.2.

3.3.2: SDS PAGE analysis and proteolytic digestion

Five µg of the IgG samples was reduced with 2-beta-mercaptoethanol (Sigma-Aldrich, St.Louis, MO) at 95°C for 10 min. The IgG was then run on a NuPage 4-12% Bis-Tris SDS-PAGE gel (Life Technologies) and stained with Coomassie G-250 (SimplyBlue SafeStain, Life Technologies). Bands were excised, cut into pieces, washed with 25 mM ammonium bicarbonate (ABC, Sigma-Aldrich), and dehydrated with acetonitrile (Biosolve, Valkenswaard, The Netherlands). The IgG was then again treated with a reducing agent by adding 50 µl of a 10 mM DL-dithiothreitol (DTT; Sigma-Aldrich) 25 mM ABC solution for 30 min at 55°C. The gel pieces were subsequently dehydrated by the addition of acetonitrile. Alkylation of the cysteine residues was achieved by incubation with 50 µl of a 55 mM iodoacetamide (Sigma-Aldrich) 25 mM ABC solution in the dark for 20 min. The gel pieces were then washed with 25 mM ABC and dehydrated with acetonitrile. The washing and dehydration was repeated a second time, and the samples were subsequently dried down completely in a centrifugal vacuum concentrator (Eppendorf, Hamburg, Germany).

For proteolytic digestion to take place, 30 µl of 25 mM ABC containing either trypsin (sequencing grade modified trypsin, Promega, Madison, WI), proteinase K (from *Tritirachium album*; Sigma-Aldrich) or chymotrypsin (sequencing grade from bovine pancreas, Roche Applied Sciences, Mannheim, Germany) was added to the dried gel pieces. An IgG:enzyme (w/w) ratio of 1:20 for trypsin, 1:3 for proteinase K and 1:20 for chymotrypsin was used. The samples were kept on ice for 1 h, to allow the enzyme to enter the gel pieces. If the gel pieces were not fully submerged, a further 10-20 µl of 25 mM ABC was added. The samples were incubated overnight at 37°C. The solution surrounding the gel pieces was collected the next morning. Following the addition of another 20 µl of 25 mM ABC, the gel pieces were incubated at 37°C for 1 h. The solution was then again collected and added to the first fraction, and stored at -20°C.

Alternatively, several IgG3 samples were digested in solution without reduction alkylation: 3 µg of IgG3 was incubated with 0.3 µg of trypsin in a total volume of 25 µl 25 mM ABC at 37°C overnight.

Endoproteinase AspN (NewEngland Biolabs, Ipswich, MA) was used to further digest trypsin-generated (glyco)peptides. Digestion was performed by adding 1.5 µl of AspN and 15 µl of 2x AspN buffer (100 mM Tris-HCl, 5 mM zinc sulfate, NewEngland Biolabs) to 15 µl of trypsin-digested IgG3, and incubating overnight at 37°C.

3.3.3: Exoglycosidase digestion

Exoglycosidase digestion was performed on tryptic IgG glycopeptides. The trypsin-digested IgG3 was first heated to 95°C for 5 min to inactivate the trypsin. The sample was then dried in a centrifugal vacuum concentrator (Eppendorf), and resuspended by the addition of 16 µl of Milli-Q-purified water, 2 µl 50 mM sodium acetate (pH 5.5), 1 µl sialidase (Glyko sialidase A, Prozyme, Hayward, CA) and 1 µl of galactosidase (Glyko beta-galactosidase, Prozyme). The samples were incubated overnight at 37°C.

3.3.4: NanoLC-ESI-IT-MS(/MS) analysis

The IgG3 (glyco)peptides were analyzed with nanoLC-reversed phase (RP)-electrospray (ESI)-ion trap (IT)-MS(/MS) on an Ultimate 3000 RSLCnano system (Dionex/Thermo Scientific) coupled to an amaZon speed ESI-IT-MS (Bruker Daltonics, Bremen, Germany). A precolumn (Acclaim PepMap C18 capillary column, 300 µm x 5 mm, particle size 5 µm, Dionex/Thermo Scientific) was used to wash and concentrate the sample, and separation was achieved on an Acclaim PepMap RSLC C18 nanocolumn (75 µm x 150 mm, particle size 2 µm, Dionex/Thermo Scientific) with a flow rate of 500 nl/min. The following linear gradient was used, with solvent A consisting of 0.1% formic acid in water and solvent B of 95% acetonitrile, 5% water: t=0 min, 1% solvent B; t=5 min, 1% B; t=20 min, 25% B; t=25 min, 70% B; t=30 min, 70% B; t=31 min, 1% B; t=55 min, 1% B. The sample was ionized in positive ion mode with an ESI-nanosprayer (4500 V) using a bare fused silica capillary (internal diameter of 20 µm). The solvent was evaporated at 180°C with a nitrogen flow of 5 l/min. A CaptiveSpray nanoBooster (Bruker Daltonics) was mounted onto the mass spectrometer and saturated the nitrogen flow with ACN to enhance the sensitivity. The MS1 ion detection window was set at *m/z* 350-1400, and the MS2 window at *m/z* 140-2200. The three highest non-singly charged peaks in each MS1 spectrum were automatically fragmented through collision-induced dissociation (CID). In order to identify the peptide sequence of proteinase K- and trypsin-generated *O*-glycopeptides, MS3 analysis was performed on manually selected precursors: the MS2 peak representing the peptide without sugars attached

was targeted for fragmentation. In a separate LC-MS run, electron transfer dissociation (ETD) fragmentation was done on selected precursor ions.

3.3.5: t-ITP-CE-ESI-qTOF-MS(/MS) analysis

Transient isotachophoresis (ITP)-capillary electrophoresis (CE)-ESI-qTOF-MS/MS analysis was performed on a tryptic sialidase- and galactosidase-treated IgG3 sample derived from pooled plasma. Separation was achieved on a CESI 8000 system (AB Sciex, Framingham, MA), coupled via porous sheathless interfacing to an ultra-high resolution (UHR)-qTOF maXis Impact MS system (Bruker Daltonics) operating in positive ion mode. The sample migrated over a 90-cm bare fused capillary (i.d. 30 µm, o.d. 150 µm, AB Sciex). A 10% acetic acid solution was used as background electrolyte and a 50 mM ammonium acetate solution as leading electrolyte. A voltage of 20 kV was applied and 70 nl was injected during 1 min. The ion detection window for both MS1 and MS2 was set at *m/z* 50-2200.

3.3.6: Data processing

The LC-MS(/MS) data was analyzed using DataAnalysis 4.2 software (Bruker Daltonics). Within this program, the function Compounds – AutoMS(n) was used to generate 300 compound spectra (with sum spectra generated for compounds within an *m/z* window of 0.5 Th over a chromatographic peak width of 0.5 min), and this data was deconvoluted and exported as a mascot generic file. Protein identification through primary sequence database searching was performed using the MASCOT search algorithm (MASCOT Daemon version 2.2.2; Matrix Science, London, UK). The following MASCOT settings were used: taxonomy: *Homo sapiens*; database: SwissProt; enzyme: trypsin (for trypsin digests) / no enzyme (for proteinase K digests) / chymotrypsin (for chymotrypsin digests); fixed modifications: carbamidomethyl (C); variable modifications: oxidation (M); max missed cleavages: 1; MS1 peptide tolerance: 0.3 Da; MS/MS tolerance: 0.3 Da; #13C: 0.

The fragmentation spectra were screened manually for common oxonium fragment ions, which are characteristic for glycopeptide fragmentation: *m/z* 366.14, [1 HexNAc (*N*-acetylhexosamine) + 1 Hex (hexose) + H]$^+$; *m/z* 292.10, [1 NeuAc (*N*-acetylneuraminic acid) + H]$^+$; *m/z* 274.09, [1 NeuAc – H_2O + H]$^+$; *m/z* 657.23, [1 HexNAc + 1 Hex + 1 NeuAc + H]$^+$. From the MS/MS spectra of *O*-glycopeptides, the composition of the glycan and the mass of the peptide moiety could be deduced. This peptide mass was used to generate matching IgG peptide sequences using the ExPASY FindPept software tool

(http://www.expasy.org/tools/findpept.html). The MS3 spectrum of the peptide moiety was then used to confirm the peptide sequence, by comparing the peaks in the spectrum to the b and y ions expected according to the Protein Prospector MS-Product tool (http://prospector.ucsf.edu/prospector/cgi-bin/msform.cgi?form=msproduct).

Relative quantification of the *O*-glycans present on the tryptic IgG3 peptide SCDTPPPCPR was done by summing LC-MS spectra over a fixed time window of 0.5 min surrounding the elution of each (glyco)peptide, and then summing the background-corrected intensities of the first 3 isotopic peaks for each *O*-glycopeptide. If the compound was present in multiple charge states, the background-corrected peak intensities of the different charge states were summed followed by normalizing the data so that the total was 100%. A separate correction factor was applied to each of the glycopeptides to correct for the fact that higher mass compounds have a lower percentage of signal intensity present in the first 3 isotopic peaks. First, the percentage of signal intensity present in each isotopic peak was calculated using IDCalc version 0.3 (University of Washington). The correction factor consists of the % of signal intensity present in the first 3 isotopic peaks of the peptide divided by the % of signal intensity present in the first 3 isotopic peaks of the *O*-glycopeptide.

In order to obtain a more accurate determination of the percentage of oligosaccharide occupation of the tryptic IgG3 peptide SCDTPPPCPR, relative quantification was done using LC-MS analysis of a sialidase- and galactosidase-treated tryptic digest sample. The ratio between the peptide and the peptide + HexNAc was determined in the same way as described above.

Relative quantification of *N*-glycosylation of IgG3 was performed using an adjusted version of the method reported by Selman *et al* (31). Targeted alignment was done using a novel in-house tool, which aligned nanoLC-ESI-IT-MS spectra according to a list of calibrant *m/z* and retention time values. Various IgG3 *N*-glycopeptides were used as calibrants. The algorithm examines the *m/z* region within a given time window around each calibrant and isolates the local maxima. The observed retention times of these maxima and the desired retention times are then taken as an input array for a second degree polynomial fit, returning a function which is used to transform the observed retention time of the whole spectrum, resulting in well-aligned spectra. The in-house tool 3D Max Extractor was used to extract signal intensities within specific *m/z* windows. The program examines all datapoints in *m/z*-retention

time space around a given analyte and reports the maximum intensity observed per analyte. Background-corrected intensities of the first three isotopic peaks belonging to IgG2/3 glycopeptides with a charge state of 2+, 3+ or 4+ were determined from the spectra and summed. The glycopeptide values were normalized by dividing by the summed intensity of all glycopeptide values. Glycopeptides were included if they exhibited a signal-to-noise ratio over 3 in at least 25% of the samples. The tryptic peptide that contains the *N*-glycosylation site has the same mass in both IgG3 and IgG2, and thus with this method we could not distinguish between IgG3 and IgG2 glycopeptides.

3.4: Results

3.4.1: *O*-glycosylation of IgG3

Various types of IgG3 samples were obtained: polyclonal IgG3 samples purified from the serum of 6 donors (44.5 ± 9 years, 3 male + 3 female; details in Supplemental Table S3.1); polyclonal IgG3 purified from pooled plasma; and two recombinant monoclonal anti-GDob1 IgG3 allotypes (G3m(g) and G3m(s)) produced in human embryonic kidney (HEK) cells. Analysis of these samples by SDS-PAGE in reducing condition followed by Coomassie staining revealed an upper band at approximately 60 kDa corresponding to the heavy chain of IgG3 and a lower band at approximately 30 kDa corresponding to the kappa and lambda light chains (Supplemental Figure S3.1). The IgG3m(s) sample exhibits a slightly lower mass, which is expected since this IgG3 allotype lacks one of the hinge repeat motifs. The single donor samples were visibly less pure than the other IgG3 samples, which is likely due to differences in sample preparation. The bands were excised and the proteins were reduced using DTT followed by alkylation of cysteine residues and subsequently overnight digestion with either trypsin or proteinase K. The samples were then analyzed by nanoLC-RP-ESI-IT-MS(/MS), and the resulting data was subjected to automated primary sequence database searching for protein identification (Supplemental Table S3.3). All bands at approximately 60 kDa were confirmed to contain the IgG3 heavy chain, while the lower bands at 25-30 kDa contained either kappa light chain (in the monoclonal samples) or both kappa and lambda light chains (in the polyclonal samples). The lower band at approximately 52 kDa which was visible in the single donor samples (Supplemental Figure S3.1) was found to contain mainly IgG1, 2 and 3, as determined by examining subclass-specific peptides (data not shown).

O-glycopeptides were detected by searching the LC-MS/MS fragmentation spectra for oxonium fragment ions, which are characteristic for glycopeptide fragmentation: *m/z* 366.14 $[HexNAc + Hex + H]^+$; *m/z* 292.10 $[NeuAc + H]^+$; *m/z* 274.09 $[NeuAc - H_2O + H]^+$; and *m/z* 657.23 $[HexNAc + Hex + NeuAc + H]^+$. Three types of *O*-glycans were identified in the trypsin and proteinase K digests of all IgG3 samples: [1 HexNAc + 1 Hex], [1 HexNAc + 1 Hex + 1 NeuAc], and [1 HexNAc + 1 Hex + 2 NeuAc]. The fragmentation spectra of the tryptic glycopeptides are depicted in Figure 3.1.

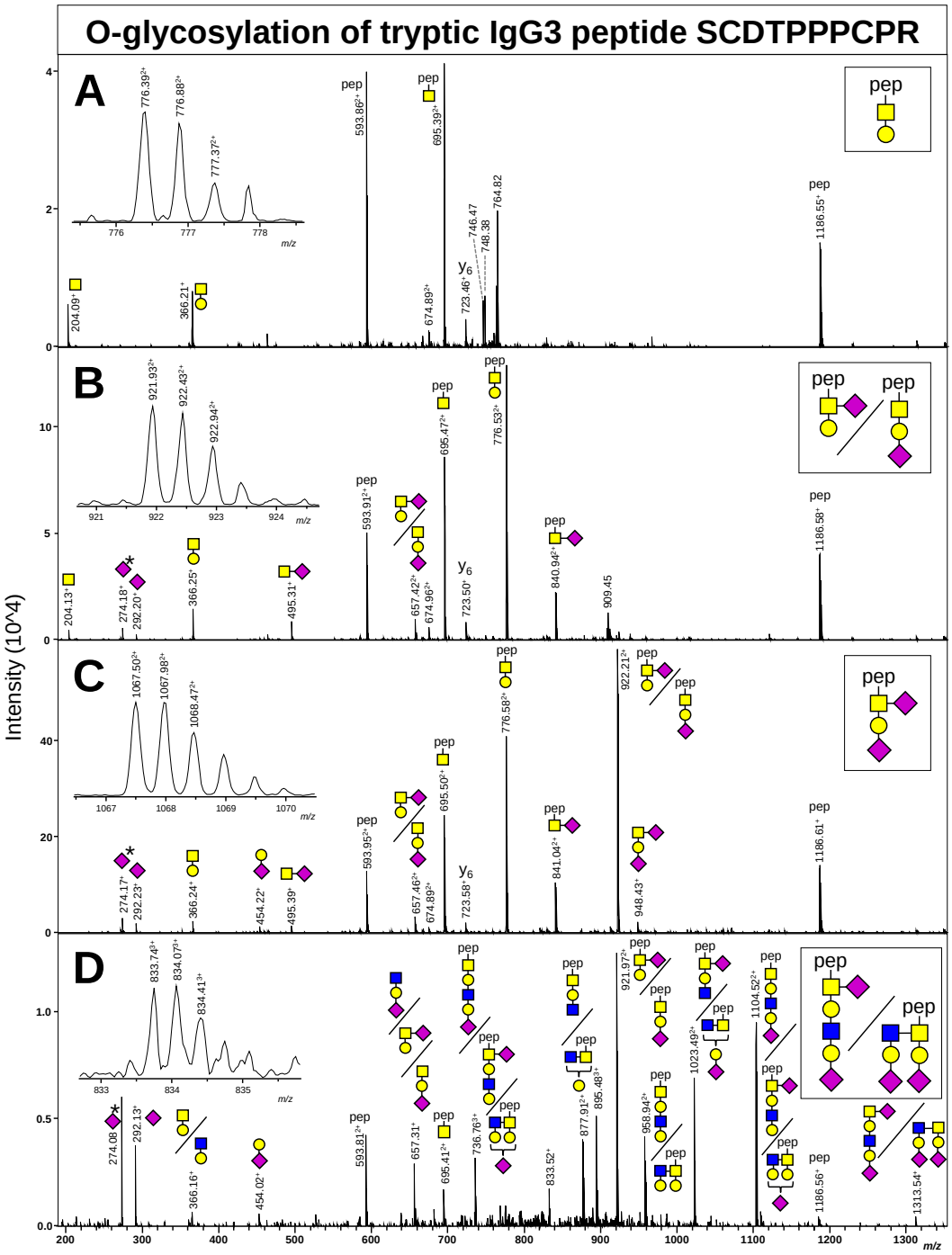

Figure 3.1: NanoLC-ESI-IT-CID spectra showing fragmentation of various trypsin-generated recombinant IgG3m(g) *O*-glycopeptides. Non-, mono- and disialylated core 1 type *O*-glycans (A-C) were seen attached to the peptide SCDTPPPCPR, as well as a disialylated *O*-glycan with an *N*-acetyllactosamine (*N*-acetylglucosamine + galactose) (D). These structures are partially based on literature, since it is difficult to distinguish between different types of hexoses and *N*-acetylhexosamines with mass spectrometry. The triply charged peak at *m/z* 895.48 in panel D has a higher mass than the precursor mass, and thus likely originates from a contaminant. The MS1 precursor peak is shown for each fragmentation spectrum. Pep = peptide; yellow square = *N*-acetylgalactosamine, yellow circle = galactose; blue square = *N*-acetylglucosamine; purple diamond = *N*-acetylneuraminic acid.

While mass spectrometry does not reveal the exact identity of the monosaccharides, digestion of these glycopeptides by sialidase and galactosidase led to complete trimming of the oligosaccharides (Supplemental Figure S3.2), thereby confirming the presence of α2-linked *N*-acetylneuraminic acid and β1-linked galactose. Based on literature, we expect the HexNAc attached to the peptide to be an *N*-acetylgalactosamine (32). The encountered glycan structures are therefore presumably a non-, mono- and disialylated core 1 type *O*-glycan. A minor fraction but distinct fourth type of *O*-glycan was seen only in the monoclonal recombinant IgG3 samples: [2 HexNAc + 2 Hex + 2 NeuAc] (Figure 3.1D). The peak at 1313.54^{1+} in the MS/MS spectrum corresponds to the intact *O*-glycan B-ion (the nomenclature for glycan fragmentation is described by Domon and Costello (33)), indicating a hexasaccharide *O*-glycan which may be a core 1 or core 2 type. A comprehensive overview of the *m/z* values in MS1 and MS2 spectra corresponding to the *O*-glycopeptides can be found in Supplemental Table S3.4.

3.4.2: Localization of the IgG3 *O*-glycosylation site

The amino acid sequence of the trypsin- and proteinase K-generated *O*-glycopeptides was identified through MS3 fragmentation of the peptide. In tryptic digests, the same peptides were also seen without glycans attached, demonstrating that the *O*-glycosylation sites are only partially occupied. The peptide sequences could be traced back to a triple repeat sequence within the IgG3 hinge region (Figure 3.2). This region contains 6 potential *O*-glycosylation sites: 3 threonine residues and 3 serine residues. The conventional EU notation for IgG3 (34), which is based on homology between all IgG subclasses, does not cover the triple repeat sequence, and therefore an alternative notation method was introduced to refer to amino acid residues within the IgG3 hinge region. The IgG3 hinge covers four exons, the last three of which encode for the same amino acid sequence (allotype IgG3m(s) forms an exception since it has only two repeats). The location of an amino acid within the hinge region will be specified as ‘HX-Y’, with ‘X’ standing for the exon number (1/2/3/4) and Y for the amino acid number within the exon (1-17).

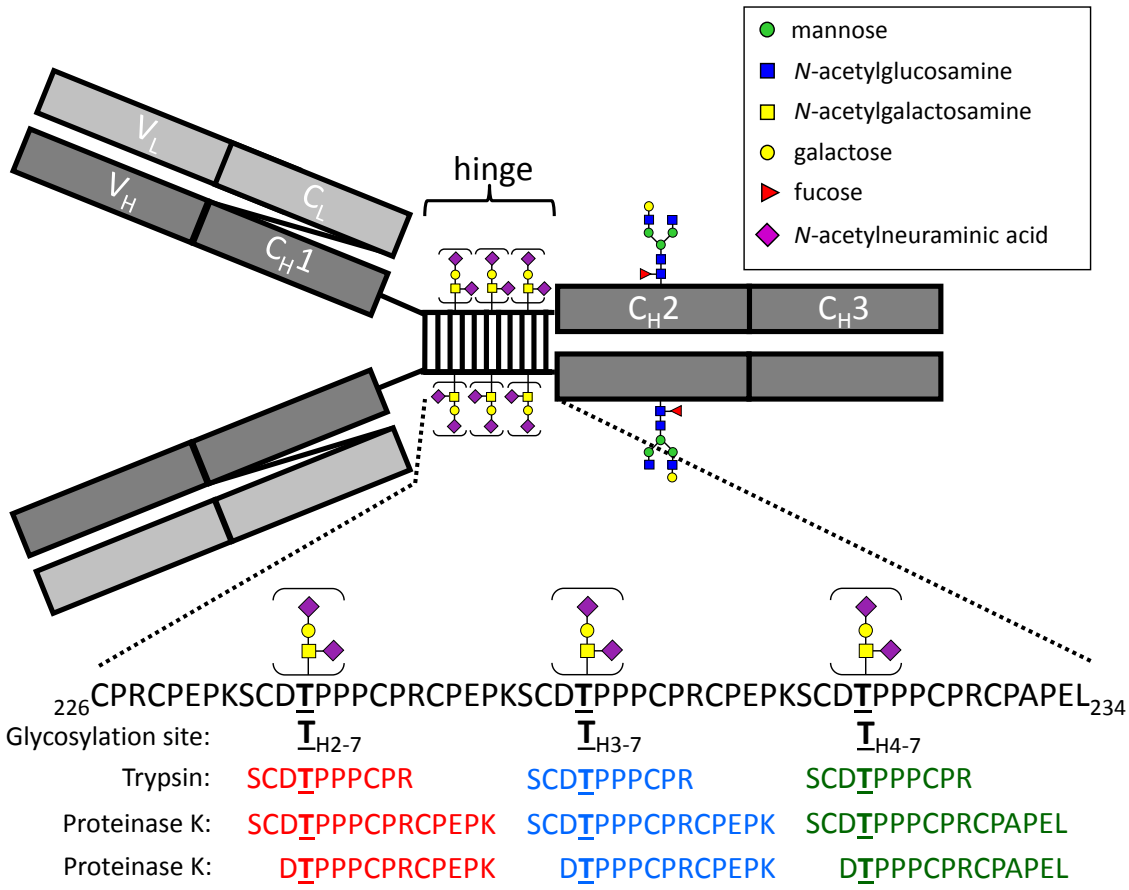

Figure 3.2: A schematic overview of IgG3, which consists of two heavy chains (shown in dark grey, 1 variable and 3 conserved domains) and two light chains (light grey, 1 variable and 1 conserved domain). Black bars represent interchain disulfide bonds. An *N*-glycosylation site is present in domain CH2. Each IgG3 heavy chain contains three hinge repeat sequences with two or three partially occupied *O*-glycosylation sites. The peptide sequences of the major trypsin- and proteinase K-generated *O*-glycopeptides are shown.

The proteinase K-generated glycopeptide $_{H4-6}$DTPPPCPRCPAPEL$_{234}$ demonstrates that T_{H4-7} is occupied, while $_{H2/3-6}$DTPPPCPRCPEPK$_{H3/4-3}$ demonstrates that either T_{H2-7} or T_{H3-7} or both are also occupied. However, the proteinase K digest did not allow us to either confirm or disprove that serine residues were also occupied, since all *O*-glycopeptides which contain a serine residue also contain a threonine residue.

We therefore attempted to use endoproteinase AspN in order to further digest trypsin-generated *O*-glycopeptides derived from monoclonal IgG3 from 'SCDTPPPCPR' to 'SC' and 'DTPPPCPR'. However, while the majority of the non-glycosylated tryptic hinge repeat peptides were cleaved by AspN, the *O*-glycopeptides with the same peptide sequence remained undigested. The *O*-glycopeptides also remained resistant to AspN-digestion after

the tryptic *O*-glycopeptides were treated with sialidase and galactosidase, trimming most of the *O*-glycans down to a single *N*-acetylhexosamine (data not shown).

In order to obtain further evidence about the position of the *O*-glycans within the IgG3 hinge region, we performed nanoLC-ESI-IT-MS/MS analysis with electron transfer dissociation (ETD) on a sialidase- and galactosidase-treated tryptic digest of IgG3m(s). Peptide backbone fragmentation with retention of the glycan moiety could be observed in the resulting mass spectrum and this appeared to be in line with occupation of the threonine residue (Figure 3.3A). NanoLC-ESI-IT-MS/MS with CID fragmentation also revealed signals which appear to show peptide backbone fragmentation with glycan retention, but the signal intensity was too low be definitive (data not shown). By using the more sensitive technique t-ITP-CE-ESI-qTOF-MS/MS with CID fragmentation to analyze sialidase- and galactosidase-treated trypsin-digested IgG3 derived from pooled plasma (Figure 3.3B-C), we were able to observe minor peaks (y7 and y8) pertaining to peptide backbone fragmentation without glycan loss, indicating occupation of the threonine residue.

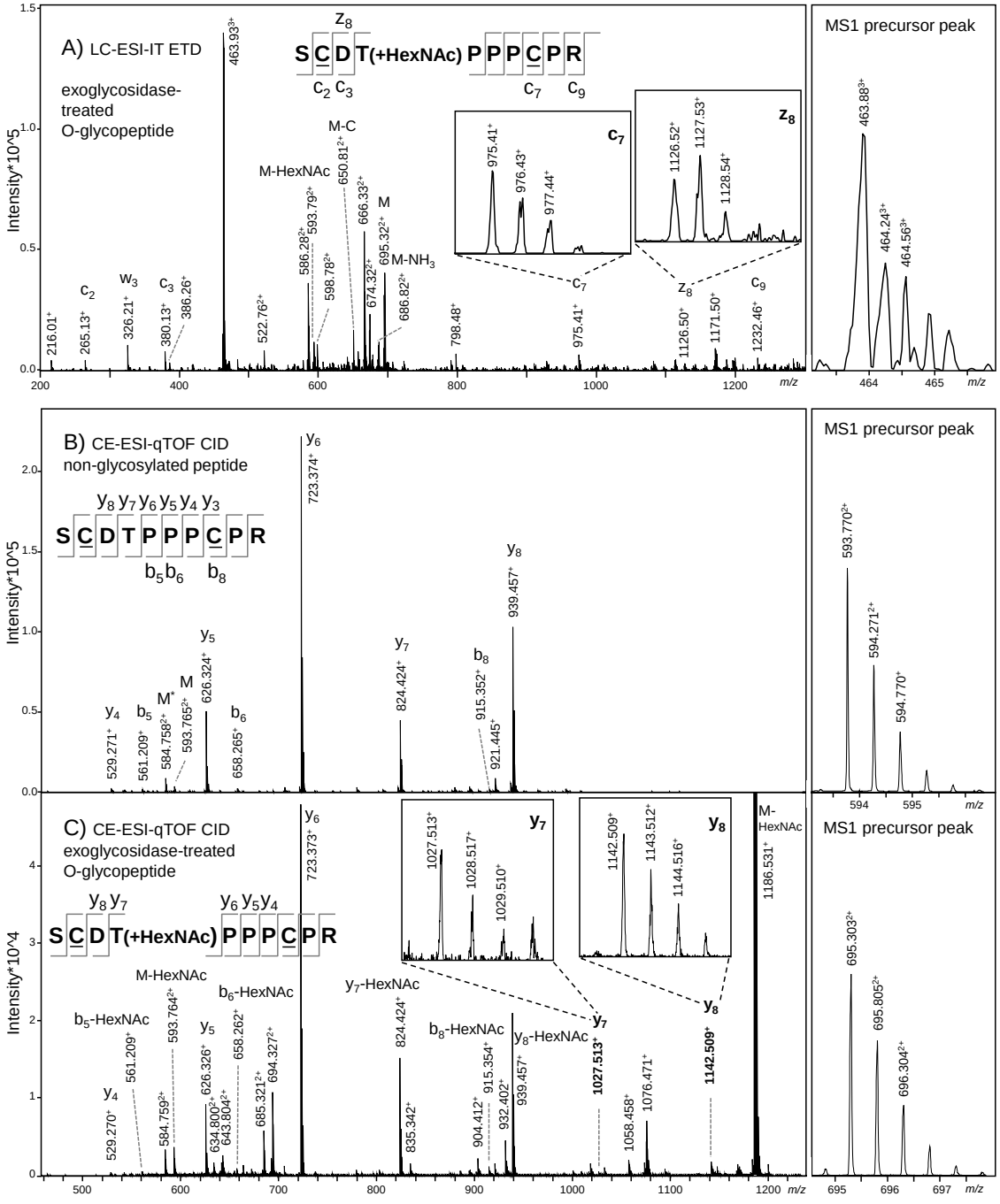

Figure 3.3 A) NanoLC-ESI-IT-MS/MS with electron transfer dissociation (ETD) fragmentation of a sialidase- and galactosidase-treated tryptic glycopeptide of recombinant IgG3m(s). Peptide backbone fragmentation (c- and z-ions) and loss of the *N*-acetylhexosamine (HexNAc) or cysteine side chain (C) were observed. B-C) CE-ESI-beam-type CID analysis was done on sialidase- and galactosidase-treated tryptic peptides of IgG3 derived from pooled plasma, and fragmentation spectra are shown for B) the unoccupied tryptic hinge peptide SCDTPPPCPR and C) the *O*-glycosylated version of the same peptide with a single *N*-acetylgalactosamine attached. The b- and y-ions are annotated. The MS1 precursor peak is shown on the right. The doubly charged peak at *m/z* 694.327 in panel C is likely a coeluting compound which appears in the spectrum because it was present within the precursor *m/z* window, and the peak at *m/z* 694.321 is the same compound after loss of water. The cysteine residues have been underlined to denote carbomidomethylation.

To further establish that the *O*-glycan resides only on the threonine residue, several recombinant anti-TNP IgG3m(g) proteins were produced, in which either the three serines, the three threonines or all six potential *O*-glycosylation sites in the hinge repeat region were replaced by alanine, along with wild type IgG3m(g) as a control (protein sequences are listed in Supplemental Table S3.2). As expected, LC-MS/MS analysis of the wild type IgG3, digested with trypsin or proteinase K, revealed *O*-glycosylation of the hinge region, while no *O*-glycosylation was seen on the IgG3 in which all six potential *O*-glycosylation sites had been replaced by alanine. IgG3 that only lacked the hinge region serines contained the same *O*-glycans seen in wild type IgG3. No *O*-glycopeptides were found in IgG3 lacking threonines in the hinge repeat, again suggesting that the *O*-glycans within the IgG3 hinge region reside only on the threonine residue and not on serine (Supplemental Figure S3.3).

3.4.3: Relative quantification of IgG3 *O*- and *N*-glycosylation

Relative quantification of the *O*-glycosylation was done using LC-MS data of trypsin-digested IgG3. The abundances of the different glycans attached to the peptide SCDTPPPCPR were normalized to the total of all glycopeptides (Figure 3.4A). When the *O*-glycopeptide values were normalized on the sum of both *O*-glycopeptides and unoccupied peptide, we found the following *O*-glycopeptide abundances: 3.3% (standard deviation +/- 0.6) for IgG3 from pooled plasma; 21.9% (+/- 2.9) for recombinant IgG3m(g) with three hinge repeats; 18.5% (+/- 1.8) for IgG3m(s) with two hinge repeats; and 11.6 % (+/- 1.9) on average for single donor-derived IgG3 (Supplemental Table S3.5). We observed a slight fluctuation in the ratio of the signals of IgG3-hinge-derived *O*-glycopeptides vs. unoccupied peptide, which results in a larger technical variation than when we normalize on *O*-glycopeptides only. It is known that large glycans moieties may result in a considerably lowered ionization of the glycopeptide as compared to the corresponding non-glycosylated peptide (35), making it difficult to compare peptide and glycopeptide signal intensities. Therefore, in an attempt to obtain reliable relative quantification data, tryptic IgG3 *O*-glycopeptides were treated with exoglycosidases, which should trim all *O*-glycans down to a single *N*-acetylgalactosamine, with the exception of the minor hexasaccharide glycoform which likely contains an *N*-acetylglucosamine. We observed a low intensity signal at *m/z* 877.85 which appears to be an exoglycosidase digestion product of this hexasaccharide glycan with 2 HexNAc and 1 Hex remaining, indicating that the glycan may be core 1 type. LC-MS analysis of the exoglycosidase-treated tryptic IgG3 (*O*-glyco)peptides showed that

approximately 10% of the *O*-glycosylation sites within IgG3 derived from each of the six donors carried an *O*-glycan (Figure 3.4B), and the inter-individual differences appear to be relatively small. Monoclonal IgG3 exhibited a slightly higher degree of *O*-glycosylation, with approximately 12-14% of the sites occupied. IgG3 derived from pooled plasma showed a much lower level of *O*-glycosylation (5%), as well as a markedly lower abundance of the disialylated *O*-glycan [1 HexNAc + 1 Hex + 2 NeuAc], while showing increased levels of monosialylated *O*-glycans compared to the other IgG3 samples (Figure 3.4A). Upon calculation of the number of *N*-acetylneuraminic acids per *O*-glycan (Figure 3.4C), the deviation of IgG3 derived from pooled plasma became even more apparent.

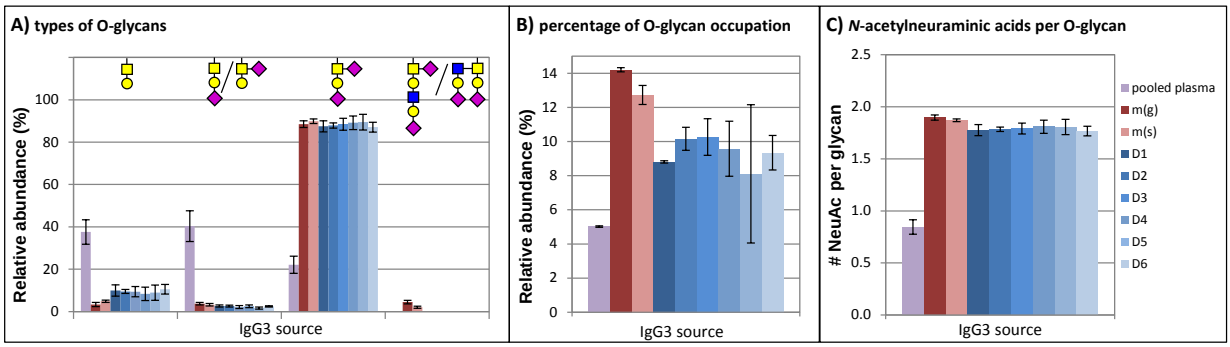

Figure 3.4: A) Relative quantification of IgG3 *O*-glycosylation based on nanoLC-ESI-IT-MS analysis of tryptic glycopeptides from various IgG3 samples (IgG3 derived from pooled plasma, 2 monoclonal IgG3 allotypes and IgG3 purified from six donors (D1-6)). The signal intensities were normalized on the sum of all hinge-derived *O*-glycopeptides. The relative abundance and technical variation are based on LC-MS analyses of 4 distinct tryptic digests, each of them measured twice. The values given for glycopeptide NHS are expected to be significantly lower than the actual values, because the triply charged compound overlapped with the doubly charged hinge peptide with a putative acetylation modification in all samples, leaving only the doubly charged peak for relative quantification. B) An estimate of the total percentage of *O*-glycosylation was derived from relative quantification of tryptic (glyco)peptides which had been treated with exoglycosidases, trimming all *O*-glycans down to a single HexNAc. The averages and standard deviation are based on 2 LC-MS analyses of the same sample. C) The number of *N*-acetylneuraminic acids per *O*-glycan was calculated from the same *O*-glycopeptide data listed under A). A comprehensive list of values is available in Supplemental Table S3.5.

In all IgG3 samples, a modified version of the hinge peptide SCDTPPPCPR was observed, with a mass increase of +42.04 Da which could consist of acetylation. This modification was observed on both the non-glycosylated and glycosylated peptide, and the percentage of modified peptide was found to be stable at approximately 15% regardless of the type of *O*-glycan attached or the IgG3 sample source. LC-ESI-IT-MS/MS spectra show that the modification appears to be present on the N-terminal serine or cysteine residue. When IgG3 was digested in-solution without reduction alkylation (data not shown), the modification was

not observed on the resulting disulfide bridge-linked hinge peptide dimer, indicating that the modification is an artefact of the sample processing. Furthermore, peaks with masses corresponding to the a hinge peptide with an acrylamide adduct (*m/z* 600.75 (2+)) or with an oxidized disulphide bridge (*m/z* 535.70 (2+)) were also seen, but since their signal intensity was only around 5% or less than 2%, respectively, of the signal intensity of the main peptide peak, we do not expect these modifications to significantly influence our results with regard to glycopeptide quantification.

Because the type and quantity of *O*-glycosylation appeared similar in IgG3 derived from different single donors, we also investigated inter-individual differences in Fc *N*-glycosylation at position N297. Relative quantification of Fc *N*-glycosylation was done using tryptic digests of single donor IgG3 (Supplemental Figure S3.4 and Supplemental Table S3.6). Minor differences were observed between the IgG2/3 *N*-glycosylation of these donors, most pronounced for the degree of galactosylation.

In-solution trypsin digestion of IgG3 without reduction alkylation produces a dimer of the hinge repeat peptide held together by two interchain disulfide bridges. Mono-glycosylated dimers were observed in all IgG3 samples. In the monoclonal IgG3 samples, a dimer with two disialylated glycans attached was seen at a very low abundance (approximately 1.0% (G3m(g)) and 0.4% (G3m(s)) of the total of *O*-glycopeptides + peptide) (Supplemental Table S3.7); in the polyclonal IgG3 samples we did not observe a di-glycosylated dimer, which may be due to the fact that these samples were less pure than the monoclonal samples and thus had a higher background in LC-MS.

3.4.4: *O*-glycosylation of Fc constructs with an IgG4 hinge

Four recombinant IgG Fc constructs produced in HEK cells, all carrying an IgG4 hinge (30), were also found to carry *O*-glycans (Supplemental Figure S3.5). The Fc-domains consisted either of the G3m(b) or G3m(c3c5) allotypes for IgG3 or IgG4 with V397M or V397M and K392N; protein sequences can be reviewed in Supplemental Table S3.2. The *O*-glycopeptides observed in LC-MS(/MS) analysis of chymotrypsin and proteinase K digests contained one potential glycosylation site: a serine residue in the hinge region at what in intact IgG4 would be position 228; the peptide sequences of the encountered *O*-glycopeptides are listed in Supplemental Table S3.4.

Because of these findings, we also investigated whether *O*-glycosylation was present on whole IgG4. We obtained IgG4 from the serum of a patient with high IgG4 levels and from the serum of a rheumatoid arthritis patient, as well as an IgG4 sample produced in HEK cells and a humanized murine IgG4 therapeutic antibody. LC-MS(/MS) analysis of trypsin and proteinase K digests revealed the peptide covering S228, but no *O*-glycans were observed.

3.5: Discussion

IgG3 stands out from the other IgG subclasses due to its elongated hinge region and enhanced effector functions. In this paper we demonstrate for the first time partial *O*-glycosylation of threonine residues within the triple repeat sequence in the hinge region of each IgG3 heavy chain. Non-, mono- and disialylated core 1 type *O*-glycans were identified in IgG3 from various sources. A hexasaccharide disialylated *O*-glycan was also present at a very low abundance, but only in the monoclonal IgG3 samples.

3.5.1: Relative abundance and distribution of IgG3 *O*-glycosylation

An estimate of the relative abundance of the various *O*-glycans was determined from nanoLC-ESI-IT-MS analysis of trypsin-generated (glyco)peptides. It should be noted that because the signal of the monosialylated *O*-glycopeptide in triply charged state overlapped with the doubly charged peak of the hinge repeat peptide with a putative acetylation modification in all samples, only the doubly charged signal of the monosialylated *O*-glycopeptide was quantified, thereby leading to an underestimation of this *O*-glycoform. Furthermore, it is known that glycopeptides with different glycan structures can have different response factors (35), and thus the relative abundances we measured may not accurately reflect the real ratios. In order to obtain a more reliable estimate of the percentage of the hinge repeat motif bearing an *O*-glycan, tryptic IgG peptides were incubated with exoglycosidases, trimming all *O*-glycans down to a single *N*-acetylhexosamine. A previous study of quantitative measurements of a single glycosylated peptide using nanoLC-ESI-IT-MS found that the glycopeptide with a single *N*-acetylglucosamine produced signal strengths similar to the non-glycosylated peptide (35). Given the structural similarities between *N*-acetylglucosamine and *N*-acetylgalactosamine, we expect our method of relative quantification of de-sialylated and de-galactosylated *O*-glycopeptides to give a reliable estimate of the degree of *O*-glycosylation.

Approximately 10% of the hinge repeat threonines carry an *O*-glycan in polyclonal IgG3 derived from donor sera. Despite differences in the age and sex of the donors, the degree and type of *O*-glycosylation appears similar in all 6 samples. This is in contrast to the *N*-glycosylation profiles of these samples, which do show inter-individual differences in agreement with literature (36). In the two monoclonal IgG3 allotypes we examined, IgG3m(g) and IgG3m(s), approximately 12-14% of the *O*-glycosylation sites were occupied;

this increase may be due to the expression system (HEK cells) in which these antibodies were produced (37).

A clear difference in *O*-glycosylation was seen between the commercially obtained IgG3 sample derived from pooled plasma and the other IgG3 samples: the former exhibited a much lower level of terminal *N*-acetylneuraminic acids per *O*-glycan, as well as a lower level of *O*-glycosylation overall. Two explanations could be found in the details of the preparation process which were supplied by the manufacturer of this IgG3 sample: boric acid was used for precipitation and a jacalin column was used to remove a minor IgA contaminant. Acidic treatment has been known to cause loss of terminal *N*-acetylneuraminic acid (38). However, the *N*-glycans of pooled plasma-derived IgG3 did not show a decrease in sialylation compared to single donor-derived IgG3, which makes it unlikely that boric acid treatment is responsible for the lower level of *O*-glycan sialylation. Jacalin is a plant lectin with affinity for core 1 type *O*-glycans; it binds *O*-glycosylated proteins such as IgA1, as well as several animal IgGs which are suspected of carrying *O*-glycosylation (39, 40). However, it has been reported that jacalin has a higher affinity for non-sialylated than for sialylated *O*-glycans in the case of fetuin (40), and the same was observed for monoclonal IgG3 which was run over a jacalin column and found to be depleted for non-sialylated and partially depleted for monosialylated but not for disialylated *O*-glycans (unpublished data). This does not explain why the pooled plasma-derived IgG3 would exhibit lower levels of disialylated *O*-glycans and higher levels of monosialylated *O*-glycans compared to single donor serum-derived IgG3. In any case, it is difficult to say anything about possible depletion without being able to observe the *O*-glycosylation profile of the original non-jacalin-treated pooled plasma sample. Because it was shown that jacalin interacts with the *O*-glycosylated IgG3 hinge and because of the deviating *O*-glycosylation profile obtained from the jacalin-treated pooled plasma-derived sample vs IgG3 from single human donors obtained without jacalin-depletion, the results obtained for this IgG3 sample will not be deemed representative for the overall human population.

It is likely that the *O*-glycosylation is distributed randomly among all IgG3s, since monoclonal cell cultures were found to produce partially *O*-glycosylated instead of either fully or non-*O*-glycosylated IgG3. Furthermore, hinge peptide-dimer repeats linked by interchain disulfide bridges rarely carry two *O*-glycans, which indicates that the *O*-glycosylation is not clustered on a subset of the IgG3 molecules. If the *O*-glycosylation is

distributed randomly, approximately half (1 – probability of 6 unoccupied sites = 1–((1-0.10)^6) = 47%) of the IgG3s would be expected to carry at least 1 *O*-glycan. We observed that less than 1% of hinge peptide-dimer repeats carried 2 disialylated *O*-glycans in monoclonal IgG3 samples, whereas the expected value assuming random *O*-glycosylation site occupancy would be approximately 3.8% (G3m(g)) and 2.8% (G3m(s)). These findings indicate that addition of *O*-linked glycans is inhibited if a glycan is already present at the adjacent site on the opposing heavy chain, thus dispersing the *O*-glycosylation across a higher percentage of IgG3s.

3.5.2: Criteria determining IgG hinge-region *O*-glycosylation

Based on the amino acid sequence of the IgG3 hinge repeat region, it is not surprising that it forms a target for *O*-glycosylation. It is known that *O*-glycosylation occurs in sequences with a high abundance of proline residues, preferentially at position -1 and +3 relative to the glycosylation site (41). In the IgG3 hinge repeat, 6 of the 16 amino acid residues consist of prolines, including one at position +3 relative to the glycosylation site. Furthermore, due to its extended formation, the IgG3 hinge region has a high degree of surface accessibility (42), which is also associated with *O*-glycosylation (43). Surface accessibility may be responsible for the slightly lower degree of *O*-glycosylation observed in recombinant IgG3m(s) compared to m(g): the shorter length of the hinge region of IgG3m(s), which contains two hinge repeats instead of three, could decrease the accessibility for glycosyltransferases. No *O*-glycosylation was observed at the threonine residues at the N-terminal end of the hinge, T_{H1-4}, T_{H1-9} and T_{H1-10}, which may be due to either the local amino acid sequence or the secondary structure of this region.

O-glycosylation was also found to be present on the IgG4 hinge of Fc constructs with IgG4 or IgG3 CH2 and CH3 domains. This is not surprising considering the high abundance of proline residues (at position -4, -3, -1, 2 and 4 relative to *O*-glycosylation site S228) in the IgG4 hinge region, which are a well-known marker for *O*-glycosylation (41). However, intact IgG4, whether purified from serum or expressed in the same HEK cell expression system as the Fc constructs, was not found to carry hinge region *O*-glycosylation. It is therefore likely that the presence of the Fab fragment influences the accessibility of the hinge region, preventing the attachment of an *O*-glycan in the Golgi apparatus in the case of intact IgG4. Similarly, *O*-glycosylation was recently reported on an IgG1 Fc-fragment produced in HEK and CHO cells, but not on intact IgG1 produced under the same circumstances (44). This re-

enforces the notion that accessibility is essential for the attachment of *O*-glycans (43). For human IgG3 this is provided by the extensive length of its IgG3 hinge which in the intact IgG molecules for other IgG subclasses is shielded by the Fab fragments.

3.5.3: Function of IgG3 *O*-glycosylation

The function of the *O*-glycans found on the IgG3 hinge region has not been investigated, but previous findings give rise to several options. Firstly, the hinge glycosylation might prohibit proteolytic degradation. The IgG hinge is the target of a number of bacterial or endogenous proteases (45, 46), and the extended structure of the IgG3 hinge is presumably the reason that IgG3 is more susceptible to proteolytic degradation than the other IgG subclasses (47-49). We found that tryptic IgG3 *O*-glycopeptides were resistant against endoprotease AspN digestion, while the corresponding non-glycosylated peptides were not, thus providing evidence that the hinge region *O*-glycans can shield the hinge region from proteolytic cleavage. In contrast, we did not observe any evidence of incomplete trypsin digestion in the form of miscleaved *O*-glycopeptides. *O*-glycosylation has also been found to mediate protease resistance in other immunoglobulins, such as mouse IgG2b and IgA (23, 27). Another function for the hinge region oligosaccharides could consist of helping the hinge region maintain an extended conformation, which might contribute to the flexibility and orientation of the Fab fragments and thereby influence divalent binding to target antigens.

Furthermore, it could be speculated that deviations in the *O*-glycosylation of IgG3 may have pathological effects, as has been described for IgA nephropathy (50). Aberrant glycosylation of IgA1 is known to play a causal role in IgA nephropathy: the truncated *O*-glycans are recognized by immunoglobulins, leading to the formation of antibody complexes which are deposited on blood vessel walls near the glomerulus (50, 51). A similar mechanism involving IgG3 *O*-glycosylation could be theorized to play a role in IgG nephropathy. It has been shown that patients with membranoproliferative glomerulonephritis, a subtype of primary glomerulopathy, have IgG deposits which consist predominantly of IgG3, which may be in line with a causal role for IgG3 *O*-glycosylation (52). Further research is required to determine the exact nature and functional consequences of IgG3 hinge glycosylation.

References

1. Stoop, J. W., Zegers, B. J., Sander, P. C., and Ballieux, R. E. (1969) Serum immunoglobulin levels in healthy children and adults. *Clin Exp Immunol* 4, 101-112
2. Morell, A., Terry, W. D., and Waldmann, T. A. (1970) Metabolic properties of IgG subclasses in man. *J Clin Invest* 49, 673-680
3. Vidarsson, G., Dekkers, G., and Rispens, T. (2014) IgG subclasses and allotypes: from structure to effector functions. *Front Immunol* 5, 520
4. Roux, K. H., Strelets, L., and Michaelsen, T. E. (1997) Flexibility of human IgG subclasses. *J Immunol* 159, 3372-3382
5. Dangl, J. L., Wensel, T. G., Morrison, S. L., Stryer, L., Herzenberg, L. A., and Oi, V. T. (1988) Segmental flexibility and complement fixation of genetically engineered chimeric human, rabbit and mouse antibodies. *EMBO J* 7, 1989-1994
6. Scharf, O., Golding, H., King, L. R., Eller, N., Frazier, D., Golding, B., and Scott, D. E. (2001) Immunoglobulin G3 from polyclonal human immunodeficiency virus (HIV) immune globulin is more potent than other subclasses in neutralizing HIV type 1. *J Virol* 75, 6558-6565
7. Cavacini, L. A., Emes, C. L., Power, J., Desharnais, F. D., Duval, M., Montefiori, D., and Posner, M. R. (1995) Influence of heavy chain constant regions on antigen binding and HIV-1 neutralization by a human monoclonal antibody. *J Immunol* 155, 3638-3644
8. Redpath, S., Michaelsen, T., Sandlie, I., and Clark, M. R. (1998) Activation of complement by human IgG1 and human IgG3 antibodies against the human leucocyte antigen CD52. *Immunology* 93, 595-600
9. Norderhaug, L., Brekke, O. H., Bremnes, B., Sandin, R., Aase, A., Michaelsen, T. E., and Sandlie, I. (1991) Chimeric mouse human IgG3 antibodies with an IgG4-like hinge region induce complement-mediated lysis more efficiently than IgG3 with normal hinge. *Eur J Immunol* 21, 2379-2384
10. Natsume, A., In, M., Takamura, H., Nakagawa, T., Shimizu, Y., Kitajima, K., Wakitani, M., Ohta, S., Satoh, M., Shitara, K., and Niwa, R. (2008) Engineered antibodies of IgG1/IgG3 mixed isotype with enhanced cytotoxic activities. *Cancer Res* 68, 3863-3872
11. Hogarth, P. M., and Pietersz, G. A. (2012) Fc receptor-targeted therapies for the treatment of inflammation, cancer and beyond. *Nat Rev Drug Discov* 11, 311-331
12. Canfield, S. M., and Morrison, S. L. (1991) The Binding-Affinity of Human-Igg for Its High-Affinity Fc Receptor Is Determined by Multiple Amino-Acids in the Ch2 Domain and Is Modulated by the Hinge Region. *Journal of Experimental Medicine* 173, 1483-1491
13. Stapleton, N. M., Andersen, J. T., Stemerding, A. M., Bjarnarson, S. P., Verheul, R. C., Gerritsen, J., Zhao, Y., Kleijer, M., Sandlie, I., de Haas, M., Jonsdottir, I., van der Schoot, C. E., and Vidarsson, G. (2011) Competition for FcRn-mediated transport gives rise to short half-life of human IgG3 and offers therapeutic potential. *Nat Commun* 2, 599
14. Einarsdottir, H., Ji, Y., Visser, R., Mo, C., Luo, G., Scherjon, S., van der Schoot, C. E., and Vidarsson, G. (2014) H435-containing immunoglobulin G3 allotypes are transported efficiently across the human placenta: implications for alloantibody-mediated diseases of the newborn. *Transfusion* 54, 665-671
15. Dard, P., Lefranc, M. P., Osipova, L., and Sanchez-Mazas, A. (2001) DNA sequence variability of IGHG3 alleles associated to the main G3m haplotypes in human populations. *Eur J Hum Genet* 9, 765-772
16. Jefferis, R., and Lefranc, M. P. (2009) Human immunoglobulin allotypes: possible implications for immunogenicity. *MAbs* 1, 332-338
17. Dard, P., Huck, S., Frippiat, J. P., Lefranc, G., Langaney, A., Lefranc, M. P., and Sanchez-Mazas, A. (1997) The IGHG3 gene shows a structural polymorphism characterized by different hinge lengths: sequence of a new 2-exon hinge gene. *Hum Genet* 99, 138-141

18. Anthony, R. M., and Nimmerjahn, F. (2011) The role of differential IgG glycosylation in the interaction of antibodies with FcgammaRs in vivo. *Curr Opin Organ Transplant* 16, 7-14
19. Shields, R. L., Lai, J., Keck, R., O'Connell, L. Y., Hong, K., Meng, Y. G., Weikert, S. H., and Presta, L. G. (2002) Lack of fucose on human IgG1 N-linked oligosaccharide improves binding to human Fcgamma RIII and antibody-dependent cellular toxicity. *J Biol Chem* 277, 26733-26740
20. Kapur, R., Kustiawan, I., Vestrheim, A., Koeleman, C. A., Visser, R., Einarsdottir, H. K., Porcelijn, L., Jackson, D., Kumpel, B., Deelder, A. M., Blank, D., Skogen, B., Killie, M. K., Michaelsen, T. E., de Haas, M., Rispens, T., van der Schoot, C. E., Wuhrer, M., and Vidarsson, G. (2014) A prominent lack of IgG1-Fc fucosylation of platelet alloantibodies in pregnancy. *Blood* 123, 471-480
21. Kaneko, Y., Nimmerjahn, F., and Ravetch, J. V. (2006) Anti-inflammatory activity of immunoglobulin G resulting from Fc sialylation. *Science* 313, 670-673
22. Karsten, C. M., Pandey, M. K., Figge, J., Kilchenstein, R., Taylor, P. R., Rosas, M., McDonald, J. U., Orr, S. J., Berger, M., Petzold, D., Blanchard, V., Winkler, A., Hess, C., Reid, D. M., Majoul, I. V., Strait, R. T., Harris, N. L., Kohl, G., Wex, E., Ludwig, R., Zillikens, D., Nimmerjahn, F., Finkelman, F. D., Brown, G. D., Ehlers, M., and Kohl, J. (2012) Anti-inflammatory activity of IgG1 mediated by Fc galactosylation and association of FcgammaRIIB and dectin-1. *Nat Med* 18, 1401-1406
23. Kim, H., Yamaguchi, Y., Masuda, K., Matsunaga, C., Yamamoto, K., Irimura, T., Takahashi, N., Kato, K., and Arata, Y. (1994) O-glycosylation in hinge region of mouse immunoglobulin G2b. *J Biol Chem* 269, 12345-12350
24. Mattu, T. S., Pleass, R. J., Willis, A. C., Kilian, M., Wormald, M. R., Lellouch, A. C., Rudd, P. M., Woof, J. M., and Dwek, R. A. (1998) The glycosylation and structure of human serum IgA1, Fab, and Fc regions and the role of N-glycosylation on Fcalpha receptor interactions. *J Biol Chem* 273, 2260-2272
25. Takahashi, N., Tetaert, D., Debuire, B., Lin, L. C., and Putnam, F. W. (1982) Complete amino acid sequence of the delta heavy chain of human immunoglobulin D. *Proc Natl Acad Sci U S A* 79, 2850-2854
26. Takayasu, T., Suzuki, S., Kametani, F., Takahashi, N., Shinoda, T., Okuyama, T., and Munekata, E. (1982) Amino acid sequence of galactosamine-containing glycopeptides in the hinge region of a human immunoglobulin D. *Biochem Biophys Res Commun* 105, 1066-1071
27. Reinholdt, J., Tomana, M., Mortensen, S. B., and Kilian, M. (1990) Molecular aspects of immunoglobulin A1 degradation by oral streptococci. *Infect Immun* 58, 1186-1194
28. Kruijsen, D., Einarsdottir, H. K., Schijf, M. A., Coenjaerts, F. E., van der Schoot, E. C., Vidarsson, G., and van Bleek, G. M. (2013) Intranasal administration of antibody-bound respiratory syncytial virus particles efficiently primes virus-specific immune responses in mice. *J Virol* 87, 7550-7557
29. Vink, T., Oudshoorn-Dickmann, M., Roza, M., Reitsma, J. J., and de Jong, R. N. (2014) A simple, robust and highly efficient transient expression system for producing antibodies. *Methods* 65, 5-10
30. Rispens, T., Davies, A. M., Ooijevaar-de Heer, P., Absalah, S., Bende, O., Sutton, B. J., Vidarsson, G., and Aalberse, R. C. (2014) Dynamics of inter-heavy chain interactions in human immunoglobulin G (IgG) subclasses studied by kinetic Fab arm exchange. *J Biol Chem* 289, 6098-6109
31. Selman, M. H., Derks, R. J., Bondt, A., Palmblad, M., Schoenmaker, B., Koeleman, C. A., van de Geijn, F. E., Dolhain, R. J., Deelder, A. M., and Wuhrer, M. (2012) Fc specific IgG glycosylation profiling by robust nano-reverse phase HPLC-MS using a sheath-flow ESI sprayer interface. *J Proteomics* 75, 1318-1329
32. Tarp, M. A., and Clausen, H. (2008) Mucin-type O-glycosylation and its potential use in drug and vaccine development. *Biochim Biophys Acta* 1780, 546-563
33. Domon, B., and Costello, C. E. (1988) A Systematic Nomenclature for Carbohydrate Fragmentations in Fab-Ms Ms Spectra of Glycoconjugates. *Glycoconjugate Journal* 5, 397-409

34. Edelman, G. M., Cunningham, B. A., Gall, W. E., Gottlieb, P. D., Rutishauser, U., and Waxdal, M. J. (1969) The covalent structure of an entire gamma G immunoglobulin molecule. *J Immunol* 173, 5335-5342
35. Stavenhagen, K., Hinneburg, H., Thaysen-Andersen, M., Hartmann, L., Varon Silva, D., Fuchser, J., Kaspar, S., Rapp, E., Seeberger, P. H., and Kolarich, D. (2013) Quantitative mapping of glycoprotein micro-heterogeneity and macro-heterogeneity: an evaluation of mass spectrometry signal strengths using synthetic peptides and glycopeptides. *J Mass Spectrom* 48, 627-639
36. Bakovic, M. P., Selman, M. H., Hoffmann, M., Rudan, I., Campbell, H., Deelder, A. M., Lauc, G., and Wuhrer, M. (2013) High-throughput IgG Fc N-glycosylation profiling by mass spectrometry of glycopeptides. *J Proteome Res* 12, 821-831
37. Croset, A., Delafosse, L., Gaudry, J. P., Arod, C., Glez, L., Losberger, C., Begue, D., Krstanovic, A., Robert, F., Vilbois, F., Chevalet, L., and Antonsson, B. (2012) Differences in the glycosylation of recombinant proteins expressed in HEK and CHO cells. *J Biotechnol* 161, 336-348
38. Chen, F. T., Dobashi, T. S., and Evangelista, R. A. (1998) Quantitative analysis of sugar constituents of glycoproteins by capillary electrophoresis. *Glycobiology* 8, 1045-1052
39. Pedroso, M. M., Pesquero, N. C., Thomaz, S. M., Roque-Barreira, M. C., Faria, R. C., and Bueno, P. R. (2012) Jacalin interaction with human immunoglobulin A1 and bovine immunoglobulin G1: affinity constant determined by piezoelectric biosensoring. *Glycobiology* 22, 326-331
40. Hortin, G. L., and Trimpe, B. L. (1990) Lectin affinity chromatography of proteins bearing O-linked oligosaccharides: application of jacalin-agarose. *Anal Biochem* 188, 271-277
41. Wilson, I. B., Gavel, Y., and von Heijne, G. (1991) Amino acid distributions around O-linked glycosylation sites. *Biochem J* 275 (Pt 2), 529-534
42. Johnson, P. M., Michaelsen, T. E., and Scopes, P. M. (1975) Conformation of the hinge region and various fragments of human IgG3. *Scand J Immunol* 4, 113-119
43. Julenius, K., Molgaard, A., Gupta, R., and Brunak, S. (2005) Prediction, conservation analysis, and structural characterization of mammalian mucin-type O-glycosylation sites. *Glycobiology* 15, 153-164
44. Ahmed, A. A., Giddens, J., Pincetic, A., Lomino, J. V., Ravetch, J. V., Wang, L. X., and Bjorkman, P. J. (2014) Structural characterization of anti-inflammatory immunoglobulin g fc proteins. *J Mol Biol* 426, 3166-3179
45. Brezski, R. J., and Jordan, R. E. (2010) Cleavage of IgGs by proteases associated with invasive diseases: an evasion tactic against host immunity? *MAbs* 2, 212-220
46. Brezski, R. J., Vafa, O., Petrone, D., Tam, S. H., Powers, G., Ryan, M. H., Luongo, J. L., Oberholtzer, A., Knight, D. M., and Jordan, R. E. (2009) Tumor-associated and microbial proteases compromise host IgG effector functions by a single cleavage proximal to the hinge. *Proc Natl Acad Sci U S A* 106, 17864-17869
47. Baici, A., Knopfel, M., Fehr, K., Skvaril, F., and Boni, A. (1980) Kinetics of the different susceptibilities of the four human immunoglobulin G subclasses to proteolysis by human lysosomal elastase. *Scand J Immunol* 12, 41-50
48. Virella, G., and Parkhouse, R. M. (1971) Papain sensitivity of heavy chain sub-classes in normal human IgG and localizaton of antigenic determinants for the sub-classes. *Immunochemistry* 8, 243-250
49. Turner, M. W., Bennich, H. H., and Natvig, J. B. (1970) Pepsin digestion of human G-myeloma proteins of different subclasses. I. The characteristic features of pepsin cleavage as a function of time. *Clin Exp Immunol* 7, 603-625
50. Tomana, M., Novak, J., Julian, B. A., Matousovic, K., Konecny, K., and Mestecky, J. (1999) Circulating immune complexes in IgA nephropathy consist of IgA1 with galactose-deficient hinge region and antiglycan antibodies. *J Clin Invest* 104, 73-81
51. Lehoux, S., Mi, R., Aryal, R. P., Wang, Y., Schjoldager, K. T., Clausen, H., van Die, I., Han, Y., Chapman, A. B., Cummings, R. D., and Ju, T. (2014) Identification of distinct glycoforms of IgA1 in

plasma from patients with immunoglobulin a (IgA) nephropathy and healthy individuals. *Mol Cell Proteomics* 13, 3097-3113
52. Imai, H., Hamai, K., Komatsuda, A., Ohtani, H., and Miura, A. B. (1997) IgG subclasses in patients with membranoproliferative glomerulonephritis, membranous nephropathy, and lupus nephritis. *Kidney Int* 51, 270-276

Supplemental information

A complete overview of the supplemental information is available online at http://www.mcponline.org/content/14/5/1373/suppl/DC1.

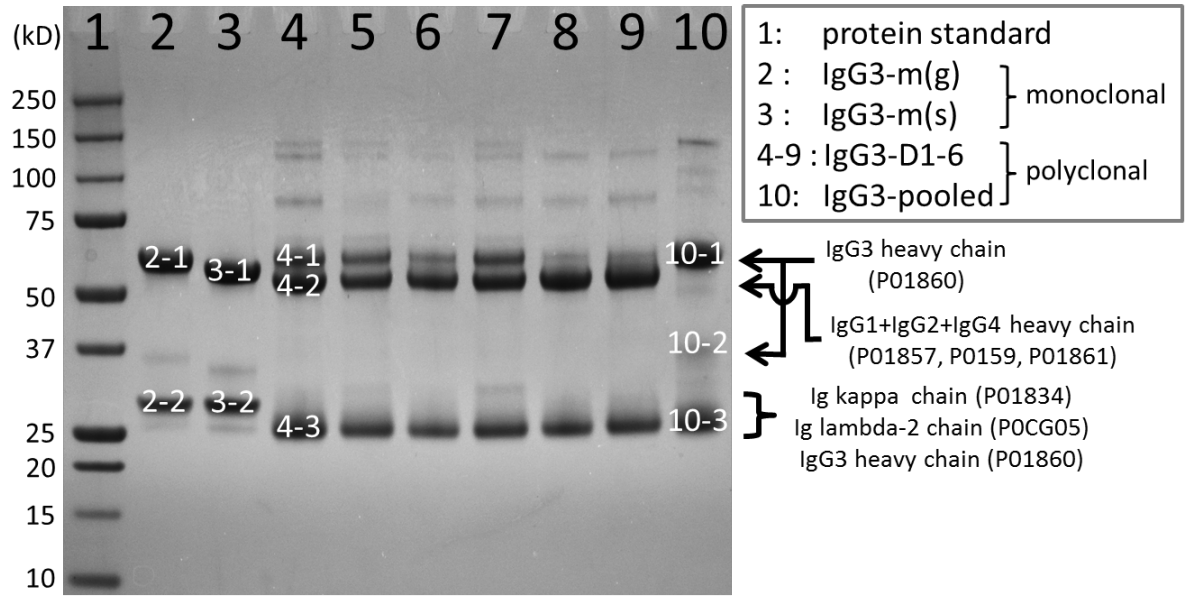

Supplemental Figure S3.1: SDS-PAGE analysis of various IgG3 samples. The bands denoted with a numerical code were excised and the embedded proteins were digested with trypsin, followed by LC-ESI-IT-MS(/MS) analysis. Automated primary sequence database searching using MASCOT was used to identify the IgG3 heavy chain, as well as both kappa and lambda (in polyclonal samples) or only kappa (in monoclonal samples) light chains, which are listed here with their primary UniProt accession number. A more comprehensive list of the identified proteins can be seen in Supplemental Table S3.3.

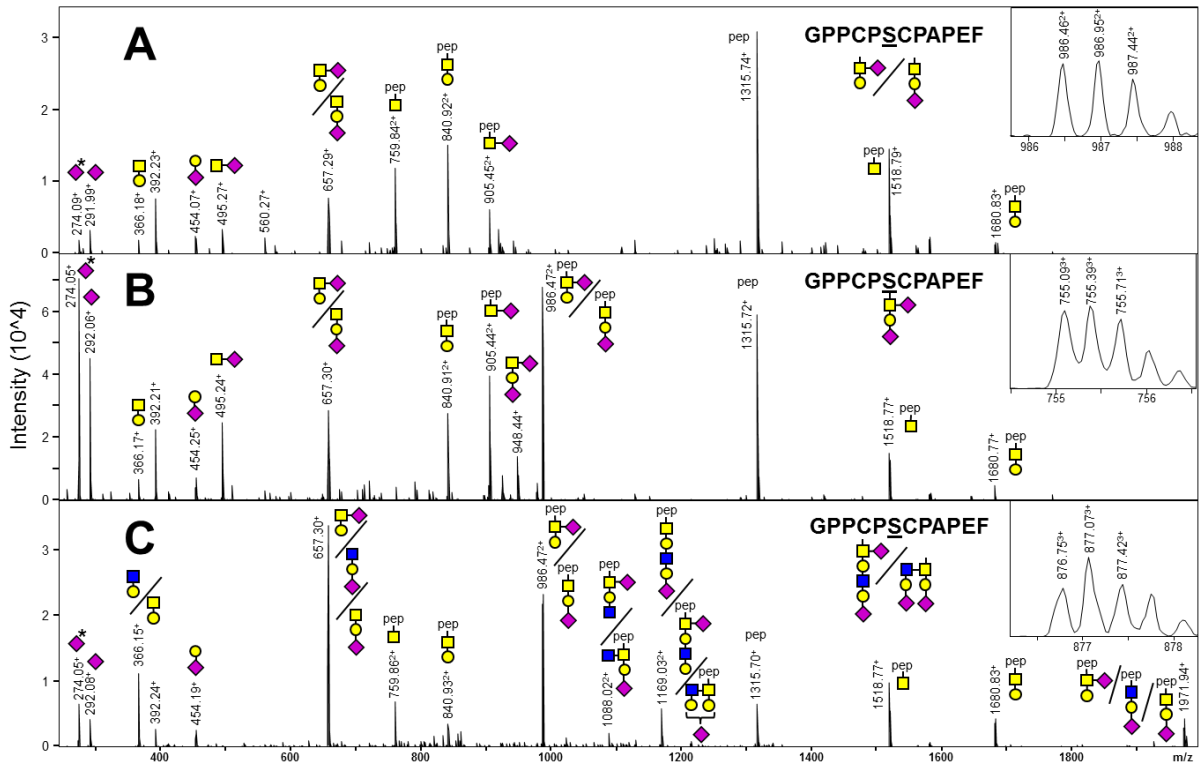

Supplemental Figure S3.5: NanoLC-ESI-IT-CID spectra showing fragmentation of the proteinase K-generated glycopeptide GPPCPSCPAPEF belonging to an IgG4 Fc construct (IgG4-Fc-V397MA). The following glycan structures were observed: A) a monosialylated core 1 type *O*-glycan; B) a disialylated core 1 type *O*-glycan; C) a disialylated *O*-glycan with an *N*-acetyllactosamine (GlcNAc + Gal). This structure interpretation is partially based on literature, since mass spectrometry cannot distinguish between different types of hexoses and *N*-acetylhexosamines. The MS1 precursor peak of each MS2 spectrum is shown in the right-upper corner. Pep = peptide; yellow circle = galactose; yellow square = *N*-acetylgalactosamine; blue square = *N*-acetylglucosamine; purple diamond = *N*-acetylneuraminic acid.

Chapter 4:

Galactosylation and sialylation levels of IgG predict relapse in patients with PR3-ANCA associated vasculitis

Adapted from: *EBioMedicine* 2017, 17, 108-118

Authors: M.J. Kemna*[,1,2], R. Plomp*[,3], Pieter van Paassen[1,2], Carolien A.M. Koeleman[3], Bas C. Jansen[3,4], Jan G.M.C. Damoiseaux[5], Jan Willem Cohen Tervaert[§,1], Manfred Wuhrer[§,3]

* the authors should be considered joint first author
§ the authors should be considered joint last author
[1]*Cardiovascular Research Institute Maastricht (CARIM), Maastricht University, Maastricht, The Netherlands;*
[2]*Department of Internal Medicine, Division of Nephrology and Clinical Immunology, Maastricht University Medical Center, Maastricht, The Netherlands;*
[3]*Center for Proteomics and Metabolomics, Leiden University Medical Center, Leiden, The Netherlands;*
[4]*present address: Ludger, Oxford, The United Kingdom;*
[5]*Central Diagnostic Laboratory, Maastricht University Medical Center, Maastricht, The Netherlands*

Table of Contents

4.1: Summary

Objective:

The objective of our study is to investigate the Fc glycosylation profiles of both antigen-specific IgG targeted against proteinase 3 (PR3-ANCA) and total IgG as prognostic markers of relapse in patients with Granulomatosis with Polyangiitis (GPA).

Methods:

Seventy-five patients with GPA and a PR3-ANCA rise during follow-up were included, of whom 43 patients relapsed within a median period of 8 (2-16) months. The *N*-glycan at Asn297 of affinity-purified and denatured total IgG and PR3-ANCA was determined by mass spectrometry of glycopeptides in samples obtained at the time of the PR3-ANCA rise and at the time of the relapse or time-matched during remission.

Results:

Patients with total IgG1 exhibiting low galactosylation or low sialylation were highly prone to relapse after an ANCA rise (HR 3.46 [95%-CI 1.73-6.96], p<0.0001 and HR 3.22 [95%-CI 1.52-6.83], p=0.002, respectively).

In relapsing patients, total IgG1 galactosylation, sialylation and bisection significantly decreased and fucosylation significantly increased from the time of the PR3-ANCA rise to the relapse (p<0.0001, p=0.0087, p<0.0001 and p=0.0025), while the glycosylation profile remained similar in non-relapsing patients. PR3-ANCA IgG1 galactosylation, sialylation and fucosylation of PR3-ANCA IgG1 decreased in relapsing patients (p=0.0073, p=0.0049 and p=0.0205), but also in non-relapsing patients (p=0.0007, p=0.0114 and p=0.0002), while bisection increased only in non-relapsing patients (P<0.0001).

Conclusion:

While Fc glycosylation profiles have been associated with clinically manifest autoimmune diseases, in the present study we show that low galactosylation and sialyation in total IgG1 but not PR3-ANCA IgG1 predicts disease reactivation in patients with GPA who experience an ANCA rise during follow-up. We postulate that glycosylation profiles may be useful in pre-emptive therapy studies using ANCA rises as guideline.

4.2: Introduction

Granulomatosis with Polyangiitis (GPA; Wegener's), Microscopic Polyangiitis (MPA) and Eosinophilic Granulomatosis with Polyangiitis (EGPA; Churg Strauss Syndrome) are inflammatory disease entities affecting small to medium vessels. They are characterized by the presence of anti-neutrophil cytoplasmic antibodies (ANCA) against proteinase-3 (PR3) or myeloperoxidase (MPO) and are frequently grouped together under the term ANCA-associated vasculitis (AAV) (1).

The pathogenic potential of ANCA to cause necrotizing glomerulonephritis (NCGN) is well established in mouse models (2-4). Patients with severe NCGN are almost always positive for either PR3- or MPO-ANCA (5), while ANCA are less often detected in patients with localized forms of vasculitis (6, 7). After remission induction, a rise in the ANCA titer is detected in some patients and disease reactivation may occur shortly thereafter (8). However, the relation between longitudinal ANCA measurements and disease reactivation is far from absolute since many ANCA rises are not followed by a relapse and relapses may occur without a preceding ANCA rise (9, 10). Recently, it has been shown that ANCA rises are highly predictive for disease activity in patients with severe vasculitic disease, e.g. NCGN or alveolar hemorrhage, but not in patients with limited granulomatous disease (11-14). Our current hypothesis is that the pathogenicity of an ANCA rise is modulated by the quality of the auto-antibody, for which the glycosylation profile is an important factor.

The glycosylation profile of the crystallizable fragment (Fc) of the immunoglobulin G (IgG) is characterized by a single *N*-linked glycan attached to each heavy chain at the asparagine-297 (15). The Fc *N*-glycan composition affects Fcy receptor (FcγR) affinity (15-18) and can influence complement activation (19). The lack of a core fucose, *N*-acetylneuraminic (sialic) acids and galactose residues on the Fc *N*-glycan have been found to increase the inflammatory capacity of IgG, at least in mice (20-22). The Fc *N*-glycan is essential for the pathogenicity of the antibody, since deglycosylation of MPO-ANCA significantly attenuates ANCA-mediated neutrophil activation and reduces glomerular crescent formation in a mouse model (23).

Already in the early eighties, it was recognized that total IgG in patients with rheumatoid arthritis (RA) contained less galactose and sialic acid at the non-reducing termini compared

to healthy controls (24). A difference in the glycosylation profile of total IgG has since been demonstrated in patients with various other auto-immune diseases when compared to healthy controls, including systemic lupus erythematosus, inflammatory bowel disease, myasthenic gravis, ankylosing spondylitis, primary Sjögren's syndrome, psoriatic arthritis and multiple sclerosis (25-29). Furthermore, significant differences have been observed in the glycosylation profile of total IgG and specific auto-antibodies, such as anti-citrullinated protein antibodies (ACPA), anti-β2GP1 and anti-histone IgG (30-33). Finally, Fc glycosylation of auto-antibodies may change during disease development. For example, the glycosylation profile of ACPA changes prior to the onset of RA towards a more inflammation-associated phenotype (31, 34).

In patients with PR3-ANCA, it was previously shown with lectin assays that total IgG exhibits a lower degree of galactosylation when compared to healthy controls (35, 36). In addition, the degree of sialylation of PR3-ANCA is lower during active disease compared to inactive disease (37). Recently, it has been shown with mass spectrometric IgG Fc glycosylation analysis that total IgG Fc of patients with severe AAV exhibits lower levels of galactosylation, sialylation and bisecting *N*-acetylglucosamine (GlcNAc) compared to healthy controls (38). This finding was more pronounced for PR3-ANCA compared to total IgG (38). Correlations were observed between the glycosylation profile of PR3-ANCA and several cytokine concentrations, suggesting that the glycosylation of ANCA may be driven by T-cell activation in an antigen-specific manner (38). Potential differences and similarities in the glycosylation profile of total IgG and antigen-specific IgG between patients with PR3-ANCA and patients with MPO-ANCA associated vasculitis have not yet been investigated.

The objective of our study is to investigate differences in the glycosylation profile of both PR3-ANCA and total IgG and the prognostic value at the time of a rise in PR3-ANCA in patients with GPA. The primary question is whether patients with a particular glycosylation profile are more prone to relapse. Furthermore, upon an ANCA rise, changes in glycosylation profiles associated with a relapse are examined. To increase the homogeneity of our cohort, we included only GPA patients that are PR3-ANCA positive, the disease subgroup that is most prevalent in our area.

4.3: Methods

4.3.1: Inclusion criteria

All patients who visited the clinic at the Maastricht University Medical Center (MUMC) between January 1, 2000 and November 1, 2011 were evaluated. Inclusion criteria were a diagnosis of GPA according to the EMA classification system and a rise in PR3-ANCA during remission (11, 39, 40).

Clinical characteristics were recorded in all subjects according to the Dutch law on Medical Treatment Act (WGBO), the Personal Data Protection Act (Wbp) and the Code of Conduct for Health Research (Federa) (41). Ethics approval was waived by our local ethics committee.

4.3.2: Classification of patients

Renal involvement was preferably determined by a kidney biopsy showing pauci-immune necrotizing glomerulonephritis (42, 43). However, surrogate markers such as haematuria in combination with red cell casts, dysmorphic erythrocytes (>10) and/or proteinuria sufficed (40). All patients have been treated according to the European League against Rheumatism (EULAR) guidelines (43, 44).

The definitions recommended by the EULAR of 2007 were applied to define disease activity states (39). Remission was defined as absence of disease activity attributable to active disease during maintenance immunosuppressive therapy of a prednisone dosage of 7.5mg or lower. A relapse was defined as re-occurrence or new onset of disease attributable to active disease combined with an increase or addition of immunosuppressive treatment. Relapses were further subdivided in 'major' or 'minor' depending on whether the relapse was potentially organ- or life-threatening or not (39).

4.3.3: ANCA measurements

Patients were routinely evaluated during follow-up, generally every three months during the first two years after diagnosis and/or a relapse and 2-3 per year later on. At every visit, patients were screened for potential symptoms of a relapse (39) and blood was drawn.

Antigen-specific solid-phase ANCA tests were performed for the detection and quantification of PR3-ANCA. Initially, commercially available direct PR3-ANCA enzyme linked immunosorbent assays (ELISA) were used (Euro Diagnostica, Malmö, Sweden) (45). On October 1, 2005, this assay was replaced by a fluorescent-enzyme immune-assay (FEIA) for

PR3-ANCA (EliA, Thermo Fisher, Freiburg, Germany) (46). During the transition, ANCA measurements were performed using both methods.

4.3.4: Definition of an ANCA rise

For the detection of an ANCA rise, the ANCA titer was compared to all measurements made with the same assay in the past 6 months. We defined a rise using the slope of an increase as previously described (11), thereby taking into account the relative increase (in %) and the time between measurements (in days). A receiver operating characteristics (ROC) curve was calculated to determine the optimal cut-off value of the slope. The chosen cut-off values as determined by the ELISA and FEIA method were 2.56 and 2.25 %/day, respectively. This is equivalent to a relative increase of 78% and 68% over one month or 233% and 205% over three months.

To ensure that small elevations were above the intra-assay coefficient of variation, a rise had to constitute to a relative increase of at least 25% and an absolute increase equivalent to a doubling of the lowest value of a borderline result (at least 10 AU for the ELISA and 5 U/ml for the FEIA). Because our analysis is focused on patients in remission, only serum samples drawn at least 3 months after the previous disease activity were eligible for detection of an ANCA rise (11).

4.3.5: Serum selection

In all 75 patients, a serum sample was selected at the time of an ANCA rise (‘T1’) (11). In relapsing patients, either renal or non-renal, a second serum sample was selected prior to the start of the immunosuppressive induction therapy at the time of the relapse (‘T2rel’). In non-relapsing patients, a second serum sample was selected after the ANCA rise during remission (‘T2rem’), of which the time between the first and second sample was matched with the time between the first and second sample in the renal relapsing patients. For 4 relapsing patients no serum sample was available at the time of the relapse, and therefore only 71 T2 serum samples were analyzed.

4.3.6: Total IgG purification

For total IgG purification, the wells of two filter plates (Multiscreen filter plates with Durapore membrane, pore size 0.65 µm; Merck Millipore, Darmstadt, Germany) were filled with 15 µl of Protein G Sepharose 4 Fast Flow beads (GE Healthcare, Uppsala, Sweden) in 200 µl PBS, followed by the addition of 2 µl of the serum samples. Furthermore, 10 of the

serum samples were purified in duplicate. Fifteen wells were filled with 2 µl Milli-Q-purified water to serve as negative control and 20 wells were filled with 2 µl of the serum of a healthy donor to serve as positive control. The plates were incubated on a shaker at room temperature for 1 hour. The samples were then washed on a vacuum manifold with 4x 200 µl PBS and 3x 200 µl Milli-Q-purified water, followed by the addition of 100 µl 100 mM formic acid (Fluka, Steinheim, Germany) for elution into a V-bottom 96-well plate (Greiner Bio-One, Frickenhausen, Germany), which has been shown to result in near-complete denaturation of IgG (47). Eluates were dried in a centrifugal vacuum concentrator (Eppendorf, Hamburg, Germany) at 60 °C for approximately 2 hours.

4.3.7: PR3-ANCA purification

An ELISA kit (Wieslab PR3-ANCA; Euro Diagnostica) was used for purification of PR3-ANCA. Eighty µl diluent containing PBS (Wieslab kit) and 20 µl of the serum samples were added to two PR3-coated 96-well plates. Ten of the serum samples were purified in duplicate in separate wells. Fifteen wells were filled with 20 µl Milli-Q-purified water to serve as negative control and 20 wells were filled with 20 µl of the serum of a healthy donor to serve as a further negative control. The samples were incubated on a shaker at room temperature for 1 hour, followed by washing 4x with 250 µl wash buffer (Wieslab kit) and 1x with 150 µl 50 mM ammonium bicarbonate buffer (Sigma-Aldrich, St. Louis, MO). The PR3-ANCA was eluted by adding 100 µl 100 mM formic acid to the wells and collected into a V-bottom 96-well plate. The samples were then dried in a centrifugal vacuum concentrator at 60°C for approximately 2 hours.

4.3.8: PR3-ANCA purification

The dried total IgG and PR3-ANCA samples were resuspended in 20 µl 50 mM ammonium bicarbonate and incubated on a shaker at room temperature for 15 minutes. Twenty µl of 0.01 µg/µl trypsin (sequencing grade modified trypsin, Promega, Madison, WI) was then added to each well. The samples were again incubated on a shaker at room temperature for 15 minutes, followed by overnight incubation at 37°C. Samples were stored at -20°C.

4.3.9: LC-MS/MS analysis

The digested samples were analyzed by nanoLC-reversed phase (RP)-electrospray ionization (ESI) –quadrupole time-of-flight (qTOF)-MS on an Ultimate 3000 HPLC system (Dionex/Thermo Scientific, Sunnyvale, CA) coupled to a MaXis Impact (Bruker Daltonics, Bremen, Germany). The samples were concentrated on a Dionex Acclaim PepMap100 C18

trap column (particle size 5 µm, internal diameter 300 µm, length 5 mm) and separated on an Ascentis Express C18 nano column (2.7 µm HALO fused core particles, internal diameter 75 µm, length 50 mm; Supelco, Bellefonte, PA). The following linear gradient was applied, with solvent A consisting of 0.1% trifluoroacetic acid (TFA; Fluka) and solvent B of 95% acetonitrile (Biosolve, Valkenswaard, The Netherlands): t=0 min, 3% solvent B; t=2, 6%; t=4.5, 18%; t=5, 30%; t=7, 30%; t=8, 1%; t=10.9, 1%. The sample was ionized in positive ion mode with a CaptiveSprayer (Bruker Daltonics) at 1100 V. A nanoBooster (Bruker Daltonics) was used to enrich the nitrogen gas with acetonitrile to enhance the ionization efficacy. A mass spectrum was acquired every second (frequency of 1 Hz), with the ion detection window set at *m/z* 550-1800. In between every 12 measurements an external IgG standard was run. A mass spectrum of both total IgG and PR3-ANCA can be seen in Figure 4.1.

4.3.10: Data processing

Mass spectrometric identification and processing of tryptic IgG glycopeptide data was done as described previously (48), with a few differences as stated below, and was performed blindly in order to prevent bias. The LC-MS data files were examined in Compass DataAnalysis 4.2 software (Bruker Daltonics). Negative controls were inspected and found to contain no significant intensity of IgG signals.

First, the *m/z* axis of the mass spectra was calibrated internally using several known IgG glycopeptides masses. Next, the files were converted to the .mzXML data format using the MSconvert program from the ProteoWizard 3.0 suite (49). The m/z and retention times of all the tryptic IgG glycopeptides were manually determined using MZmine 2.10 (50) and can be found in Supplemental Table S4.1. The time axes were aligned based on a list of the most prominent IgG glycopeptide peaks and their retention times, using an alignment tool designed in-house (51). The intensity of the first three isotopes of every analyte was extracted using a window of ± 0.04 Thomson and ± 10 s around the manually determined retention time. This was achieved using the in-house developed 3D Total Extractor (3DTE) program (software code can be found in the supplemental data). A list of analytes is provided to 3DTE, which then uses a binary search to find the retention time and mass region around each analyte. Afterwards, the maximum intensity of each analyte is determined per mass spectrum that falls within the retention time window. The value that is reported for each analyte by 3DTE is the sum of the highest intensity values from the individual mass spectra. Lastly, the program

generates a tab-separated output file that lists all the compositions and their respective total intensities. Background correction was optimized to minimize intensity biases in the determination of glycopeptide ratios. In Excel 14.0, the background-corrected signal intensities of the three isotopic peaks in both 2+ and 3+ charge state were summed to obtain a single value for each glycopeptide. IgG1 G2 and G2S2 were excluded because of overlap with contaminant peaks. Isotopic peaks for several other IgG1 glycopeptides were also excluded due to peak overlap, and these values were replaced by an estimate based on the remaining isotopic peaks and the theoretical isotopic pattern (these isotopic peaks account for less than 3% of the total glycopeptide signal intensity). Afucosylated IgG4 glycopeptides were excluded due to peak overlap with IgG1 glycopeptides. In order to obtain a percentage value for each glycopeptide, this value was then divided by the sum of all signal intensities of glycopeptides, and this was done separately for IgG1, IgG2/3 and IgG4. In Caucasian populations the tryptic glycopeptide of IgG3 generally has the same peptide sequence as IgG2 (52). Therefore it was not possible to distinguish between IgG2 and IgG3 glycopeptides with the methods we used, and these glycopeptides will be referred to as IgG2/3. The IgG percentage data can be seen in Supplemental Table S4.2. Several glycosylation features were calculated from this data: fucosylation (% of glycans bearing a core fucose), bisection (% of glycans with a bisecting GlcNAc), galactosylation (% of antennae carrying a galactose) and sialylation (% of antennae carrying a sialic acid, see supplemental data for the exact definitions).

In order to guard the quality of the acquired data, an intensity threshold was set. If the sum of the signal intensities of G0F, G1F and G2F in triple charge state for an IgG subclass did not exceed this threshold, all data for that subclass was excluded. Additionally, data was excluded if the signal/background of the highest peak per subclass did not exceed 20. Finally, because of the chance of overlap between IgG4 glycopeptide peaks and later eluting IgG2/3 peaks, IgG2/3 data was excluded if more IgG4 was present than IgG2/3 (as determined by G0F+G1F+G2F (3+) signals). Lastly, we determined the average relative standard deviation (RSD) of eight prominent glycans (G0F, G1F, G2F, G0FN, G1FN, G2FN, G1FS and G2FS) to further examine the quality of the data.

4.3.11: Statistical analysis

Numerical variables were expressed as median (interquartile range [IQR]) and categorical variables as relative abundances (percentages). Two unpaired variables were compared with

the Mann Whitney U test. Two paired variables were compared with the Wilcoxon signed rank test. Continuous variables were correlated with the Spearman test.

Receiver operating characteristic (ROC) curves were constructed for galactosylation, sialylation, fucosylation and bisection at the time of an ANCA rise to discriminate relapsing patients from patients who remained in remission. If a trend towards significance was observed in an ROC curve, an optimal cut-off value was derived that was closest to the upper left corner (the cut-off value with the highest sum of sensitivity and specificity). Patients were subsequently categorized as high (above or equal to the cut-off) or low (below cut-off) level for the concerning glycosylation trait. Differences in the time to relapse between high and low were assessed using the log-rank test. The time to relapse was estimated using the Kaplan-Meier method. An event was defined as a relapse at the time of the start or increase of immunosuppressive treatment. Subjects were censored at the time of last follow-up. Hazard ratios (HR) with the 95% confidence interval were derived using the Cox regression analysis, adjusted for age and sex. The proportional hazards assumption was assessed by visually inspecting log-log plots.

All statistical analyses were performed using GraphPad Prism version 6.04 for Windows (GraphPad Software, La Jolla, California, USA) and SPSS statistics for Windows, version 23.0 (IBM, Armonk, NY, USA). Bonferroni corrections were applied to the statistical testing, in which a p-value of <0.0125 was considered significant and <0.05 was considered as a trend.

4.4: Results

4.4.1: Patient characteristics

Seventy-five patients with Granulomatosis with Polyangiitis positive for PR3-ANCA were included in this study, of whom 51 patients had renal involvement in the past and 24 patients did not (see Table 4.1). Forty-three (57.3%) patients relapsed within a median time of 8 (2-16) months since the ANCA rise.

Table 4.1: Patient characteristics. The organ involvement refers the organ involvement during any previous periods of disease activity in the past (at the diagnosis or any previous relapse). The induction treatment refers to the treatment regimen that was used to induce remission during the most recent period of disease activity only. Abbreviations: SD, standard deviation. GC, glucocorticosteroid therapy. *This patient was included after a minor relapse which was treated with GC monotherapy, while remission was induced after diagnosis using cyclophosphamide + GC. ±The follow-up time refers to the time from the most recent disease activity to the endpoint of the study (at the time of relapse or at the last time of follow-up).

	Renal		Non-renal	
	Relapse (n=31)	Remission (n=20)	Relapse (n=12)	Remission (n=12)
Demographics				
Age (in years + SD)	58.2 (14.5)	54.7 (14.2)	58.1 (9.0)	66.2 (11.3)
Male	23 (74.2%)	13 (65%)	6 (50%)	4 (33.3%)
Organ involvement at previous disease activities				
Arthralgia	19 (61.3%)	10 (50%)	7 (58.3%)	5 (41.7%)
Cutaneous	13 (41.9%)	3 (15%)	2 (16.7%)	0 (0%)
Eyes	8 (25.8%)	5 (25%)	3 (25%)	3 (25%)
Ear, nose, throat	26 (83.4%)	17 (85%)	10 (83.3%)	11 (91.7%)
Lung	23 (74.2%)	14 (70%)	10 (83.3%)	10 (83.3%)
Cardiovascular	1 (3.2%)	2 (10%)	0 (0%)	0 (0%)
Renal	31 (100%)	20 (100%)	0 (0%)	0 (0%)
Central nervous system	1 (3.2%)	0 (0%)	0 (0%)	1 (8.3%)
Peripheral nervous system	7 (22.6%)	4 (20%)	1 (8.3%)	2 (16.7%)
Induction treatment at previous disease activity resulting in remission				
Cyclophosphamide + GC	19 (61.3%)	14 (70%)	6 (50%)	10 (83.3%)
Rituximab + GC	1 (3.2%)	3 (15%)	0 (0%)	0 (0%)
Methothrexate + GC	5 (16.1%)	0 (0%)	4 (33.3%)	1 (8.3%)
Mofetil mycophenolate + GC	3 (9.7%)	3 (15%)	0 (0%)	0 (0%)
Gusperimus + GC	2 (6.4%)	0 (0%)	1 (8.3%)	0 (0%)
GC monotherapy	1 (3.2%)*	0 (0%)	1 (8.3%)	1 (8.3%)
Immunosuppressive therapy at the time of the ANCA rise				
Immunosuppressive therapy	27 (87.1%)	16 (80%)	8 (66.7%)	8 (66.7%)
None	4 (12.9%)	4 (20%)	4 (33.3%)	4 (33.3%)
Follow-up				
Follow-up time (in months + SD) ±	12.9 (20.4)	42.0 (20.8)	13.9 (16.1)	45.6 (35.3)
Persistently ANCA positive	10 (32.3%)	6 (30%)	2 (16.7%)	3 (25%)
Relapse				
Major	18 (58.1%)	-	4 (33.3%)	-
Minor	13 (41.9%)	-	8 (66.7%)	-

Out of 156 samples total (75 at the time of ANCA rise, 71 at a second time point, and 10 duplicates), PR3-ANCA IgG1 data was excluded in 16 samples, total IgG1 data in 0 samples, total IgG2/3 data in 14 samples and total IgG4 in 20 samples. Because the signal intensity of PR3-ANCA IgG2/3 and IgG4 in the majority of samples did not surpass the threshold, we excluded this data group altogether. For 8 prominent glycoforms, the external IgG standard

run in between every 12 measurements showed an average RSD of 4.2% for IgG1, 4.0% for IgG2/3 and 7.1% for IgG4. The on-plate healthy donor serum-derived total IgG samples exhibited an average RSD of 4.0% for IgG1, 3.0% for IgG2/3 and 3.5% for IgG4. Finally, for the aforementioned 8 glycoforms, the 10 ANCA serum samples which were processed in duplicate showed an average RSD of 2.3%, 1.5% and 1.3% for total IgG1, IgG2/3 and IgG4, and 3.1% for PR3-ANCA IgG1. Two LC-MS spectra of total IgG and PR3-ANCA IgG, belonging to an AAV patient at the time of relapse, can be seen in Figure 4.1.

For better readability, the results of total IgG1 and PR3-ANCA IgG1 are presented in the manuscript, while the results of total IgG2/3 and total IgG4, which exhibit the same general trend as total IgG1, can be found in the supplemental data.

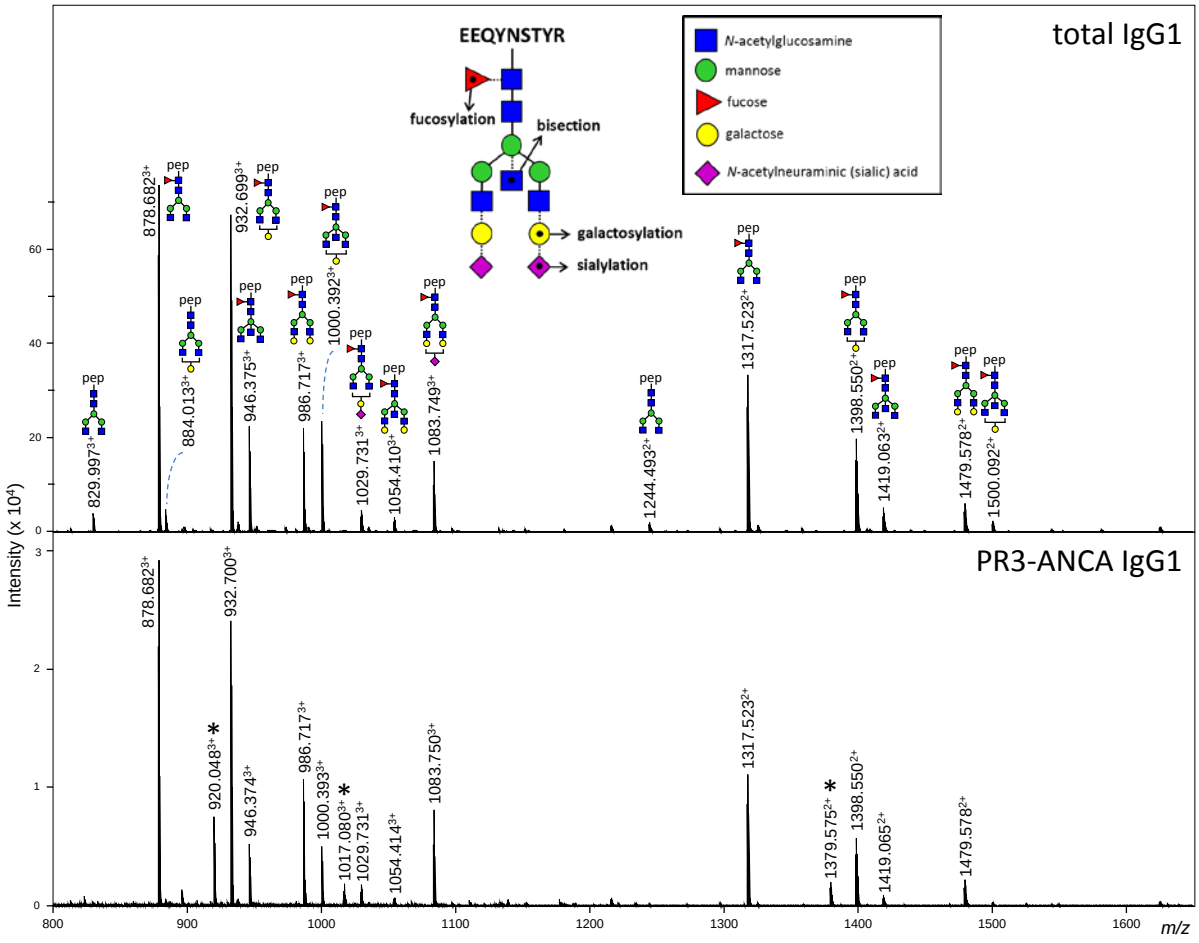

Figure 4.1: LC-MS spectra showing tryptic IgG1 glycopeptides for total IgG and PR3-ANCA belonging to an AAV patient (#9; details in Supplemental Table 4.1) at the time of relapse. The peaks denoted with an asterisk belong to a co-enriched contaminant (an apolipoprotein *O*-glycopeptide). Pep=peptide.

4.4.2: IgG1 Fc glycosylation of total IgG and PR3-ANCA at the time of the ANCA rise

At the time of the ANCA rise, we analyzed whether there were differences in the glycosylation profile of total IgG1 and PR3-ANCA IgG1. The degree of galactosylation, sialylation and fucosylation of total IgG1 was lower compared to PR3-ANCA IgG1 (46.0% [39.1-49.7%] versus 47.4% [40.4-57.5%], p=0.0175; 6.2% [5.2-7.1%] versus 6.9 [5.1-9.0%]; p=0.0289 and 93.3% [89.9-95.5%] versus 98.4% [97.3-99.0%], p<0.0001, respectively). In contrast, the level of bisection of total IgG1 was higher compared to PR3-ANCA IgG1 (19.0 [15.9-21.7%] versus 11.4% [10.1-13.9%], p<0.0001, see Supplemental Figure S4.1).

4.4.3: IgG1 Fc glycosylation as a predictor of a relapse at the time of an ANCA rise

Thereafter, we investigated whether patients with a particular IgG1 Fc glycosylation profile at the time of an ANCA rise are more prone to relapse after an ANCA rise. The ROC curve of total IgG1 galactosylation and sialylation were found to differentiate relapsing patients from non-relapsing patients (Supplemental Figure S4.2; AUC 0.6533, p=0.02385 and AUC 0.6563, p=0.02131, respectively). Total IgG1 bisection and fucosylation did not yield significant discrimination between relapsing and non-relapsing patients (p=0.9488 and p=0.9402, respectively; data not shown). The ROC curve of PR3-ANCA IgG1 was not significant for any of the glycosylation traits (data not shown). An optimal cut-off value was derived from the significant ROC curves, and patients were classified as ‘low galactosylation’ if the galactosylation rate of total IgG1 was lower than 46.1% and as ‘low sialylation’ if the sialylation rate of total IgG1 was lower than 6.9% (see Supplemental Figure S4.2).

Forty-one of 75 (54.7%) patients were classified as low galactosylation, of whom 30 (73.2%) patients relapsed within a median of 6 (1-15) months after the ANCA rise. In comparison, only 13 of 34 (38.2%) patients who were classified as high galactosylation relapsed in a median of 10 (2.5-17.5) months. Thus, patients with low galactosylation total IgG1 were highly prone to relapse after an ANCA rise (HR 3.46 [95%-CI 1.73-6.96], p<0.0001, adjusted for age and sex, see Figure 4.2A).

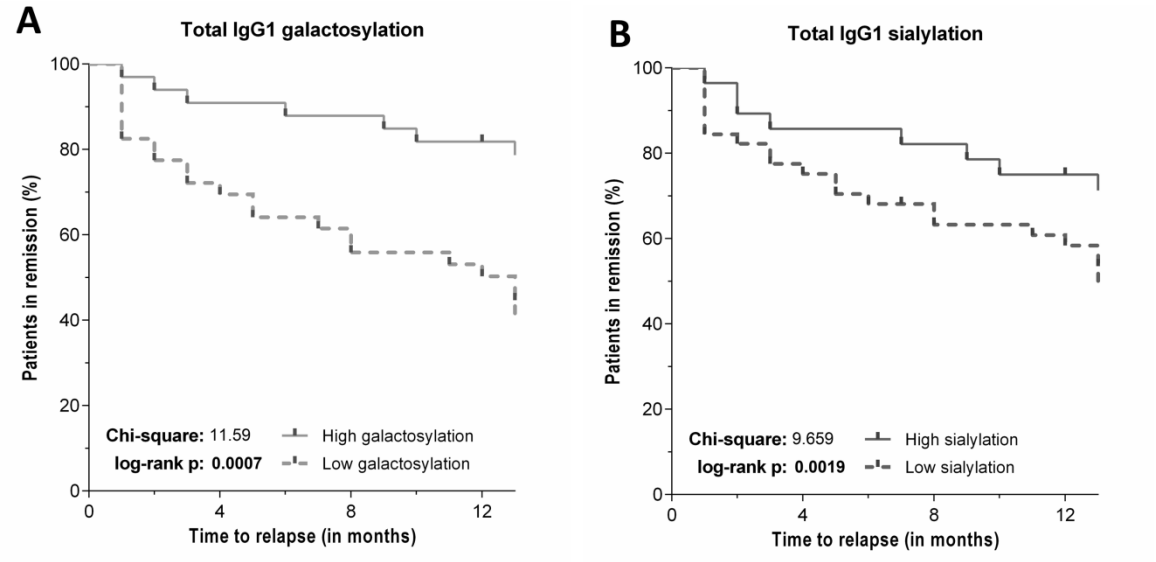

Figure 4.2: Time to relapse after an ANCA rise, (A) according to the degree of galactosylation of total IgG 1 Fc and (B) according to the degree of sialylation of total IgG 1 Fc.

Similar results were found for the degree of sialylation. Forty-seven of 75 (62.7%) patients were classified as low sialylation, of whom 34 (72.3%) patients relapsed within a median of 8 (1-17) months after the ANCA rise. In comparison, only 9 of 28 (32.1%) patients with a high sialylation relapsed in a median of 7 (2-12) months. Low sialylation patients were highly prone to relapse after an ANCA rise (HR 3.22 [95%-CI 1.52-6.83], p=0.002, adjusted for age and sex; see Figure 4.2B).

Because the degree of sialylation and galactosylation are highly correlated (terminal *N*-acetylneuraminic acid is attached to galactose), we in addition calculated the sialic acid per galactose. No association was observed between the sialic acid per galactose and the time to relapse (see Supplemental Figure S4.3 and S4.4).

4.4.4: Changes in IgG1 Fc glycosylation during follow-up

Next, we looked at potential changes of the glycosylation profile during follow-up. With regards to the total IgG1, the degree of galactosylation, sialylation and bisection significantly decreased and fucosylation significantly increased in relapsing patients (p<0.0001, p=0.0087, p<0.0001 and p=0.0025, respectively), while the glycosylation profile remained similar in patients who remained in remission (see Figure 4.3 and figure S4.5 and S4.6 in the supplemental data).

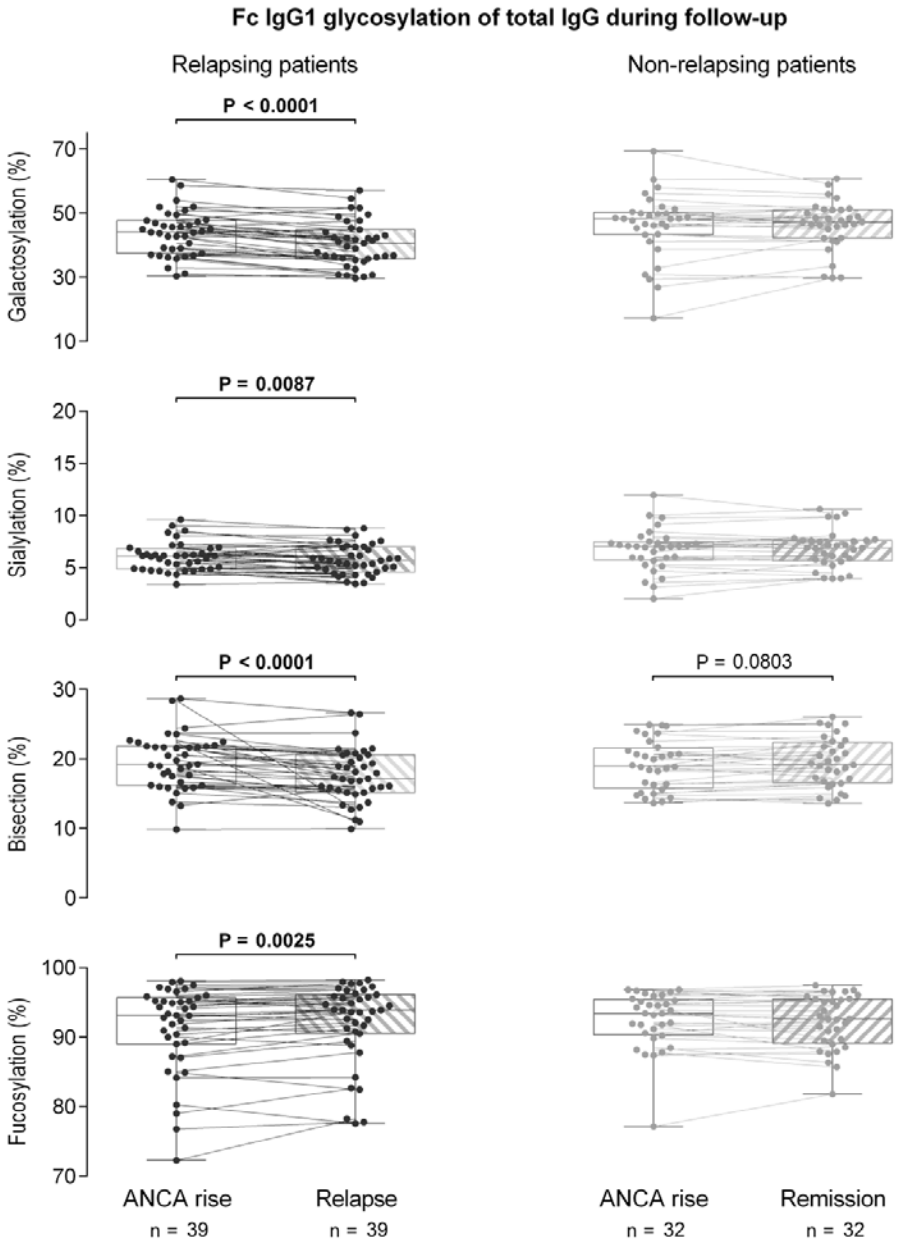

Figure 4.3: The glycosylation profile of total IgG1 Fc at the time of an ANCA rise (T1) and at the time of a relapse (T2rel) in relapsing patients (black dots) and time-matched during remission (T2rem) in patients who remain in remission (gray dots). Dots represent individual patients, lines indicate corresponding pairs. The box represents the median with interquartile range, the whiskers delineate the min-max range. Significant differences were evaluated using the Wilcoxon signed rank test, P-values are shown if <0.10 and in bold if <0.0125.

With regard to PR3-ANCA IgG1, in relapsing patients, a significant reduction in the degree of galactosylation and sialylation and a trend towards a reduction in fucosylation were observed from the ANCA rise to the time of the relapse (p=0.0073, p=0.0049 and p=0.0205, respectively, see Figure 4.4). Similarly, in patients who remained in remission, a significant reduction in the degree of galactosylation, sialylation and fucosylation was observed from the

ANCA rise to the time of the second sample (p=0.0007, p=0.0114 and p=0.0002, respectively). Moreover, the proportion of bisection of PR3-ANCA IgG1 significantly increased from the ANCA rise to the time-matched sample during remission (p<0.0001).

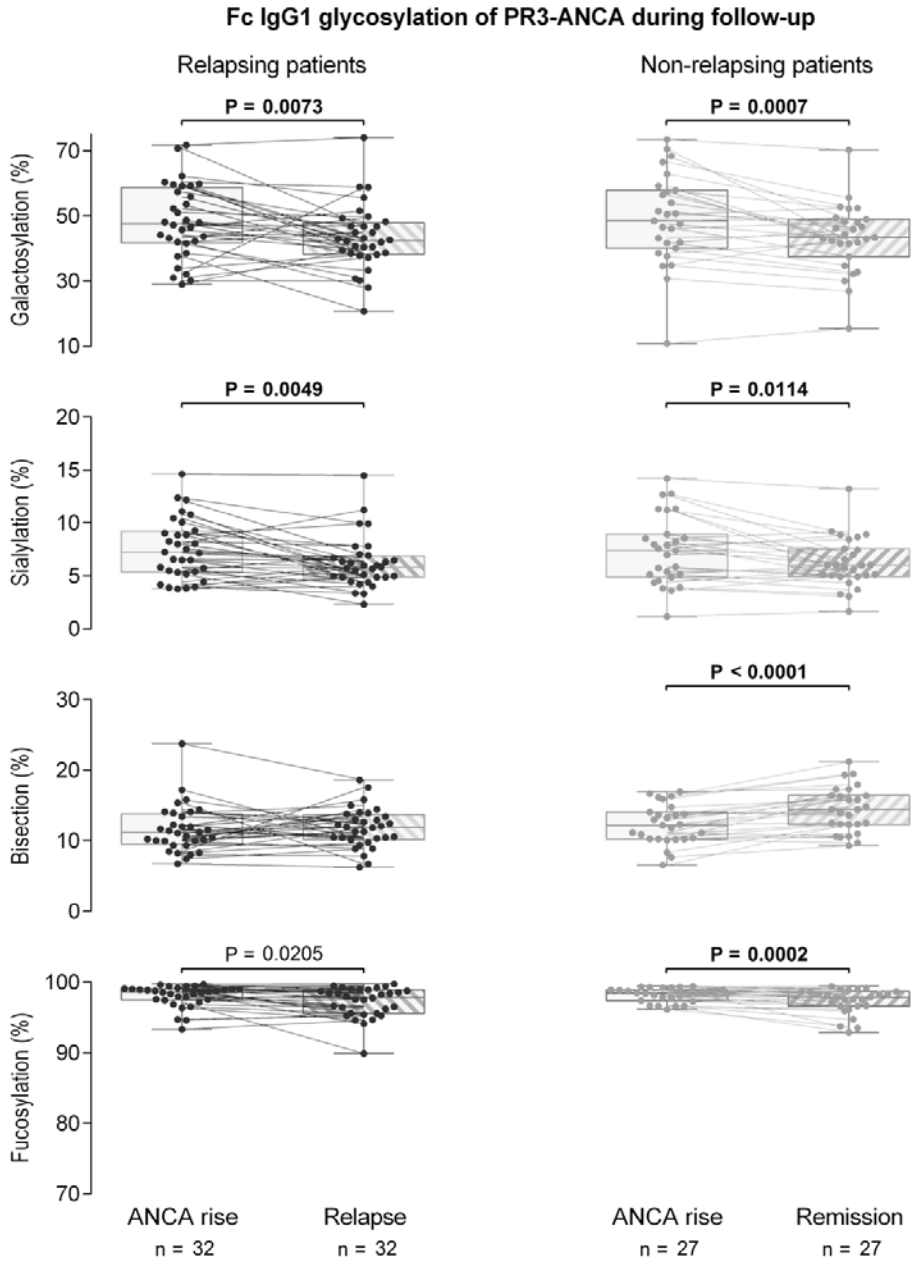

Figure 4.4: The glycosylation profile of antigen specific PR3-ANCA IgG1 Fc at the time of an ANCA rise (T1) and at the time of a relapse (T2rel) in relapsing patients (black dots) and time-matched during remission (T2rem) in patients who remain in remission (gray dots). Dots represent individual patients, lines indicate corresponding pairs. The box represents the median with interquartile range, the whiskers delineate the min-max range. Significant differences were evaluated using the Wilcoxon signed rank test, P-values are shown if <0.10 and in bold if <0.0125.

4.4.5: IgG1 Fc glycosylation at the time of relapse or time-matched during remission

The changes in the glycosylation profile over time lead to significant differences between patients in relapse or in remission at the second time point. With regard to total IgG1, a significantly lower degree of galactosylation and sialylation and a trend towards a lower degree of bisection was observed in relapsing patients compared to patients who remain in remission ($p=0.0015$, $p=0.0120$ and $p=0.0443$, respectively, see Figure 4.5 and Figure S4.7 in the supplemental data). Conversely, the glycosylation profile of PR3-ANCA was only significantly different with regard to bisection, which was lower in relapsing patients compared to patients who remained in remission ($p=0.0009$).

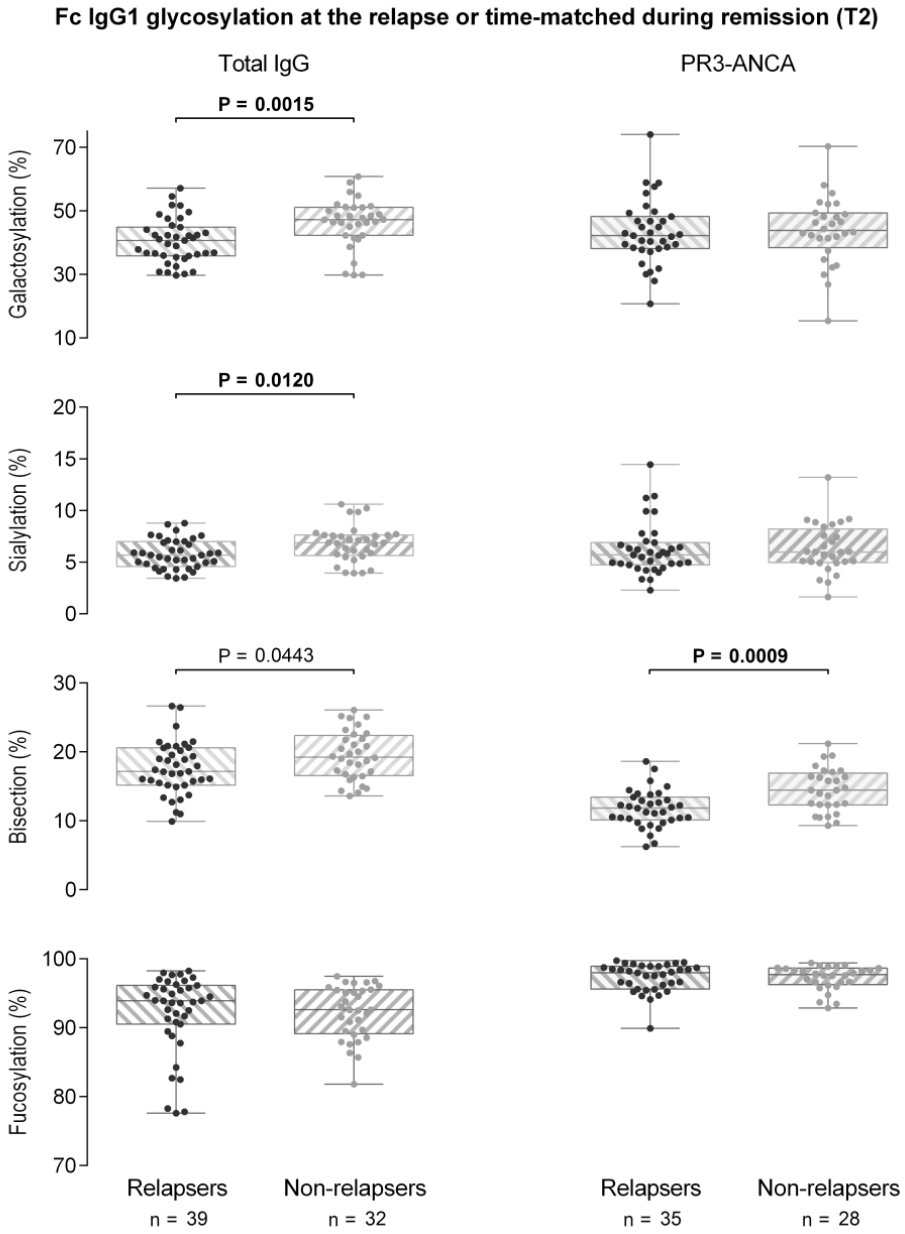

Figure 4.5: The glycosylation profile at the time of a relapse in relapsing patients and time-matched during remission in patients who remain in remission (gray dots). IgG1 Fc glycosylation of total IgG (left side, white background) and antigen specific PR3-ANCA (right side, yellow background) is shown. Dots represent individual patients. The box represents the median with interquartile range, the whiskers delineate the min-max range. Significant differences were evaluated using the Mann Whitney U test, P-values are shown if <0.10 and in bold if <0.0125.

4.5: Discussion

In this study we investigate with mass spectrometry the changes in Fc glycosylation over time in both total IgG and PR3-ANCA of patients with AAV. In patients who were in clinical remission, a first serum sample was taken at the time of an ANCA rise, whereas a second sample was acquired either after relapse but before therapy was started, or for patients who remained in remission, after a similar length of time. Analysis of the two longitudinal samples revealed a significant reduction in galactosylation, sialylation and bisection and an increase in fucosylation in total IgG Fc of relapsing patients, while these glycosylation traits did not change significantly in patients who remain in remission. Most importantly, the Fc glycosylation profile of total IgG at the time of an ANCA rise predicts a relapse. Namely, patients with low galactosylation or low sialylation in total IgG are more prone to relapse compared to patients with high galactosylation or sialylation in total IgG. In addition, we observed that the level of sialylation and galactosylation of PR3-ANCA is decreased over time, both in relapsing and non-relapsing patients. Therefore, it appears that PR3-ANCA gains a more inflammation-associated phenotype during follow-up in both groups of patients, independent of disease course.

While IgG with a low degree of galactosylation has repeatedly been found to be associated with pro-inflammatory autoimmune responses, the underlying mechanisms are still largely elusive (53-56). In addition, highly galactosylated IgG may confer anti-inflammatory activities through the association with the inhibiting receptor FcyRIIb and the C-type lectin-like receptor Dectin-1 in mice (21). This latter pathway has been shown to block C5a effector functions in vitro and C5a-dependent inflammatory responses in animal mouse models (21). This is highly relevant in AAV, since C5a plays a pivotal role in the pathophysiology (1, 57). Mouse models have shown that the blocking of C5a or C5a receptor (C5aR) ameliorates anti-MPO induced necrotizing glomerulonephritis (58, 59). The safety and efficacy in the treatment of non-life-threatening AAV with CCX168, a C5aR inhibitor, is currently being tested in a phase 2 study (EudraCT Number: 2011-001222-15). The addition of galactose to the glycan structure also no longer enables the interaction of MBL with IgG, and may thereby block the lectin pathway (19). The clinical relevance of the lectin pathway in AAV is questionable however, since mannose-binding lectin (MBL) deposition in the kidney was found in only a minority of patients and complement activation in AAV occurs predominantly via the alternative pathway (57).

Sialylated IgG has been reported to have anti-inflammatory properties likely mediated through interaction with the murine C-type lectin receptor SIGN-R1 (a homologue of the human DC-SIGN) and FcyRIIb (22, 60). In our study, we found that total IgG preserved an anti-inflammatory glycosylation profile in patients who remained in remission, but changed to an inflammation-associated phenotype in relapsing patients. It remains unclear whether this change merely represent a bystander acute-phase reaction or whether the loss of anti-inflammatory effector function of total IgG enabled PR3-ANCA to induce disease reactivation. Notably, low galactosylation and sialylation at the ANCA rise predicts disease reactivation, suggesting that the change of total IgG towards an inflammation-associated phenotype precedes the onset of disease reactivation. We hypothesize that these anti-inflammatory mechanisms of total IgG are involved in the suppression of active disease in our AAV patients who remain in remission.

One may wonder what causes the change of the glycosylation profile of total IgG from an anti-inflammatory towards a pro-inflammatory phenotype. One study observed an average reduction of total IgG sialylation by 40% upon antigenic challenge in a mouse model (22). Based on our findings, we speculate that a second hit that is not related to the presence of PR3-ANCA nor the glycosylation profile of PR3-ANCA is required for a relapse after an ANCA rise (the “first hit”). Several candidates for such a second hit have been postulated, such as microorganisms (61), environmental factors (62, 63), and/or other auto-antibodies (64). No functional data are currently available regarding the role of the glycosylation profile of total IgG and/or antigen-specific IgG in the capacity of PR3-ANCA to induce inflammation and this should be further studied.

A recent study reported a novel correlation between bisection of PR3-ANCA and disease state (38). In our study we find a correlation between bisection and relapse/remission. The level of bisection of total IgG decreases significantly in relapsing patients, while it stays stable in non-relapsing patients. In PR3-ANCA the level of bisection remains stable in relapsing patients, while it increases in non-relapsing patients. While the effect of a bisecting GlcNAc on IgG effector functions is minor compared to that of the other glycosylation features, it has been reported that bisection can enhance antibody-dependent cellular cytotoxicity (ADCC) through increased FcγRIIIa affinity (65, 66). Since a reduction in bisection is seen during AAV relapse, it is likely that the minor anti-inflammatory effect of decreased bisection is overshadowed by effects of other changes in glycosylation and that

ADCC may only play a minor role in the pathogenesis of AAV (67). A decrease in IgG bisection has not been reported for any other autoimmune disorders, while an increase in bisection has been observed for Lambert-Eaton Myasthenic Syndrome (LEMS) (29). A slight increase in fucosylation over time was seen in total IgG of relapsing patients. In contrast, PR3-ANCA showed a minor decrease in fucosylation for both relapsing and non-relapsing patients. While the absence of a core fucose can greatly enhance the inflammatory properties of IgG through increased FcγRIIIa affinity, the differences in fucosylation in our study cohort are likely too small to be of much influence.

Our findings regarding the glycosylation profile of total IgG compared to antigen-specific PR3 markedly differ from those of a previous study, which reported a reduction of galactosylation, sialylation and bisection of PR3-ANCA as compared to total IgG, while we observe that bisection, but not galactosylation and sialylation is reduced in PR3-ANCA. These differences may be largely caused by the pronounced differences in study design (38). First, we included patients with severe AAV as well as patients with more limited forms of AAV, while the previous report only included patients with severe AAV (38). Second, our patients were in remission at the time of sampling, while the patients of Wuhrer et al. were sampled at the time of active disease (38). Interestingly, both studies observe a lower degree of bisection in PR3-ANCA compared to total IgG.

Our study is limited by the amount of included patients, hence only the *N*-glycan analysis was included in the statistical evaluation. Future validation in other, larger study cohorts is warranted in which the predictive value of a multitude of factors, in particular the IgG *N*-glycan analysis, should be evaluated using multivariate techniques, including principle components analysis. A strong aspect of our study is that our patients are highly characterized and we only included patients with GPA positive for PR3-ANCA. Yet differences still remain in organ involvement and immunosuppressive therapy. Our findings, however, may not apply to patients with MPA or patients positive for MPO-ANCA and this should be further investigated.

Most importantly, we addressed the clinical value of the aberrant glycosylation which we observe in AAV patients. Changes in IgG glycosylation, especially galactosylation and sialylation, might be useful to screen patients for their risk of relapse. Our data indicates that analysis of total IgG would be sufficient for this purpose. Already in the first serum sample,

acquired a median time of 8 months before the time of relapse, we could identify patients that are at risk for a future disease relapse. Differences in the glycosylation profile between relapsing and non-relapsing patients becomes more pronounced as the time of relapse approaches. Longitudinal acquisition of serum samples taken every few months would reveal changes in the personal glycosylation profile of each patient that could possibly help as a guide when to start treatment in these patients. It remains to be studied, however, whether treatment based on this information will be able to minimize tissue and organ damage.

References

1. Wilde, B., van Paassen, P., Witzke, O., and Cohen Tervaert, J. W. (2011) New pathophysiological insights and treatment of ANCA-associated vasculitis. *Kidney Int* 79, 599-612
2. Xiao, H., Heeringa, P., Hu, P., Liu, Z., Zhao, M., Aratani, Y., Maeda, N., Falk, R. J., and Jennette, J. C. (2002) Antineutrophil cytoplasmic autoantibodies specific for myeloperoxidase cause glomerulonephritis and vasculitis in mice. *J Clin Invest* 110, 955-963
3. Little, M. A., Al-Ani, B., Ren, S., Al-Nuaimi, H., Leite, M., Jr., Alpers, C. E., Savage, C. O., and Duffield, J. S. (2012) Anti-Proteinase 3 Anti-Neutrophil Cytoplasm Autoantibodies Recapitulate Systemic Vasculitis in Mice with a Humanized Immune System. *PLoS ONE* 7, e28626
4. Huugen, D., Xiao, H., van Esch, A., Falk, R. J., Peutz-Kootstra, C. J., Buurman, W. A., Tervaert, J. W. C., Jennette, J. C., and Heeringa, P. (2005) Aggravation of Anti-Myeloperoxidase Antibody-Induced Glomerulonephritis by Bacterial Lipopolysaccharide: Role of Tumor Necrosis Factor-α. *The American Journal of Pathology* 167, 47-58
5. Tervaert, J. W., Goldschmeding, R., Elema, J. D., van der Giessen, M., Huitema, M. G., van der Hem, G. K., The, T. H., von dem Borne, A. E., and Kallenberg, C. G. (1990) Autoantibodies against myeloid lysosomal enzymes in crescentic glomerulonephritis. *Kidney Int* 37, 799-806
6. Nolle, B., Specks, U., Ludemann, J., Rohrbach, M. S., DeRemee, R. A., and Gross, W. L. (1989) Anticytoplasmic autoantibodies: their immunodiagnostic value in Wegener granulomatosis. *Ann Intern Med* 111, 28-40
7. Cohen Tervaert, J. W., and Damoiseaux, J. G. M. C. (2012) Antineutrophil cytoplasmic autoantibodies: how are they detected and what is their use for diagnosis, classification and follow-up? *Clin Rev Allergy Immunol* 43, 211-219
8. Cohen Tervaert, J., van der Woude, F., Fauci, A., Ambrus, J., Velosa, J., Keane, W., Meijer, S., van der Giessen, M., van der Hem, G., and The, T. (1989) Association between active Wegener's granulomatosis and anticytoplasmic antibodies. *Arch Intern Med* 159, 2461-2465
9. Boomsma, M. M., Stegeman, C. A., Van Der Leij, M. J., Oost, W., Hermans, J., Kallenberg, C. G. M., Limburg, P. C., and Tervaert, J. W. C. (2000) Prediction of relapses in Wegener's granulomatosis by measurement of antineutrophil cytoplasmic antibody levels: A prospective study. *Arthritis Rheum* 43, 2025-2033
10. Birck, R., Schmitt, W. H., Kaelsch, I. A., and van der Woude, F. J. (2006) Serial ANCA Determinations for Monitoring Disease Activity in Patients With ANCA-Associated Vasculitis: Systematic Review. *American Journal of Kidney Diseases* 47, 15-23
11. Kemna, M. J., Damoiseaux, J. G. M. C., Austen, J., Winkens, B., Peters, J., van Paassen, P., and Cohen Tervaert, J. W. (2015) ANCA as a predictor of relapse: useful in patients with renal involvement but not in patients with nonrenal disease. *J Am Soc Nephrol* 26, 537-542
12. Fussner, L. A., Hummel, A. M., Schroeder, D. R., Silva, F., Cartin-Ceba, R., Snyder, M. R., Hoffman, G. S., Kallenberg, C. G., Langford, C. A., Merkel, P. A., Monach, P. A., Seo, P., Spiera, R. F., St Clair, E. W., Tchao, N. K., Stone, J. H., and Specks, U. (2016) Factors Determining the Clinical Utility of Serial Measurements of Antineutrophil Cytoplasmic Antibodies Targeting Proteinase 3. *Arthritis Rheum* 68, 1700-1710
13. Koh, J. H., Kemna, M. J., Cohen Tervaert, J. W., and Kim, W. U. (2016) Can an Increase in Antineutrophil Cytoplasmic Autoantibody Titer Predict Relapses in Antineutrophil Cytoplasmic Antibody-Associated Vasculitis? *Arthritis Rheum* 68, 1571-1573
14. Yamaguchi, M., Ando, M., Kato, S., Katsuno, T., Kato, N., Kosugi, T., Sato, W., Tsuboi, N., Yasuda, Y., Mizuno, M., Ito, Y., Matsuo, S., and Maruyama, S. (2015) Increase of Antimyeloperoxidase Antineutrophil Cytoplasmic Antibody (ANCA) in Patients with Renal ANCA-associated Vasculitis: Association with Risk to Relapse. *The Journal of Rheumatology* 42, 1853-1860
15. Anthony, R. M., Wermeling, F., and Ravetch, J. V. (2012) Novel roles for the IgG Fc glycan. *Ann N Y Acad Sci* 1253, 170-180
16. Brady, L. J., Velayudhan, J., Visone, D. B., Daugherty, K. C., Bartron, J. L., Coon, M., Cornwall, C., Hinckley, P. J., and Connell-Crowley, L. (2015) The criticality of high-resolution N-linked

carbohydrate assays and detailed characterization of antibody effector function in the context of biosimilar development. *MAbs* 7, 562-570
17. Subedi, G. P., and Barb, A. W. (2016) The immunoglobulin G1 N-glycan composition affects binding to each low affinity Fc γ receptor. *MAbs* 8, 1512-1524
18. Thomann, M., Schlothauer, T., Dashivets, T., Malik, S., Avenal, C., Bulau, P., Rüger, P., and Reusch, D. (2015) In Vitro Glycoengineering of IgG1 and Its Effect on Fc Receptor Binding and ADCC Activity. *PLoS ONE* 10, e0134949
19. Malhotra, R., Wormald, M. R., Rudd, P. M., Fischer, P. B., Dwek, R. A., and Sim, R. B. (1995) Glycosylation changes of IgG associated with rheumatoid arthritis can activate complement via the mannose-binding protein. *Nat Med* 1, 237-243
20. Anthony, R. M., and Nimmerjahn, F. (2011) The role of differential IgG glycosylation in the interaction of antibodies with FcγRs in vivo. *Curr Opin Organ Transplant* 16, 7-14
21. Karsten, C. M., Pandey, M. K., Figge, J., Kilchenstein, R., Taylor, P. R., Rosas, M., McDonald, J. U., Orr, S. J., Berger, M., Petzold, D., Blanchard, V., Winkler, A., Hess, C., Reid, D. M., Majoul, I. V., Strait, R. T., Harris, N. L., Kohl, G., Wex, E., Ludwig, R., Zillikens, D., Nimmerjahn, F., Finkelman, F. D., Brown, G. D., Ehlers, M., and Kohl, J. (2012) Anti-inflammatory activity of IgG1 mediated by Fc galactosylation and association of FcγRIIB and dectin-1. *Nat Med* 18, 1401-1406
22. Kaneko, Y., Nimmerjahn, F., and Ravetch, J. V. (2006) Anti-Inflammatory Activity of Immunoglobulin G Resulting from Fc Sialylation. *Science* 313, 670-673
23. van Timmeren, M. M., van der Veen, B. S., Stegeman, C. A., Petersen, A. H., Hellmark, T., Collin, M., and Heeringa, P. (2010) IgG Glycan Hydrolysis Attenuates ANCA-Mediated Glomerulonephritis. *Journal of the American Society of Nephrology* 21, 1103-1114
24. Parekh, R. B., Dwek, R. A., Sutton, B. J., Fernandes, D. L., Leung, A., Stanworth, D., Rademacher, T. W., Mizuochi, T., Taniguchi, T., Matsuta, K., and et al. (1985) Association of rheumatoid arthritis and primary osteoarthritis with changes in the glycosylation pattern of total serum IgG. *Nature* 316, 452-457
25. Watson, M., Rudd, P. M., Bland, M., Dwek, R. A., and Axford, J. S. (1999) Sugar printing rheumatic diseases: a potential method for disease differentiation using immunoglobulin G oligosaccharides. *Arthritis Rheum* 42, 1682-1690
26. Wuhrer, M., Selman, M. H., McDonnell, L. A., Kumpfel, T., Derfuss, T., Khademi, M., Olsson, T., Hohlfeld, R., Meinl, E., and Krumbholz, M. (2015) Pro-inflammatory pattern of IgG1 Fc glycosylation in multiple sclerosis cerebrospinal fluid. *J Neuroinflammation* 12, 235
27. Vuckovic, F., Kristic, J., Gudelj, I., Teruel, M., Keser, T., Pezer, M., Pucic-Bakovic, M., Stambuk, J., Trbojevic-Akmacic, I., Barrios, C., Pavic, T., Menni, C., Wang, Y., Zhou, Y., Cui, L., Song, H., Zeng, Q., Guo, X., Pons-Estel, B. A., McKeigue, P., Leslie Patrick, A., Gornik, O., Spector, T. D., Harjacek, M., Alarcon-Riquelme, M., Molokhia, M., Wang, W., and Lauc, G. (2015) Association of systemic lupus erythematosus with decreased immunosuppressive potential of the IgG glycome. *Arthritis Rheum* 67, 2978-2989
28. Trbojevic Akmacic, I., Ventham, N. T., Theodoratou, E., Vuckovic, F., Kennedy, N. A., Kristic, J., Nimmo, E. R., Kalla, R., Drummond, H., Stambuk, J., Dunlop, M. G., Novokmet, M., Aulchenko, Y., Gornik, O., Campbell, H., Pucic Bakovic, M., Satsangi, J., and Lauc, G. (2015) Inflammatory bowel disease associates with proinflammatory potential of the immunoglobulin G glycome. *Inflamm Bowel Dis* 21, 1237-1247
29. Selman, M. H., Niks, E. H., Titulaer, M. J., Verschuuren, J. J., Wuhrer, M., and Deelder, A. M. (2011) IgG fc N-glycosylation changes in Lambert-Eaton myasthenic syndrome and myasthenia gravis. *J Proteome Res* 10, 143-152
30. Scherer, H. U., van der Woude, D., Ioan-Facsinay, A., el Bannoudi, H., Trouw, L. A., Wang, J., Haupl, T., Burmester, G. R., Deelder, A. M., Huizinga, T. W., Wuhrer, M., and Toes, R. E. (2010) Glycan profiling of anti-citrullinated protein antibodies isolated from human serum and synovial fluid. *Arthritis Rheum* 62, 1620-1629

31. Rombouts, Y., Ewing, E., van de Stadt, L. A., Selman, M. H., Trouw, L. A., Deelder, A. M., Huizinga, T. W., Wuhrer, M., van Schaardenburg, D., Toes, R. E., and Scherer, H. U. (2015) Anti-citrullinated protein antibodies acquire a pro-inflammatory Fc glycosylation phenotype prior to the onset of rheumatoid arthritis. *Ann Rheum Dis* 74, 234-241
32. Magorivska, I., Muñoz, L. E., Janko, C., Dumych, T., Rech, J., Schett, G., Nimmerjahn, F., Bilyy, R., and Herrmann, M. (2016) Sialylation of anti-histone immunoglobulin G autoantibodies determines their capabilities to participate in the clearance of late apoptotic cells. *Clinical & Experimental Immunology* 184, 110-117
33. Fickentscher, C., Magorivska, I., Janko, C., Biermann, M., Bilyy, R., Nalli, C., Tincani, A., Medeghini, V., Meini, A., Nimmerjahn, F., Schett, G., Mu, #xf1, oz, L. E., Andreoli, L., and Herrmann, M. (2015) The Pathogenicity of Anti-β2GP1-IgG Autoantibodies Depends on Fc Glycosylation. *Journal of Immunology Research* 2015, 12
34. Ercan, A., Cui, J., Chatterton, D. E., Deane, K. D., Hazen, M. M., Brintnell, W., O'Donnell, C. I., Derber, L. A., Weinblatt, M. E., Shadick, N. A., Bell, D. A., Cairns, E., Solomon, D. H., Holers, V. M., Rudd, P. M., and Lee, D. M. (2010) Aberrant IgG galactosylation precedes disease onset, correlates with disease activity, and is prevalent in autoantibodies in rheumatoid arthritis. *Arthritis Rheum* 62, 2239-2248
35. Holland, M., Yagi, H., Takahashi, N., Kato, K., Savage, C. O. S., Goodall, D. M., and Jefferis, R. (2006) Differential glycosylation of polyclonal IgG, IgG-Fc and IgG-Fab isolated from the sera of patients with ANCA-associated systemic vasculitis. *Biochimica et Biophysica Acta* 1760, 669-677
36. Holland, M., Takada, K., Okumoto, T., Takahashi, N., Kato, K., Adu, D., Ben-Smith, A., Harper, L., Savage, C. O. S., and Jefferis, R. (2002) Hypogalactosylation of serum IgG in patients with ANCA-associated systemic vasculitis. *Clinical & Experimental Immunology* 129, 183-190
37. Espy, C., Morelle, W., Kavian, N., Grange, P., Goulvestre, C., Viallon, V., Chéreau, C., Pagnoux, C., Michalski, J.-C., Guillevin, L., Weill, B., Batteux, F., and Guilpain, P. (2011) Sialylation levels of anti–proteinase 3 antibodies are associated with the activity of granulomatosis with polyangiitis (Wegener's). *Arthritis Rheum* 63, 2105-2115
38. Wuhrer, M., Stavenhagen, K., Koeleman, C. A., Selman, M. H., Harper, L., Jacobs, B. C., Savage, C. O., Jefferis, R., Deelder, A. M., and Morgan, M. (2015) Skewed Fc glycosylation profiles of anti-proteinase 3 immunoglobulin G1 autoantibodies from granulomatosis with polyangiitis patients show low levels of bisection, galactosylation, and sialylation. *J Proteome Res* 14, 1657-1665
39. Hellmich, B., Flossmann, O., Gross, W. L., Bacon, P., Cohen Tervaert, J. W., Guillevin, L., Jayne, D., Mahr, A., Merkel, P. A., Raspe, H., Scott, D. G. I., Witter, J., Yazici, H., and Luqmani, R. A. (2007) EULAR recommendations for conducting clinical studies and/or clinical trials in systemic vasculitis: focus on anti-neutrophil cytoplasm antibody-associated vasculitis. *Annals of the Rheumatic Diseases* 66, 605-617
40. Watts, R., Lane, S., Hanslik, T., Hauser, T., Hellmich, B., Koldingsnes, W., Mahr, A., Segelmark, M., Cohen Tervaert, J. W., and Scott, D. (2007) Development and validation of a consensus methodology for the classification of the ANCA-associated vasculitides and polyarteritis nodosa for epidemiological studies. *Ann Rheum Dis* 66, 222-227
41. Central Commitee on Research Involving Human Subjects. Non WMO Research. [Internet. Accessed June 22, 2016.] Available from: http://www.ccmo.nl/en/non-wmo-research.
42. Berden, A. E., Ferrario, F., Hagen, E. C., Jayne, D. R., Jennette, J. C., Joh, K., Neumann, I., Noel, L. H., Pusey, C. D., Waldherr, R., Bruijn, J. A., and Bajema, I. M. (2010) Histopathologic classification of ANCA-associated glomerulonephritis. *J Am Soc Nephrol* 21, 1628-1636
43. Hilhorst, M., Wilde, B., van Breda Vriesman, P., van Paassen, P., and Cohen Tervaert, J. W. (2013) Estimating Renal Survival Using the ANCA-Associated GN Classification. *J Am Soc Nephrol* 24, 1371-1375
44. Mukhtyar, C., Guillevin, L., Cid, M. C., Dasgupta, B., de Groot, K., Gross, W., Hauser, T., Hellmich, B., Jayne, D., Kallenberg, C. G. M., Merkel, P. A., Raspe, H., Salvarani, C., Scott, D. G. I., Stegeman, C., Watts, R., Westman, K., Witter, J., Yazici, H., Luqmani, R., and Group, f. t. E. V. S.

(2009) EULAR recommendations for the management of primary small and medium vessel vasculitis. *Annals of the Rheumatic Diseases* 68, 310-317
45. Boomsma, M. M., Damoiseaux, J. G. M. C., Stegeman, C. A., Kallenberg, C. G., Patnaik, M., Peter, J. B., and Tervaert, J. W. (2003) Image analysis: a novel approach for the quantification of antineutrophil cytoplasmic antibody levels in patients with Wegener's granulomatosis. *J Immunol Methods* 274, 27-35
46. Damoiseaux, J. G. M. C., Slot, M. C., Vaessen, M., Stegeman, C. A., Van Paassen, P., and Cohen Tervaert, J. W. (2005) Evaluation of a New Fluorescent-Enzyme Immuno-Assay for Diagnosis and Follow-up of ANCA-Associated Vasculitis. *Journal of Clinical Immunology* 25, 202-208
47. Falck, D., Jansen, B. C., Plomp, R., Reusch, D., Haberger, M., and Wuhrer, M. (2015) Glycoforms of Immunoglobulin G Based Biopharmaceuticals Are Differentially Cleaved by Trypsin Due to the Glycoform Influence on Higher-Order Structure. *J Proteome Res* 14, 4019-4028
48. Selman, M. H., Derks, R. J., Bondt, A., Palmblad, M., Schoenmaker, B., Koeleman, C. A., van de Geijn, F. E., Dolhain, R. J., Deelder, A. M., and Wuhrer, M. (2012) Fc specific IgG glycosylation profiling by robust nano-reverse phase HPLC-MS using a sheath-flow ESI sprayer interface. *J Proteomics* 75, 1318-1329
49. Chambers, M. C., Maclean, B., Burke, R., Amodei, D., Ruderman, D. L., Neumann, S., Gatto, L., Fischer, B., Pratt, B., Egertson, J., Hoff, K., Kessner, D., Tasman, N., Shulman, N., Frewen, B., Baker, T. A., Brusniak, M. Y., Paulse, C., Creasy, D., Flashner, L., Kani, K., Moulding, C., Seymour, S. L., Nuwaysir, L. M., Lefebvre, B., Kuhlmann, F., Roark, J., Rainer, P., Detlev, S., Hemenway, T., Huhmer, A., Langridge, J., Connolly, B., Chadick, T., Holly, K., Eckels, J., Deutsch, E. W., Moritz, R. L., Katz, J. E., Agus, D. B., MacCoss, M., Tabb, D. L., and Mallick, P. (2012) A cross-platform toolkit for mass spectrometry and proteomics. *Nat Biotechnol* 30, 918-920
50. Pluskal, T., Castillo, S., Villar-Briones, A., and Oresic, M. (2010) MZmine 2: modular framework for processing, visualizing, and analyzing mass spectrometry-based molecular profile data. *BMC Bioinformatics* 11, 395
51. Plomp, R., Dekkers, G., Rombouts, Y., Visser, R., Koeleman, C. A., Kammeijer, G. S., Jansen, B. C., Rispens, T., Hensbergen, P. J., Vidarsson, G., and Wuhrer, M. (2015) Hinge-Region O-Glycosylation of Human Immunoglobulin G3 (IgG3). *Mol Cell Proteomics* 14, 1373-1384
52. Zauner, G., Selman, M. H., Bondt, A., Rombouts, Y., Blank, D., Deelder, A. M., and Wuhrer, M. (2013) Glycoproteomic analysis of antibodies. *Mol Cell Proteomics* 12, 856-865
53. Bondt, A., Selman, M. H., Deelder, A. M., Hazes, J. M., Willemsen, S. P., Wuhrer, M., and Dolhain, R. J. (2013) Association between galactosylation of immunoglobulin G and improvement of rheumatoid arthritis during pregnancy is independent of sialylation. *J Proteome Res* 12, 4522-4531
54. Matsumoto, A., Shikata, K., Takeuchi, F., Kojima, N., and Mizuochi, T. (2000) Autoantibody activity of IgG rheumatoid factor increases with decreasing levels of galactosylation and sialylation. *J Biochem* 128, 621-628
55. Albrecht, S., Unwin, L., Muniyappa, M., and Rudd, P. M. (2014) Glycosylation as a marker for inflammatory arthritis. *Cancer Biomark* 14, 17-28
56. Rademacher, T. W., Williams, P., and Dwek, R. A. (1994) Agalactosyl glycoforms of IgG autoantibodies are pathogenic. *Proc Natl Acad Sci U S A* 91, 6123-6127
57. Hilhorst, M., van Paassen, P., van Rie, H., Bijnens, N., Heerings-Rewinkel, P., van Breda Vriesman, P., and Cohen Tervaert, J. W. (2015) Complement in ANCA-associated glomerulonephritis. *Nephrology Dialysis Transplantation* Epub ahead of print
58. Xiao, H., Dairaghi, D. J., Powers, J. P., Ertl, L. S., Baumgart, T., Wang, Y., Seitz, L. C., Penfold, M. E. T., Gan, L., Hu, P., Lu, B., Gerard, N. P., Gerard, C., Schall, T. J., Jaen, J. C., Falk, R. J., and Jennette, J. C. (2014) C5a Receptor (CD88) Blockade Protects against MPO-ANCA GN. *Journal of the American Society of Nephrology* 25, 225-231
59. Huugen, D., van Esch, A., Xiao, H., Peutz-Kootstra, C. J., Buurman, W. A., Tervaert, J. W., Jennette, J. C., and Heeringa, P. (2007) Inhibition of complement factor C5 protects against anti-myeloperoxidase antibody-mediated glomerulonephritis in mice. *Kidney Int* 71, 646-654

60. Collin, M., and Ehlers, M. (2013) The carbohydrate switch between pathogenic and immunosuppressive antigen-specific antibodies. *Exp Dermatol* 22, 511-514
61. Popa, E. R., Stegeman, C. A., Kallenberg, C. G., and Cohen Tervaert, J. W. (2002) Staphylococcus aureus and Wegener's granulomatosis. *Arthritis Res* 4, 77-79
62. Gatenby, P. A., Lucas, R. M., Engelsen, O., Ponsonby, A.-L., and Clements, M. (2009) Antineutrophil cytoplasmic antibody–associated vasculitides: Could geographic patterns be explained by ambient ultraviolet radiation? *Arthritis Care & Research* 61, 1417-1424
63. de Lind van Wijngaarden, R. A. F., van Rijn, L., Hagen, E. C., Watts, R. A., Gregorini, G., Cohen Tervaert, J. W., Mahr, A. D., Niles, J. L., de Heer, E., Bruijn, J. A., and Bajema, I. M. (2008) Hypotheses on the Etiology of Antineutrophil Cytoplasmic Autoantibody–Associated Vasculitis: The Cause Is Hidden, but the Result Is Known. *Clinical Journal of the American Society of Nephrology* 3, 237-252
64. Kain, R., Tadema, H., McKinney, E. F., Benharkou, A., Brandes, R., Peschel, A., Hubert, V., Feenstra, T., Sengölge, G., Stegeman, C., Heeringa, P., Lyons, P. A., Smith, K. G. C., Kallenberg, C., and Rees, A. J. (2012) High Prevalence of Autoantibodies to hLAMP-2 in Anti–Neutrophil Cytoplasmic Antibody–Associated Vasculitis. *J Am Soc Nephrol* 23, 556-566
65. Davies, J., Jiang, L., Pan, L. Z., LaBarre, M. J., Anderson, D., and Reff, M. (2001) Expression of GnTIII in a recombinant anti-CD20 CHO production cell line: Expression of antibodies with altered glycoforms leads to an increase in ADCC through higher affinity for FC gamma RIII. *Biotechnol Bioeng* 74, 288-294
66. Shinkawa, T., Nakamura, K., Yamane, N., Shoji-Hosaka, E., Kanda, Y., Sakurada, M., Uchida, K., Anazawa, H., Satoh, M., Yamasaki, M., Hanai, N., and Shitara, K. (2003) The absence of fucose but not the presence of galactose or bisecting N-acetylglucosamine of human IgG1 complex-type oligosaccharides shows the critical role of enhancing antibody-dependent cellular cytotoxicity. *J Biol Chem* 278, 3466-3473
67. Mayet, W. J., Schwarting, A., and Meyer zum Buschenfelde, K. H. (1994) Cytotoxic effects of antibodies to proteinase 3 (C-ANCA) on human endothelial cells. *Clin Exp Immunol* 97, 458-465

Supplemental Information

A complete overview of the supplemental information is available online at https://www.ncbi.nlm.nih.gov/pmc/articles/PMC5360573.

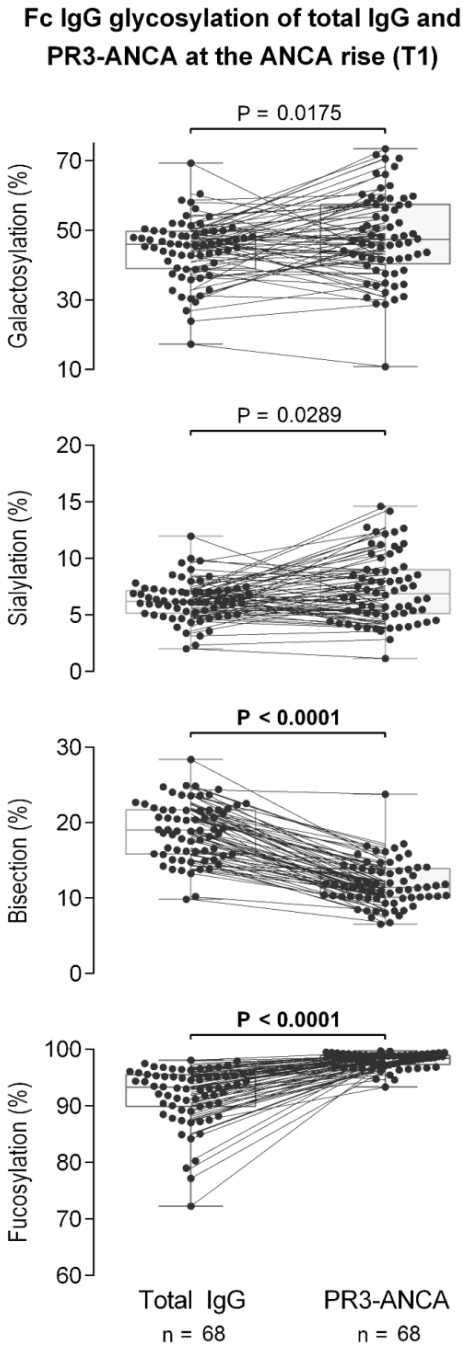

Supplemental Figure S4.2: The glycosylation profile of total IgG (white background) differs significantly compared to PR3-ANCA (yellow background) at the time of an ANCA rise (T1). IgG1 Fc glycosylation is shown. Dots represent individual patients. The box represents the median with interquartile range, the whiskers delineate the min-max range. Significant differences were evaluated using the Mann Whitney U test, P-values are shown if <0.10 and in bold if <0.0125.

Chapter 5:

Subclass-specific IgG glycosylation is associated with markers of inflammation and metabolic health

Manuscript submitted to *Scientific Reports*

Authors: R. Plomp[1], L. R. Ruhaak[1,2], H. Uh[3], K. R. Reiding[1], M. Selman[1,4], J. J. Houwing-Duistermaat[5], P. E. Slagboom[5], M. Beekman[5], M. Wuhrer[1]

[1]*Center for Proteomics and Metabolomics, Leiden University Medical Center, Leiden, The Netherlands;*
[2]*Department of Clinical Chemistry and Laboratory Medicine, Leiden University Medical Center, Leiden, The Netherlands;*
[3]*Department of Medical Statistics and Bioinformatics, Leiden University Medical Center, Leiden, The Netherlands;*
[4]*present address: Pharming Group N.V., Leiden, The Netherlands;*
[5]*Department of Molecular Epidemiology, Leiden University Medical Center, Leiden, The Netherlands*

Table of Contents

5.1: Summary

This study indicates that glycosylation of immunoglobulin G, the most abundant antibody in human blood, may convey useful information with regard to inflammation and metabolic health. IgG occurs in the form of different subclasses, of which the effector functions show significant variation. Our method provides subclass-specific IgG glycosylation profiling, while previous large-scale studies neglected to measure IgG2-specific glycosylation.

We analysed the plasma Fc glycosylation profiles of IgG1, IgG2 and IgG4 in a cohort of 1826 individuals by liquid chromatography-mass spectrometry. For all subclasses, a low level of galactosylation and sialylation and a high degree of core fucosylation associated with poor metabolic health, i.e. increased inflammation as assessed by C-reactive protein, low serum high-density lipoprotein cholesterol and high triglycerides, which are all known to indicate increased risk of cardiovascular disease. IgG2 consistently showed weaker associations of its galactosylation and sialylation with the metabolic markers, compared to IgG1 and IgG4, while the direction of the associations were overall similar for the different IgG subclasses.

These findings demonstrate the potential of IgG glycosylation as a biomarker for inflammation and metabolic health, and further research is required to determine the additive value of IgG glycosylation on top of biomarkers which are currently used.

5.2: Introduction

Glycosylation is known to reflect the physiological state of an organism and changes thereof (1). For immunoglobulin G (IgG), which occupies a central role in the immune system, it is known that the conserved *N*-glycan located at asparagine 297 on the fragment crystallisable (Fc) part of IgG can modulate inflammatory responses: a lack of core fucose, galactose and *N*-acetylneuraminic (sialic) acid increases the ability of IgG to induce antibody-dependent cell-mediated cytotoxicity (ADCC) in mice (2-4). Furthermore, glycosylation of IgG is associated with various pathologies. Autoimmune diseases are generally associated with decreased galactosylation and sialylation of IgG Fc, which is a hallmark of the inflammatory state of these pathologies (5-10). Different types of cancer (11-13) and viral infections (14, 15) have been shown to exhibit low galactosylation and sialylation of IgG *N*-glycans similar to inflammatory conditions. IgG glycosylation, specifically low galactosylation and sialylation, has also been proposed as a biomarker of inflammageing, the state of chronic weak inflammation in elderly individuals (16), or more generally as a marker of immune activation (17).

Since IgG glycosylation appears to be altered during a state of inflammation, it is not surprising that associations between certain glycoforms and the inflammatory marker C-reactive protein (CRP) have been reported (18-20). Inflammation often goes hand in hand with ageing and poor metabolic health, which are all associated with a higher risk for cardiovascular disease (21). However, an overview is lacking of the associations between IgG glycosylation and an assortment of clinical markers related to metabolic health in healthy individuals. Furthermore, other large cohort studies (>100 healthy participants) on IgG glycosylation report either a released glycan profile (22, 23), which does not contain any subclass-specific information, or a joint profile for IgG2 and IgG3 (24, 25). This is due to the shared peptide sequence of the tryptic glycopeptides of these two subclasses, which prevents separate analysis by mass spectrometry, and thereby prevents separate examination of IgG2 glycosylation. While little is known about the differences in effector functions between IgG subclasses *in vivo*, *in vitro* assays ascribe to IgG2 a lower overall binding affinity to Fc gamma receptors (FcγRs) (26-28) and ADCC capacity (29, 30).

In order to evaluate the merit of IgG Fc *N*-glycosylation as a systemic biomarker of metabolic health, we here analysed glycosylation of IgG1, 2 and 4 in a cohort of 1826 healthy

individuals to investigate associations with known markers related to inflammation and metabolic health. The population analysed in this study is part of the Leiden Longevity Study, aimed at determining the biological foundation of healthy ageing. In this study we investigate the glycosylation of IgG in relation to measurements of inflammation, such as plasma levels of C-reactive protein (CRP) and interleukin-6 (IL-6), and of metabolism such as lipids and thyroid hormone. IgG glycosylation analysis has previously been performed on this cohort with MALDI-MS to facilitate the measurement of 6 *N*-glycopeptides for IgG1 and IgG2 each, allowing only the assessment of galactosylation and bisection (18). The current analysis is performed with nanoLC-ESI-QTOF-MS, which offers enhanced sensitivity and a more extensive glycoprofiling of the samples: 20 *N*-glycopeptides were identified for IgG1 and IgG2 and 10 for IgG4, providing novel information on the sialylation and fucosylation of these samples.

5.3: Methods

5.3.1: Cohort participants and study design

This study was performed on 1995 available plasma samples from 1170 offspring of nonagenarian siblings of the Leiden Longevity cohort and 656 of their partners as controls (31). Families were included if the parents were over 91 (for females) or over 89 (for males) years of age. Previously we have shown that comparison of the middle-aged offspring of long-lived parents and their partners as controls reveals parameters associating with familial metabolic health, thereby demonstrating that offspring have a beneficial immune-metabolic health (32-34). An overview of the age and sex distribution of the participants can be seen in Table 1. All participants have given informed consent prior to sample collection, in accordance with the Declaration of Helsinki. The study design and protocols were approved by the Ethical Committee of the Leiden University Medical Center. Venous blood was collected under non-fasting conditions.

5.3.2: Metabolic parameter analysis

Various parameters related to metabolic health were determined for the participants of the Leiden Longevity cohort. High-sensitivity measurements of CRP, glucose, total cholesterol (TC), high-density lipoprotein cholesterol (HDLC) and triglycerides (TG) in blood samples were performed on the Hitachi Modular P-800, while free triiodothyronine (T3) levels were assessed using a Modular E-170 (both Roche Diagnostics, Almere, the Netherlands) (35-37). Low-density lipoprotein cholesterol (LDLC) was derived from these measurements using the Friedewald formula (LDLC = TC - HDLC - TG/5) (38). If the level of TG exceeded 4.52 mmol/L, LDLC was listed as missing. The level of insulin in blood was assessed with an Immulite 2500 (DPC, Los Angeles, CA) (37). Interleukin 6 (IL-6) levels were determined with an enzyme-linked immunosorbent assay (ELISA) (Sanquin Reagents, Amsterdam, The Netherlands). Furthermore, the self-reported current smoking status of the participants was registered. An ELISA was done on serum to determine if the participants had antibodies against cytomegalovirus (PKS Assay, Medac, Wedel, Germany). The distributions of these metabolic parameters within the cohort are listed in Table 1.

5.3.3: IgG glycopeptide sample preparation

IgGs were purified in 96-well format as described previously (18). An amount of 2 µL of plasma was incubated with 15 µL Protein A Sepharose Fast Flow beads (GE Healthcare, Uppsala, Sweden) and 150 µL phosphate buffered saline (PBS) on a 96-well filter plate for 1

hour at room temperature while shaking. The IgG samples were washed three times with PBS and three times with MilliQ-purified water, followed by elution with 100 µL 100 mM formic acid. The samples were then dried in a vacuum concentrator for 2 hours at 60 °C and resuspended in 40 µL 25 mM ammonium bicarbonate with 200 ng of trypsin (sequencing grade modified trypsin, Promega, Madison, WI). Digestion took place overnight at 37 °C. Two of the 96-well plates were prepared twice to assess interbatch variation.

5.3.4: NanoLC-ESI-QTOF-MS analysis

The IgG glycopeptide samples were analysed using liquid chromatography coupled to mass spectrometry (LC-MS), in a setup described previously (39). An amount of 2.5 µL of the samples was injected in an Ultimate 3000 RSLCnano liquid chromatography system (Dionex, Sunnyvale, CA). The samples were first washed on an Acclaim PepMap100 C18 trap column (5 mm x 300 µm i.d., Dionex, Sunnyvale, CA), and subsequently separated on an Ascentis Express C18 nanoLC column (50 mm x 75 µm i.d., 2.7 µm HALO fused core particles; Supelco, Bellefonte, PA) with a flow rate of 0.9 µL/min. The following linear gradient was used, with solvent A consisting of 0.1% trifluoroacetic acid and B of 95% acetonitrile (ACN): t=0, 3% solvent B; t=2, 6%; t=4.5, 18%; t=5, 30%; t=7, 30%; t=8, 0%; t=11, 0%.

Via a sheath-flow electrospray (ESI) interface (Agilent Technologies, Santa Clara, CA), the LC was coupled to a Maxis Impact quadrupole time-of-flight (QTOF)-MS system (micrOTOF-Q; Bruker Daltonics, Bremen, Germany). A sheath-flow consisting of 50% isopropanol, 20% propionic acid (Merck) and 30% MilliQ-purified water was applied at 2 µL/min, and nitrogen gas was applied at 4 L/min. MS1 spectra were acquired with a frequency of 0.5 Hz and within an *m/z* range of 600-2000. An IgG standard and two blank injections were run in between every 12 runs.

5.3.5: Glycosylation data processing

Glycosylation profiles were extracted from the data files as described previously (39). The three subclass-specific types of tryptic glycopeptides (IgG1: EEQYNSTYR, IgG2: EEQFNSTFR, IgG4: EEQFNSTYR) eluted at different time points, with the retention times of differentially glycosylated variants of each subclass clustered closely together, since the secondary interaction between sialic acids and the silica column which usually leads to later elution of sialylated glycopeptides was negated by the use of TFA in the mobile phase (Supplemental Figure S1). Based on their mass and previous characterizations of IgG *N*-

glycan structures (40-42), 20 *N*-glycans were identified for both IgG1 and IgG2 (Supplemental Table S1). For IgG4, only 10 glycopeptides could be identified, as the mass of the minor afucosylated species overlapped with the much more abundant IgG1 fucosylated glycopeptides, and could thus not be reliably distinguished from tailing of the latter (Supplemental Table S1).

LC-MS data was examined and calibrated in Compass Data Analysis 4.2 (Bruker Daltonics), based on a list of four of the most abundant *N*-glycopeptides (G0F, G1F, G2F, G2FS) in both double and triple charge state. The data was then exported in mzXML file format. Alignment of the retention times was done using MSalign. Next, the in-house developed software tool Xtractor 2D (43) was used to extract the signal intensity of the first three isotopic peaks of various glycopeptides in both double and triple charge state, within an *m/z* window of $\pm$ 0.04 Thompson and a time window of $\pm$ 10 s surrounding the retention time. These *N*-glycopeptides were inputted from a list of *m/z* values (Supplemental Table S1) encompassing 20 IgG1 glycopeptides, 20 IgG2 glycopeptides and 10 IgG4 glycopeptides (afucosylated IgG4 species overlapped with IgG1 glycopeptides and thus could not be properly analysed).

For each *N*-glycopeptide, the signal intensity of the three isotopic peaks in double and triple charge state were background-corrected and summed. IgG2-G1FNS1 (the IgG2 glycan carrying 1 galactose (G1), 1 sialic acid (S1), a core fucose (F) and a bisecting N-acetylglucosamine) and IgG2-G2FNS1, which each represented less than 0.4% of the total IgG2 glycopeptide abundance, were excluded from the data due to a severe batch effect. The *N*-glycopeptide signals were normalised by dividing each by the total signal intensity of all *N*-glycopeptides belonging to that subclass, yielding percentage data amounting to 100% per subclass.

An intensity threshold was determined based on the percentage of the signal intensity which was derived from *N*-glycopeptides with a signal-to-background ratio larger than 3. If the total intensity per subclass did not exceed the threshold, data from that subclass was excluded. After this exclusion, IgG1 data remained for 1825 individuals, IgG2 for 1826 and IgG4 for 1742.

5.3.6: Data preprocessing

From the individual *N*-glycan percentage data, five glycosylation features were determined for each IgG subclass (calculations can be found in Supplemental Table S2): fucosylation (% of fucosylated *N*-glycopeptides), bisection (% of *N*-glycopeptides carrying a bisecting *N*-acetylglucosamine (GlcNAc)), galactosylation (% of galactoses per antennae), sialylation (% of sialic acids per antennae) and sialic acid per galactose (% of sialic acids per galactose). Fucosylation could not be determined for IgG4, since no afucosylated IgG4 glycopeptides were measured due to overlap with IgG1 glycopeptides.

The three most abundant glycopeptides (G0F, G1F, G2F) of the standard IgG samples run in between every twelve samples showed a relative standard deviation (RSD) of 4.7%. The average intraplate RSD was 1.9%, based on standard IgG samples run during the measurement of each plate, and the interplate RSD was 3.3%. Therefore, batch correction was done using the ComBat package (44) in R 3.0.1, with the 96-well plates as batches (45). Furthermore, any glycosylation feature value which deviated more than 5 standard deviations (SD) from the mean was replaced by 5 x SD from the mean.

The glycosylation features and several of the metabolic parameters (CRP, IL-6, glucose, insulin, TG, free T3) underwent natural logarithm transformation, in order to make these parameters more normally distributed.

5.3.7: Reproducibility of the analysis

Two 96-well plates with samples were purified and analysed twice, to assess the reproducibility of our method. To assess the level of correlation between these sample plates, a Pearson's correlation test was performed in R using the function cor.test(). The glycosylation features on the different plates showed a high level of correlation, i.e. Pearson's correlation coefficients (r) of 0.97 (fucosylation), 0.95 (bisection), 0.98 (galactosylation), 0.93(sialylation) and 0.80 (SA per gal) for IgG1. From the two plates which were prepared twice, the plate which showed the highest signals was used for further data analysis.

5.3.8: Statistical association analysis

Statistical analyses were done in R 3.0.1 (45). A paired t-test from the R stats package was performed to see if there was a significant difference in glycosylation features between different subclasses. Regression analysis was done using the generalised estimating equation package (geepack) (46) to account for family relationship. A linear model with formula

'glycosylation feature Y ~ β_1*metabolic parameter X + β_2*age + β_3*sex + β_4*(age*sex) + error' was fitted to the data, to assess the association between each glycosylation feature and metabolic parameter, while correcting for confounders, taking into account within-family relatedness and under the assumption of an exchangeable correlation structure. The output of this regression analysis consisted of a p_1-value, β_1 coefficient and its standard error (SE(β_1)) describing the association between each glycosylation feature and metabolic parameter, and from this the t statistic was derived using t=β_1/SE(β_1). To assess the relation of IgG glycosylation with familial metabolic health, a logistic regression model was applied using the same software, with familial metabolic health as dependent variable Y, coded as 0 for controls and 1 for members of long-lived families, and IgG glycosylation features as independent variable X, while correcting for the same confounders and within-family relatedness, and under the assumption of an independent correlation structure.

Significance was defined as a *p*-value below the Bonferroni-corrected threshold α = 0.000714 (7.14 x 10^{-4}). This threshold was derived from the standard threshold α = 0.05 divided by 70, which is the number of analyses between 14 variables (metabolic parameters + age + sex) and 5 glycosylation features (subclass-specific versions of the same glycosylation feature were disregarded since they are highly intercorrelated).

5.3.9: Data visualization

Before plotting, glycosylation data was corrected for either age-specific differences or for both age- and sex-specific differences, by fitting the linear model (geepack) 'glycosylation feature ~ age' or 'glycosylation feature ~ age + sex', and then taking the residuals. The ggplot2 package in R was used for visualization of the data (47). A linear trendline was fitted to plots with the geom_smooth function. A heatmap was generated in R with the weighted correlation network analysis (WGCNA) package (48).

5.4: Results

By performing nanoLC-ESI-QTOF-MS analysis on tryptic IgG glycopeptides, Fc glycosylation profiles of IgG1, IgG2 and IgG4 were determined for nearly 2000 participants of the Leiden Longevity study. After data curation, IgG1, IgG2 and IgG4 data remained for respectively 1825, 1826 and 1742 participants. From the individual *N*-glycan data five glycosylation features were derived (the calculations can be found in Supplemental Table S2): fucosylation, bisection, galactosylation, sialylation and sialic acid per galactose (SA per gal). The distribution of the age and sex of the study population, as well as the average measurements of metabolic parameters and IgG glycosylation features, can be found in Table 1. IgG glycosylation was observed to be age-dependent and differences were seen between males and females (Supplemental Figure S2), as has been described in earlier reports (25, 49-51). We observe minor but significant differences between the glycosylation features of the three IgG subclasses: t-tests revealed a *p*-value below 1.0×10^{-10} for all comparisons of glycosylation features between IgG subclasses (1 vs 2, 1 vs 4 and 2 vs 4). IgG2 exhibits a higher level of fucosylation (IgG1: 91.2 ± 4.1% (mean ± SD); IgG2: 97.4 ± 0.9%; IgG4 fucosylation could not be determined), but a lower level of bisection (IgG1: 19.1 ± 3.3%, IgG2: 13.9 ± 2.7%, IgG4: 19.6 ± 4.4%) and galactosylation (IgG1: 50.1 ± 6.4%, IgG2: 39.5 ± 6.2%, IgG4: 43.7 ± 6.9%).

Table 5.1: Distribution of age, sex, glycosylation features and metabolic parameters within the Leiden Longevity study population. The mean, standard deviation (SD), range (minimum and maximum value) and number of included samples (N) are given. Samples that were excluded based on data quality criteria were not used for calculation of values in this table.

	mean	SD	range	N
Age (years)	59.1	+/-6.7	30.2 - 79.2	1826
Sex	47.1 % male	-	-	1826
CRP (mg/L)	2.86	+/-9.5	0.2 - 228.7	1813
IL-6 (pg/mL)	0.67	+/-1.2	0 - 19.6	1705
Glucose (mmol/L)	5.94	+/-1.5	2.5 - 26.3	1816
Insulin (mU/L)	23.23	+/-22.1	2 - 238	1766
TC (mmol/L)	5.55	+/-1.2	1.4 - 10.8	1820
LDLC (mmol/L)	3.33	+/-1.0	0.7 - 7.9	1772
HDLC (mmol/L)	1.42	+/-0.4	0.2 - 3.2	1819
TG (mmol/L)	1.82	+/-1.2	0.2 – 21.2	1820
free T3 (pmol/L)	4.12	+/-0.8	1.8 – 14.3	1819
smoking	13.6 % smoking	-	-	1587
CMV serostatus	45.9 % positive	-	-	1437
longevity	64.1 % offspring	-	-	1826
IgG1 fucosylation	91.2 %	+/-4.1	69.3 - 99.5	1825
IgG2 fucosylation	97.4 %	+/-0.9	92.6 - 99.1	1826
IgG1 bisection	19.1 %	+/-3.3	6.5 - 35.8	1825
IgG2 bisection	13.9 %	+/-2.7	6.4 - 26.5	1826
IgG4 bisection	19.6 %	+/-4.4	8.8 - 41.3	1742
IgG1 galactosylation	50.1 %	+/-6.4	24.6 - 70.8	1825
IgG2 galactosylation	39.5 %	+/-6.2	9.0 - 61.3	1826
IgG4 galactosylation	43.7 %	+/-6.9	14.5 - 66.0	1742
IgG1 sialylation	6.8 %	+/-1.4	2.5 - 14.0	1825
IgG2 sialylation	6.2 %	+/-1.4	1.4 - 11.9	1826
IgG4 sialylation	9.1 %	+/-2.0	3.2 - 18.9	1742
IgG1 sialic acid per gal	13.6 %	+/-1.6	9.0 - 21.5	1825
IgG2 sialic acid per gal	15.5 %	+/-1.7	9.4 - 22.5	1826
IgG4 sialic acid per gal	20.7 %	+/-2.0	13.8 - 30.8	1742

5.4.1: Association between IgG glycosylation and immune-metabolic parameters

To investigate the relationship between IgG glycosylation and metabolic health parameters, we performed regression analysis. The resulting associations between IgG glycosylation features and metabolic parameters are visualised in a heatmap (Figure 1, Supplemental Table S3).

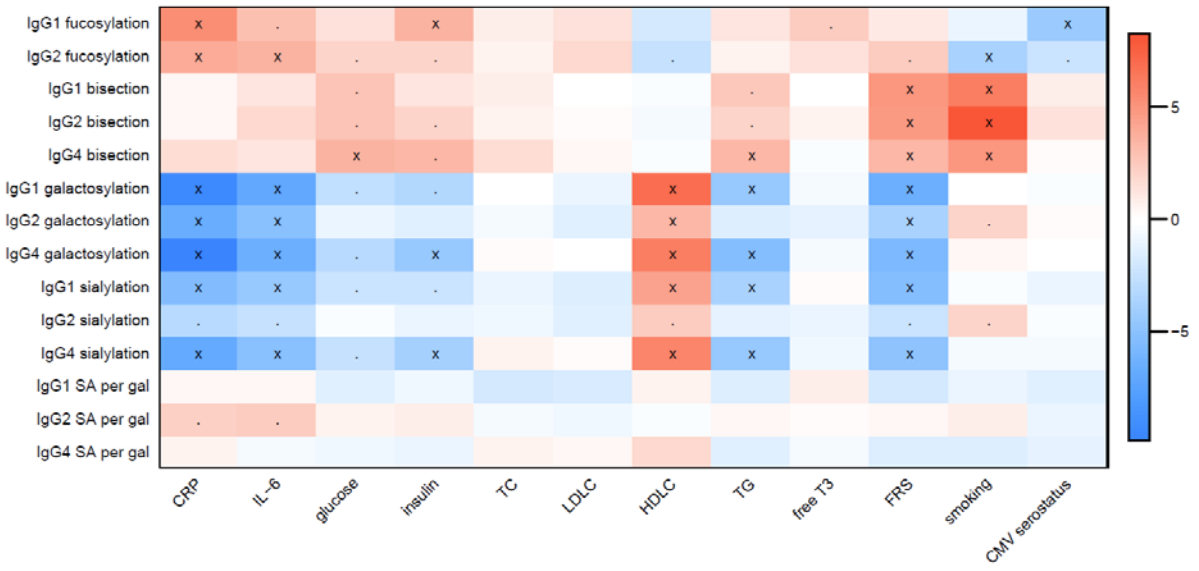

Figure 5.1: Associations between glycosylation features (y-axis) and metabolic parameters (x-axis). The colors indicate the magnitude of the association as represented by the t statistic ($t_1=\beta_1/SE(\beta_1)$), with positive associations shown in red and negative in blue. Associations with a p_1-value below 0.05 are marked with a point, while associations with a p_1-value below 7.14×10^{-4}, which are significant after Bonferroni correction, are marked with an X.

5.4.1.1: Inflammation markers

Low galactosylation and high fucosylation of IgG were associated with low-grade inflammation, as determined by the well-known inflammation markers CRP and IL-6 (Figure 2) ($p_1 < 1.0 \times 10^{-4}$ for all but IgG1 fucosylation, for which $p_1 = 2.0 \times 10^{-3}$). IgG sialylation was also found to be significantly associated with CRP and IL-6 ($p_{1,IgG1} < 1.0 \times 10^{-4}$), but sialic acid per galactose was not ($p_{1,IgG1} = 6.2 \times 10^{-1}$, $p_{1,IgG2} = 1.9 \times 10^{-2}$ for CRP). Notably, CRP only has a small contribution to the variance of IgG galactosylation ($R^2 = 0.0569$ with a linear model for IgG1).

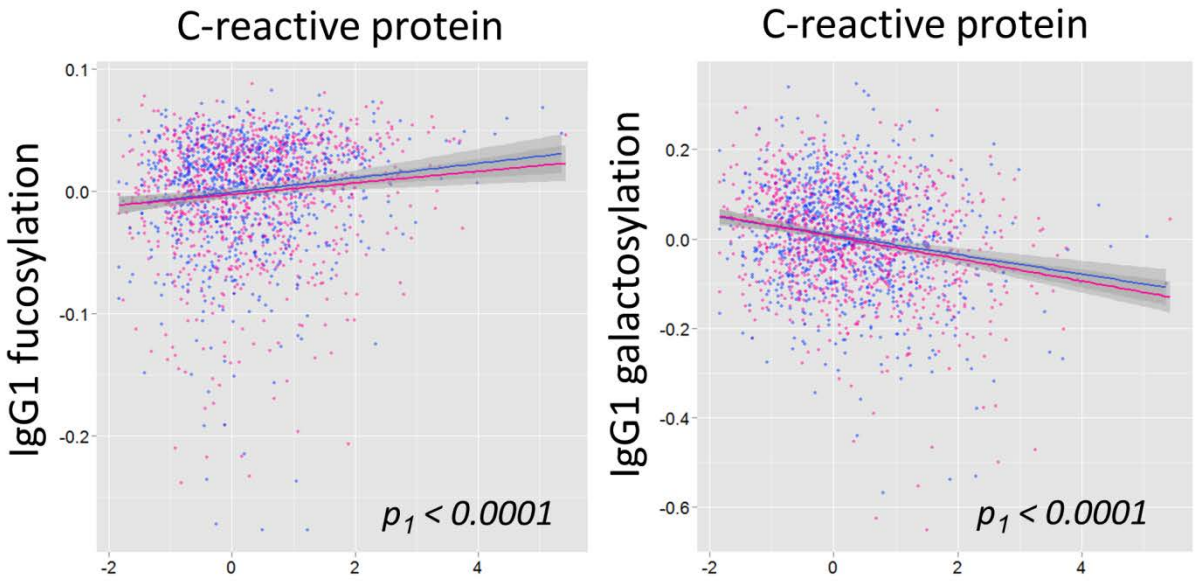

Figure 5.2: IgG1 galactosylation and fucosylation are associated with CRP. Both parameters were log transformed, and the glycosylation features were subsequently corrected for age. Males are shown in blue and females in pink. A trend line is shown with a 95% confidence interval. P_1-values and β_1 coefficients are shown for the total population (males and females).

5.4.1.2: Metabolic markers

An increase in IgG galactosylation and sialylation ($p_{1,IgG1} < 1.0 \times 10^{-4}$), as well as a non-significant decrease in fucosylation ($p_{1,IgG1} = 5.2 \times 10^{-2}$; $p_{1,IgG2} = 1.3 \times 10^{-2}$) was found to be associated with high levels of HDLC and low levels of triglycerides (TG), which together form beneficial risk profiles for cardiovascular disease, type 2 diabetes and obesity (52, 53). A negative association of galactosylation and a positive association of fucosylation were seen with insulin and glucose, which are markers for diabetes type 2 and are also known to associate with inflammation (54). Interestingly, IgG bisection exhibited a positive association with glucose and insulin ($p_{1,IgG4} = 3.1 \times 10^{-4}$ for glucose). Total cholesterol (TC) and LDLC did not significantly influence IgG glycosylation.

5.4.1.3: CMV and smoking

The presence of antibodies against cytomegalovirus (CMV), a common herpes virus which remains latent in many individuals after infection, was found to be associated with low levels of IgG fucosylation. Fucosylation generally shows little variation between individuals (91.2 ± 4.1% for IgG1), so while the difference in IgG1 fucosylation between seronegative and seropositive individuals was small (91.7 ± 3.7% versus 90.6 ± 4.3%), it was nonetheless

significant ($p_{1,IgG1} < 1.0 \times 10^{-4}$, Figure 3A). The other glycosylation features did not show any association with CMV serostatus.

Furthermore, smokers showed significantly higher levels of bisection compared to non-smokers ($p_1 < 1.0 \times 10^{-4}$ for all IgG subclasses, Figure 3B), as well as a low level of IgG2 fucosylation. Individuals who smoked at the time of sample collection showed a mean IgG1 bisection of 20.1±3.4% versus 18.9±3.2% in non-smokers.

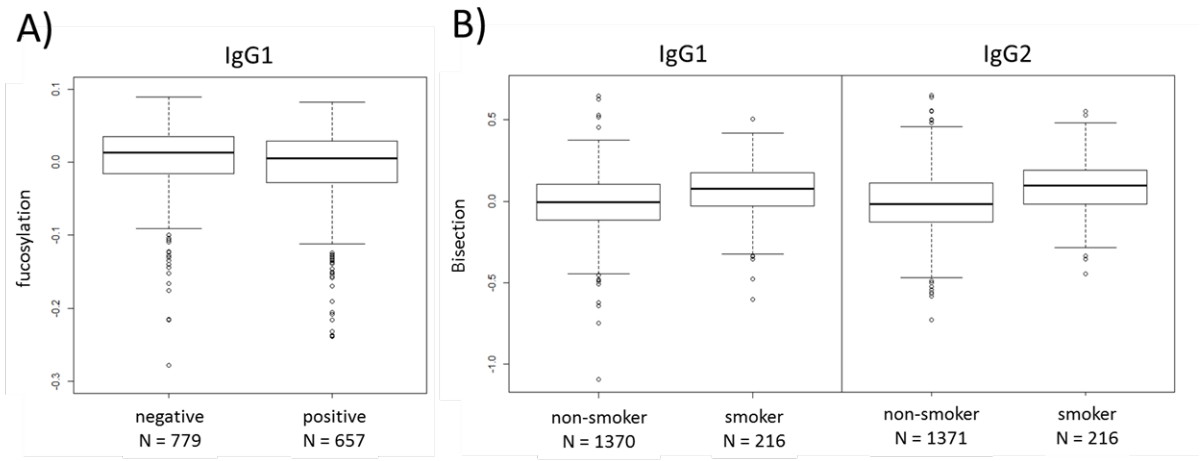

Figure 5.3: A) IgG1 fucosylation of individuals with and without cytomegalovirus infection. B) IgG1 and IgG2 bisection of smokers/non-smokers. The interquartile range is shown. Glycosylation data was log transformed and adjusted for age and sex.

5.4.2: Familial metabolic health

Since we observed various associations between IgG glycosylation and parameters related to metabolic health, we were interested to know whether metabolically healthier middle-aged offspring from nonagenarians differed from controls. None of the glycosylation features showed, however, a significant difference between these groups, although several trends could be observed (Supplemental Table S4). IgG4 galactosylation was increased in offspring ($p_{1,IgG4} < 2.2 \times 10^{-2}$), which is consistent with a 'younger' and less inflammatory IgG glycosylation profile. Furthermore, weak trends towards lower levels of IgG bisection ($p_{1,IgG4} = 1.4 \times 10^{-1}$) and fucosylation ($p_{1,IgG2} = 5.1 \times 10^{-2}$) could be observed in members of long-lived families.

5.5: Discussion

In the current study we were able to measure IgG2-specific glycosylation features, in addition to those of IgG1 and IgG4. IgG2-specific glycosylation features showed similar associations with inflammation and metabolic health markers compared to IgG1 and 4, though IgG2 glycosylation levels showed in general weaker associations for galactosylation and sialylation. Low levels of galactosylation and sialylation, as well as a high degree of fucosylation, appear to reflect an inflammatory state, poor metabolic health and potentially cardiovascular disease risk. In contrast, sialic acid per galactose was not associated with any of the metabolic markers. Furthermore, fucosylation is lower in individuals infected with cytomegalovirus, reflecting a low grade chronic inflammatory state, and current smokers show higher bisecting GlcNAc levels.

5.5.1: IgG subclass-specific glycosylation differences

Tryptic *N*-glycopeptides of IgG2 and IgG3 share the same peptide sequence in Caucasians (55, 56), and so the commonly used protein G enrichment of IgG gives a joint profile for both IgG2 and IgG3. In this study we use Protein A for IgG purification, which does not capture IgG3 and thus allows for separate glycoprofiling of IgG2.

The IgG subclasses display subtle differences in their Fc glycosylation, with IgG2 exhibiting a higher degree of fucosylation and a lower level of bisection and galactosylation compared to the other subclasses, confirming observations from a previous study which examined only four blood samples (57). In addition, we find that galactosylation and sialylation of IgG2 generally display a weaker association (i.e. lower β coefficient) with markers of inflammation and metabolic health compared to IgG1 and IgG4. This corresponds with literature, in which it is described that IgG2 exhibits the lowest overall affinity for FcγRs (26-28) and has the lowest ADCC capacity (29) compared to other IgG subclasses. One may speculate that the lower capacity of IgG2 to trigger inflammatory responses, either pro-inflammatory via FcγRI, IIa, IIc, and IIIa, or anti-inflammatory via FcγRIIb, could result in a weaker association with inflammation and metabolic health as compared to the other subclasses. Furthermore, it has been reported that IgG2 antibody production is primarily triggered during T-cell independent immune reactions (27, 30), which would also contribute to the weaker association with T-cell-secreted IL-6 and IL-6-stimulated CRP. Together this points towards a more limited role of IgG2 with regard to inflammation compared to the other IgG subclasses.

5.5.2: Galactosylation and sialylation

Low galactosylation and sialylation are associated with a state of inflammation, which is in concordance with previous work based on MALDI-MS measurements within the same cohort (18, 58) and in children (17). Our observations also agree with observations of decreased galactosylation and sialylation in autoimmune diseases (5-10, 59-61) and with several experimental findings that IgG without galactose and/or sialic acid has a higher inflammatory capacity (3, 4, 62). The mechanism by which IgG galactosylation influences inflammation is not yet fully resolved, but the *N*-glycan in the Fc region is known to confer changes to the IgG structure and influence the binding of IgG with Fc gamma receptors (FcγRs) (63-65). The association between low galactosylation and sialylation and inflammation may thus reflect an active role of IgG glycosylation in the regulation of immune activation.

Levels of sialylation and galactosylation are highly correlated, reflecting the fact that the attachment of a sialic acid requires the presence of a galactose. We find that galactosylation and sialylation exhibit very similar associations with metabolic parameters, but the association with sialylation is generally slightly weaker than with galactosylation. The presence of sialic acid on IgG *N*-glycans is thought to confer an anti-inflammatory effect (3, 62). However, we did not observe any significant association with sialic acid per galactose, i.e. the percentage of galactoses which carry a sialic acid, indicating that associations with sialylation may be mediated by its close correlation with galactosylation. This is in line with several previous studies which concluded that galactosylation of human IgG, rather than sialylation, appears to show a pronounced negative association with clinical parameters and infection (5, 66). Together, this supports the notion that IgG Fc galactosylation may be involved in modulating inflammation.

5.5.3: Fucosylation

We find that IgG fucosylation is higher in individuals with a higher level of inflammation. Despite the fact that functional studies have shown that the lack of a core fucose in IgG glycosylation greatly increases the inflammatory capacity through increased binding to FcγRIIIa (63, 64, 67, 68), an increase in IgG fucosylation is sometimes observed in autoimmune patients (59-61). Furthermore, a previous study using UHPLC found that high CRP levels were associated with high fucosylation in non-galactosylated IgG *N*-glycans (69), further demonstrating that IgG fucosylation is increased during a state of inflammation.

In individuals who tested seropositive for cytomegalovirus (CMV), a common virus which can remain in the body in a latent state after infection, a significantly lower level of fucosylation of IgG was observed than in non-infected individuals. Low IgG fucosylation has also been observed in alloantibody reactions against platelets and red blood cells during pregnancy or blood transfusion (70) and in anti-HIV antibodies, and has been suggested to be a defence mechanism by B-cells to increase antiviral control (71). It may be interesting to investigate autoantibodies against CMV, as well as other types of infectious agents, to determine whether low fucosylation of IgG might be a hallmark of viral infections.

5.5.4: Bisection

In our cohort, incidence of a bisecting GlcNAc is higher in current smokers than in non-smokers. Smoking is associated with inflammation and can enact changes in the levels of various cytokines (72). Since cytokine expression has been shown to affect IgG glycosylation, including bisection (73), it can be speculated that these smoking-associated IgG glycosylation changes are mediated through cytokines. A high degree of bisection is further associated with high levels of glucose and triglycerides. This association between higher IgG bisection and poor metabolic health could, as a consequence of the association between smoking and an unhealthy diet and lifestyle (74), reflect the higher prevalence of type 2 diabetes among smokers.

Though we find that the IgG glycosylation reflects poor metabolic health, we were unable to find significant differences between middle-aged members of long-lived families and controls, who are known to differ on various metabolic measures (32, 36, 75). Previous work which applied MALDI-MS to the same set of samples reported a significant decrease in the level of bisection of offspring of long-lived people, but only in individuals below 60 years of age (18), and IgG glycosylation features contributed to the differentiation of controls and members of long-lived families (76). While in the current dataset we indeed observe a similar trend towards decreased bisection in the offspring of long-lived individuals, this was not significant in either the total cohort ($p_{1,IgG4} = 4.3 \times 10^{-1}$), or among individuals below the age of 60 ($p_{1,IgG1} = 5.2 \times 10^{-2}$, $p_{1,IgG4} = 6.3 \times 10^{-1}$; Supplemental Table S4), even without multiple testing correction. From a biological viewpoint the non-significant trends we see are consistent with the age-dependence of IgG glycosylation. Bisection is known to increase with age , so the changes observed in offspring of long-lived individuals are exemplary of a ‘younger’ profile. These trends fit the expectation that individuals prone to longevity show

delayed ageing which is reflected in their IgG glycosylation profile. A recent investigation into the released *N*-glycan profile of plasma samples within the Leiden Longevity cohort also could not find any association with longevity, while replicating several of the associations we find between *N*-glycans which likely originate from IgG and metabolic markers (58).

5.5.5: Biomarker potential of IgG glycosylation

Our study design does not allow for estimation of whether IgG glycosylation features offer a predictive value for cardiovascular disease in addition to traditional markers of inflammation. However, we did test whether IgG parameters associate with metabolic health markers and which of the subclasses features the strongest association. We show that low levels of galactosylation and sialylation and high levels of fucosylation correspond with a state of low-grade inflammation and a detrimental lipid profile. This is likely due to the fact that a chronic level of inflammation is a known risk factor for cardiovascular disease (77). This high risk profile is also characteristic for ageing – in older individuals, galactosylation and sialylation decrease, while bisection increases (Supplemental Figure 2).

IgG glycosylation is known to be directly involved in the interaction with Fcγ receptors and complement, modulating the inflammatory capacity of the antibody (3, 78), whereas CRP influences opsonisation of pathogens and complement activation (79). Considering the complexity of the immune system and the multitude of pathways therein, these regulatory mechanisms might well be (partially) additive rather than overlapping. Furthermore, while IgG2 glycosylation appears to be of less consequence for low-grade inflammation, IgG2 is more involved in T-cell independent immune reactions compared to the other IgG subclasses and CRP (27, 30). This could provide a reason to further investigate associations of this IgG subclass with health and disease phenotype. Finally, the complexity of IgG glycosylation with its multiple features has the advantage that it could provide more information than the level of a single analyte such as CRP, as shown by the IgG glycosylation features exhibiting different associations with metabolic markers. For these reasons, subclass-specific glycosylation of IgG, independently or in combination with the traditional inflammation marker CRP, might be a more informative biomarker regarding inflammation and metabolic health than CRP on its own. Further studies are required to review the added value of IgG glycosylation as a biomarker in light of prospective data on cardiovascular incidence and morbidity.

References

1. Varki, A. (1993) Biological roles of oligosaccharides: all of the theories are correct. *Glycobiology* 3, 97-130
2. Collin, M., and Ehlers, M. (2013) The carbohydrate switch between pathogenic and immunosuppressive antigen-specific antibodies. *Exp Dermatol* 22, 511-514
3. Kaneko, Y., Nimmerjahn, F., and Ravetch, J. V. (2006) Anti-inflammatory activity of immunoglobulin G resulting from Fc sialylation. *Science* 313, 670-673
4. Karsten, C. M., Pandey, M. K., Figge, J., Kilchenstein, R., Taylor, P. R., Rosas, M., McDonald, J. U., Orr, S. J., Berger, M., Petzold, D., Blanchard, V., Winkler, A., Hess, C., Reid, D. M., Majoul, I. V., Strait, R. T., Harris, N. L., Kohl, G., Wex, E., Ludwig, R., Zillikens, D., Nimmerjahn, F., Finkelman, F. D., Brown, G. D., Ehlers, M., and Kohl, J. (2012) Anti-inflammatory activity of IgG1 mediated by Fc galactosylation and association of FcgammaRIIB and dectin-1. *Nat Med* 18, 1401-1406
5. Bondt, A., Selman, M. H., Deelder, A. M., Hazes, J. M., Willemsen, S. P., Wuhrer, M., and Dolhain, R. J. (2013) Association between galactosylation of immunoglobulin G and improvement of rheumatoid arthritis during pregnancy is independent of sialylation. *J Proteome Res* 12, 4522-4531
6. Matsumoto, A., Shikata, K., Takeuchi, F., Kojima, N., and Mizuochi, T. (2000) Autoantibody activity of IgG rheumatoid factor increases with decreasing levels of galactosylation and sialylation. *J Biochem* 128, 621-628
7. Holland, M., Yagi, H., Takahashi, N., Kato, K., Savage, C. O., Goodall, D. M., and Jefferis, R. (2006) Differential glycosylation of polyclonal IgG, IgG-Fc and IgG-Fab isolated from the sera of patients with ANCA-associated systemic vasculitis. *Biochim Biophys Acta* 1760, 669-677
8. Wuhrer, M., Stavenhagen, K., Koeleman, C. A., Selman, M. H., Harper, L., Jacobs, B. C., Savage, C. O., Jefferis, R., Deelder, A. M., and Morgan, M. (2015) Skewed Fc glycosylation profiles of anti-proteinase 3 immunoglobulin G1 autoantibodies from granulomatosis with polyangiitis patients show low levels of bisection, galactosylation, and sialylation. *J Proteome Res* 14, 1657-1665
9. Vuckovic, F., Kristic, J., Gudelj, I., Teruel, M., Keser, T., Pezer, M., Pucic-Bakovic, M., Stambuk, J., Trbojevic-Akmacic, I., Barrios, C., Pavic, T., Menni, C., Wang, Y., Zhou, Y., Cui, L., Song, H., Zeng, Q., Guo, X., Pons-Estel, B. A., McKeigue, P., Leslie Patrick, A., Gornik, O., Spector, T. D., Harjacek, M., Alarcon-Riquelme, M., Molokhia, M., Wang, W., and Lauc, G. (2015) Association of systemic lupus erythematosus with decreased immunosuppressive potential of the IgG glycome. *Arthritis Rheumatol* 67, 2978-2989
10. Youinou, P., Pennec, Y. L., Casburn-Budd, R., Dueymes, M., Letoux, G., and Lamour, A. (1992) Galactose terminating oligosaccharides of IgG in patients with primary Sjogren's syndrome. *J Autoimmun* 5, 393-400
11. Theodoratou, E., Thaci, K., Agakov, F., Timofeeva, M. N., Stambuk, J., Pucic-Bakovic, M., Vuckovic, F., Orchard, P., Agakova, A., Din, F. V., Brown, E., Rudd, P. M., Farrington, S. M., Dunlop, M. G., Campbell, H., and Lauc, G. (2016) Glycosylation of plasma IgG in colorectal cancer prognosis. *Sci Rep* 6, 28098
12. Saldova, R., Wormald, M. R., Dwek, R. A., and Rudd, P. M. (2008) Glycosylation changes on serum glycoproteins in ovarian cancer may contribute to disease pathogenesis. *Dis Markers* 25, 219-232
13. Ren, S., Zhang, Z., Xu, C., Guo, L., Lu, R., Sun, Y., Guo, J., Qin, R., Qin, W., and Gu, J. (2016) Distribution of IgG galactosylation as a promising biomarker for cancer screening in multiple cancer types. *Cell Res* 26, 963-966
14. Moore, J. S., Wu, X., Kulhavy, R., Tomana, M., Novak, J., Moldoveanu, Z., Brown, R., Goepfert, P. A., and Mestecky, J. (2005) Increased levels of galactose-deficient IgG in sera of HIV-1-infected individuals. *Aids* 19, 381-389
15. Ho, C. H., Chien, R. N., Cheng, P. N., Liu, J. H., Liu, C. K., Su, C. S., Wu, I. C., Li, I. C., Tsai, H. W., Wu, S. L., Liu, W. C., Chen, S. H., and Chang, T. T. (2015) Aberrant serum immunoglobulin G

glycosylation in chronic hepatitis B is associated with histological liver damage and reversible by antiviral therapy. *J Infect Dis* 211, 115-124
16. Dall'Olio, F., Vanhooren, V., Chen, C. C., Slagboom, P. E., Wuhrer, M., and Franceschi, C. (2013) N-glycomic biomarkers of biological aging and longevity: a link with inflammaging. *Ageing Res Rev* 12, 685-698
17. de Jong, S. E., Selman, M. H., Adegnika, A. A., Amoah, A. S., van Riet, E., Kruize, Y. C., Raynes, J. G., Rodriguez, A., Boakye, D., von Mutius, E., Knulst, A. C., Genuneit, J., Cooper, P. J., Hokke, C. H., Wuhrer, M., and Yazdanbakhsh, M. (2016) IgG1 Fc N-glycan galactosylation as a biomarker for immune activation. *Sci Rep* 6, 28207
18. Ruhaak, L. R., Uh, H. W., Beekman, M., Koeleman, C. A., Hokke, C. H., Westendorp, R. G., Wuhrer, M., Houwing-Duistermaat, J. J., Slagboom, P. E., and Deelder, A. M. (2010) Decreased levels of bisecting GlcNAc glycoforms of IgG are associated with human longevity. *PLoS One* 5, e12566
19. Gardinassi, L. G., Dotz, V., Hipgrave Ederveen, A., de Almeida, R. P., Nery Costa, C. H., Costa, D. L., de Jesus, A. R., Mayboroda, O. A., Garcia, G. R., Wuhrer, M., and de Miranda Santos, I. K. (2014) Clinical severity of visceral leishmaniasis is associated with changes in immunoglobulin g fc N-glycosylation. *MBio* 5, e01844
20. Dube, R., Rook, G. A., Steele, J., Brealey, R., Dwek, R., Rademacher, T., and Lennard-Jones, J. (1990) Agalactosyl IgG in inflammatory bowel disease: correlation with C-reactive protein. *Gut* 31, 431-434
21. Guarner, V., and Rubio-Ruiz, M. E. (2015) Low-grade systemic inflammation connects aging, metabolic syndrome and cardiovascular disease. *Interdiscip Top Gerontol* 40, 99-106
22. Kristic, J., Vuckovic, F., Menni, C., Klaric, L., Keser, T., Beceheli, I., Pucic-Bakovic, M., Novokmet, M., Mangino, M., Thaqi, K., Rudan, P., Novokmet, N., Sarac, J., Missoni, S., Kolcic, I., Polasek, O., Rudan, I., Campbell, H., Hayward, C., Aulchenko, Y., Valdes, A., Wilson, J. F., Gornik, O., Primorac, D., Zoldos, V., Spector, T., and Lauc, G. (2014) Glycans are a novel biomarker of chronological and biological ages. *J Gerontol A Biol Sci Med Sci* 69, 779-789
23. Pucic, M., Knezevic, A., Vidic, J., Adamczyk, B., Novokmet, M., Polasek, O., Gornik, O., Supraha-Goreta, S., Wormald, M. R., Redzic, I., Campbell, H., Wright, A., Hastie, N. D., Wilson, J. F., Rudan, I., Wuhrer, M., Rudd, P. M., Josic, D., and Lauc, G. (2011) High throughput isolation and glycosylation analysis of IgG-variability and heritability of the IgG glycome in three isolated human populations. *Mol Cell Proteomics* 10, M111.010090
24. Lauc, G., Huffman, J. E., Pucic, M., Zgaga, L., Adamczyk, B., Muzinic, A., Novokmet, M., Polasek, O., Gornik, O., Kristic, J., Keser, T., Vitart, V., Scheijen, B., Uh, H. W., Molokhia, M., Patrick, A. L., McKeigue, P., Kolcic, I., Lukic, I. K., Swann, O., van Leeuwen, F. N., Ruhaak, L. R., Houwing-Duistermaat, J. J., Slagboom, P. E., Beekman, M., de Craen, A. J., Deelder, A. M., Zeng, Q., Wang, W., Hastie, N. D., Gyllensten, U., Wilson, J. F., Wuhrer, M., Wright, A. F., Rudd, P. M., Hayward, C., Aulchenko, Y., Campbell, H., and Rudan, I. (2013) Loci associated with N-glycosylation of human immunoglobulin G show pleiotropy with autoimmune diseases and haematological cancers. *PLoS Genet* 9, e1003225
25. Bakovic, M. P., Selman, M. H., Hoffmann, M., Rudan, I., Campbell, H., Deelder, A. M., Lauc, G., and Wuhrer, M. (2013) High-throughput IgG Fc N-glycosylation profiling by mass spectrometry of glycopeptides. *J Proteome Res* 12, 821-831
26. Canfield, S. M., and Morrison, S. L. (1991) The binding affinity of human IgG for its high affinity Fc receptor is determined by multiple amino acids in the CH2 domain and is modulated by the hinge region. *J Exp Med* 173, 1483-1491
27. Bruhns, P., Iannascoli, B., England, P., Mancardi, D. A., Fernandez, N., Jorieux, S., and Daeron, M. (2009) Specificity and affinity of human Fcgamma receptors and their polymorphic variants for human IgG subclasses. *Blood* 113, 3716-3725
28. Hogarth, P. M., and Pietersz, G. A. (2012) Fc receptor-targeted therapies for the treatment of inflammation, cancer and beyond. *Nat Rev Drug Discov* 11, 311-331

29. Michaelsen, T. E., Aase, A., Norderhaug, L., and Sandlie, I. (1992) Antibody dependent cell-mediated cytotoxicity induced by chimeric mouse-human IgG subclasses and IgG3 antibodies with altered hinge region. *Mol Immunol* 29, 319-326
30. Vidarsson, G., Dekkers, G., and Rispens, T. (2014) IgG subclasses and allotypes: from structure to effector functions. *Front Immunol* 5, 520
31. Schoenmaker, M., de Craen, A. J., de Meijer, P. H., Beekman, M., Blauw, G. J., Slagboom, P. E., and Westendorp, R. G. (2006) Evidence of genetic enrichment for exceptional survival using a family approach: the Leiden Longevity Study. *Eur J Hum Genet* 14, 79-84
32. Rozing, M. P., Westendorp, R. G., de Craen, A. J., Frolich, M., de Goeij, M. C., Heijmans, B. T., Beekman, M., Wijsman, C. A., Mooijaart, S. P., Blauw, G. J., Slagboom, P. E., and van Heemst, D. (2010) Favorable glucose tolerance and lower prevalence of metabolic syndrome in offspring without diabetes mellitus of nonagenarian siblings: the Leiden longevity study. *J Am Geriatr Soc* 58, 564-569
33. Postmus, I., Deelen, J., Sedaghat, S., Trompet, S., de Craen, A. J., Heijmans, B. T., Franco, O. H., Hofman, A., Dehghan, A., Slagboom, P. E., Westendorp, R. G., and Jukema, J. W. (2015) LDL cholesterol still a problem in old age? A Mendelian randomization study. *Int J Epidemiol* 44, 604-612
34. Derhovanessian, E., Maier, A. B., Beck, R., Jahn, G., Hahnel, K., Slagboom, P. E., de Craen, A. J., Westendorp, R. G., and Pawelec, G. (2010) Hallmark features of immunosenescence are absent in familial longevity. *J Immunol* 185, 4618-4624
35. Rozing, M. P., Mooijaart, S. P., Beekman, M., Wijsman, C. A., Maier, A. B., Bartke, A., Westendorp, R. G., Slagboom, E. P., and van Heemst, D. (2011) C-reactive protein and glucose regulation in familial longevity. *Age (Dordr)* 33, 623-630
36. Rozing, M. P., Westendorp, R. G., de Craen, A. J., Frolich, M., Heijmans, B. T., Beekman, M., Wijsman, C., Mooijaart, S. P., Blauw, G. J., Slagboom, P. E., and van Heemst, D. (2010) Low serum free triiodothyronine levels mark familial longevity: the Leiden Longevity Study. *J Gerontol A Biol Sci Med Sci* 65, 365-368
37. Rozing, M. P., Westendorp, R. G., Frolich, M., de Craen, A. J., Beekman, M., Heijmans, B. T., Mooijaart, S. P., Blauw, G. J., Slagboom, P. E., and van Heemst, D. (2009) Human insulin/IGF-1 and familial longevity at middle age. *Aging (Albany NY)* 1, 714-722
38. Friedewald, W. T., Levy, R. I., and Fredrickson, D. S. (1972) Estimation of the concentration of low-density lipoprotein cholesterol in plasma, without use of the preparative ultracentrifuge. *Clin Chem* 18, 499-502
39. Selman, M. H., Derks, R. J., Bondt, A., Palmblad, M., Schoenmaker, B., Koeleman, C. A., van de Geijn, F. E., Dolhain, R. J., Deelder, A. M., and Wuhrer, M. (2012) Fc specific IgG glycosylation profiling by robust nano-reverse phase HPLC-MS using a sheath-flow ESI sprayer interface. *J Proteomics* 75, 1318-1329
40. Parekh, R. B., Dwek, R. A., Sutton, B. J., Fernandes, D. L., Leung, A., Stanworth, D., Rademacher, T. W., Mizuochi, T., Taniguchi, T., Matsuta, K., and et al. (1985) Association of rheumatoid arthritis and primary osteoarthritis with changes in the glycosylation pattern of total serum IgG. *Nature* 316, 452-457
41. Stadlmann, J., Pabst, M., Kolarich, D., Kunert, R., and Altmann, F. (2008) Analysis of immunoglobulin glycosylation by LC-ESI-MS of glycopeptides and oligosaccharides. *Proteomics* 8, 2858-2871
42. Takahashi, N., Ishii, I., Ishihara, H., Mori, M., Tejima, S., Jefferis, R., Endo, S., and Arata, Y. (1987) Comparative structural study of the N-linked oligosaccharides of human normal and pathological immunoglobulin G. *Biochemistry* 26, 1137-1144
43. Palmblad, M. (2009) Xtractor. Creative Commons Attribution
44. Johnson, W. E., Li, C., and Rabinovic, A. (2007) Adjusting batch effects in microarray expression data using empirical Bayes methods. *Biostatistics* 8, 118-127
45. R Core Team (2013) R: A language and environment for statistical computing. R Foundation for Statistical Computing, Vienna, Austria

46. Hojsgaard, S., Halekoh, U., and Yan, J. (2006) The R Package geepack for Generalized Estimating Equations. *Journal of Statistical Software* 15, 1-11
47. Wickam, H. (2009) *ggplot2: elegant graphics for data analysis*
48. Langfelder, P., and Horvath, S. (2008) WGCNA: an R package for weighted correlation network analysis. *BMC Bioinformatics* 9, 559
49. Shikata, K., Yasuda, T., Takeuchi, F., Konishi, T., Nakata, M., and Mizuochi, T. (1998) Structural changes in the oligosaccharide moiety of human IgG with aging. *Glycoconj J* 15, 683-689
50. Parekh, R., Roitt, I., Isenberg, D., Dwek, R., and Rademacher, T. (1988) Age-related galactosylation of the N-linked oligosaccharides of human serum IgG. *J Exp Med* 167, 1731-1736
51. Yamada, E., Tsukamoto, Y., Sasaki, R., Yagyu, K., and Takahashi, N. (1997) Structural changes of immunoglobulin G oligosaccharides with age in healthy human serum. *Glycoconj J* 14, 401-405
52. Rigotti, A., and Krieger, M. (1999) Getting a handle on "good" cholesterol with the high-density lipoprotein receptor. *N Engl J Med* 341, 2011-2013
53. Smith, S. C., Jr. (2007) Multiple risk factors for cardiovascular disease and diabetes mellitus. *Am J Med* 120, S3-S11
54. Haffner, S. M. (2003) Insulin resistance, inflammation, and the prediabetic state. *Am J Cardiol* 92, 18-26
55. Plomp, R., Bondt, A., de Haan, N., Rombouts, Y., and Wuhrer, M. (2016) Recent Advances in Clinical Glycoproteomics of Immunoglobulins (Igs). *Mol Cell Proteomics* 15, 2217-2228
56. Dard, P., Lefranc, M. P., Osipova, L., and Sanchez-Mazas, A. (2001) DNA sequence variability of IGHG3 alleles associated to the main G3m haplotypes in human populations. *Eur J Hum Genet* 9, 765-772
57. Wuhrer, M., Stam, J. C., van de Geijn, F. E., Koeleman, C. A., Verrips, C. T., Dolhain, R. J., Hokke, C. H., and Deelder, A. M. (2007) Glycosylation profiling of immunoglobulin G (IgG) subclasses from human serum. *Proteomics* 7, 4070-4081
58. Reiding, K. R., Ruhaak, L. R., Uh, H. W., El Bouhaddani, S., van den Akker, E. B., Plomp, R., McDonnell, L. A., Houwing-Duistermaat, J. J., Slagboom, P. E., Beekman, M., and Wuhrer, M. (2016) Human plasma N-glycosylation as analyzed by MALDI-FTICR-MS associates with markers of inflammation and metabolic health. *Mol Cell Proteomics* 16, 228-242
59. Flogel, M., Lauc, G., Gornik, I., and Macek, B. (1998) Fucosylation and galactosylation of IgG heavy chains differ between acute and remission phases of juvenile chronic arthritis. *Clin Chem Lab Med* 36, 99-102
60. Rombouts, Y., Ewing, E., van de Stadt, L. A., Selman, M. H., Trouw, L. A., Deelder, A. M., Huizinga, T. W., Wuhrer, M., van Schaardenburg, D., Toes, R. E., and Scherer, H. U. (2015) Anti-citrullinated protein antibodies acquire a pro-inflammatory Fc glycosylation phenotype prior to the onset of rheumatoid arthritis. *Ann Rheum Dis* 74, 234-241
61. Sjowall, C., Zapf, J., von Lohneysen, S., Magorivska, I., Biermann, M., Janko, C., Winkler, S., Bilyy, R., Schett, G., Herrmann, M., and Munoz, L. E. (2015) Altered glycosylation of complexed native IgG molecules is associated with disease activity of systemic lupus erythematosus. *Lupus* 24, 569-581
62. Scallon, B. J., Tam, S. H., McCarthy, S. G., Cai, A. N., and Raju, T. S. (2007) Higher levels of sialylated Fc glycans in immunoglobulin G molecules can adversely impact functionality. *Mol Immunol* 44, 1524-1534
63. Lu, J., Chu, J., Zou, Z., Hamacher, N. B., Rixon, M. W., and Sun, P. D. (2015) Structure of FcgammaRI in complex with Fc reveals the importance of glycan recognition for high-affinity IgG binding. *Proc Natl Acad Sci U S A* 112, 833-838
64. Ferrara, C., Grau, S., Jager, C., Sondermann, P., Brunker, P., Waldhauer, I., Hennig, M., Ruf, A., Rufer, A. C., Stihle, M., Umana, P., and Benz, J. (2011) Unique carbohydrate-carbohydrate interactions are required for high affinity binding between FcgammaRIII and antibodies lacking core fucose. *Proc Natl Acad Sci U S A* 108, 12669-12674

65. Jefferis, R., and Lund, J. (2002) Interaction sites on human IgG-Fc for FcgammaR: current models. *Immunol Lett* 82, 57-65
66. Kemna, M. J., Plomp, R., van Paassen, P., Koeleman, C. A., Jansen, B. C., Damoiseaux, J. G., Cohen Tervaert, J. W., and Wuhrer, M. (2017) Galactosylation and Sialylation Levels of IgG Predict Relapse in Patients With PR3-ANCA Associated Vasculitis. *EBioMedicine* 17, 108-118
67. Niwa, R., Natsume, A., Uehara, A., Wakitani, M., Iida, S., Uchida, K., Satoh, M., and Shitara, K. (2005) IgG subclass-independent improvement of antibody-dependent cellular cytotoxicity by fucose removal from Asn297-linked oligosaccharides. *J Immunol Methods* 306, 151-160
68. Shields, R. L., Lai, J., Keck, R., O'Connell, L. Y., Hong, K., Meng, Y. G., Weikert, S. H., and Presta, L. G. (2002) Lack of fucose on human IgG1 N-linked oligosaccharide improves binding to human Fcgamma RIII and antibody-dependent cellular toxicity. *J Biol Chem* 277, 26733-26740
69. Menni, C., Keser, T., Mangino, M., Bell, J. T., Erte, I., Akmacic, I., Vuckovic, F., Pucic Bakovic, M., Gornik, O., McCarthy, M. I., Zoldos, V., Spector, T. D., Lauc, G., and Valdes, A. M. (2013) Glycosylation of immunoglobulin g: role of genetic and epigenetic influences. *PLoS One* 8, e82558
70. Sonneveld, M. E., van der Schoot, C. E., and Vidarsson, G. (2016) The Elements Steering Pathogenesis in IgG-Mediated Alloimmune Diseases. *J Clin Immunol* 36 Suppl 1, 76-81
71. Ackerman, M. E., Crispin, M., Yu, X., Baruah, K., Boesch, A. W., Harvey, D. J., Dugast, A. S., Heizen, E. L., Ercan, A., Choi, I., Streeck, H., Nigrovic, P. A., Bailey-Kellogg, C., Scanlan, C., and Alter, G. (2013) Natural variation in Fc glycosylation of HIV-specific antibodies impacts antiviral activity. *J Clin Invest* 123, 2183-2192
72. Lee, J., Taneja, V., and Vassallo, R. (2012) Cigarette smoking and inflammation: cellular and molecular mechanisms. *J Dent Res* 91, 142-149
73. Wang, J., Balog, C. I., Stavenhagen, K., Koeleman, C. A., Scherer, H. U., Selman, M. H., Deelder, A. M., Huizinga, T. W., Toes, R. E., and Wuhrer, M. (2011) Fc-glycosylation of IgG1 is modulated by B-cell stimuli. *Mol Cell Proteomics* 10, M110.004655
74. Willi, C., Bodenmann, P., Ghali, W. A., Faris, P. D., and Cornuz, J. (2007) Active smoking and the risk of type 2 diabetes: a systematic review and meta-analysis. *Jama* 298, 2654-2664
75. Westendorp, R. G., van Heemst, D., Rozing, M. P., Frolich, M., Mooijaart, S. P., Blauw, G. J., Beekman, M., Heijmans, B. T., de Craen, A. J., and Slagboom, P. E. (2009) Nonagenarian siblings and their offspring display lower risk of mortality and morbidity than sporadic nonagenarians: The Leiden Longevity Study. *J Am Geriatr Soc* 57, 1634-1637
76. Beekman, M., Uh, H. W., van Heemst, D., Wuhrer, M., Ruhaak, L. R., Gonzalez-Covarrubias, V., Hankemeier, T., Houwing-Duistermaat, J. J., and Slagboom, P. E. (2016) Classification for Longevity Potential: The Use of Novel Biomarkers. *Front Public Health* 4, 233
77. Koene, R. J., Prizment, A. E., Blaes, A., and Konety, S. H. (2016) Shared Risk Factors in Cardiovascular Disease and Cancer. *Circulation* 133, 1104-1114
78. Anthony, R. M., and Nimmerjahn, F. (2011) The role of differential IgG glycosylation in the interaction of antibodies with FcgammaRs in vivo. *Curr Opin Organ Transplant* 16, 7-14
79. Murphy, K., and Weaver, C. (2016) *Janeway's Immunobiology*, 9th edition Ed., Garland Science, New York

Supplemental Information

A complete overview of the supplemental information will be made available online upon publication.

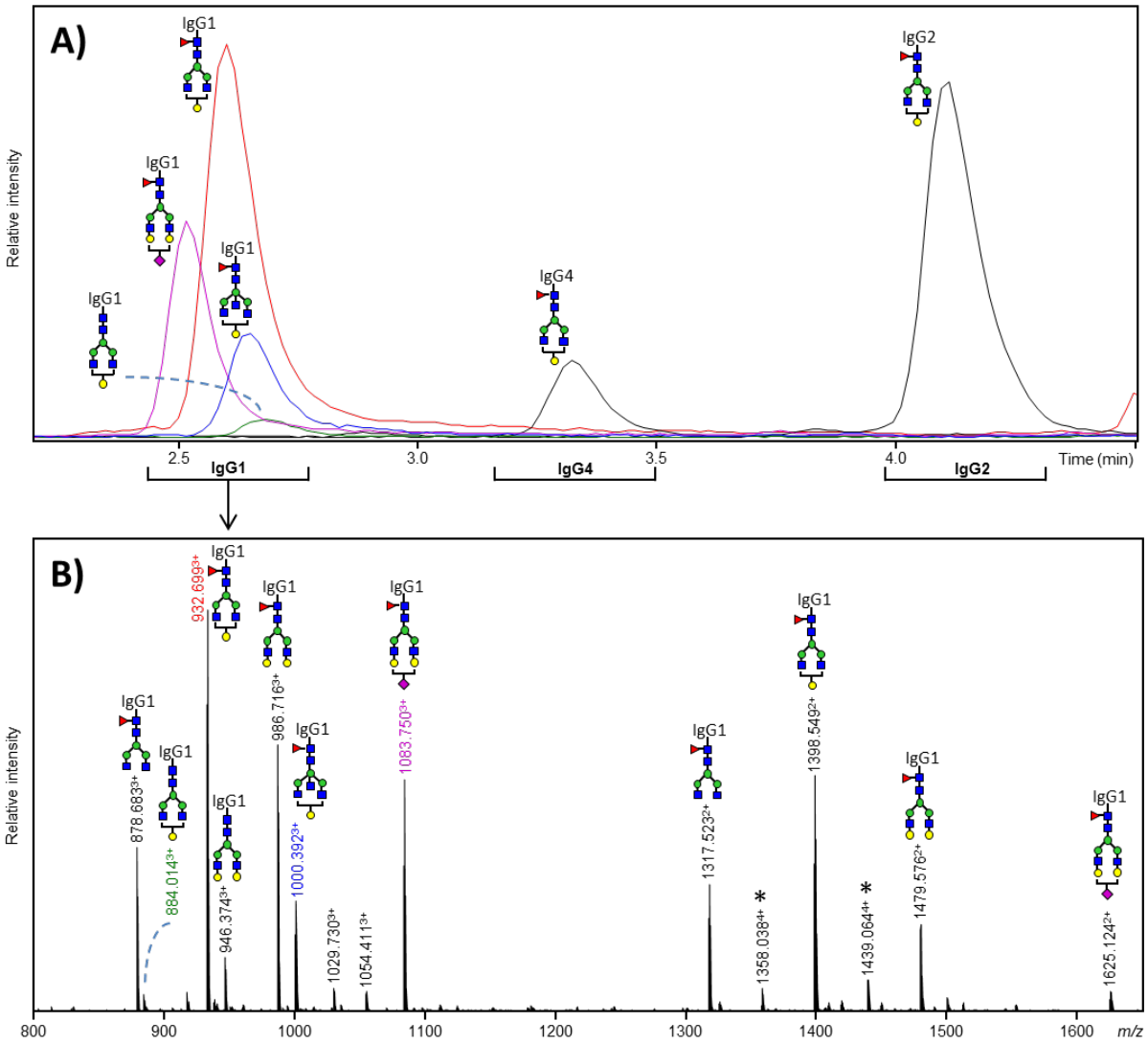

Supplemental Figure S5.1: A) Extracted ion chromatograms (EICs) of various IgG glycopeptides, showing that IgG1 glycopeptides elute first, followed by IgG4 and lastly IgG2. B) A mass spectrum of IgG1 glycopeptides in both 2+ and 3+ charge state. The peaks marked with an asterisk are quadruply charged dimers of two IgG1 glycopeptides.

Supplemental Table S5.2: Calculation of glycosylation features from individual *N*-glycan percentages. The difference between glycosylation feature calculations for different IgG subclasses arises from the exclusion of IgG2 *N*-glycopeptides G1FNS1 and G2FNS1 and afucosylated IgG4 *N*-glycopeptides. F=core fucose, N=bisecting *N*-acetylglucosamine, G=galactose, S=*N*-acetylneuraminic (sialic) acid.

glycosylation feature	description	calculation
IgG1 fucosylation	% of IgG1 *N*-glycans carrying a core fucose	G0F + G1F + G2F + G0FN + G1FN + G2FN + G1FS1 + G2FS1 + G1FNS1 + G2FNS1
IgG1 bisection	% of IgG1 *N*-glycans carrying a bisecting GlcNAc	G0FN + G1FN + G2FN + G1FNS1 + G2FNS1 + G0N + G1N + G2N + G1NS1 + G2NS1
IgG1 galactosylation	% of IgG1 *N*-glycan antennae carrying a galactose	(G1F + G1FN + G1FS1 + G1FNS1 + G1 + G1N + G1S1 + G1NS1)*0.5 + (G2F + G2FN + G2FS1 + G2FNS1 + G2 + G2N + G2S1 + G2NS1)*1
IgG1 sialylation	% of IgG1 *N*-glycan antennae carrying a sialic acid	(G1FS1 + G2FS1 + G1FNS1 + G2FNS1 + G1S1 + G2S1 + G1NS1 + G2NS1)*0.5
IgG1 sialic acid per galactose	% of galactoses carrying a sialic acid on IgG1	(IgG1 sialylation/IgG1 galactosylation) * 100
IgG2 fucosylation	% of IgG2 *N*-glycans carrying a core fucose	G0F + G1F + G2F + G0FN + G1FN + G2FN + G1FS1 + G2FS1
IgG2 bisection	% of IgG2 *N*-glycans carrying a bisecting GlcNAc	G0FN + G1FN + G2FN + G0N + G1N + G2N + G1NS1 + G2NS1
IgG2 galactosylation	% of IgG2 *N*-glycan antennae carrying a galactose	(G1F + G1FN + G1FS1 + G1 + G1N + G1S1 + G1NS1)*0.5 + (G2F + G2FN + G2FS1 + G2 + G2N + G2S1 + G2NS1)*1
IgG2 sialylation	% of IgG2 *N*-glycan antennae carrying a sialic acid	(G1FS1 + G2FS1 + G1S1 + G2S1 + G1NS1 + G2NS1)*0.5
IgG2 sialic acid per galactose	% of galactoses carrying a sialic acid on IgG2	(IgG2 sialylation/IgG2 galactosylation) * 100
IgG4 bisection	% of IgG4 *N*-glycans carrying a bisecting GlcNAc	G0FN + G1FN + G2FN + G1FNS1 + G2FNS1
IgG4 galactosylation	% of IgG4 *N*-glycan antennae carrying a galactose	(G1F + G1FN + G1FS1 + G1FNS1)*0.5 + (G2F + G2FN + G2FS1 + G2FNS1)*1
IgG4 sialylation	% of IgG4 *N*-glycan antennae carrying a sialic acid	(G1FS1 + G2FS1 + G1FNS1 + G2FNS1 + G1S1 + G2S1 + G1NS1 + G2NS1)*0.5
IgG4 sialic acid per galactose	% of galactoses carrying a sialic acid on IgG4	(IgG4 sialylation/IgG4 galactosylation) * 100

Chapter 6:

Discussion

Table of Contents

6.1: General thoughts on glycosylation

At a first glance, glycan synthesis in humans may seem to be an energetically costly and needlessly elaborate system. The glycosylation machinery takes up an estimated 1% of genes in humans (1), and many of the enzymes involved in glycosylation have similar tasks, the most egregious offender being the GalNAc-transferase, of which approximately 20 isoforms exist in humans (2). Furthermore, during *N*-glycan synthesis various building blocks are added which are removed in subsequent steps. One may well ask whether this level of complexity is necessary, especially since some of the structural alterations in proteins mediated by glycosylation could likely be achieved by other means as well. This is evidenced by the fact that the rat homologue of a human glycoprotein was found not to be glycosylated, but instead exhibited similar properties (i.e. receptor binding) through changes in the protein sequence (3), and similarly, glycosylation sites are not always conserved in related proteins (4). On the other hand, it cannot be stated that there is a high level of redundancy, as the loss of a single enzyme, even among the GalNAc-transferases, can result in serious developmental disorders (2, 5).

Glycosylation can thus be seen as a useful process which, due to its multifaceted nature, has been integrated into many different pathways over the course of evolution. One advantage of glycosylation in contrast to mutations in single protein genes, is the fact that mutations in genes involved in the glycosylation machinery can affect a large number of proteins simultaneously. In simple, single-celled eukaryotes such as yeast, *N*-glycans vary only in the number and branching of mannoses. As multicellular organisms emerged and grew continuously more complex, glycosylation was embedded into new pathways, such as cellular adhesion, signalling and degradation of asialylated glycoproteins. Simultaneously, glycosylation became more diverse, with a larger number of glycan monosaccharides, linkages and motifs, likely to accommodate the growing number of functions, although pathogen evasion has also been argued to play a role.

6.2: Analytical challenges

6.2.1: Partial occupancy of glycosylation

Chapter 3 describes the novel discovery of *O*-glycans in the hinge region of IgG3. The *O*-glycosylation sites were not fully occupied, as an *O*-glycan was only present at approximately 10% of the sites, but considering the total number of potential *O*-glycosylation sites, it is

possible that roughly half of all IgG3s carry at least one *O*-glycan. The fact that this structural feature evaded notice for over seventy years since the IgG protein was discovered (6) and over half a century since the first description of its *N*-glycosylation (7), is a testament to the fact that novel glycosylation discoveries are not limited to less-characterized proteins.

Partial site-occupancy of post-translational modifications (PTMs), including glycosylation, could be present on many proteins that have been sequenced in the past decades. If a modification is only present on a fraction of the protein molecules, the non-modified peptide will still be identified using a bottom-up proteomics approach. Hence, without specific attention to a modification, it can easily be missed using the automatic search routines. Therefore, in order to discover modifications, such as glycosylation, one must actively look for them, and for many PTMs this option is already available in commonly used software, e.g. MASCOT (8). However, for glycosylation this is not as straightforward due to the large number of possible glycan structures. Nonetheless, several software programs capable of analyzing glycopeptide fragmentation data are available (9-11). Alternatively, the chemical cleavage and labelling of glycosylation sites before their analysis may circumvent the problem of glycan structure heterogeneity (12-14). Another approach bypasses structural diversity by producing *O*-glycoproteins in a cellular system modified to generate only truncated *O*-glycans (SimpleCell) (15, 16), but unfortunately this method encompasses a lectin-purification step, thus eliminating the possibility of assessing the occupancy of *O*-glycosylation sites.

Potential *N*-glycosylation sites are easily identified due to their consensus sequence, which forms an easy target for investigation. Partial occupation of *N*-glycosylation sites occasionally goes unnoticed, as evidenced by the recent finding of a second *N*-glycan in IgG3 (17), but in general, for well-characterized proteins, sites of *N*-glycosylation are known, even if the exact range of glycan structures is often unexplored (18).

O-glycans are much more likely to go unnoticed, for various reasons. Firstly, *N*-glycans can easily be released using the enzyme *N*-glycosidase F, but for *O*-glycans chemical methods are required, which do not work as well. Secondly, the lack of a single sequence-specific *O*-GalNActransferase, and therefore lack of a consensus sequence for *O*-glycosylation, makes it difficult to predict where *O*-glycans are likely to show up (19). Hence, the prediction tools which are available are not yet very accurate. For example, two software tools deemed all

three IgG3 *O*-glycosylation sites described in chapter 3 'not *O*-glycosylated', based on the IgG3 protein sequence, while assigning the status '*O*-glycosylated' to 17 or 37 other amino acid residues in IgG3 (GPP (20) and YinOYang1.2 (21), respectively). A third tool assigned a 50% chance of *O*-glycosylation to the three identified *O*-glycosylation sites, but also assigned a higher chance to 13 other threonine and serine residues within IgG3 (NetOGlyc 4.0 (16)).

A third reason that *O*-glycosylation analysis is challenging is the heterogeneity in occupation of *O*-glycosylation sites (macroheterogeneity). Potential *O*-glycosylation sites often occur in clusters, with some sites occupied and others not, and the pattern of occupied sites can be influenced by environmental factors (13). The hinge regions of IgA1 and IgD are good examples of this: IgA1 isomers with differentially occupied *O*-glycosylation sites have been described to occur naturally in human plasma (22). Different *O*-glycosylation sites have been described for IgD, indicating that *O*-glycosylation isomers could also be present there (23, 24). While it is difficult to determine due to the sparseness of studies on glycosylation occupancy in general and *O*-glycosylation specifically, we expect that partial occupancy is more widespread among *O*-glycosylation sites than *N*-glycosylation sites.

6.2.2: Cell-bound immunoglobulins

Another aspect of Ig glycosylation which has not yet been explored is cell-bound Ig. Glycosylation analysis of Igs has up to now been focused solely on soluble Igs, since these are easily extracted from body fluids. However, immunoglobulins are also present in cell surface-bound state as B cell receptors. B cell receptors originate from the same genes as the secreted Igs by way of differential mRNA splicing, with a transmembrane section at their C-terminus. Before B-cell maturation, all Igs in B cells are surface-bound, and upon antigen exposure the secreted variant is produced (25). It has not been studied whether these surface-bound Igs express glycosylation similar to that of soluble Igs. Many of the interactions that cell-bound Igs undergo are not shared with soluble Igs, such as the interaction with glycoproteins Ig-α (CD79A) and Ig-β (CD79B) to induce signalling reactions necessary for B cell survival and development, and whether these interactions are influenced by Ig glycosylation has not been investigated (25). Therefore, glycans which appear to have no discernible function on soluble Ig should be evaluated in the context of membrane-bound Ig as well.

Immunoglobulins can also be bound to the cell surface in a different way: by non-covalent binding to cell-bound receptors. Due to the high concentration of IgG in blood and the low binding affinity between FcγRs and non-antigen-bound IgG, the receptor-bound fraction of IgG is expected to be relatively small (26). However, *N*-glycosylation of Fc IgG has been shown to affect FcγR binding affinity, with the most influential factor being the core fucose: afucosylated glycoforms possess a 50-100x greater affinity for FcγRIIIa (27-29). While the level of afucosylated IgGs is on average less than 10% in blood (Chapter 5), one may speculate that the IgG fraction bound to FcγRIIIa on immune cells could show considerably lower fucosylation. Likewise, preferential binding of afucosylated IgGs to cellular Fcγ receptors may contribute to the depletion of these antibodies from the soluble pool.

In contrast to IgG, a substantial fraction of IgE is bound to FcεRI receptors on mast cells and basophils, due to both the exceptionally high affinity between IgE and FcεRI, as well as proximity between IgE-producing B cells and FcεRI-expressing cells (26, 30). It has not been evaluated whether the type of glycans attached to IgE influences binding to FcεRI, but any such preference would greatly influence the distribution of IgE glycoforms between the receptor-bound and free fraction. Furthermore, release of FcεRI-bound IgE could facilitate a higher yield of IgE from biological samples. The low concentration of IgE in plasma, at approximately 150-300 ng/ml (31-33), compared to 10 mg/ml for IgG in healthy individuals, is now often a limiting factor for analysis.

6.3: Functional aspects of Ig glycosylation

6.3.1: Immunoglobulin E

Since the publication of the IgE glycosylation analysis described in chapter 2, additional studies have been done on the functionality of the glycans on IgE. In their 2015 paper, Shade *et al.* convincingly show that the glycan at N394 (N275 in Uniprot) is essential for binding to the Fcε receptor I, and that the removal of this glycan – either enzymatically using the high mannose-specific endoglycosidase F1 (Endo F1) or through targeted mutation of the glycosylation site – abolishes binding (34). In addition, a second study used streptococcal endoglycosidase S (Endo S) to cleave the glycan at N394, and also showed that this inhibited receptor binding and mast cell activation (35).

Furthermore, Shade *et al.* adopted the site-specific IgE glycopeptide analysis method described in chapter 2 to characterize the glycosylation of their recombinant IgE samples. They managed to improve on the method, since they only reported the use of two enzymes – trypsin and chymotrypsin – to observe the glycosylation at each of the six IgE glycosylation sites, while the original method required a third enzyme – proteinase K – to observe the glycosylation at N265 (N146 in Uniprot). Unfortunately, Shade *et al.* did not list the glycopeptide sequences or *m/z* values which they observed, which makes it difficult to compare both methods. They reported using trypsin to observe the glycopeptides at N265, which, for the standard IgE sequence as listed by Uniprot (36), would result in a peptide mass of over 7 kDa. Considering that most of the N265 glycopeptide masses would then be above 9 kDa and our measuring range only went up to *m/z* 1800, which would allow only observation of 6+ or higher charged ion species, it is not surprising that we did not observe this glycopeptide.

Shade *et al.* further report high mannose glycosylation at N394, while the other IgE sites show mostly complex-type glycosylation, which is in agreement with our results as described in chapter 2. However, they find a high degree of tetra-antennary glycans (over 50% in two of the IgE sites), as well as LacdiNAc structures and antennary fucosylation, which we did not observe in IgE derived from healthy individuals. This can be attributed to the fact that their IgE was produced in HEK cells, which can result in different glycosylation (37, 38). Probably for the same reason, Danzer *et al.* report both high mannose and complex *N*-glycans at N394, while we found solely high mannose *N*-glycans at this site (35). Moreover, the HEK cell origin of the IgE could have been the reason why Shade *et al.* encounter glycosylation at N383 (N264 Uniprot), while in chapter 2 we report that this site was unoccupied on our IgE samples. This is supported by another recent study, which confirmed that N383 was unoccupied in patient-derived IgE (39). To have a clearer picture of the influence of IgE glycosylation on FcεRI binding, experiments with polyclonal IgE samples are warranted.

A subject of further study should be whether the type of high mannose glycans (i.e. the number of mannoses) at N394 can modulate the interaction between IgE and FcεRI. To this end, a setup similar to that of Shade *et al.* could be utilized, with pre-treatment of IgE with mannosidases or mannosyltransferases to generate high mannose glycans with a varying number of mannoses. Of note, addition of mannose residues with mannosyltransferases has the drawback that this could generate structures with over nine mannoses, which are not

normally present in humans. Cleavage of mannoses, with mannosidases carefully chosen to match the different mannose linkages present in high mannose glycans, therefore appears a more appropriate strategy.

6.3.2: Immunoglobulin G

Homologous to N394 on IgE is the glycosylation site N297 on IgG, which is occupied by diantennary complex-type *N*-glycans and has been implicated in the effector functions of IgG. Despite a significant number of studies devoted to the effect of IgG glycosylation on immune reactions using various types of assays, the outcomes are often inconsistent and the exact role of IgG Fc glycosylation and its pathogenicity in autoimmune disorders remains unclear.

In autoimmune patients, IgG is often known to exhibit a decreased level of galactosylation and sialylation and an increase in fucosylation (40, 41), as described for relapsed ANCA vasculitis patients in chapter 4. This is in line with the association between IgG agalactosylation and the inflammation marker CRP (chapter 5). Sialic acid attachment requires a galactose residue, and therefore sialylation is highly correlated with galactosylation and both show similar associations with disease or metabolic markers. However, after correction for galactosylation, sialylation did not appear to be associated with either autoimmune disorders (chapter 4) (42) or CRP levels (chapter 5).

In vivo studies in mice have shown that sialylated IgG has an anti-inflammatory effect in an arthritis mouse model; sialidase-treated IgG failed to induce such an effect, indicating that sialylation, and not galactosylation, is responsible (43). Several other studies also observed that sialylated IgG shows decreased FcγR binding and/or ADCC capacity (44, 45). However, other studies did not find a negative effect of IgG sialylation on FcγR binding or ADCC capacity (46, 47). In contrast, galactosylation is described to augment FcγR-mediated effector functions (46-50).

Complement adds another layer of complexity to the interaction between IgG glycosylation and effector functions. Both galactosylation and sialylation show a positive effect on the ability of IgG to activate the classical complement pathway according to C1q-binding and cell-based assays (47, 51). The lectin pathway, which is triggered by binding of IgG to mannose binding lectin (MBL), has been proposed to be involved in immune activation by

aglycosylated IgGs in autoimmune patients (52), but recent studies have not observed any involvement of MBL (47, 53). Furthermore, a recent paper by Karsten *et al.* describes a novel pathway by which IgG interacts with inhibitory FcγRIIB and Dectin-1, leading to suppression of C5a-dependent inflammatory reactions, but only if the IgG is highly galactosylated (sialylation played no role) (54). However, these reports clash with the study by Nimmerjahn *et al.*, which reported that complement did not play a role in the *in vivo* activity of either galactosylated or agalactosylated IgG (53).

To summarize, we have the following conundrums: according to several *in vivo* studies sialylation mediates anti-inflammatory reactions, but patient IgG profiles do not show a direct association of disease activity or inflammatory parameters with sialylation after correction for galactosylation. Furthermore, galactosylation is low in autoimmune patients, but high galactosylation appears to be a more effective immune activator according to *in vitro* ADCC studies. The exact way in which IgG glycosylation and inflammatory responses are linked is thus poorly understood.

6.4: IgG glycosylation as a biomarker

In chapter 4, we described the changes seen in ANCA vasculitis patients who relapsed, compared to patients who remained in remission: IgG of relapsers exhibited a significantly lower level of galactosylation and sialylation, as well as a non-significantly higher fucosylation and lower bisection. In chapter 5, we described that individuals with a high level of inflammation, as determined by high CRP and IL-6, also showed a significantly lower level of galactosylation and sialylation and a higher level of fucosylation. As discussed above, it is not known exactly how, or even if, the glycosylation of IgG can modulate immune reactions. However, similar glycosylation patterns have been seen in many auto-immune diseases and are thought to reflect a state of inflammation (40, 55). As such, the glycosylation of IgG could be utilized as a biomarker for autoimmune diseases or relapse thereof.

The complexity of IgG glycosylation analysis, with various glycosylation features derived from individual glycan measurements, may appear to be a disadvantage, but can also be seen as a strength. The multidimensionality of IgG glycosylation measurements could provide a more specific indication as to the ailment of a patient than the level of a single clinical

parameter such as CRP. The aforementioned combination of low galactosylation and sialylation and high fucosylation is seen in many autoimmune diseases, while low fucosylation appears to be associated with certain infections, as will be discussed below.

In chapter 5 we described that individuals with a cytomegalovirus (CMV) infection exhibit a significantly lower degree of IgG fucosylation within the LLS cohort: seropositive individuals exhibited 90.6% fucosylation, while 91.7% was seen in others. While these differences are relatively small, it should be noted that these are individuals with a latent, asymptomatic CMV-infection, and the amount of CMV-specific IgG as a proportion of the total IgG is therefore likely small. We also examined CMV-specific IgG of three unrelated samples, and this antigen-specific IgG subpopulation showed a much lower degree of fucosylation, at approximately 70% (unpublished data). Literature also reports several instances of antigen-specific IgG with low fucosylation: HIV-specific antibodies have been reported to exhibit approximately 75% fucosylation (56). Extremely low IgG fucosylation levels (as low as 12%) have also been observed for maternal IgGs against foetal red blood cells in haemolytic disease (57). In contrast, PR3 ANCA-specific IgGs exhibit significantly higher fucosylation compared to total IgG (chapter 4), similar to several other auto-immune conditions (40, 41). Thus, it appears that specific glycosylation changes can be induced in antigen-specific IgG, and that these vary depending on the nature of the inflammation. Autoantibodies show increased fucosylation, while antibodies against foreign compounds repeatedly appeared to carry afucosylated *N*-glycans, which in the case of the often predominant IgG1 subclass is considered to be more inflammatory with respect to induction of ADCC (27-29). However, the division is likely not as clear-cut as this, since no fucosylation difference was reported in total IgG in chronic hepatitis patients before and after treatment (58) or in antigen-specific IgG after influenza or tetanus vaccination (59).

A disadvantage of IgG glycosylation as biomarker is the large inter-individual variation. Part of this variation is age- and sex-related, and in fact this may reflect underlying differences in inflammation: older individuals are generally known to have a more inflammatory immune system, and also display lower galactosylation. Furthermore, post-menopausal women have the lowest degree of galactosylation (chapter 5), which fits with the higher abundance of auto-immune diseases in this group (60). The problem of large inter-individual variation could be circumvented by using IgG glycosylation as a personal biomarker for inflammation, for instance in individuals at risk for relapse, as we suggested in chapter 4.

In chapter 5 we did not find an association between IgG glycosylation and predisposition to longevity. This may be because a high level of immune activation can be either advantageous or detrimental, depending on the situation. Many elderly people die of opportunistic infections which their immune system is not able to handle. Furthermore, cancer occurs when an uncontrolled cell escapes the constraints of the immune system, and occurs more often in immunocompromised individuals (61). In both of these cases, it can be generally said that an active immune system is advantageous. On the other hand, inflammation is associated with and possibly contributes to heart disease, the leading cause of death in industrialized countries (62). Moreover, an overactive immune system can lead to auto-immune conditions, which, while they are often not fatal, can severely impact the quality of life. We expect that in individuals with a genetic predisposition for longevity, the immune system is finely balanced to avoid both under- and over-activity. For this reason, in future mortality analysis in the LLS study, it may be worthwhile to categorize mortality cases based on the cause of death, with two broad groups containing deaths related to over- and underactivity of the immune system.

References

1. Varki, A., Cummings, R. D., Esko, J. D., Stanley, P., Hart, G., Aebi, M., Darvill, A., Kinoshita, T., Packer, N. H., Prestegard, J. J., Schnaar, R. L., and Seeberger, P. H. (2015) *Essentials of Glycobiology*, 3rd Edition Ed., Cold Spring Harbor Laboratory Press, Cold Spring Harbor (NY)
2. Bennett, E. P., Mandel, U., Clausen, H., Gerken, T. A., Fritz, T. A., and Tabak, L. A. (2012) Control of mucin-type O-glycosylation: a classification of the polypeptide GalNAc-transferase gene family. *Glycobiology* 22, 736-756
3. Wyss, D. F., Choi, J. S., Li, J., Knoppers, M. H., Willis, K. J., Arulanandam, A. R., Smolyar, A., Reinherz, E. L., and Wagner, G. (1995) Conformation and function of the N-linked glycan in the adhesion domain of human CD2. *Science* 269, 1273-1278
4. Tan, N. Y., Bailey, U. M., Jamaluddin, M. F., Mahmud, S. H., Raman, S. C., and Schulz, B. L. (2014) Sequence-based protein stabilization in the absence of glycosylation. *Nat Commun* 5, 3099
5. Jaeken, J. (2010) Congenital disorders of glycosylation. *Ann N Y Acad Sci* 1214, 190-198
6. Black, C. A. (1997) A brief history of the discovery of the immunoglobulins and the origin of the modern immunoglobulin nomenclature. *Immunol Cell Biol* 75, 65-68
7. Rothfus, J. A., and Smith, E. L. (1963) Glycopeptides. IV. The periodate oxidation of glycopeptides from human gamma-globulin. *J Biol Chem* 238, 1402-1410
8. Perkins, D. N., Pappin, D. J., Creasy, D. M., and Cottrell, J. S. (1999) Probability-based protein identification by searching sequence databases using mass spectrometry data. *Electrophoresis* 20, 3551-3567
9. Dallas, D. C., Martin, W. F., Hua, S., and German, J. B. (2013) Automated glycopeptide analysis--review of current state and future directions. *Brief Bioinform* 14, 361-374
10. Wu, S. W., Pu, T. H., Viner, R., and Khoo, K. H. (2014) Novel LC-MS(2) product dependent parallel data acquisition function and data analysis workflow for sequencing and identification of intact glycopeptides. *Anal Chem* 86, 5478-5486
11. Hufnagel, P., Resemann, A., Jabs, W., Marx, K., and U., S.-H. (2014) Automated detection and identification of N- and O-glycopeptides. *Discovering the Subtleties of Sugars: Proceedings of the 3rd Beilstein Glyco-Bioinformatics Symposium*, Logos Verlag Berlin Gmbh, Potsdam, Germany
12. Gerken, T. A. (2012) O-glycoprotein biosynthesis: site localization by Edman degradation and site prediction based on random peptide substrates. *Methods Mol Biol* 842, 81-108
13. Jensen, P. H., Kolarich, D., and Packer, N. H. (2010) Mucin-type O-glycosylation--putting the pieces together. *Febs j* 277, 81-94
14. Pan, S., Chen, R., Aebersold, R., and Brentnall, T. A. (2011) Mass spectrometry based glycoproteomics--from a proteomics perspective. *Mol Cell Proteomics* 10, R110.003251
15. Steentoft, C., Vakhrushev, S. Y., Vester-Christensen, M. B., Schjoldager, K. T., Kong, Y., Bennett, E. P., Mandel, U., Wandall, H., Levery, S. B., and Clausen, H. (2011) Mining the O-glycoproteome using zinc-finger nuclease-glycoengineered SimpleCell lines. *Nat Methods* 8, 977-982
16. Steentoft, C., Vakhrushev, S. Y., Joshi, H. J., Kong, Y., Vester-Christensen, M. B., Schjoldager, K. T., Lavrsen, K., Dabelsteen, S., Pedersen, N. B., Marcos-Silva, L., Gupta, R., Bennett, E. P., Mandel, U., Brunak, S., Wandall, H. H., Levery, S. B., and Clausen, H. (2013) Precision mapping of the human O-GalNAc glycoproteome through SimpleCell technology. *Embo j* 32, 1478-1488
17. Stavenhagen, K., Plomp, R., and Wuhrer, M. (2015) Site-Specific Protein N- and O-Glycosylation Analysis by a C18-Porous Graphitized Carbon-Liquid Chromatography-Electrospray Ionization Mass Spectrometry Approach Using Pronase Treated Glycopeptides. *Anal Chem* 87, 11691-11699
18. Hoffmann, M., Marx, K., Reichl, U., Wuhrer, M., and Rapp, E. (2016) Site-specific O-Glycosylation Analysis of Human Blood Plasma Proteins. *Mol Cell Proteomics* 15, 624-641
19. Ten Hagen, K. G., Fritz, T. A., and Tabak, L. A. (2003) All in the family: the UDP-GalNAc:polypeptide N-acetylgalactosaminyltransferases. *Glycobiology* 13, 1r-16r
20. Hamby, S. E., and Hirst, J. D. (2008) Prediction of glycosylation sites using random forests. *BMC Bioinformatics* 9, 500
21. Gupta, R., and Brunak, S. (2002) Prediction of glycosylation across the human proteome and the correlation to protein function. *Pac Symp Biocomput*, 310-322
22. Takahashi, K., Smith, A. D., Poulsen, K., Kilian, M., Julian, B. A., Mestecky, J., Novak, J., and Renfrow, M. B. (2012) Naturally occurring structural isomers in serum IgA1 o-glycosylation. *J Proteome Res* 11, 692-702

23. Takayasu, T., Suzuki, S., Kametani, F., Takahashi, N., Shinoda, T., Okuyama, T., and Munekata, E. (1982) Amino acid sequence of galactosamine-containing glycopeptides in the hinge region of a human immunoglobulin D. *Biochem Biophys Res Commun* 105, 1066-1071
24. Takahashi, N., Tetaert, D., Debuire, B., Lin, L. C., and Putnam, F. W. (1982) Complete amino acid sequence of the delta heavy chain of human immunoglobulin D. *Proc Natl Acad Sci U S A* 79, 2850-2854
25. Gauld, S. B., Dal Porto, J. M., and Cambier, J. C. (2002) B cell antigen receptor signaling: roles in cell development and disease. *Science* 296, 1641-1642
26. Murphy, K., and Weaver, C. (2016) *Janeway's Immunobiology*, 9th edition Ed., Garland Science, New York
27. Ferrara, C., Grau, S., Jager, C., Sondermann, P., Brunker, P., Waldhauer, I., Hennig, M., Ruf, A., Rufer, A. C., Stihle, M., Umana, P., and Benz, J. (2011) Unique carbohydrate-carbohydrate interactions are required for high affinity binding between FcgammaRIII and antibodies lacking core fucose. *Proc Natl Acad Sci U S A* 108, 12669-12674
28. Niwa, R., Natsume, A., Uehara, A., Wakitani, M., Iida, S., Uchida, K., Satoh, M., and Shitara, K. (2005) IgG subclass-independent improvement of antibody-dependent cellular cytotoxicity by fucose removal from Asn297-linked oligosaccharides. *J Immunol Methods* 306, 151-160
29. Shields, R. L., Lai, J., Keck, R., O'Connell, L. Y., Hong, K., Meng, Y. G., Weikert, S. H., and Presta, L. G. (2002) Lack of fucose on human IgG1 N-linked oligosaccharide improves binding to human Fcgamma RIII and antibody-dependent cellular toxicity. *J Biol Chem* 277, 26733-26740
30. Gould, H. J., Sutton, B. J., Beavil, A. J., Beavil, R. L., McCloskey, N., Coker, H. A., Fear, D., and Smurthwaite, L. (2003) The biology of IGE and the basis of allergic disease. *Annu Rev Immunol* 21, 579-628
31. King, C. L., Poindexter, R. W., Ragunathan, J., Fleisher, T. A., Ottesen, E. A., and Nutman, T. B. (1991) Frequency analysis of IgE-secreting B lymphocytes in persons with normal or elevated serum IgE levels. *J Immunol* 146, 1478-1483
32. Johansson, S. G. (1967) Raised levels of a new immunoglobulin class (IgND) in asthma. *Lancet* 2, 951-953
33. Ghory, A. C., Patterson, R., Roberts, M., and Suszko, I. (1980) In vitro IgE formation by peripheral blood lymphocytes from normal individuals and patients with allergic bronchopulmonary aspergillosis. *Clin Exp Immunol* 40, 581-585
34. Shade, K. T., Platzer, B., Washburn, N., Mani, V., Bartsch, Y. C., Conroy, M., Pagan, J. D., Bosques, C., Mempel, T. R., Fiebiger, E., and Anthony, R. M. (2015) A single glycan on IgE is indispensable for initiation of anaphylaxis. *J Exp Med* 212, 457-467
35. Sjögren, J. (2015) Bacterial modulation of host glycosylation - in infection, biotechnology, and therapy. *Factulty of Medicine*, Lund University, Lund, Sweden
36. (2015) UniProt: a hub for protein information. *Nucleic Acids Res* 43, D204-212
37. Bohm, E., Seyfried, B. K., Dockal, M., Graninger, M., Hasslacher, M., Neurath, M., Konetschny, C., Matthiessen, P., Mitterer, A., and Scheiflinger, F. (2015) Differences in N-glycosylation of recombinant human coagulation factor VII derived from BHK, CHO, and HEK293 cells. *BMC Biotechnol* 15, 87
38. Costa, A. R., Rodrigues, M. E., Henriques, M., Oliveira, R., and Azeredo, J. (2014) Glycosylation: impact, control and improvement during therapeutic protein production. *Crit Rev Biotechnol* 34, 281-299
39. Wu, G., Hitchen, P. G., Panico, M., North, S. J., Barbouche, M. R., Binet, D., Morris, H. R., Dell, A., and Haslam, S. M. (2016) Glycoproteomic studies of IgE from a novel hyper IgE syndrome linked to PGM3 mutation. *Glycoconj J* 33, 447-456
40. Rombouts, Y., Ewing, E., van de Stadt, L. A., Selman, M. H., Trouw, L. A., Deelder, A. M., Huizinga, T. W., Wuhrer, M., van Schaardenburg, D., Toes, R. E., and Scherer, H. U. (2015) Anti-citrullinated protein antibodies acquire a pro-inflammatory Fc glycosylation phenotype prior to the onset of rheumatoid arthritis. *Ann Rheum Dis* 74, 234-241
41. Sjowall, C., Zapf, J., von Lohneysen, S., Magorivska, I., Biermann, M., Janko, C., Winkler, S., Bilyy, R., Schett, G., Herrmann, M., and Munoz, L. E. (2015) Altered glycosylation of complexed native IgG molecules is associated with disease activity of systemic lupus erythematosus. *Lupus* 24, 569-581
42. Bondt, A., Selman, M. H., Deelder, A. M., Hazes, J. M., Willemsen, S. P., Wuhrer, M., and Dolhain, R. J. (2013) Association between galactosylation of immunoglobulin G and improvement of rheumatoid arthritis during pregnancy is independent of sialylation. *J Proteome Res* 12, 4522-4531
43. Kaneko, Y., Nimmerjahn, F., and Ravetch, J. V. (2006) Anti-inflammatory activity of immunoglobulin G resulting from Fc sialylation. *Science* 313, 670-673

44. Scallon, B. J., Tam, S. H., McCarthy, S. G., Cai, A. N., and Raju, T. S. (2007) Higher levels of sialylated Fc glycans in immunoglobulin G molecules can adversely impact functionality. *Mol Immunol* 44, 1524-1534
45. Naso, M. F., Tam, S. H., Scallon, B. J., and Raju, T. S. (2010) Engineering host cell lines to reduce terminal sialylation of secreted antibodies. *MAbs* 2, 519-527
46. Thomann, M., Schlothauer, T., Dashivets, T., Malik, S., Avenal, C., Bulau, P., Ruger, P., and Reusch, D. (2015) In vitro glycoengineering of IgG1 and its effect on Fc receptor binding and ADCC activity. *PLoS One* 10, e0134949
47. Dekkers, G., Treffers, L., Plomp, R., Bentlage, A. E. H., de Boer, M., Koeleman, C. A., Lissenberg-Thunissen, S., Visser, R., Brouwer, M., Mok, J. Y., van Esch, W. C., Aalberse, R., Kuijpers, T., Wouters, D., Rispens, T., Wuhrer, M., and Vidarsson, G. (2016) IgG Fc-glycosylation differentially affects FcγR binding and complement *Manuscript submitted for publication*
48. Houde, D., Peng, Y., Berkowitz, S. A., and Engen, J. R. (2010) Post-translational modifications differentially affect IgG1 conformation and receptor binding. *Mol Cell Proteomics* 9, 1716-1728
49. Kumpel, B. M., Wang, Y., Griffiths, H. L., Hadley, A. G., and Rook, G. A. (1995) The biological activity of human monoclonal IgG anti-D is reduced by beta-galactosidase treatment. *Hum Antibodies Hybridomas* 6, 82-88
50. Kumpel, B. M., Rademacher, T. W., Rook, G. A., Williams, P. J., and Wilson, I. B. (1994) Galactosylation of human IgG monoclonal anti-D produced by EBV-transformed B-lymphoblastoid cell lines is dependent on culture method and affects Fc receptor-mediated functional activity. *Hum Antibodies Hybridomas* 5, 143-151
51. Boyd, P. N., Lines, A. C., and Patel, A. K. (1995) The effect of the removal of sialic acid, galactose and total carbohydrate on the functional activity of Campath-1H. *Mol Immunol* 32, 1311-1318
52. Malhotra, R., Wormald, M. R., Rudd, P. M., Fischer, P. B., Dwek, R. A., and Sim, R. B. (1995) Glycosylation changes of IgG associated with rheumatoid arthritis can activate complement via the mannose-binding protein. *Nat Med* 1, 237-243
53. Nimmerjahn, F., Anthony, R. M., and Ravetch, J. V. (2007) Agalactosylated IgG antibodies depend on cellular Fc receptors for in vivo activity. *Proc Natl Acad Sci U S A* 104, 8433-8437
54. Karsten, C. M., Pandey, M. K., Figge, J., Kilchenstein, R., Taylor, P. R., Rosas, M., McDonald, J. U., Orr, S. J., Berger, M., Petzold, D., Blanchard, V., Winkler, A., Hess, C., Reid, D. M., Majoul, I. V., Strait, R. T., Harris, N. L., Kohl, G., Wex, E., Ludwig, R., Zillikens, D., Nimmerjahn, F., Finkelman, F. D., Brown, G. D., Ehlers, M., and Kohl, J. (2012) Anti-inflammatory activity of IgG1 mediated by Fc galactosylation and association of FcgammaRIIB and dectin-1. *Nat Med* 18, 1401-1406
55. de Jong, S. E., Selman, M. H., Adegnika, A. A., Amoah, A. S., van Riet, E., Kruize, Y. C., Raynes, J. G., Rodriguez, A., Boakye, D., von Mutius, E., Knulst, A. C., Genuneit, J., Cooper, P. J., Hokke, C. H., Wuhrer, M., and Yazdanbakhsh, M. (2016) IgG1 Fc N-glycan galactosylation as a biomarker for immune activation. *Sci Rep* 6, 28207
56. Ackerman, M. E., Crispin, M., Yu, X., Baruah, K., Boesch, A. W., Harvey, D. J., Dugast, A. S., Heizen, E. L., Ercan, A., Choi, I., Streeck, H., Nigrovic, P. A., Bailey-Kellogg, C., Scanlan, C., and Alter, G. (2013) Natural variation in Fc glycosylation of HIV-specific antibodies impacts antiviral activity. *J Clin Invest* 123, 2183-2192
57. Kapur, R., Della Valle, L., Sonneveld, M., Hipgrave Ederveen, A., Visser, R., Ligthart, P., de Haas, M., Wuhrer, M., van der Schoot, C. E., and Vidarsson, G. (2014) Low anti-RhD IgG-Fc-fucosylation in pregnancy: a new variable predicting severity in haemolytic disease of the fetus and newborn. *Br J Haematol* 166, 936-945
58. Ho, C. H., Chien, R. N., Cheng, P. N., Liu, J. H., Liu, C. K., Su, C. S., Wu, I. C., Li, I. C., Tsai, H. W., Wu, S. L., Liu, W. C., Chen, S. H., and Chang, T. T. (2015) Aberrant serum immunoglobulin G glycosylation in chronic hepatitis B is associated with histological liver damage and reversible by antiviral therapy. *J Infect Dis* 211, 115-124
59. Selman, M. H., de Jong, S. E., Soonawala, D., Kroon, F. P., Adegnika, A. A., Deelder, A. M., Hokke, C. H., Yazdanbakhsh, M., and Wuhrer, M. (2012) Changes in antigen-specific IgG1 Fc N-glycosylation upon influenza and tetanus vaccination. *Mol Cell Proteomics* 11, M111.014563
60. Fairweather, D., and Rose, N. R. (2004) Women and autoimmune diseases. *Emerg Infect Dis* 10, 2005-2011
61. Riminton, D. S., Hartung, H. P., and Reddel, S. W. (2011) Managing the risks of immunosuppression. *Curr Opin Neurol* 24, 217-223
62. Libby, P. (2006) Inflammation and cardiovascular disease mechanisms. *Am J Clin Nutr* 83, 456s-460s

Appendix

Table of Contents

Summary (English)

Glycosylation of immunoglobulins is suspected to play a key role in the regulation of the immune system. Glycosylation of IgG has been shown to influence various effector functions, while IgE glycosylation is essential for receptor binding. Furthermore, various diseases have been associated with aberrant Ig glycosylation profiles – for instance, low galactosylation and sialylation of IgG *N*-glycans in autoimmune disorders, and low galactosylation of IgA *O*-glycans in IgA nephropathy.

Glycans can occupy multiple positions within Igs: each heavy chain harbors at least one *N*-glycan, which can affect receptor binding; the hinge region of several isotypes carries *O*-glycans; and the variable sequence in the Fab part can contain any number of glycans. To distinguish between glycans at different positions, glycoproteomics methods can be used to generate a site-specific glycosylation profile. Protease-generated glycopeptides can be analyzed using LC-MS/MS, which provides both a relatively high throughput and a good overview of glycan compositions.

In this thesis, mass spectrometry-based glycoproteomics methods were used to characterize the glycosylation of various immunoglobulins. While the field of glycomics is rapidly expanding, antibody glycosylation studies have up to now focused almost solely on IgG, ignoring the other antibody isotypes. This can be partially attributed to the high abundance of IgG in blood and the relatively low complexity of its glycosylation, which simplifies its analysis. Glycosylation of the other isotypes remains largely unstudied, especially for the low-abundant Igs such as IgD and IgE.

Structural Ig glycosylation analysis

Immunoglobulin E exhibits the lowest abundance of all the Igs in blood, but at the same time it has the capacity to ellicit the strongest immune reactions. IgE is involved in protection against parasites, but is mainly known for causing allergic reactions. It's protein sequence contains seven potential *N*-glycosylation sites, but in literature there was no clear consensus as to whether all of these were occupied. In **Chapter 2**, we describe the development of a glycoproteomics method to analyze IgE glycosylation: IgE was digested using three different proteases, and the resulting glycopeptides were identified using LC-MS(/MS). Using this we were able to show that six of the seven potential *N*-glycosylation sites were occupied, and presented a site-specific overview of the *N*-glycans present at each site. We further showed that myeloma-derived IgE exhibited aberrant glycosylation – specifically a higher degree of

tri- and tetra-antennary glycans and a lower degree of bisecting GlcNAc – while IgE from a hyperimmune donor did not, although both these observations were derived from only a single sample. It has since been shown that one of the IgE glycans is essential for binding to the high affinity receptor FcεRI.

In **Chapter 3** we reported partial *O*-glycosylation of IgG3. IgG3 is unique among the IgG subclasses in having an extended hinge region which contains a triple repeat sequence. From LC-MS(/MS) analyses of tryptic glycopeptides, we found that this repeat may contain up to 3 sites of *O*-glycosylation, which carry mainly mono- and di-sialylated core 1-type *O*-glycans. However, only 10% of each site is occupied by a glycan, with little variation in either the occupancy or the type of *O*-glycans seen in six individuals. It can be speculated that the *O*-glycans are involved in protection of IgG3 against bacterial proteases, since they were observed to inhibit digestion with endoproteinase AspN, and because *O*-glycosylation of the IgA1 and IgD hinge has also been shown to confer protease resistance.

Ig glycosylation analysis in population studies

In addition to structural glycosylation research, we also analyzed antibody glycosylation in population cohorts. In **Chapter 4** and **Chapter 5**, IgG Fc glycopeptide analysis was performed on blood samples using LC-MS(/MS). We found that a low degree of galactosylation and sialylation, and a high degree of fucosylation were associated with a state of inflammation.

In a cohort of 76 ANCA vasculitis patients, low galactosylation and sialylation of IgG was associated with a higher chance of future relapse. In relapsing patients, the degree of galactosylation, sialylation and bisection of IgG significantly decreased, while in patients who remained in remission they did not. Interestingly, PR3-specific IgG was not a better predictor of relapse than total IgG, though it reflected the same trends as seen in total IgG.

In the approximately 1800 participants of the Leiden Longevity study (LLS), low galactosylation and sialylation of IgG, together with high fucosylation, showed association with markers of inflammation. Low galactosylation and sialylation also associated with low levels of high-density lipoprotein cholesterol (HDLC) and high levels of tryglycerides, which are known risk factors for cardiovascular disease. Together this points towards a potential role for IgG glycosylation as a biomarker of inflammation and metabolic health. However, the significant inter-individual differences complicate this.

Interestingly, galactosylation and sialylation of IgG2 showed a consistently weaker association with metabolic markers compared to the other IgG subclasses. This could be indicative of a minor role of this IgG subclass *in vivo*, which is supported by *in vitro* receptor affinity studies in literature. Furthermore, in both the LLS and the ANCA vasculitis cohort, we found that after correction for galactosylation, IgG sialylation no longer showed association with metabolic markers or functioned as a predictor for ANCA vasculitis relapse. This supports the theory that mainly galactosylation, and not sialylation, mediates the inflammatory capacity of human IgG. Finally, we found that participants with a latent cytomegalovirus infection exhibited a lower degree of fucosylation, while current smokers exhibited a higher level of bisection.

Conclusion and future prospects

We hope that the novel data presented in this thesis may contribute to the elucidation of the role of antibody glycosylation in the immune system, of which the understanding is currently still very limited. Overall, our data indicates that IgG glycosylation may hold value as a biomarker of inflammation and metabolic health, but the biology behind this proposition is not yet clear. Functional studies have shed some light on the role of IgG glycosylation in receptor binding and other immune reactions, but at the same time this data often clashes with results from *in vivo* associations studies. Therefore, more comprehensive functional studies on IgG glycosylation are warranted, in models which should resemble the human physiology as closely as possible, as well as functional studies on glycosylation of other Igs, which up to now have been scarce.

The sensitivity of current (LC-MS) techniques is rapidly increasing, and we hope that this will enable investigation of Igs such as IgE and IgD, of which the low amount in blood is now a complicating factor for their analysis. Furthermore, in recent years new software tools have been developed to facilitate the analysis of mass spectrometric glycosylation data, which will be of great use for the analysis of antibodies which carry a large number of glycosylation sites, such as IgE and IgM. We therefore expect that high-throughput analysis of glycosylation of all Igs will be within reach shortly.

Samenvatting (Nederlands)

De glycosylering van immunoglobulinen (Ig) lijkt een belangrijke rol te spelen bij de regulering van het immuunsysteem. Van glycosylering van IgG is aangetoond dat het invloed heeft op de functionele werking, en glycosylering van IgE is essentieel voor binding aan receptoren. Daarnaast zijn verscheidene ziekten geassocieerd met afwijkende Ig glycosyleringsprofielen – onder andere lage galactosylering en sialylering van IgG *N*-glycanen bij auto-immuunziekten, en lage galactosylering van IgA *O*-glycanen bij IgA nefropathie.

Glycanen kunnen meerdere posities bezetten op immunoglobulinen: elke zware keten draagt ten minste één *N*-glycaan, welke invloed kan uitoefenen op de binding met receptoren; het scharniergebied van verschillende Ig klassen kan bedekt zijn met *O*-glycanen; en tenslotte kan de variabele sequentie van het Fab gedeelte eveneens glycanen bevatten. Om onderscheid te maken tussen glycanen op verschillende posities kan gebruik gemaakt worden van glycoproteomics methoden om een site-specifiek glycosyleringsprofiel te bepalen. Proteolytisch-gegenereerde glycopeptiden kunnen met LC-MS/MS worden geanalyseerd, wat zowel een relatief hoge high throughput als een goed overzicht van de composities van de glycanen verschaft.

In dit proefschrift zijn glycoproteomics methoden op basis van massa spectrometrie gebruikt om de glycosylering van verschillende immunoglobulinen te karakteriseren. Hoewel het terrein van glycomics zich in rap tempo uitbreidt, zijn studies op het gebied van glycosylering van antilichamen tot nu toe bijna geheel op IgG gefocust. Dit kan deels worden toegeschreven aan de hoge concentratie van IgG in bloed en de lage complexiteit van de bijbehorende glycosylering, wat de analyse relatief eenvoudig maakt. De glycosylering van andere Ig klassen is voor het overgrote deel onontgonnen gebied, met name voor de immunoglobulinen met een lage concentratie zoals IgD en IgE.

Structurele analyse van Ig glycosylering

Immunoglobuline E vertoont de laagste concentratie van alle immunoglobulinen in het bloed, maar bezit tegelijkertijd de capaciteit om de sterkste immuunreacties te ontlokken. IgE is betrokken bij de bescherming tegen parasieten, maar staat vooral bekend als de oorzaak van allergische reacties. De eiwitsequentie van IgE bevat zeven potentiële *N*-glycosyleringsites, maar in de literatuur was geen duidelijke consensus omtrent de vraag of deze allen bezet waren. In **Hoofdstuk 2** beschrijven wij de ontwikkeling van een glycoproteomics methode

om de glycosylering van IgE te analyseren: IgE is gedigesteerd met drie verschillende proteases, en de resulterende glycopeptiden zijn geïdentificeerd met behulp van LC-MS/MS. Hiermee konden we laten zien dat zes van de zeven potentiële *N*-glycosyleringssites bezet waren en hebben we een site-specifiek overzicht gepresenteerd van de *N*-glycanen die op elke site aanwezig zijn. Wij laten daarnaast zien dat IgE afkomstig van myeloma patienten afwijkende glycosylering vertoonde – met name een hoger niveau van tri- en tetra-antennaire glycanen en minder bisecting GlcNAc – terwijl dit bij IgE van een hyperimmuun donor niet het geval was, al moet gezegd worden dat beide observaties op slechts èèn enkel monster gebaseerd waren. Sindsdien is aangetoond dat één van de IgE glycanen essentieel is voor de binding met de hoge-affiniteitsreceptor FcεRI.

In **Hoofdstuk 3** rapporteerden wij gedeeltelijke *O*-glycosylering van IgG3. Uniek aan IgG3 vergeleken met de andere IgG subklassen is het verlengde scharniergebied dat een drievoudige herhalende sequentie bevat. Uit LC-MS(/MS) analyses van tryptische glycopeptiden konden wij opmaken dat deze sequentie tot drie sites van *O*-glycosylering kan bevatten, met voornamelijk mono- en di-gesialyleerde core 1-type *O*-glycanen. Echter, slechts 10% van elke site wordt bezet door een glycaan en tussen zes individuen werd weinig variatie gevonden in zowel de bezetting als het soort *O*-glycanen. Men kan speculeren dat de *O*-glycanen betrokken zijn bij bescherming van IgG3 tegen bacteriële proteases, aangezien de *O*-glycanen digestie met endoproteïnase AspN belemmerden, en omdat van *O*-glycosylering in het scharniergebied van IgA1 en IgD ook is aangetoond dat het resistentie tegen proteases verleent.

Analyse van Ig glycosylering in populatie studies

Naast structurele analyse van glycosylering hebben wij ook de glycosylering van antilichamen in populatiecohorten gemeten. In **Hoofdstuk 4** en **Hoofdstuk 5** is IgG Fc glycopeptide analyse uitgevoerd op bloedmonsters met gebruik van LC-MS. Wij vonden dat een laag gehalte van galactosylering en sialylering en een hoog gehalte van fucosylering geassocieerd waren met een staat van inflammatie.

In een cohort van 76 ANCA vasculitis patiënten was lage galactosylering en sialylering van IgG geassocieerd met een hogere kans op een terugval in patiënten die op dat moment in remissie waren. In patiënten die een terugval hadden was het niveau van galactosylering, sialylering, en bisecting GlcNAc van IgG significant afgenomen, terwijl dat in patiënten die

in remissie bleven niet het geval was. Interessant genoeg was PR3-specifiek IgG geen betere voorspeller van een terugval dan de totale pool van IgG, alhoewel het dezelfde trends vertoonde.

In de circa 1800 participanten van de Leiden Longevity studie (LLS) zagen we dat lage galactosylering en sialylering van IgG samen met hoge fucosylering associatie vertoonde met markers van inflammatie. Lage galactosylering en sialylering waren ook geassocieerd met een laag gehalte van hoge-dichtheid lipoproteïne cholesterol (HDLC) en een hoog gehalte van triglyceriden, waarvan bekend is dat het risicofactoren zijn voor cardiovasculaire ziekten. Dit tezamen indiceert een potentiële rol voor IgG glycosylering als een biomarker van inflammatie en metabole gezondheid. Dit wordt echter bemoeilijkt door de substantiële interindividuele verschillen.

Interessant genoeg toonde galactosylering en sialylering van IgG2 een consistent zwakkere associatie met metabole markers in vergelijking met de andere IgG subklasssen. Dit kan duiden op een ondergeschikte rol van deze subklasse *in vivo*, wat ondersteund wordt door onderzoek naar *in vitro* receptor binding in de literatuur. Daarenboven vonden wij dat, in zowel het LLS als het ANCA vasculitis cohort na correctie voor galactosylering, IgG sialylering niet langer associatie vertoonde met metabole markers, noch als voorspeller voor een ANCA vasculitis relapse. Dit pleit voor de theorie dat voornamelijk galactosylering, en niet sialylering, invloed heeft op de inflammatoire capaciteit van humaan IgG. Tenslotte zagen we dat participanten met een latente cytomegalovirus infectie een lager gehalte aan fucosylering vertoonden, terwijl huidige rokers een hoger niveau van bisecting GlcNAc in hun IgG hadden.

Conclusie en toekomstperspectief

Wij hopen dat de nieuwe data die in dit proefschrift wordt gepresenteerd bijdraagt aan de opheldering van de rol van glycosylering van antilichamen in het immuunsysteem, waarvan het huidige begrip nog zeer gelimiteerd is. In het algemeen wijst ons onderzoek aan dat de glycosylering van IgG van waarde kan zijn als biomarker van inflammatie en metabole gezondheid, maar de biologische mechanismen die achter dit voorstel schuilen zijn nog niet duidelijk. Functionele studies hebben een tipje van de sluier opgelicht wat betreft de rol van IgG glycosylering bij binding aan receptoren en andere immuunreacties, maar tegelijkertijd botst deze data vaak met resultaten van *in vivo* onderzoek. Diepgaand functioneel onderzoek

naar de rol van IgG glycosylering zijn daarom nodig, met modellen die zo dicht mogelijk de humane fysiologie nabootsen, evenals functionele studies naar de glycosylering van andere immunoglobulinen, die tot op heden schaars zijn.

De sensitiviteit van huidige (LC-MS) technieken neemt in rap tempo toe en wij hopen dat dit de gelegenheid geeft tot onderzoek naar immunoglobulinen zoals IgE en IgD, waarvan de lage concentratie in bloed nu een obstakel is. Daarnaast zijn de laatste jaren nieuwe software tools ontwikkeld om de analyse van massa spectrometrische glycosyleringsdata te faciliteren, die van grote waarde zullen zijn voor de analyse van antilichamen met een groot aantal glycosyleringssites, zoals IgE en IgM. Wij verwachten daarom dat high-throughput analyse van de glycosylering van alle immunoglobulinen binnenkort binnen bereik zal zijn.

List of abbreviations

AA	2-aminobenzoic acid
AAV	ANCA-associated vasculitis
ABC	ammonium bicarbonate
ACN	acetonitrile
ACPA	anti-citrullinated protein antibodies
ADCC	antibody-dependent cellular cytotoxicity
ANCA	anti-neutrophil cytoplasmic antibodies
C1q	complement component 1 q
CDC	complement-dependent cellular cytotoxicity
CE	capillary electrophoresis
CGE-LIF	capillary gel electrophoresis with laser-induced fluorescence
CH	conserved heavy chain
CID	collision-induced dissociation
CMV	cytomegalovirus
CRP	c-reactive protein
DC-SIGN	dendritic cell-specific intercellular adhesion molecule-3 grabbing non-integrin
DHB	2,5-dihydroxybenzoic acid
DTT	dithiothreitol
EGPA	eosinophilic granulomatosis with polyangiitis
ELISA	enzyme-linked immunosorbent assay
Endo S	endoglycosidase S
ER	endoplasmic reticulum
ERLIC	electrostatic repulsion HILIC
ESI	electrospray ionization
ETD	electron-transfer dissociation
FA	formic acid
Fab	fragment antigen binding
Fc	fragment crystallizable
FcεR	Fc-epsilon receptor
FcγR	Fc-gamma receptor
FEIA	fluorescent-enzyme immune assay
FRS	Framingham risk score
GBP	glycan-binding protein
GC	glucocorticosteroid therapy
GDob1	chimeric MN12H2 antibodies with V genes from the human monoclonal IgG2 antibody DOB1
GlcNAc	*N*-acetylglucosamine
GPA	granulomatosis with polyangiitis
HDLC	high density lipoprotein cholesterol
HEK	human embryonic kidney
Hex	hexose
HexNAc	*N*-acetylhexosamine
HILIC	hydrophilic interaction liquid chromatography
HIV	human immunodeficiency virus
HPLC	high performance liquid chromatography
HR	hazard ratio

Ig	immunoglobulin
IL	interleukin
IT	ion trap
IVIg	intravenous Immunoglobulin
LC	liquid chromatography
LDLC	low density lipoprotein cholesterol
LEMS	lambert-Eaton Myasthenic Syndrome
MALDI	matrix-assisted laser desorption ionization
MBL	mannose-binding lectin
MPA	microscopic polyangiitis
MPO	myeloperoxidase
MRM	multiple reaction monitoring
MS	mass spectrometry
NCGN	necrotizing glomerulonephritis
NeuAc	*N*-acetylneuraminic acid
PBS	phosphate buffered saline
PR3	proteinase 3
PNGase F	*N*-glycosidase F
PTM	post-translational modification
qTOF	quadropole TOF
RA	rheumatoid arthritis
ROC	receiver operating characteristic
RP	reversed phase
RSD	relative standard deviation
SA	sialic acid
SD	standard deviation
SDS-PAGE	sodium dodecyl sulfate polyacrylamide gel electrophoresis
SIGN-R1	specific intercellular adhesion molecule-3 grabbing non-integrin related 1
t-ITP	transient isotachophoresis
T3	triiodothyronine
TC	total cholesterol
TFA	trifluoroacetic acid
TG	triglycerides
TNP	trinitrophenol
TOF	time-of-flight
UHPLC	ultra high performance liquid chromatography
ZIC HILIC	zwitterionic HILIC

Acknowledgements

Looking back at the past 5 years, my PhD at the Center for Proteomics and Metabolomics has been a wonderful experience surrounded by great people. I remember having a lot of doubts before I started, wondering whether a PhD was the right fit for me. I can now say I have much enjoyed doing research and it has been a very fulfilling experience. I would like to express my gratitude to the many people who helped me along the way and brought me to where I am now, at the end of my thesis.

First of all I would like to thank my promotor Manfred, for his dedication and his guidance. While he had plenty on his plate, first as head of the glyco group, professor at the VU Amsterdam and finally head of the CPM, he was always available for questions and discussions. When I sent him a manuscript I would always get detailed feedback within a few days, often at odd hours of the night. Thank you for your direction and encouragement!

I would also like to thank André, my original promotor. Although he left soon after I started, from what I've heard he was the driving force behind my selection despite my admittedly not stellar job interview. I would like to thank him for his confidence in me.

I would like to thank Paul, my co-promotor, for his help in shaping my thesis and propositions, and for sharing his knowledge of proteomics.

I would further like to thank Carolien, Agnes and Irina for their guidance in the lab and their supervision of the machinery which enabled me and everyone in the group to measure tens of thousands of samples. At the same time I would like to apologize for all of the mistakes which I've made, after which I came running to you for help; thank you for having my back!

My current colleagues I owe a great deal due to their contributions to both my development as a researcher and the friendly and encouraging environment in the group. Karli started just two weeks before me and was always game for fun discussions, glyco-related or not. I would like to thank him for all his technical and bioinformatic support. Noortje joined us later and was also frequently subjected to my questions, as well as many friendly conversations. In addition, I would like to thank her for the organisational skills she shared with me when we organised a small lab outing. Thank you both for being my paranymphs! Albert guided me during my first experiment as a PhD student; I would like to thank him for his guidance, as well as for the Christmas tree which now adorns my desk. Further thanks to David who has boosted my understanding of analytics and introduced me to new and exciting board games. Stephi, thank you for the organisational skills which helped support the literal backbone of

this thesis! Bas, thank you for all the technical support, and sorry for all of the bugs I encountered which should not have been possible! Further thanks to Viktoria, Guinevere, Gerda, Kathrin, Florent, Cees, and all of the others at the CPM!

I would also like to thank my former colleagues, Yoann, Gerhild and Maurice, for showing me the ropes of glycoanalysis. Yoann aided me in writing several publications and gave me a lot of useful advice. Gerhild taught me how to interpret mass spectrometric data and Maurice was always ready to impart (an often lengthy monologue of) his vast repository of knowledge.

In addition, I would like to thank Hae-Won, Marian, Jeanine and Eline for expanding my view on statistics and aiding in the processing of large datasets.

To my collaborators in Amsterdam and Maastricht: it was a pleasure to work with you! Michael, Gillian, Myrthe and Sanne: thank you for your contributions to my thesis and good luck with yours as well! Gestur, Theo and Jan Willem: thank you for your guidance.

I would also like to thank the students I had the pleasure of supervising: Lisette, Shivani and Jayshri. I learned a lot from supervising you, as I hope you did too!

I would further like to thank Manu for guiding me through the bureaucratic jungle known as ‘Converis’.

Finally, I would like to address the support I got from home, from Jan and my family. Thank you for the afternoons and evenings when you looked after Leander so that I could work on my thesis, and for the second opinions on various pieces of writing. I would also like to thank Jan for all of his encouragement and for the confidence he has given me.

Curriculum Vitae

Henriëtte Rosina Plomp was born on Friday the 13th of November, 1987 in Leiderdorp, The Netherlands. After receiving the bulk of her primary education in international schools, she attended the Stedelijk Gymnasium Leiden and graduated in 2006. During the next three years, she was enrolled in the Bachelor program Life Science and Technology, a collaboration between Leiden University and the Technical University Delft. In her final year there, she followed an internship at the Department of Molecular Cell Biology at the Leiden University Medical Center, supervised by Dr. A. Zaldumbide and Prof. Dr. R. C. Hoeben, investigating the migration of human mesenchymal stem cells from different biological sources.

Following that, Rosina enrolled in the Master study Forensic Science at the University of Amsterdam, receiving a degree in 2011. In that year she also performed an internship at the Department of Forensic Molecular Biology at the Erasmus Medical Center, supervised by Dr. K. Ackermann and Prof. Dr. M. Kayser. During this time she conducted research into the expression of circadian biomarkers in human blood.

In 2012 Rosina joined the Center for Proteomics and Metabolomics at the Leiden University Medical Center as a PhD student under the supervision of Prof. Dr. M. Wuhrer, Prof. Dr. A.M. Deelder and Dr. P. Hensbergen. During her PhD, which was funded by the HighGlycan Project of the European Union's Seventh Framework Programme, Rosina investigated glycosylation of immunoglobulins using a mass spectrometry-based proteomics approach, which resulted in this thesis. Since completing her thesis, she has continued in the field of glycoproteomics as a post-doctoral researcher in the same group.

List of publications

1. Ackermann, K., **Plomp, R.**, Lao, O., Middleton, B., Revell, V. L., Skene, D. J., and Kayser, M. (2013) Effect of sleep deprivation on rhythms of clock gene expression and melatonin in humans. *Chronobiol Int* 30, 901-909

2. **Plomp, R.**, Hensbergen, P. J., Rombouts, Y., Zauner, G., Dragan, I., Koeleman, C. A., Deelder, A. M., and Wuhrer, M. (2014) Site-specific N-glycosylation analysis of human immunoglobulin e. *J Proteome Res* 13, 536-546

3. Huffman, J. E., Pucic-Bakovic, M., Klaric, L., Hennig, R., Selman, M. H., Vuckovic, F., Novokmet, M., Kristic, J., Borowiak, M., Muth, T., Polasek, O., Razdorov, G., Gornik, O., **Plomp, R.**, Theodoratou, E., Wright, A. F., Rudan, I., Hayward, C., Campbell, H., Deelder, A. M., Reichl, U., Aulchenko, Y. S., Rapp, E., Wuhrer, M., and Lauc, G. (2014) Comparative performance of four methods for high-throughput glycosylation analysis of immunoglobulin G in genetic and epidemiological research. *Mol Cell Proteomics* 13, 1598-1610

4. Nagelkerke, S. Q., Dekkers, G., Kustiawan, I., van de Bovenkamp, F. S., Geissler, J., **Plomp, R.**, Wuhrer, M., Vidarsson, G., Rispens, T., van den Berg, T. K., and Kuijpers, T. W. (2014) Inhibition of FcγR-mediated phagocytosis by IVIg is independent of IgG-Fc sialylation and FcγRIIb in human macrophages. *Blood* 124, 3709-3718

5. **Plomp, R.**, Dekkers, G., Rombouts, Y., Visser, R., Koeleman, C. A., Kammeijer, G. S., Jansen, B. C., Rispens, T., Hensbergen, P. J., Vidarsson, G., and Wuhrer, M. (2015) Hinge-Region O-Glycosylation of Human Immunoglobulin G3 (IgG3). *Mol Cell Proteomics* 14, 1373-1384

6. Falck, D., Jansen, B. C., **Plomp, R.**, Reusch, D., Haberger, M., and Wuhrer, M. (2015) Glycoforms of Immunoglobulin G Based Biopharmaceuticals Are Differentially Cleaved by Trypsin Due to the Glycoform Influence on Higher-Order Structure. *J Proteome Res* 14, 4019-4028

7. Stavenhagen, K., **Plomp, R.**, and Wuhrer, M. (2015) Site-Specific Protein N- and O-Glycosylation Analysis by a C18-Porous Graphitized Carbon-Liquid Chromatography-Electrospray Ionization Mass Spectrometry Approach Using Pronase Treated Glycopeptides. *Anal Chem* 87, 11691-11699

8. **Plomp, R.**, Bondt, A., de Haan, N., Rombouts, Y., and Wuhrer, M. (2016) Recent Advances in Clinical Glycoproteomics of Immunoglobulins (Igs). *Mol Cell Proteomics* 15, 2217-2228

9. Dekkers, G., **Plomp, R.**, Koeleman, C. A., Visser, R., von Horsten, H. H., Sandig, V., Rispens, T., Wuhrer, M., and Vidarsson, G. (2016) Multi-level glyco-engineering techniques to generate IgG with defined Fc-glycans. *Sci Rep* 6, 36964

10. Sonneveld, M. E., Koelewijn, J., de Haas, M., Admiraal, J., **Plomp, R.**, Koeleman, C. A., Hipgrave Ederveen, A. L., Ligthart, P., Wuhrer, M., van der Schoot, C. E., and Vidarsson, G. (2016) Antigen specificity determines anti-red blood cell IgG-Fc alloantibody glycosylation and thereby severity of haemolytic disease of the fetus and newborn. Br J Haematol 176(4), 651-660

11. Reiding, K. R., Ruhaak, L. R., Uh, H. W., El Bouhaddani, S., van den Akker, E. B., **Plomp, R.**, McDonnell, L. A., Houwing-Duistermaat, J. J., Slagboom, P. E., Beekman, M., and Wuhrer, M. (2016) Human plasma N-glycosylation as analyzed by MALDI-FTICR-MS associates with markers of inflammation and metabolic health. *Mol Cell Proteomics* 16(2), 228-242

12. Kemna, M. J., **Plomp**, R., van Paassen, P., Koeleman, C. A. M., Jansen, B. C., Damoiseaux, J. G. M. C., Tervaert J. W., Wuhrer, M. (in press) Galactosylation and sialylation levels of IgG predict relapse in patients with PR3-ANCA associated vasculitis. *EBioMedicine* 17, 108-118

13. **Plomp**, R., Ruhaak, L. R., Uh, H., Reiding, K. R., Selman, M., Houwing-Duistermaat, J. J., Slagboom, P. E., Beekman, M., Wuhrer, M. (2017) Subclass-specific IgG glycosylation is associated with markers of inflammation and metabolic health. Manuscript submitted for publication.